Development of a post-mitotic, neuronal-astrocytic cell system, for the prediction of acute neurotoxicity in humans.

Elizabeth Kristen Woehrling

Doctor of Philosophy

ASTON UNIVERSITY

May 2007

Aston University

Development of a post-mitotic, neuronal-astrocytic cell system, for the prediction of acute neurotoxicity in humans.

Elizabeth Kristen Woehrling
Doctor of Philosophy

May 2007

Thesis Summary

These studies describe the development of a human, post-mitotic, neuronal-astrocytic cell system, which could be applied to a variety of neurological research approaches, including the screening of compounds for acute human neurotoxic potential.

The human NT2.D1 cell line was differentiated to form both a 1:2 co-culture of post-mitotic NT2 neuronal and NT2 astrocytic (NT2.N/A) cells and a pure NT2.N culture. The respective sensitivities to several test chemicals of the NT2.N/A, the NT2.N, and the NT2.D1 cells were evaluated and compared with the CCF-STTG1 astrocytoma cell line, using a combination of basal cytotoxicity and biochemical endpoints.

Using the MTT assay, the basal cytotoxicity data estimated the comparative toxicities of the test chemicals (chronic neurotoxin 2,5-hexanedione, cytotoxins 2,3- and 3,4-hexanedione and acute neurotoxins tributyltin- and trimethyltin- chloride) and also provided the non-cytotoxic concentration-range for each compound.

Biochemical endpoints examined over the non-cytotoxic range included assays for ATP levels, oxidative status (H_2O_2 and GSH levels) and caspase-3 levels as an indicator of apoptosis. Although the endpoints did not demonstrate the known neurotoxicants to be consistently more toxic to the cell systems with the greatest number of neuronal properties, the NT2 astrocytes appeared to contribute positively to NT2 neuronal health following exposure to all the test chemicals. The NT2.N/A co-culture generally maintained superior ATP and GSH levels and reduced H_2O_2 levels in comparison with the NT2.N mono-culture. In addition, the pure NT2.N culture showed a significantly lower level of caspase-3 activation compared with the co-culture, suggesting NT2 astrocytes may be important in modulating the mode of cell death following toxic insult. Overall, these studies provide evidence that an *in vitro* integrated population of post-mitotic human neurons and astrocytes may offer significant relevance to the human *in vivo* heterogeneous nervous system, when initially screening compounds for acute neurotoxic potential.

KEYWORDS: Neurotoxicity, NT2.N/A, NT2.N, co-culture, post-mitotic

Acknowledgements

I will be forever grateful to Dr Mike Coleman for giving me the opportunity to read for this thesis and for his guidance, encouragement and good humour throughout the course of my PhD. Special thanks are extended to my colleagues Dr Eric Hill, Dr Mel Grant and Dr Sally Picton and fellow PhD students Tom Zilz, Ray Ransley and Lindsay Holden, for their valued friendship, help and expertise. Heartfelt thanks are also extended to all other friends and colleagues within the department, who have provided much welcomed advice and technological assistance. Thanks also to colleagues in the wider field of *in vitro* neurotoxicology and also the IVTS, ESTIV and ECVAM, whose knowledge and enthusiasm for the subject has proved invaluable.

I would like to thank my husband Ethan with all my heart, whose love, understanding and flair for vegetarian cooking has supported and motivated me since the day we met. Special thanks to my parents for their limitless love and support throughout the years and the chemistry set that began it all. Thanks to my sister and all my family and friends both near and far for staying in touch, convincing me I can achieve my goals and providing laughs, wine and wisdom.

Finally I would like to acknowledge the Humane Research Trust for the grant that made this study possible. The trustees are warm-hearted and visionary and their promotion of a humane, economical and relevant approach to human health research is truly inspirational.

List of contents

List of tables

List of figures

Abbreviations

2,3-HD	2,3-Hexanedione
2,5-HD	2,5-Hexanedione
3,4-HD	3,4-Hexanedione
3D	Three dimensional
A_{590}	Absorbance at 590 nm
ADME	Absorption, distribution, metabolism and excretion
AMC	Aminomethylcoumarin
Amplex red	N-acetyl-3,7,-dihydroxyphenoxazine
Apaf-1	Apoptotic protease-activating factor-1
AR	Amplex® red
ARAC	Cytosine arabinoside
ATP	Adenosine triphosphate
BBB	Blood brain barrier
BSA	Bovine serum albumin
Ca^{2+}	Calcium cation
CAD	C activated domain
CAS	Chemical abstracts service
CGC	Cerebellar granule cell
Cmax	Maximum concentration
Cmax/2	Half maximum concentration
CNS	Central nervous system
Cyt-c	Cytochrome-c
DA	Dopaminergic
DAPI	4',6-diamidino-2-phenylindole
DAT	Dopamine transporter
DBT-Cl	Dibutyltin chloride
DMEM-HG	Dulbecco's Modified Eagle Medium, high-glucose
DMSO	Dimethyl sulfoxide
DNA	Deoxyribonucleic acid
DTNB	5,5'-dithiobis(2-nitrobenzoic) acid
EC	European Commission

EC cells	Embryonal carcinoma cells
ECVAM	European Centre for the Validation of Alternative Methods
ESTIV	European Society of Toxicology In Vitro
ETC	Electron transport chain
EU	European Union
$FADH_2$	Dihydroflavine-adenine dinucleotide
FBS	Foetal bovine serum
FDU	Fluorodeoxyuridine
FITC	Fluoroscein isothiocyanate
GABA	Gamma-aminobutyric acid
GAP43	Growth associated protein 43
GFAP	Glial fibrillary acidic protein
GLAST	Glutamate/aspartate transporter
GLT-1	Glutamate transporter 1
GLUT-1	Glucose transporter 1
GPx	Glutathione peroxidase
GSH	Glutathione
GSR	Glutathione reductase
GSSG	Glutathione disulphide
GTP	Guanosine triphosphate
H^+	Hydrogen cation
H_2O	Water
H_2O_2	Hydrogen peroxide
HBSS	HANKS Balanced Salt Solution
HRP	Horseradish peroxidase
IC_{50}	Concentration at which 50 % of cell viability is affected
IVTS	In Vitro Toxicology Society
JECFA	Joint FAO/WHO Expert Committee on Food Additives
LD_{50}	Dose which results in 50 % lethality
LDH	Lactate dehydrogenase
Lg	L-glutamine
MAP	Microtubule-associated protein
MI	Mitotic inhibitor

MPP^+	1-Methyl-4-phenylpyridinium
1-MPTP	1-Methyl 4-phenyl 1,2,3,6-tetrahydropyridine
MTT	3-(4,5-dimethylthazol-2-yl)-2,5-diphenyl tetrazolium bromide
NADH	Hydronicotinamide-adenine dinucleotide
NCAM	Neural cell adhesion molecule
NeuN	Neuronal nuclei
NF	Neurofilament
NF68	Neurofilament 68
NGF	Nerve growth factor
NMDA	N-methyl-D-aspartic acid
NOAEL	No Observed Adverse Effect Level
NSE	Neuron-specific enolase
NT2	NTERA-2
NT2.A	NTERA-2 clone D1 derived astrocytes
NT2.D1	NTERA-2 clone D1
NT2.N	NTERA-2 clone D1 derived neurons
NT2.N/A	Mixed culture of NTERA-2 clone D1 derived neurons and astrocytes
Nurr1	Nuclear receptor related 1
O_2	Oxygen
$O_2^{-\bullet}$	Superoxide radical anion
OECD	Organisation for Economic Co-operation and Development
OGC	Oxoglutarate carrier
$^{\bullet}OH$	Hydroxyl radical/hydroxide
PAGE	Polyacrylamide gel electrophoresis
PARP	Poly-(ADP-ribose)polymerase
PBS	Phosphate buffered saline
pdl/lam	Poly-D-lysine and laminin
Pen/strep	Penicillin/streptomycin
PNS	Peripheral nervous system
PPM	Parts per million
PVC	Polyvinyl chloride
PVDF	Polyvinylidene difluoride
RA	All-trans retinoic acid

RB	Reaction buffer
REACH	Registration, Evaluation and Authorisation of CHemicals
Resorufin	7-hydroxy-^{3}H-phenoxazine-3-one
RN	Registry number
RNA	Ribonucleic acid
ROS	Reactive oxygen species
SDS	Sodium dodecyl sulfate
SEM	Standard error of the mean
SH	Thiol group
SOD	Superoxide dismutase
SP	Sodium pyruvate
SSA	Sulfosalicylic acid
TBT	Tributyltin
TBT-Cl	Tributyltin chloride
TCA	Tricarboxylic acid
TH	Tyrosine hydroxylase
TMT	Trimethyltin
TMT-Cl	Trimethyltin chloride
TNB	5-thio-2-nitrobenzoic acid
TNF-α	Tumor necrosis factor-alpha

Chapter 1 - Introduction

1.1 Overview of the nervous system

The nervous system is an incredibly complex network of nerve cells linked together in a highly organised manner to form the rapid control system of the body. At the control centre are the brain and the spinal cord which together form the central nervous system (CNS) (Kleinsmith and Kish, 1995). The peripheral nervous system (PNS) consists of collections of neuronal cell bodies and nerves which extend outside the CNS to serve the limbs and organs, or extend from sensory organs to the CNS (Seeley *et al.*, 1998b).

The brain is made up of distinct anatomical regions that are associated with different functions. For example, the cerebrum, which is the largest portion of the brain and is divided into two hemispheres, contains centres associated with perception, memory, learning and voluntary actions (Silverthorn, 1998a). The cerebellum is concerned with the control and integration of muscular movements, as well as maintenance of muscle tone and equilibrium, whilst the medulla oblongata contains the centres that control life support systems. The thalamus acts as an information processing centre for sensory and motor related pathways and the hypothalamus integrates the autonomic nervous system with the control of endocrine functions (Buckley, 1997). The hypothalamus is located within the limbic system, which houses the structures in the human brain involved in motivation and emotional association with memory.

1.1.1 The blood brain barrier

The nervous system is protected from the adverse effects of many potential toxicants by the blood brain barrier (BBB). The BBB ensures that only certain substances can pass from the blood into the nervous tissue of the brain and spinal cord, whilst allowing the exchange of nutrients and waste products between neurons and the blood and preventing fluctuations in the composition of the blood from affecting brain function (Seeley *et al.*, 1998b).

The BBB is formed by endothelial cells of the blood vessels which are joined by 'tight junctions'. Consequently, substances cannot pass between the cells and generally only

lipid soluble molecules can diffuse through endothelial cell membranes and enter the brain. For example, older antihistamines were lipid-soluble amines that readily crossed the BBB and acted on centres controlling alertness, causing drowsiness. Newer drugs are generally less lipid soluble and do not have a sedative effect (Silverthorn, 1998b). Water soluble molecules, such as amino acids and glucose must be moved across the BBB by mediated transport (Seeley *et al.*, 1998b). Thus, the penetration of toxicants or their metabolites into the nervous system is largely related to their lipid solubility and ability to pass through the BBB. There are exceptions where a small number of sites experience a discontinuity in the barrier, allowing entry of some drugs and selective neurotoxins (Anthony *et al.*, 2001).

Unlike the CNS, the PNS is not protected by the BBB, rendering it more vulnerable to toxins and mechanical injuries. However, the brain, spinal cord and peripheral nerves are additionally covered with a continuous lining of specialised cells - known as the meningeal surface in the brain and spinal cord and perineural cells in the PNS - that limits entry of molecules from adjacent tissue (Anthony *et al.*, 2001).

1.1.2 Cells of the nervous system

The nervous system includes neurons that receive stimuli and conduct action potentials to other neurons or effector organs and non-neural cells (glia), which support and protect neurons (Seeley *et al.*, 1998b).

1.1.2.1 Neurons

A typical neuron is composed of a cell body (also known as perikaryon or soma) and a series of emerging thin cytoplasmic processes called dendrites and axons, which are organised to form complex networks (Kleinsmith and Kish, 1995). Each cell body contains a relatively large, centrally located nucleus surrounded by extensive rough endoplasmic reticulum, golgi apparatuses, a large number of mitochondria and other organelles (Seeley *et al.*, 1998b).

Dendrites increase the surface area of the neuron so that it can communicate with

multiple other neurons. They are short (< 1 mm), usually highly branched cytoplasmic extensions that emerge in large numbers from the cell body and are tapered from their bases to their tips. Functionally, dendrites conduct impulses towards the cell body and their surfaces have small extensions called dendritic spines with which to form synapses with axons of other neurons (Silverthorn, 1998a). Functionally, axons conduct action potentials from the neuronal cell body to the synapse and in most neurons a single axon arises from the cell body and can remain as a single structure or branch. Axons terminate by branching to form small extensions with enlarged ends called presynaptic terminals (Kleinsmith and Kish, 1995). They are longer than dendrites (up to a metre or more in length), to allow direct contact with cells at the far ends of the body (Reine, 1998). To facilitate communication between distant regions of the body that is rapid and highly targeted, action potentials in one cell can result in action potentials being produced in another cell at the synapse, via release of neurotransmitters from the presynaptic membrane (Kleinsmith and Kish, 1995).

1.1.2.2 Glial cells

Glia are far more numerous than neurons and account for more than half the brain's weight. They fill the spaces between neuronal cell bodies, surround the axons and dendrites and communicate with each other and neurons using electrical and chemical signals (Silverthorn, 1998a). Glial cells were long believed to be simple support cells but they are now known to have a complex and dynamic interaction with neurons (Lopachin and Aschner, 1993).

Types of glia include ependymal cells, which line the cavities of the brain and the central canal of the spinal cord; and microglia which are specialised macrophages that become mobile and phagocytic in response to cellular damage in the CNS (Seeley *et al.*, 1998b). The CNS also possesses oligodendrocytes, with cytoplasmic extensions that form layers of phospholipid rich membranes called myelin sheaths around axons to aid action potential propagation. In the PNS the equivalent myelin forming glial cells are called Schwann cells. The myelin sheath has interruptions called the nodes of Ranvier which play an important role in the conduction of action potentials along the axon (Seeley *et al.*, 1998b).

1.1.2.3 Astrocytes

Astrocytes are a category of glial cells that outnumber neurons by at least 10:1 and are involved in key aspects of neuronal function and survival, as well as the provision of structural support. They are star-shaped because of cytoplasmic processes that contain a large number of intermediate filaments composed of glial fibrillary acidic protein (GFAP). These processes extend from the cell body to cover the surfaces of neurons and blood vessels, aiding the transfer of nutrients between the two (Silverthorn, 1998a) and also closely encapsulate synapses and aid efficient synaptic function (Ye and Sontheimer, 1999). Astrocytes are also an important component of the BBB, influencing the formation of tight junctions (Seeley *et al.*, 1998b). Additionally they have numerous other essential supportive and protective functions, incorporating influences on nervous tissue growth, morphology, behaviour, survival and repair; some of which are discussed in section 1.3.2.

1.1.3 The cytoskeleton

The eukaryotic cytoskeleton is a flexible, changeable, scaffolding of actin microfilaments, intermediate filaments and microtubules that interconnect and extend through the cytoplasm in all directions. The integrity of the cytoskeleton requires the participation of all three components, with the resulting framework functioning to support the cell, organise the cell interior and stabilise cell shape and also to generate movement of organelles and materials within the cytoplasm (Seeley *et al.*, 1998b).

Microtubules are hollow tubules composed primarily of tubulin, which provide support and structure to the cytoplasm of the cell and are involved in mitotic spindle formation during cell division (Seeley *et al.*, 1998a). Additionally, neuronal microtubules are directly involved in neuronal morphogenesis and their assembly and dynamics are modulated by microtubule-associated proteins (MAP). In particular, the MAP 'tau' is thought to be involved in the extension of large neuritic processes and axons as well as in the stabilisation of microtubular polymers along these processes (Ramirez *et al.*, 1999).

Actin microfilaments are small fibrils that form bundles or networks in the cytoplasm, providing structure to the cytoplasm and support for the plasma membrane and thus cell shape. Additionally, microfilaments have an important role in the formation of growth cones in the developing nervous system. Growth cones are the dynamic extensions of a developing axon seeking its synaptic target and they are supported and continually built up through construction of actin microfilaments and extension of the plasma membrane via vesicle fusion (Kandel *et al.*, 2000).

Intermediate filaments are protein fibres about 10 nm in diameter which are typically the most stable part of the cytoskeleton and provide mechanical strength to the cells. In the nervous system an important subset of these are known as neurofilaments, occurring in the highest concentration in axons, where they are organised into longitudinal crosslinked arrays that provide crucial support to the often long cytoplasmic extensions (Kirkpatrick and Brady, 1998).

1.1.4 Axonal transport

The axon is filled with many types of fibres but lacks ribosomes and endoplasmic reticulum, therefore any proteins destined for the axon and it's distant terminal must be synthesised in the cell body. They are then packaged into vesicles and moved down the axon by axonal transport. Microtubules lie along the axis of the axon and provide the main cytoskeletal 'tracks' for axonal transport which has two components. Fast transport goes in both directions and takes synaptic and secretory vesicles and mitochondria from the cell body to the pre-synaptic terminal, with retrograde transport returning damaged organelles and old membrane components to the cell body for recycling. Slow transport moves material from the cell body to the terminal via axoplasmic flow and carries components not rapidly consumed by the cell such as enzymes and cytoskeleton proteins (Seeley *et al.*, 1998b; Silverthorn, 1998a).

1.2 Neurotoxicology

Neurotoxicology deals with the adverse effects of exposure to a biological, chemical or physical agent on the structure or function of the nervous system (Harris and Blain,

2004). Functional changes due to neurotoxicity may result from exposures to industrial chemicals, cosmetic ingredients, pharmaceuticals, food additives and naturally occurring chemicals and may involve either neuronal or glial cell types, following acute or chronic exposure. Acute neurotoxic effects can be observed even after a single exposure to a compound, whereas chronic effects can be observed due to repeated low-dose exposure (Coecke *et al.*, 2006). Cellular toxicity depends on the specific sensitivity of the cell and also the extracellular concentration of the toxic compound and may be due to the primary toxicant but often due to bioactivation and subsequent response to a metabolite (Harry *et al.*, 1998).

1.2.1 Susceptibility of the nervous system to toxic damage

The exact mechanism by which many substances cause neurotoxicity is often incompletely understood. However, the nervous system is complex and has several unique anatomical and physiological features that make it exquisitely vulnerable to toxins; indeed, damage to even a small part may lead to diverse and severe clinical signs which may exert a disproportionate impact on an organism's behaviour and survival (Buckley, 1997).

1.2.1.1 Dependence on aerobic oxidation of glucose

The brain has a massive demand for cellular energy that reflects the need to maintain large volumes of cytoplasm and extensive cell membranes, as well as transport of ions against their concentration gradients and other functions. The nervous system has special metabolic requirements, as in contrast to most other tissues there is little glycogen storage and the brain normally derives almost all of its energy from the aerobic oxidation of glucose (Reine, 1998; Silverthorn, 1998b). To meet the high glucose and oxygen needs of the human brain (an organ which is less than 2% of average body weight), its blood flow accounts for approximately 15 % of cardiac output and 20 % of total oxygen consumption (Seeley *et al.*, 1998b). Dependence on a continual supply of oxygen and glucose places neurons in a vulnerable position and interruption of the brain's blood supply can rapidly lead to aberrations of cerebral function and ultimately, cell death (Anthony *et al.*, 2001). Glial cells are less sensitive

than neurons to oxygen and nutrient deprivation but may be affected in severe cases (Buckley, 1997).

1.2.1.2 High oxygen consumption

In mammalian cells, reactive oxygen species (ROS) are continuously generated during aerobic metabolism (Dringen *et al.*, 1999a). Due to the high oxygen consumption of the brain and the prevalence of polyunsaturated fatty acids, this organ must be well protected from oxidative damage. Indeed, oxidative stress has been postulated to play a role in the action of various neurotoxins and neurodegenerative processes (Watts *et al.*, 2005), aspects of which are discussed in section 1.8.2.

1.2.1.3 Cell size and morphology

Neurons are the largest cells in the body, with some axons over a metre in length. As mentioned, maintaining an ionic differential across the membrane of such large cells requires expenditure of large amounts of energy. Also, all the materials required for maintenance and nutrition must be transported between the cell body and along the length of the axon. Transport processes are energy dependent and any interference in energy metabolism will lead to a rapid decline in axonal transport, followed by axonal degeneration (Buckley, 1997). Additionally, due to their unique morphology, neurons are vulnerable to attack at numerous sites, including the cell body, dendrites, axon, myelin sheath, nodes of Ranvier and at the synapase (Harris and Blain, 2004).

1.2.1.4 Post-mitotic state of neurons

In higher vertebrates, most neurons are so specialised that they lose the capacity to divide after they begin to form axons and dendrites and thus become post-mitotic. Therefore, any neurons within the CNS which are lost to toxic damage can not be replaced by the proliferation of surviving cells (Kleinsmith and Kish, 1995; Harris and Blain, 2004).

The destruction of a neuron cell body via necrosis or apoptosis following injury is

called neuropathy, which is irreversible and includes degeneration of its dendrites and axons with no potential for regeneration (Silverthorn, 1998b; Anthony *et al.*, 2001). However, if the cell body is intact and only the axon is severed, most of the neuron will survive; a condition called axonopathy. Synaptic transmission ceases as the axon degenerates distal to the point of injury due to separation from the cell body upon which it depends for nutrition. Additionally, the segment proximal to the break may become atrophic due to reduced synthesis of cytoskeletal elements by the perikaryon (Buckley, 1997). On rare occasions in the PNS, it is possible for the cell body to synthesise new axoplasm and for the axon stump to grow and regenerate; a process that does not take place at all in the CNS (Kleinsmith and Kish, 1995).

1.3 The neuronal-astrocytic relationship

Historically, neurotoxicologists considered xenobiotic-induced nervous tissue dysfunction to be purely a consequence of altered neuron activity, with involvement of astrocytes being regarded as incidental as they were considered merely passive support cells. However, it has since been determined that during embryogenesis a complex, reciprocal-relationship is established between astrocytes and neurons which has a mutual influence on both cell types (Lopachin and Aschner, 1993). Thus, the currently accepted concept is of the neuronal-astrocytic relationship as the basic unit of function in the nervous system (Lopachin and Aschner, 1993).

1.3.1 Glutamatergic communication

A notable feature of neurons is their ability to communicate with one another and transmit information over great distances, along specific pathways via synaptic transmission (Carmignoto, 2000). Additionally, a sophisticated mechanism of bidirectional glutamatergic signalling exists between neurons and astrocytes that coordinates their intimate, functional relationship and indicates an important active role of astrocytes in the normal functioning of nervous system (Lopachin and Aschner, 1993; Verderio and Matteoli, 2001).

Astrocytic processes encapsulate numerous synapses in the CNS and are able to

modulate synaptic activity (Carmignoto, 2000). Research has shown that glutamate released by neuronal cells at the synapse can activate glutamate receptors on astrocytes, inducing sustained cytosolic calcium (Ca^{2+}) elevations or periodic oscillatory activity, which propagates within and between astrocytes (Carmignoto, 2000). Ca^{2+} elevations in astrocytes cause glutamate release from the same cells, which generates a positive feedback stimulus to neurons that modulates neuronal excitability and synaptic transmission and enables astrocytes to integrate extracellular signals and exchange information (Fields and Stevens-Graham, 2002; Perea and Araque, 2002).

1.3.2 Protective roles of astrocytes

1.3.2.1 General support and protection

During neurogenesis, neuronal migration is the basis of CNS pattern formation. The developmental process is characterised by astrocyte-guided translocation of nerve cells from neuro-embryonic sites to adult locations (Lopachin and Aschner, 1993).

The exact mechanism by which astrocytes support neuronal survival is not known. However, the abundance of astrocytes, their close proximity to neurons and position at the interface of blood vessels and synapses, provide good opportunities for metabolic support via intercellular exchange of proteins, lipids and other macromolecules (Naus and Bani-Yaghoub, 1998). Astrocytes also aid the control of brain homeostasis by regulation of the local concentration of ions and neuroactive substances (Perea and Araque, 2002). Additionally, astrocytes support neurons via the delivery of nutrients, removal of metabolic waste products (Bronstein *et al.*, 1995; Bani-Yaghoub *et al.*, 1999) and the redistribution of potentially detrimental ions and metabolites over long distances via gap junctions (Pekny and Nilsson, 2005).

Elevated neuronal activity in times of stress requires an increase in nutrient availability and corresponding shifts in cerebral blood flow. Astrocyte end-feet contact endothelial cells of brain microvessels which aids increased nutrient delivery and it is also postulated that breakdown products of astrocytic glycogen may be transferred to neurons in times of need (Lopachin and Aschner, 1993).

1.3.2.2 Protection against oxidative stress

Astrocytes are able to protect against oxidative stress enzymatically, via maintenance of neuronal levels of the glutathione peroxidase substrate, glutathione (Desagher *et al.*, 1996). Additionally, they are able to non-enzymatically scavenge extracellular hydrogen peroxide via the release of pyruvate (Desagher *et al.*, 1997; Wang and Cynader, 2001). These antioxidant capabilities are further considered in sections 1.8.8.3 and 1.8.2.4.1, respectively.

1.3.2.3 Glutamate excitoxicity

Glutamate is an important nutritional amino acid (Sandhu *et al.*, 2003) and is the major excitatory neurotransmitter in the mammalian CNS, synthesised in glutamatergic neurons and then accumulated into synaptic vesicles (Ye *et al.*, 1999). In response to neuronal stimulation, glutamate is released into the synaptic cleft by calcium dependent exocytosis of synaptic vesicles, to produce a stimulus in the next neuron. Glutamate is then deactivated primarily by transport into surrounding astrocytic processes by a sodium dependent uptake system, involving astrocytic glutamate transporters such as the glutamate/aspartate transporter (GLAST) and glutamate transporter 1 (GLT-1) (Had-Aissouni *et al.*, 2002).

In addition to its transmission and nutrient functions, glutamate acts as a potent neurotoxin when present at high concentrations at glutamatergic synapses, resulting in excitotoxicity (Ye and Sontheimer, 1999; Sandhu *et al.*, 2003). The over-stimulation of excitatory amino acid receptors by glutamate results in increased levels of cytosolic Ca^{2+}, activation of calcium dependent digestive enzymes, including proteases, lipases and nucleases (Garcia and Massieu, 2003) and the production of ROS followed by mitochondrial dysfunction leading to necrosis or delayed apoptosis (Almaas *et al.*, 2002; Had-Aissouni *et al.*, 2002). Astrocytic processes closely encapsulate synapses and normally efficiently maintain extracellular glutamate concentrations at low micromolar levels (Ye *et al.*, 1999; Daniels and Brown, 2001). Thus, glutamate transport into astrocytes plays a crucial role in modulating efficient synaptic transmission and prevention of excitotoxicity (Drukarch *et al.*, 1997; Had-Aissouni *et*

al., 2002).

1.3.3 Astrocytic involvement in neurotoxicity

Whilst it is well established that the trophic and protective support offered by astrocytes to neurons may provide increased tolerance of neurons to some specific neurotoxins (Yu and Zuo, 1997; Tieu *et al.*, 2001; Zhou *et al.*, 2004), the multifaceted nature of the astrocytic-neuronal relationship provides numerous potential sites of disruption for neurotoxic chemicals (Lopachin and Aschner, 1993; Tieu *et al.*, 2001). Thus, regarding xenobiotic neurotoxic mechanisms, nerve damage induced by chemicals may not only involve direct damage to the nerve cell (Iwasaki and Tsuruta, 1984; Heijink *et al.*, 2000) but also dissociation of astrocytic-neuronal interactions (Lopachin and Aschner, 1993; Cookson *et al.*, 1995), or damage to the astrocytes themselves (O'Callaghan, 1991; Karpiak and Eyer, 1999). Additionally, there is evidence that astrocytes may be necessary for the expression of certain neuronal toxic effects, particularly via the release of cytokines (Harry *et al.*, 1998; Viviani *et al.*, 2000).

1.3.3.1 Astrocytic degeneration and activation

Astrocytes are usually less susceptible to damage than neurons but may undergo degenerative or reactive change (Buckley, 1997). The first signs of degeneration are swelling of the cell body followed by vacuolation of the cytoplasm; cellular processes then disintegrate followed by phagocytosis (Anthony *et al.*, 2001). *In vitro*, swollen astrocytes have been associated with compromised glutamate uptake and glutamate efflux (Lopachin and Aschner, 1993).

Glial cells become reactive in response to many CNS pathologies, such as stroke, neurodegenerative disease and some neurotoxins; indeed damage to all glial cell types, including astrocytes, appears to elicit this cellular response (O'Callaghan, 1991; O'Callaghan *et al.*, 1995). This reactive process, also known as astrogliosis or glial activation is not completely understood but an accepted hallmark is hypertrophy (O'Callaghan, 1991). Hypertrophy is associated with increased positive staining for

GFAP due to an increased number of astrocytic processes, rather than proliferation. Indeed, astrocyte mitosis usually only occurs when a nervous system injury creates a physical space that can be filled by dividing astrocytes (Wu and Schwartz, 1998). In addition to an increase in GFAP levels, astrocytic activation may be accompanied by increased glucose uptake and enhanced metabolic status, protein and RNA synthesis (Cookson *et al.*, 1994; Wu and Schwartz, 1998; Pekny and Nilsson, 2005).

1.3.3.2 Astrocytic activation and cytokines

Cytokines are important mediators of the host defence system and inflammatory response (Wu and Schwartz, 1998) and also play an important role in regulating the activity of cells in the CNS, serving as an additional means of communication between neurons and astrocytes (Brown, 1999). Astrocytes in the CNS can both secrete and respond to cytokines, such as tumor necrosis factor-alpha (TNF-α). TNF-α release may occur in response to a variety of biological stimuli, including activation (Wu and Schwartz, 1998; Viviani *et al.*, 2000) and may be necessary for the expression of toxicity towards neurons by some substances, for example via induction of the apoptotic cascade (Viviani *et al.*, 1998a).

1.4 Neurotoxicity hazard and risk overview

It has been estimated that there are approximately 4-5 million chemical compounds in the environment and many thousands of new chemicals enter commerce each year, some of which are highly toxic to the nervous system (Atterwill *et al.*, 1994; Coecke *et al.*, 2006).

Risk assessment in toxicology is defined as 'the characterisation of the potential adverse health effects of human exposures to a substance'. The initial step in risk assessment process is hazard identification, to identify the potential of chemical exposure to cause a particular type of toxic injury. This is followed by dose-response and exposure assessment, to define the likelihood of an adverse effect occurring under actual exposure conditions and may be used to determine a quantitative estimate of risk (Harry *et al.*, 1998; Coecke *et al.*, 2006).

1.4.1 Neurotoxicity testing

The 'Organisation for Economic Co-operation and Development (OECD) Guidelines for the Testing of Chemicals' are a collection of the most relevant internationally agreed testing methods used by government, industry and independent laboratories to characterise potential hazards of new and existing chemical substances. The current guidelines from the OECD for neurotoxic hazard identification following acute or chronic exposure are based solely on *in vivo* studies. Primary testing parameters combine behavioural methods to measure perturbations in sensory, motor and cognitive functions due to chemical exposure, with routine histopathological investigations and supplemented when required by electrophysiology (Atterwill *et al.*, 1993; Coecke *et al.*, 2006). Behavioural tests are generally quantitative and non-invasive and the same animal can be tested repeatedly during a toxicity study to provide information about the presence or absence of effects, severity of effects and the onset, duration or recovery of effects (OECD, 2004).

The recommended testing strategies are briefly considered below:

1) Tests of motor function; these include grip strength, ability to stay on a rotating rod and measurement of hind limb foot splay on landing.

2) Tests of sensory function; these include response to pain induced by a thermal stimulus or irritant and startle response to acoustic, auditory, nasal and visual stimuli.

3) Tests of cognitive function; these include aspects of perception, thinking, learning and memory, with observation of aversion to food and fluids, learning and anxiety as measured by avoidance of an aversive stimuli and accuracy of response to a maze.

4) Ability to perform a complex task; whereby animals are trained to make response (e.g. press a lever) to obtain positive reinforcement, with variation monitored.

5) Neurophysiology; electrophysiological techniques are used to measurement of spontaneous and stimulated electrical activity within the brain, in response to electrical, visual, aural, and skin stimulation.

6) Neuropathology; involving immersion, fixation and examination of paraffin sections of nervous system tissue (OECD, 2004).

1.4.2 Disadvantages associated with *in vivo* neurotoxicity testing in animals

In spite of its ability to predict chemical induced neurotoxicity, the whole animal approach is increasingly expensive and time-consuming and possesses a number of other shortfalls that are considered below.

1.4.2.1 Reliability of behavioural changes

Animal behavioural toxicology studies can be poorly predictive of the situation in humans and are increasingly ethically contentious due to the distress caused to the animals. Many changes in behaviour following exposure to chemicals may not be related to the specific action of a chemical on the nervous systems. Additionally, due to the functional reserve capacity of the nervous system, there is the possibility of an animal suffering morphological damage but still functioning within normal limits. Finally, while little or no animal training is required to conduct behavioural tests, the ability or willingness of individual animals may vary and this could lead to insensitivity or inappropriate interpretation of the data (OECD, 2004).

1.4.2.2 Species differences

There are many documented examples of human and animal neural tissues differing greatly regarding their susceptibility to neurotoxins *in vivo* that makes extrapolation to humans difficult. In fact, advances in the understanding of human brain biochemistry indicate that many disorders of the CNS and the fate of the drugs designed to treat them, depend upon cellular biochemical pathways unique to man (Ravindranath *et al.*, 1995; Ravindranath, 1998).

The importance of species differences was highlighted by a tumour-necrosis-factor-related ligand that was considered safe as it did not cause damage to non-malignant cells in laboratory animals. However, this potential cancer therapy drug caused apoptosis in normal human brain cells (Almaas *et al.*, 2002). A further example is the MPP^+ metabolite of the 'designer' drug contaminant MPTP, which resulted in permanent Parkinsonian effects in humans. Conversely, rats were protected from this toxic outcome due to their higher blood brain barrier levels of monoamine oxidase, compared with man (Kopin, 1987; Fonck and Baudry, 2003). Species differences may

also be of importance in cell culture. For example, the vulnerability of foetal human neurons to excitatory amino acids develops over a prolonged time compared with cortical rat neurons, as foetal human neurons constitutively express functional NMDA receptors at $1/10^{th}$ of the level in primary rat cultures (Almaas *et al.*, 2002; Garcia and Massieu, 2003).

1.4.2.3 Nature of toxin

Depending on the toxin being tested, within a single experiment it may be difficult to quantify the contribution of neurotoxicity versus illness, to observed behavioural effects. This may be particularly true in studies involving high doses. For example, paraquat is used to model Parkinson's disease in animals but tends to have a direct toxic effect on lung and liver before behavioural symptoms appear (McCarthy *et al.*, 2004).

1.4.2.4 Reduction of animal use

In accordance with public concern over the moral significance of animal suffering, principles for regulating animal use for experimental purposes were proposed in the UK in 1876 (Cruelty to Animals Act). Since then, legislative control has been introduced in most developed countries, with major initiatives in Europe (Animal Scientific Procedures Act, 1986) and the United States (Animal Welfare Act, 1966 and 1985) (Purchase *et al.*, 1998). A major influence on the introduction of this legislation was the publication of the "Principles of Humane Experimental Technique", by Russell and Burch in 1959. They defined the three 'Rs', Reduction, Refinement and Replacement of the use of laboratory animals, as the basis of alternatives in biomedical research (Russell and Burch, 1959). Under the Animal Scientific Procedures Act, 1986, it is law that if a non-animal method is developed, validated and accepted by all the regulatory authorities, it must be used instead of the animal method.

1.4.2.5 The REACH strategy

New, potentially neurotoxic drugs and chemicals are continually entering the development pipeline. Additionally, in 2012, the European Commission (EC) White

Paper 'Strategy for a future chemicals policy' will come into full effect (EC, 2001). It proposes that 'existing' chemicals should have the same extensive set of toxicity data profiles as required for 'new' chemicals since 1981. This update of the EC chemical testing policy will necessitate the hazard assessment, including the neurotoxic potential, of over 30,000 'existing' substances. To acquire this data, the White Paper requires the rapid establishment of a new system called REACH (Registration, Evaluation and Authorisation of Chemicals), to deal with both existing and new chemical substances. Due to the massive increase in experiments this system will entail (approximately 3.9 million test animals), a clause in this White Paper promotes the use of alternatives to animal tests due to ethical and economic considerations and time constraints (EC, 2001; Gartlon *et al.*, 2006).

1.4.3 Alternatives to the *in vivo* approach

As discussed, there is a recognised shortfall in the current whole animal approach for identifying chemical hazard in humans, including escalating costs, a low throughput that is unsuitable for screening a large number of agents, increased animal usage and a number of reservations relating to extrapolation to the human population (Veronesi, 1992; Atterwill *et al.*, 1994). Thus, complete reliance on extensive animal use is no longer reasonable and there is a need for a new approach to risk assessment (Broadhead and Bottrill, 1997; Sanfeliu *et al.*, 1999).

The use of *in vitro* cell and tissue culture data in the neurotoxic hazard identification process may greatly accelerate the rate at which species-relevant compound knowledge is produced to meet the increasing demand of the REACH strategy. Additionally, conventional neurotoxicity endpoints measured in the animal are subsequent to those initiated at the cellular level. This concept has turned the focus of neurotoxicology from observational to the provision of biochemical and neurospecific, mechanistic information on a compound, facilitating the prediction of neurotoxicity (Veronesi, 1992; Combes, 2005).

Up to now, no *in vitro* methods for evaluating the neurotoxic hazard of a chemical have been validated (Coecke *et al.*, 2006). However, *in vitro* culture techniques have been

successfully developed to systematically study the mechanisms of neurotoxicity at the cellular and molecular levels. A considerable effort has also been made to demonstrate that *in vitro* studies can be used to identify neurotoxic hazards and supplement investigations in whole animals in a way that is scientific, time-efficient, economical and ethically sound (Harry *et al.*, 1998; Coecke *et al.*, 2006).

1.4.3.1 Tiered, *in vitro* neurotoxicity test strategy

No single *in vitro* system is able to model the complexity of the *in vivo* nervous system and for over a decade a way forward has been considered to be the development of a tiered, *in vitro* neurotoxicity test strategy to measure toxicity at the cellular rather than the organismal level (Atterwill *et al.*, 1994; Coecke *et al.*, 2006). This would incorporate a battery of cell culture models and multidisciplinary measurable endpoints to more closely reconstruct the whole *in vivo* situation (Harry *et al.*, 1998). Such a stepwise approach progresses from a first-tier preliminary screening battery to differentiate neurotoxicants from cytotoxicants and rank chemicals for cytotoxic potency, to more defined mechanistic questions relating to the *in vivo* situation (Veronesi, 1992; Atterwill *et al.*, 1994).

A first-tier screening battery for differentiating cytotoxicants from neurotoxicants consists of a judicious collection of appropriate cell systems with neurospecific and non-specific endpoints, coupled with an analysis of the data produced. It is important to use a variety of cell culture models that closely mimic the intact nervous system both morphologically and biochemically, using general and neuron-specific endpoints to parallel cellular targets *in vivo* (Veronesi, 1992).

At the current stage, this tiered approach is not intended to replace existing *in vivo* testing, rather to provide a quick and inexpensive system for assessing the basic neurotoxic potential of many chemicals. Additionally, if incorporated at the earliest stage of the hazard identification process, these ideas have the potential to reduce the number of animals routinely used for testing, by identifying chemicals that have a high probability of neurotoxicity. The data provided by a preliminary neurotoxicity screen can then be incorporated into future chemical design, compound selection and direction

of animal based risk-assessment (Coecke *et al.*, 2006). The validation and inclusion of such neurotoxicity test methods into 'OECD Test Guidelines' will aid the ethical and economical testing of the 'existing' chemicals requiring classification prior to 2012.

1.4.3.2 Facilitating *in vitro/in vivo* extrapolations in neurotoxicity testing

In vivo, cellular toxicity depends on the specific sensitivity of the cell, the intracellular concentration of the test compound achieved and whether toxicity is due to the primary toxicant or an active metabolite (Harry *et al.*, 1998). Thus, when evaluating a compound *in vitro*, various factors can contribute to either an overestimation or underestimation of the extent to which it poses a neurotoxic risk to the living organism. Some of these factors and the steps that may be necessary to facilitate *in vitro* to *in vivo* extrapolation are considered below.

i) The origin of the cells utilised in the screening battery should be relevant for the exposed species *in vivo* and phenotypically reflect the *in vivo* situation both at the level of differentiation and markers expressed, as closely as possible.

ii) The nervous system is heterogeneous and *in vivo* nervous system function is dependent on the interaction between neuronal and non-neuronal cell types. Previously an advantage of cell culture was perceived as being the ability to obtain a culture enriched in one cell type and this is indeed useful for answering certain questions. However, such an isolated condition is an alien state for neuronal cells and it has been demonstrated in culture that often neurons survive poorly alone (Costa, 1998b). Similarly glial cells behave differently in an enriched culture. For example, cerebellar rat astrocytes cells show a flat undifferentiated morphology and proliferate rapidly when cultured alone but upon the addition of neurons, astrocytic cell growth is rapidly arrested and a stellate glial morphology similar to that of the *in vivo* situation is induced (Veronesi, 1992). Thus, an exciting development in tissue culture is the recognition of the necessity of specific cell interactions and the inclusion of integrated populations of cells to reflect the heterogeneous *in vivo* situation.

iii) In *in vitro* hazard assessment, the effects detected at the dose level applied to the cellular population (the external dose) must be related to the effects that would be

caused by the dose that actually reaches the target cells *in vivo* (internal dose). Several parameters affect *in vivo* bioavailability of a toxin to nervous system cells, including ability of toxin to cross the blood brain barrier (BBB), possible compromise of the BBB by the toxin and toxicokinetics affecting compound absorption, distribution, metabolism (including activation and detoxification of the compound) and excretion (ADME) (Veronesi, 1992; Combes, 2005). *In vitro* test systems lack normal methods for ADME, including the absence of a BBB and diminished or absent metabolic capacity. Therefore, it is important to assess the bioavailability and biokinetics of a substance, which may be done using *in vivo* knowledge of compound metabolism and *in silico* pharmacokinetic modelling (Combes, 2005; Coecke *et al.*, 2006). Additionally other types of cellular models have been proposed to address distinct questions which could be used synergistically with a tiered-test model (Veronesi, 1992). For example, cell-culture models have been developed which use endothelial, neuronal and astrocytic cells to functionally simulate BBB transport, in conjunction with flow conditions that mimic circulation and allow chemical delivery (Harry *et al.*, 1998; Parkinson *et al.*, 2003; Tahti *et al.*, 2003).

However, it should be remembered that when initially screening a compound, it is actually advantageous to examine the intrinsic toxicity of chemical in a controlled defined system without the complicating factors of many normal *in vivo* homeostatic mechanisms. Test chemicals dissolved in medium come into direct contact without filtration by the BBB, with minimal lipid:aqueous partitioning, with uniform toxic-exposure for a defined length of time and with no hepatic elimination influences (Harry *et al.*, 1998). Intrinsic neurotoxic hazard identification may be addressed using a first-tier preliminary screening battery with more defined questions relating to the *in vivo* situation being addressed at a later stage (Veronesi, 1992).

1.4.4 Endpoints proposed for inclusion in a neurotoxicity screening battery

Normal functioning of the nervous system requires that the many biochemical mechanisms that underlie nerve signal propagation operate properly, thus neurotoxicity can manifest as varying and multiple effects. High levels of toxicity typically result in lethal cell injury such as necrosis or apoptosis, whereas the mechanisms underlying

toxic effects of a compound are often the result of disruption to basic biochemical processes and specific molecular interactions. Thus, these two levels of toxicity should be involved in assembling a first-tier test battery to screen rapidly for neurotoxic potential. Therefore, *in vitro* neurotoxicity assessment often starts with a concentration-range finding study to identify the basal- and non-cytotoxic range, in order to then test for neurotoxic potential at lower concentrations using a multitude of biochemical and neurospecific endpoints (Veronesi, 1992; Coecke *et al.*, 2006).

1.4.4.1 Basal cytotoxicity

A reliable *in vitro* measure of basal cytotoxicity is essential for the integrated assessment of neurotoxic potential. It may be used to establish the toxin concentration at which a certain percentage of cell viability is affected (e.g. 25, 50 or 75 %) and also allows the estimation of the non-cytotoxic range (Eisenbrand *et al.*, 2002; Ba *et al.*, 2003).

1.4.4.2 Biochemical endpoints

Although they have limited ability to detect neural-specific effects, biochemical endpoints may be rapidly collected and quantified accurately. They provide vital information on the intrinsic toxicity of chemicals and must be included in the first-tier neurotoxicity screening battery to differentiate cytotoxicity from neurotoxicity. Alterations in cellular ion homeostasis and oxidative status are among the important general cellular functions whose impairment may cause severe brain damage after acute chemical exposure (Costa, 1998a; Ba *et al.*, 2003).

1.4.4.3 Neurospecific endpoints

Neurospecific endpoints are the most sensitive indicators of neurotoxic insult and their inclusion is recommended in the later stages of the test strategy. Neurospecific endpoints may include assays for expression of neuronal receptors and activity of neural enzymes such as glutamic acid decarboxylase and dopamine hydroxylase and astrocytic specific enzymes such as glutamine synthase. Morphological effects may be

examined by quantification of antibodies against neuronal and glial filaments and measurement of chemical effects on neurite outgrowth (Veronesi, 1992; Coecke *et al.*, 2006).

1.4.5 Cell cultures proposed for inclusion in a neurotoxicity screening battery

There are many *in vitro* culture systems now available including ex *in vivo* models such as brain tissue slices, enriched or mixed primary cultures of dissociated neurons and/or glia, secondary cultures such as suspension and re-aggregated brain cultures, as well as neuronal and glial cell lines (Atterwill *et al.*, 1994; Gartlon *et al.*, 2006).

The complexity of an *in vitro* neurotoxicity model inversely correlates with the ease of obtaining and maintaining cells. The more intact models are technically arduous and expensive and usually reserved for mechanistic studies, with more cost effective primary cells and cell lines being used in routine screens (Veronesi, 1992; Coecke *et al.*, 2006). The most widely used and extensively characterised primary cultures of neuronal or glial cells being investigated for screening of neurotoxic potential are rodent based systems, usually from foetal or embryonic animals. Particular examples are primary neuronal-glial cultures of rat cerebellar granule cells (CGCs), or rat cortical cultures which contain mature differentiated neurons and a minor amount of astrocytes and so are considered to be morphologically and functionally comparable to native neuronal tissue (Schmuck *et al.*, 2000; Coecke *et al.*, 2006).

To-date, primary cultures have been recommended predominately for use in *in vitro* testing systems. However, some cell lines have been investigated for their suitability for inclusion in a screening battery of cell systems. There are a number of advantages of using cell lines for high throughput screening. They are widely available, consistent and inexpensive to maintain, may be used to produce large quantities of homogeneous material and are easily monitored with a variety of cytotoxic or neurotoxic endpoints (Atterwill *et al.*, 1993).

Cell lines proposed to date include the naturally occurring neoplastic derivatives of many neuronal cell types in the CNS, including neuroblastomas (e.g. SK-N-SH, SK-

SY-5Y) and pheochromocytomas (e.g. PC12), each with some valid neurochemical features. Additionally, some may be induced to develop neurite extensions, with an immature cytoskeleton and a number of other neuronal characteristics such as electrical excitability, expression of neurotransmitter receptors and secretion of neurotransmitters (Harry *et al.*, 1998). For example, Nerve growth factor (NGF) causes rat-derived PC12 cells to reversibly differentiate into sympathetic-like neurons. However, most lack the morphology and neuritic claborations of mature post-mitotic neurons and differentiation following treatment with exogenous factors is fully reversible and does not reflect the terminally differentiated *in vivo* state (Harry *et al.*, 1998; Gartlon *et al.*, 2006).

1.4.5.1 Human cell advantages

The development of an *in vitro* neurotoxicity test system requires a reliable source of neuronal tissue. Various groups have proposed models using primarily rodent based cell lines and organotypic primary cultures of terminally differentiated neurons (Figiel and Fiedorowicz, 2002; Jimenez *et al.*, 2004). However, as previously discussed, human and animal neural tissues may differ greatly in their susceptibility to neurotoxins and the ability to use human cells in toxicology testing would obviate the need to undertake species extrapolation when assessing human hazard (Sanfeliu *et al.*, 1999). Thus, there is a huge demand in current biomedical research for growing human cells in culture systems and if human brain cells could be generated on a large scale *in vitro*, this would greatly assist the high throughput screening of novel and existing compounds for neurotoxic potential.

Primary human CNS cells and tissues represent a very attractive alternative to animal-derived material. However, obtaining and using such material is logistically difficult and unreliable, compounded by deterioration after death, inconsistency, infection risk and high costs and is thus not practical for routine neurotoxicity testing (Atterwill *et al.*, 1994; Sladowski *et al.*, 2005). Some of these problems may be circumvented by isolation of neurons from human embryonic spinal cord but there are ethical objections. Additionally, attempts to establish neuronal cultures from human foetal brain have not always been completely successful and the consistency and reproducibility of cultures

is problematic due to variability in source material. Primary cells also exhibit limited capacity for proliferation, therefore making it difficult to build up a continuous supply of identical material for neurotoxicity-screening (Sanfeliu *et al.*, 1999; Horrocks *et al.*, 2003).

A solution may be to develop and use more appropriate transformed human cell lines which can be phenotypically manipulated to form particular differentiated cell types and are ideally easily transferable, reproducible and applicable for high throughput screening. These cell lines may prove particularly useful in the development of models with more than one cellular target, for example an integrated population of neuronal and astrocytic cell lines.

1.4.5.2 Cell line alternatives to human tissue

There are a number of human CNS cell lines available but the optimal system for the identification of neurotoxic potential is one that most closely resembles the phenotype of concern. To be useful it is important that a cell line have a short doubling time so that it is possible to accumulate enough cells for experiments. However, the more rapidly a cell line proceeds through the cell cycle, the fewer neuronal features it will develop; possibly because many differentiated properties of neurons are not fully articulated *in vivo* until they become post-mitotic (Seeley *et al.*, 1998b). The use of human-derived neuroblastoma cell lines (e.g. SK-N-SH) in neurotoxicity testing is now well established. However, this rapidly dividing neuroblastoma cell line expresses fewer receptors and antigenic markers than fully differentiated human adult neurons (Pleasure *et al.*, 1992). Therefore, the ideal cell line for inclusion in a neurotoxicity test battery would be one that divides rapidly to provide large quantities of homogeneous cells and can then be induced with an agent to exit the cell cycle and undergo an irreversible commitment to a well-characterised neuronal phenotype. Ideally these cells would subsequently elaborate extensive neuritic processes and mature to a state similar to that of primary neurons in culture (Pleasure *et al.*, 1992).

Very few human cell lines can be induced to exhibit terminally-differentiated neuronal properties. However, embryonal carcinoma (EC) cell lines satisfy some of the above

criteria. Among these lines is the well characterized EC NT2.D1 cell line, which may be induced to differentiate *in vitro* into post-mitotic neurons that far more closely resemble human neurons than any other model currently in use (Pleasure *et al.*, 1992). This cell line is reported to follow a pattern of differential gene expression similar to that of neural precursors during neurogenesis and depending on the differentiation protocol, also has the capacity to differentiate into astrocytes (Bani-Yaghoub *et al.*, 1999) (see section 1.6).

1.5 Development of a preliminary screen for detecting potential neurotoxicity

As discussed, a first-tier screening battery for differentiating cytotoxicants from neurotoxicants should consist of a judicious collection of cell systems and biochemical and specific endpoints, with appraisal using a variety of test chemicals. Regarding the identification of potential human neurotoxins, an ideal cell system for inclusion in a screening battery would be human-derived and would reflect the vital *in vivo* neuronal-astrocytic relationships. The endpoints should be relevant to the potential toxic perturbations of the nervous system and measurement should be sensitive and rapid to meet the high throughput needs of the pharmaceutical industry and REACH strategy. The test chemicals should consist of known neurotoxins and cytotoxins and cover a range of latencies and potencies. Thus with consideration of these factors, it may be seen that a number of steps are required in the development of such a preliminary neurotoxicity screen.

1.6 Step 1: Selection of neuronal and astrocytic cell lines

The origin of the cells utilised in the screening battery should be relevant for the exposed species and phenotypically reflect the *in vivo* situation. The nervous system is heterogeneous and *in vivo* nervous system function is dependent on the interaction between neuronal and astrocytic cells. Therefore, the development of an *in vitro* cell system for the prediction of neurotoxicity in humans requires a reliable and integrateable source of both human neurons and astrocytes. As mentioned previously (section 1.4.5.2), the unsuitability of primary human CNS cultures for high-throughput compound screening may be addressed through the use of a human EC cell line that

can be induced to exhibit terminally differentiated neuronal properties. Therefore, the first step is to select suitable human cell lines for use in, and/or comparison with, a neuronal and astrocytic co-culture cell system.

1.6.1 Embryonal carcinoma (EC) cells

Differentiation is the process leading to the expression of phenotypic properties characteristic of the functionally mature cell *in vivo*. Pioneering work by Jones-Villeneuve *et al.*, (1982) first demonstrated that murine embryonal carcinoma (EC) cells differentiated in response to all-trans retinoic acid (RA), to form sub-populations of neurons and glial cells. Since then, RA has also been used to induce the formation of neural derivatives from human EC cells adapted to grow *in vitro*, in particular from sub-lines of the TERA-2 lineage, which proved an exception to the poor and ill-defined capacity for differentiation found for most human EC cells (Andrews *et al.*, 1984).

1.6.2 TERA-2 and NT2.D1 cell lines

The cell line TERA-2 was established in 1984 from a lung metastasis of a 22 year old Caucasian man with a primary testicular germ cell tumour. A xenograft of TERA-2 grown in nude mouse formed a tumour containing neural elements, pieces of which were explanted into tissue culture and the NTERA-2 (NT2) EC cell line established. The clones D1, B9 and D3 were then obtained, of which NT2.D1 has been the most widely used (Andrews, 1984; Andrews *et al.*, 1984). A striking feature of human germ cell tumours is the evident relationship of their EC cells to pleuripotent embryonic stem cells (Andrews, 1988).

1.6.3 Retinoic acid (RA) as an inducer of differentiation

Vitamin A and its derivatives are essential for both normal embryonic development and maintenance of differentiation in the adult organism (Ross *et al.*, 2000). There is strong evidence that endogenous retinoic acid (RA), a biologically active metabolite of vitamin A, plays an role important role in neuronal differentiation *in vivo* (Baldassarre *et al.*, 2000). RA is also commonly used *in vitro* as an inexpensive pharmacological

agent able to induce differentiation in a large array of tumour cell lines, as well as the expression of more than 300 proteins (Andrews, 1984; McCaffery and Drager, 2000). In particular, RA treatment of NT2.D1 cells induces growth arrest and terminal differentiation along the neuronal pathway, with accumulation of cells in the senescent G1/G0 phase beginning after 7-15 days (Baldassarre *et al.*, 2000). This is important as mature mammalian neurons lose the potential to proliferate as part of their differentiation programme *in vivo* (Lee and Andrews, 1986).

1.6.4 Differentiation into NT2 neuronal (NT2.N) cells

In culture, the pleuripotent NT2.D1 cell line shows little evidence of spontaneous differentiation but as mentioned above, this line can be differentiated extensively to cells resembling post-mitotic neurons, by growth in the presence of 1-10 μM RA for four weeks (Andrews, 1988). It is considered that neural differentiation of NT2.D1 cells parallels changes seen during cellular development in the embryonic neural tube (Horrocks *et al.*, 2003).

During RA treatment, adherent NT2.D1 cells are not sub-cultured and form dense multicellular layers, with a reduction in the number of dividing cells. A percentage of cells form terminally differentiated neurons while the remainder of the culture consists of unidentified differentiated cell types and residual undifferentiated EC cells (Andrews, 1984).

1.6.4.1 Purification of the neuronal culture

Pleasure *et al.*, (1992) introduced purification steps by way of a differential adhesion protocol, mechanical manipulation and the use of mitotic inhibitors to kill off undifferentiated cells, in order to isolate highly enriched cultures of post-mitotic neurons (NT2.N) from other contaminating non-neuronal cell types.

In this method, following RA treatment, the cells were detached and replated at a lower density to allow the release of NT2.N cells buried in the midst of many layers of cells. Following replating (replate #1), the NT2.N cells tended to form a loosely attached

layer on flat non-neuronal cells and were then mechanically dislodged, replated onto a poly-D-lysine and laminin (pdl/lam) coated surface (replate #2) and enriched with a combination of mitotic inhibitors for three weeks to eliminate any remaining dividing cells (Pleasure *et al.*, 1992). During mitotic inhibitor (MI) treatment the neuronal cells migrated to form aggregates and grew numerous neuritic processes that formed extensive networks covering the whole culture surface. Some neuritic processes bound together to form thick fascicles linking adjacent islands of neural perikarya. The enriched culture took on a morphologically differentiated neuronal appearance, almost indistinguishable from primary neuronal cultures obtained from rodents (Pleasure *et al.*, 1992; Younkin *et al.*, 1993). Following MI treatment, cells were maintained in normal medium and no increase in cell number was detected over three months. The cells were demonstrated to be incapable of cell division and thus deemed permanently post-mitotic (Pleasure *et al.*, 1992). Most other neuronal cell lines are incapable of terminal differentiation. Exogenously applied factors can arrest cell division and allow expression of differentiated characteristics (e.g. treatment of PC12 cells with neuronal growth factor) but removal usually results in re-entry into the cell cycle and return to undifferentiated state (Younkin *et al.*, 1993).

This 'Plating Method' is a lengthy (approximately 7 weeks) but straightforward procedure, and has been used successfully by a number of groups to yield a highly purified population of human post-mitotic neurons from rapidly dividing, pleuripotent, NT2.D1 EC cells (Younkin *et al.*, 1993; Leypoldt *et al.*, 2001; Marchal-Victorion *et al.*, 2003). These NT2.N cells develop morphological and cytoskeletal characteristics of post-mitotic CNS neurons, have a stable neuronal phenotype and can survive for up to three months in normal medium. When produced at weekly intervals, sufficient numbers of identical, terminally differentiated, post-mitotic, human neuron-like cells, can be readily generated for neurotoxicity screening (Pleasure *et al.*, 1992).

1.6.4.2 Neuronal characteristics expressed

While it is important to consider that transformed cell lines may not share the exact features of primary neural tissue, there is no evidence to date which suggests that human NTERA-2 derived neurons differentiate in an aberrant way and instead many of

their features are conserved (Horrocks *et al.*, 2003). Pleasure *et al.*, (1992) and other groups have characterised the NT2.N cells extensively and found them to express many key marker proteins typical of neurons *in vivo* and *in vitro*.

The marker proteins expressed include the well known neurofilament (NF) triplet proteins (Lee and Andrews, 1986), neuron-specific enolase (NSE) and β-tubulin III which is neuron-specific and does not identify the β-tubulin found in glial cells (Stewart *et al.*, 2003). NT2.N cells also express the 66 kDa NF protein abundant only in CNS neurons and neuronal nuclei (NeuN), a protein specifically localised in the nucleus of terminally differentiated CNS cells. However, they do not express peripherin which is found in nearly all PNS neurons, suggesting NT2.N cells correspond to CNS neurons (Pleasure *et al.*, 1992; Megiorni *et al.*, 2005).

NT2.N cells express several neuronal cytoskeleton microtubule-associated proteins (MAP), including MAP2 (essential for dendrite formation) and tau (essential for axon outgrowth) and also surface markers, including NCAM (neural cell adhesion molecule) and GAP43 (growth associated protein concentrated in neuronal growth cones) (Pleasure *et al.*, 1992). Additionally they express markers of secretory activity typical of neurons, including synaptophysin (marker for synaptic vesicles that store and release neurotransmitters) and chromogranin (vesicles involved in neuropeptide and catecholamine synthesis) (Pleasure *et al.*, 1992).

The neurotransmission repertoire of NT2.N cells *in vitro* includes, GABAergic, catecholaminergic, cholinergic and a smaller number of serotonergic phenotypes, along with the appropriate neurotransmitter enzymes (Guillemain *et al.*, 2000). Though their dopaminergic (DA) status is yet to be determined, NT2.N cells can be stimulated to release the neurotransmitter dopamine and have been observed to possess detectable markers typical of DA midbrain neurons. These include the dopamine transporter (DAT), dopamine receptor (D2) and the rate-limiting enzyme for dopamine synthesis, tyrosine hydroxylase (TH). Additionally, NT2.N cells were found to be Nurr1-positive, the nuclear receptor shown to be essential for the development, differentiation and maintenance of midbrain DA neurons (Misiuta *et al.*, 2003; Misiuta *et al.*, 2006).

Finally, NT2.N cells exhibit both N-methyl-D-aspartate (NMDA) and non-NMDA glutamate receptor channels, as well as tetrodotoxin-sensitive sodium ion channels and regenerative membrane channels. When in contact with astrocytes they form both glutamatergic excitatory and GABAergic inhibitory functional synapses and generate action potentials with nearly identical characteristics of primary neurons in the CNS (Hartley *et al.*, 1999; Horrocks *et al.*, 2003; Paquet-Durand *et al.*, 2003). Additionally, they express synapsin I, II, and III, which are implicated in the maturation of synapses (Misiuta *et al.*, 2006).

1.6.4.3 Previous utilisation of NT2.N cells

NT2.N cells have been shown to remain post-mitotic, retain their neuronal phenotype and survive for over a year *in vivo* when transplanted into rodent brain. Indeed, these cells are considered to so closely resemble human CNS neurons that they have been employed in numerous attempts to improve behavioural deficits by transplantation into the brains of human stroke victims (Kondziolka *et al.*, 2000; Nelson *et al.*, 2002). Additionally, NT2.N cells have been used extensively *in vitro* as a model system to study various aspects of Alzheimer's, Huntington's and Parkinson's diseases (Merrick *et al.*, 1997; Tamagno *et al.*, 2000; Lee *et al.*, 2002), hypoxic-ischemic brain injury (Almaas *et al.*, 2002; Garcia and Massieu, 2003), and embryonal CNS development (Bani-Yaghoub *et al.*, 1997).

There is some documented evidence of the use of NT2.N cells in *in vitro* neurotoxicity studies, such as the examination of glutamate excitotoxicity and protective effects of glutamate receptor antagonist MK-801 (Rootwelt *et al.*, 1998; Paquet-Durand *et al.*, 2006). Additionally, Wang *et al.*, (1998) and others have studied the sensitivity of NT2.N cells to exogenously applied hydrogen peroxide. However, since NT2.N cells present many of the characteristics of primary cultures of nerve cells, there exists the potential for their use in a novel cell system for inclusion in a test battery for the preliminary screening of potential neurotoxins.

1.6.5 Neuronal and astrocytic co-culture

Some of the differences in cell behaviour between cells *in vivo* and those *in vitro*, stem from the dissociation of cells from a three dimensional (3D) geometry, leading to loss of specific heterotypic cell interactions if only one cell type is represented in the culture. Indeed, the extreme heterogeneity of the nervous system makes neurotoxicity testing complex. However, an exciting development in tissue culture is the development of integrated populations of cells that reflect the *in vivo* state more closely. As such, the importance of astrocytic cells *in vivo* with regards to neuronal function and survival (section 1.3.2) makes it necessary to include these cells in *in vitro* investigations of neurotoxic potential and offers a greater degree of relevance to the human situation (Bronstein *et al.*, 1995).

Previously, attempts to co-culture neurons and astrocytes have utilized human primary cells (Sanfeliu *et al.*, 1999) or primary rat astrocytes (Sass *et al.*, 1993; Hartley *et al.*, 1999; Van den Pol and Spencer, 2000). However, if we take into account interspecies differences and the limitations of primary cells (section 1.4.5.1), the use of a human astrocyte cell line would be best suited to a system for human neurotoxicity testing.

Initially, it was intended to culture the NT2.N cells on a layer of CCF-STTG1 human astrocytoma cells in order to produce an integrated astrocytic-neuronal culture. However, the use of a continuous astrocytic cell line would have conferred the practical problem of differing division rates, with the astrocytic cells outgrowing the post-mitotic neurons so rapidly that they would not necessarily make the intimate astrocytic-neuronal connections required for a true co-culture. Analysis of the literature revealed that an alternative useful co-culture model incorporating post-mitotic NT2 astrocytic cells had been previously developed by Bani-Yaghoub *et al.*, (1999).

1.6.5.1 Differentiation of NT2.D1 cells into a NT2 neuronal and NT2 astrocytic co-culture

In the developing CNS, neurons and astrocytes are both formed from the proliferating neuroepithelial cells incorporated into the neural tube. The prenatal neurogenesis process (4-20 weeks in humans) is followed by the formation of astrocytes (beginning at the 19th week) (Przyborski *et al.*, 2000). Bani-Yaghoub *et al.*, (1999) demonstrated

that, similar to the *in vivo* situation, the pleuripotent NT2.D1 cell line may be induced to differentiate into neurons (NT2.N), followed by astrocytes (NT2.A), to give a mixed culture of post-mitotic neurons and astrocytes (NT2.N/A), thus alleviating practical problems related to differing division rates. This discovery gave credence to the notion that NT2.D1 human EC cells are similar to human embryonal stem cells that give rise to both neuronal and astrocytic lineages.

The differentiation procedure involves the use of a lower concentration of antiproliferative agents and a later developmental window, to yield aggregations of neuronal perikarya with linking bundles of neurites on the surface of an astrocytic monolayer (Bani-Yaghoub *et al.*, 1999; Stewart *et al.*, 2003). In mixed cultures, NT2.A cells appear to support the survival of NT2N cells. Several groups have observed that alone, NT2.N cells generally survive for 2-3 months in normal media, whereas mixed NT2.N/A cultures typically survive for 6-9 months, clearly demonstrating the importance of neuronal-astrocytic interactions for neuronal maintenance (Bani-Yaghoub *et al.*, 1999; Sandhu *et al.*, 2002; Stewart *et al.*, 2003).

1.6.5.2 Astrocytic characteristics expressed by NT2.A cells

Similar to NT2.N cells, NT2.A cells are arrested in the G0/G1 phase of the cell cycle (Sandhu *et al.*, 2002). NT2.A cells express GFAP and also S100β which is considered a marker of mature astrocytes in the CNS and have been demonstrated to communicate via gap junctions (Bani-Yaghoub *et al.*, 1999; Lu *et al.*, 2005).

The NMDA receptor is made up of four receptor sub-units of which NT2.N cells express low levels, whereas NT2.N in co-culture with NT2.A express all the sub-units at higher levels and their functionality has been confirmed using glutamate and calcium sensitive dyes. NT2.A have also been demonstrated to possess high affinity, functional, glutamate transporting proteins and to contain glutamine synthase, an enzyme involved in the breakdown of toxic intracellular glutamate to non-toxic glutamine (Sandhu *et al.*, 2003), with activity comparable with that of human foetal astrocytes (Lu *et al.*, 2005). NT2 neurons in mono-culture rarely form synapses and they have weak action potentials. However, NT2.N cells grown in co-culture with primary rodent astrocytes

form functional synapses (Hartley *et al.*, 1999). It has also been demonstrated that NT2.N cells form functional synapses in co-culture with NT2.A cells (Sandhu *et al.*, 2002).

1.6.5.3 Previous utilisation of NT2.N/A co-cultures

The above described combination of NT2.N and NT2.A cells has been used as a model of human neurogenesis (Marchal-Victorion *et al.*, 2003; Stewart *et al.*, 2003), to study astrocytic protection of neurons against glutamate excitotoxicity (Langlois and Duval, 1997; Sandhu *et al.*, 2003) and to examine chemokine production and function by cells in the CNS (Lu *et al.*, 2005). However, the advantages of its use in neurotoxicity testing has been largely overlooked, thus highlighting the potential use of the NT2.N/A co-culture in a novel, wholly human, post-mitotic, screening battery for the prediction of neurotoxicity.

1.6.5.4 CCF-STTG1 cell line

It was also considered desirable to examine the response of astrocytes to neurotoxic insult, without the presence of neurons. The production of pure NT2.A culture was not undertaken as there was little literature regarding this possibility available until the later stages of the study. Thus, the CCF-STTG1 cell line was employed for this purpose.

The human astrocytoma cell line CCF-STTG1, was established from a specimen of Grade IV astrocytoma from a 68-year-old Caucasian female. This cell line was chosen as the astrocyte-specific, intermediate-filament marker GFAP has been reported to be present in 70-80 % of CCF-STTG1 cells in culture (Barna *et al.*, 1985) and it has recently been employed in the study of Multiple Sclerosis (Lily *et al.*, 2004) and Alzheimer's Disease (Mentz *et al.*, 1999). Additionally, it has been successfully used to examine some mechanisms of neurotoxic insult which may be pertinent to astrocytes, including compromise of glutamate transport (Ye *et al.*, 1999) and apoptosis (Na *et al.*, 2001; Koo *et al.*, 2002).

1.7 Step 2: Comparison of the sensitivity of the cell lines

To properly evaluate neurotoxic potential, it is first necessary to employ a reliable method for quantification of the basal cytotoxicity of a compound. Thus, the second step is to compare the sensitivity of the selected cell cultures to toxic insult, using a measure of basal cytotoxicity after a chosen duration of acute exposure to a number of test chemicals, including known human neurotoxins and non-neurotoxins (for test chemicals see section 1.9).

1.7.1 Selection of a method for measuring basal cytotoxicity

Cytotoxicity is simply the general cell-killing property of a chemical, the term does not indicate a specific mechanism of cell death, it may refer to necrosis, apoptosis, or both and is simply dependent on exposure to a high enough concentration of chemical (Ba *et al.*, 2003). The starting point is often to establish the concentration of chemical at which 50 % of cell viability is affected (IC_{50}) after a selected time of exposure, making it possible to rapidly compare the quantitative response of a compound in different cell systems or several compounds in an individual system. Additionally, it allows the estimation of the No Observed Adverse Effect Level (NOAEL; highest concentration of toxin at which no decrease in cell viability is measurable) and thus the non-cytotoxic range at a particular timepoint.

The MTT reduction assay is one of the most widely used tests for the measurement of cytotoxicity and is based on the reduction of MTT (3-(4,5-dimethylthazol-2-yl)-2,5-diphenyl tetrazolium bromide) to give a spectrophotometrically quantifiable, blue formazan product. The MTT assay detects exclusively, living, metabolically active cells (Tada *et al.*, 1986). Since a cytotoxic factor will reduce the rate of MTT turnover by a cell population (see section 3.2.2), an MTT assay may be used as a convenient, quick, simple and inexpensive method to measure chemically induced cell death. Additionally, formazan production can exceed 100 % in treated cells, thought to reflect an increase in metabolic activity above that of control cultures (Putnam *et al.*, 2002).

1.8 Step 3: Biochemical effects at non-cytotoxic concentrations

The MTT reduction assay is really limited to providing information on the basal

cytotoxic potential of a compound over a range of concentrations. However, as mentioned above, it may be used to estimate the non-cytotoxic concentration-range for a compound. The final step is to use this concentration range to examine how a compound may affect different cell-types at concentrations that do not disrupt membrane integrity or cause cell death after a chosen duration of exposure. This process may incorporate the investigation of subtle biochemical changes and the cell-specificity of a compound is expected to be more apparent when not masked by overt cytotoxicity.

Each cell in a multicellular organism carries out numerous defined programmes (e.g. division, apoptosis, secretion of substances, metabolism of nutrients). To execute the programmes, cells are equipped with a number of biochemical mechanisms, including metabolic, transport and energy producing systems, as well as structural elements, organised into macromolecular complexes, cell membranes and organelles by which they maintain their internal functions and support other cells (Gregus and Klaassen, 2001; Gartlon *et al.*, 2006). Normal functioning of the nervous system requires that the many such biochemical mechanisms that underlie nerve signal propagation operate properly. Numerous toxicants interfere with such cellular functions and the resulting neurotoxicity can manifest as varying and multiple effects that may ultimately compromise cell survival (Gregus and Klaassen, 2001).

Mitochondria are at the crossroads of several biochemical activities that may have a crucial effect on cellular maintenance and due to the high glucose-metabolic demand of neurons, the nervous system is particularly susceptible to toxicants that disrupt mitochondrial function and metabolism. It has been hypothesised that three key mitochondrial related disorders are involved in apoptotic or necrotic neuronal cell death inflicted by toxins; an increase in intracellular calcium (Ca^{2+}) levels, an increase in intracellular reactive oxygen species (ROS) commensurate with impaired antioxidant function and a decrease in energy levels (Gregus and Klaassen, 2001; Gartlon *et al.*, 2006; Van Houten *et al.*, 2006). Therefore, mechanistic endpoints concerning changes to the energy and oxidative status of the cell have been recommended for inclusion in screening systems for detecting neurotoxicity (Costa, 1998b; Harry *et al.*, 1998; Gartlon *et al.*, 2006). Methods to measure changes in such biochemical parameters that

follow toxin exposure can be rapid and inexpensive to match needs of the pharmaceutical and chemical industries and in response to the REACH strategy (Sureda *et al.*, 1999).

In an effort to distinguish acute and chronic neurotoxicants and cytotoxicants and demonstrate the suitability of inclusion of an integrated population of neuronal and astrocytic cell-types in the screening system, the biochemical endpoints chosen for this study were; measurement of adenosine triphosphate (ATP) levels, measurement of hydrogen peroxide (H_2O_2) levels as an estimate of ROS production and cellular glutathione (GSH) content as an estimate of antioxidant levels. Additionally, the mode of cell death (apoptosis or necrosis) was also considered, with measurement of caspase-3 levels as an indicator of apoptosis. In the following sections, these endpoints are illustrated. In the study itself, toxin effects on cellular Ca^{2+} levels were not determined. However, as oxidative damage, aberrant calcium homeostasis and metabolic compromise interact with each other intimately and destructively in the brain and non-neural tissues (Ying, 1996), the effects of raised intracellular Ca^{2+} are also briefly considered (section 1.8.1.3.2).

1.8.1 Adenosine triphosphate (ATP)

Adenosine 5′-triphosphate (ATP), discovered in 1929 by Karl Lohman, is a multifunctional nucleotide present in all metabolically active cells and is the major source of intracellular energy storage and transfer (McLaughlin *et al.*, 1998). As mentioned earlier (section 1.2.1.1), the brain accounts for a disproportionately high consumption of energy in relation to its mass. The vast majority of brain ATP expenditure is devoted to neuronal excitatory signalling; including the active transport of ions necessary to re-establish the electrochemical gradients dissipated by action potential propagation and the generation, release and reuptake of neurotransmitters (Stryer, 1995). The remainder is utilised in numerous biosynthetic reactions, for the activation of endogenous compounds and is incorporated into co-factors and nucleic acids. It is required for polymerisation of the cytoskeleton, vesicular transport, axonal transport and cellular motility, division and morphology. ATP also drives essential ion transporters such as Na^+,K^+-ATPase and Ca^{2+}-ATPase (Gregus and Klaassen, 2001)

and is considered an important mediator in neuronal–glial communications and glial–glial signalling (North and Verkhratsky, 2006). No more than 5 % of ATP usage is attributed to glial function (Pellerin and Magistretti, 2003; Massicotte *et al.*, 2005). Due to the high dependence on ATP for normal CNS function, energy failure has been implicated in the neurotoxic effects of a number of compounds (Marini and Nowak, 2000; Gabryel *et al.*, 2002).

1.8.1.1 ATP production in the CNS

The majority of the normal CNS energy requirement comes from oxidative metabolism of glucose to water and carbon dioxide (CO_2), resulting in the generation of 38 molecules of ATP for each molecule of glucose (Gabryel *et al.*, 2002; Seyfried and Mukherjee, 2005). The glucose transporter, GLUT-1, is enriched in brain capillary endothelial cells and mediates the facilitated diffusion of glucose through the blood brain barrier (Seyfried and Mukherjee, 2005). Chemical energy is released by the hydrolysis of ATP to adenosine di- or mono-phosphate (Gregus and Klaassen, 2001).

The overall process of oxidizing glucose to CO_2 and water is known as cellular respiration, which includes three main pathways; glycolysis, the tricarboxylic acid (TCA) cycle (also known as the Krebs cycle) and oxidative phosphorylation (Brookes *et al.*, 2004). Glycolysis is an anaerobic process whereby glucose is metabolized to pyruvate in the cytosol, generating two net molecules of ATP. Pyruvate is a cytosolic antioxidant and an important substrate for the TCA cycle (Sharma *et al.*, 2003). Two molecules of hydronicotinamide-adenine dinucleotide (NADH) are also produced, which can be oxidized via the electron transport chain (ETC) and result in the generation of additional ATP by the protein complex ATP synthase (Gregus and Klaassen, 2001).

Pyruvate enters the mitochondria of neurons and glia and is converted to acetyl-CoA, which is fully oxidized to carbon dioxide by the TCA cycle. Every "turn" of the TCA cycle produces two molecules of carbon dioxide, one molecule of the ATP equivalent guanosine triphosphate (GTP), three molecules of NADH, and one molecule of dihydroflavine-adenine dinucleotide ($FADH_2$), both of which are energy-rich electron

donors (Stryer, 1995).

Oxidative phosphorylation is the terminal process of cellular respiration in eukaryotes; involving the passage of electrons from NADH or $FADH_2$ through the electron transport chain to molecular oxygen, which is reduced to water. These redox reactions are coupled to the creation of a proton gradient across the mitochondrial inner membrane using respiratory hydrogen (H^+) pumps, with the electrochemical energy of this gradient then used to drive ATP synthesis by ATP synthase. The oxidation of an NADH molecule results in the synthesis of on average three ATP molecules and the oxidation of one $FADH_2$ yields approximately two ATP molecules (Stryer, 1995).

1.8.1.2 Problems due to ATP depletion

Cell health is highly dependent on the production and utilisation of ATP and mitochondrial synthesis of ATP is essential to maintenance of normal neuronal and astrocytic function (Massicotte *et al.*, 2005). Chemicals may compromise mitochondrial ATP synthesis in several ways. These may involve inhibition of TCA cycle components, interference with delivery of hydrogen (in the form of NADH or $FADH_2$) to the electron transport chain, inhibition of electron transport or delivery of oxygen to the terminal electron transporter, the inhibition of the activity of ATP synthase, or general mitochondrial injury (McLaughlin *et al.*, 1998; Seyfried and Mukherjee, 2005). Alterations in mitochondrial integrity and ATP depletion in neuronal cultures following exposure to neurotoxic compounds frequently occur earlier than effects on membrane permeability (Massicotte *et al.*, 2005).

1.8.1.3 Interplay between reactive oxygen species, calcium and ATP

Oxidative damage, aberrant calcium (Ca^{2+}) homeostasis and metabolic compromise interact with each other intimately, forming a deleterious network which is important regarding cell viability in both neural and non-neural tissues (Ying, 1996). This interplay between reactive oxygen species (ROS), Ca^{2+} and ATP is discussed in more detail in the following sections.

1.8.1.3.1 Reactive oxygen species

During mitochondrial oxidative phosphorylation, the stepwise reduction of oxygen (O_2) proceeds via several reactive oxygen species ($O_2 \rightarrow O_2^{-\bullet} \rightarrow H_2O_2 \rightarrow {}^{\bullet}OH \rightarrow H_2O$) which have an essential role in redox signalling but can damage cellular components such as proteins, lipids and DNA if produced in excess (Brookes *et al.*, 2004). When mitochondria are damaged and the electron transport chain is compromised, more oxygen reacts at inappropriate points in the chain, leading to increased superoxide radical anion ($O_2^{-\bullet}$) formation (Gregus and Klaassen, 2001; Brookes *et al.*, 2004). Superoxide dismutase should normally convert this into hydrogen peroxide (H_2O_2) and catalase and glutathione peroxidase should clear H_2O_2 to water (H_2O). However, in times of stress antioxidant function can become overwhelmed and H_2O_2 can react with metal ions to create hydroxyl radicals (${}^{\bullet}OH$) that react and damage proteins, lipids and membranes. ROS may inactivate thiol dependent Ca^{2+} pumps and inhibit transporters and enzymes, including those involved in energy metabolism (Gregus and Klaassen, 2001) (see also section 1.8.2.2).

1.8.1.3.2 Calcium homeostasis

Intracellular Ca^{2+} levels are highly regulated and are maintained by the impermeability of the plasma membrane to Ca^{2+}. Transport processes remove Ca^{2+} from the cytoplasm, either by extracellular clearance or sequestration in the endoplasmic reticulum and mitochondria. Toxicants may induce elevation of Ca^{2+} levels by inducing leakage from storage organelles, damage to the plasma membrane promoting its extracellular influx, or inhibition of efflux through inhibition of Ca^{2+} transporters or depletion of the ATP driving force (Gregus and Klaassen, 2001).

Excess Ca^{2+} can also lead to the disassociation of microfilaments leading to plasma membrane blebbing that predisposes the membrane to rupture and activation of Ca^{2+} dependent hydrolytic enzymes that degrade proteins, phospholipids and nucleic acids, leading to necrosis or activation of apoptotic cell death (McCarthy *et al.*, 2004). Additionally, activation of Ca^{2+} dependent phospholipase A2 results in the release of various fatty acid species which are metabolised by lipoxygenases or cyclooxygenases

with concomitant generation of ROS (Nicotera and Orrenius, 1998).

A primary role of mitochondrial Ca^{2+} is stimulation of oxidative phosphorylation. Activation of the dehydrogenases in the TCA cycle by elevated mitochondrial Ca^{2+} accelerates hydrogen output from the TCA cycle and in turn, the flux of electrons along the electron transport chain (Brookes *et al.*, 2004), which increases the generation of $O_2^{-\bullet}$ (Gregus and Klaassen, 2001). Additionally, excessive mitochondrial Ca^{2+} uptake can dissipate the mitochondrial membrane potential and inhibit ATP-synthase, increase ATP consumption by Ca^{2+}-ATPases working to eliminate excess Ca^{2+}, or lead to injury to the mitochondrial inner membrane and impairment of ATP synthesis (Gregus and Klaassen, 2001).

1.8.1.4 Necrosis-Apoptosis switch

It is thought that cellular ATP content is the key determinant in the selection between apoptosis and necrosis as some ATP dependent steps are necessarily involved in the execution of apoptosis, including caspase and endonuclease activation (Saito *et al.*, 2006). Thus, mitochondria are believed to constitute a switch between a necrotic or apoptotic mode of cell death (Gregus and Klaassen, 2001). If toxin exposure causes sudden breakdown of the mitochondrial transmembrane gradient (see section 1.8.1.1), then intracellular energy deficiency is so severe that the main functions of life are stopped leading to necrosis. However, if the cell is able to partly maintain ATP levels, the apoptosis process is commenced (Gabryel *et al.*, 2002).

1.8.1.5 Astrocytic glycolysis

In animals, lactate is constantly produced from pyruvate via the enzyme lactate dehydrogenase (LDH) in a process of fermentation during normal metabolism and exercise. In this process, glycolysis occurs normally, producing two molecules each of ATP, NADH and pyruvate. The pyruvate is then metabolised to lactate rather than being utilised in the TCA cycle (Gregus and Klaassen, 2001).

Oxidative metabolism is the preferred method of pyruvate breakdown from glycolysis

as it is much more efficient than fermentation. Indeed, in the CNS, only about 13% of glycolytic pyruvate is converted to lactate under normal conditions (Massicotte et al., 2005; Seyfried and Mukherjee, 2005). However if there is a drop in cellular ATP due to the inhibition of oxidative metabolism by mitochondrial toxins, it is postulated that astrocytes but not neurons can respond with an increase in glycolytic activity, glucose consumption and lactate production to supplement ATP levels (Almeida *et al.*, 2001). Thus, it is considered that generally astrocytes will demonstrate less vulnerability to mitochondrial toxins than will neurons (Almeida *et al.*, 2001; Pellerin and Magistretti, 2003) and that if energy levels of astrocytes can be preserved then cellular defence mechanisms may reverse or impede injury to brain cells caused by ROS release from ATP depleted cells (Sharma *et al.*, 2003).

1.8.2 Reactive oxygen species and oxidative stress

Highly reactive oxygen species (ROS) are formed as a natural consequence of a variety of essential biochemical reactions. Oxidative stress is defined as a disturbance in the oxidant-antioxidant balance in favour of oxidative species, which can severely compromise cellular function, culminating in cell death by necrosis or apoptosis (Dringen, 2000; Saito *et al.*, 2006). It may be caused by an increased production of ROS and/or a decrease in antioxidant capacity (Dringen *et al.*, 2000).

ROS include non-organic molecules, such as singlet oxygen, $O_2^{-\bullet}$, H_2O_2 and $^{\bullet}OH$, as well as organic molecules such as alkoxyl and peroxyl radicals (Dringen *et al.*, 2000). Of these, only H_2O_2 has a long half-life and is highly membrane permeable, allowing it to accumulate in the medium during cell culture (O'Donnell *et al.*, 1987).

1.8.2.1 Mitochondria as a source of reactive oxygen species

There are many potential cellular sources of endogenous ROS production. However, the bioenergetic properties of mitochondria, in combination with their high rate of oxygen turnover and large iron stores, render these organelles a major source of oxidative species (Nohl *et al.*, 2003; Erel, 2005). ROS are generated continuously during aerobic metabolism (Cardoso *et al.*, 2004), with the majority of ROS being

produced in the mitochondrial electron transport chain (ETC), since 90 % of the body's oxygen consumption is reduced to water during this process (Ji, 1999).

A significant portion of electrons may escape the ETC and NADH-ubiquinone reductase (complex 1) and ubiquinone-cytochrome-c reductase (complex 3) of the ETC are well known sites of $O_2^{\bullet-}$ generation (Van Houten *et al.*, 2006). $O_2^{-\bullet}$ may in turn generate H_2O_2, spontaneously or through reduction by mitochondrial superoxide dismutase (SOD) (McCarthy *et al.*, 2004). Following this, an iron catalysed Fenton or Haber-Weiss reaction may give rise to $^{\bullet}OH$ (Ji, 1999).

1.8.2.2 Damage caused by reactive oxygen species

Cellular production of oxygen-derived free radicals is a normal part of physiological function. Intracellular ROS generation serves mainly for host defence against infectious agents and for redox-sensitive signal transduction (Kopprasch *et al.*, 2003). However, ROS have a strong tendency to abstract electrons to reach a more chemically stable structure and are therefore capable of eliciting oxidative damage to various cellular components when produced in excess (Ji, 1999). Indeed, mitochondrial derived ROS have been frequently implicated in the pathogenic mechanism of a number of diseases and disorders; including, aging, neurodegenerative disorders such as Parkinson's and Alzheimer's diseases, cancer, ischemic injury and cytotoxicity induced by xenobiotics (Iwata-Ichikawa *et al.*, 1999; McCarthy *et al.*, 2004). Oxidative stress has been implicated as being involved in both the apoptotic and necrotic modes of cell death (McCarthy *et al.*, 2004).

It is estimated that a normal cell produces 3.3×10^{-14} moles of H_2O_2 and $O_2^{-\bullet}$ a day (Ji, 1999). The superoxide anion has limited toxic effects alone but can dismutate into H_2O_2 that is normally degraded in the mitochondria. However, at times of antioxidant depletion or excess ROS production, H_2O_2 can in turn form the highly reactive hydroxyl radical ($^{\bullet}OH$) (Van Houten *et al.*, 2006).

Hydroxide ($^{\bullet}OH$) is the major damaging radical with an extremely short half-life. Once produced it rapidly attacks polyunsaturated fatty acids by hydrogen abstraction to

initiate lipid peroxidation. ROS are also capable of causing DNA strand breaks and both structural and functional modification of carbohydrates and proteins, including inhibition of transporters and enzymes (Gregus and Klaassen, 2001), such as those involved in energy metabolism (Ying, 1996) (see section 1.8.1.3). In turn, lipid peroxidation leads to the generation of a variety of reactive toxicants capable of damaging macromolecules, such as the lipid peroxyl and alkoxyl radicals (Ferraris *et al.*, 2002). ROS alteration of the phospholipid structure in the mitochondrial membrane may compromise the functionality of the electron transport chain leading to energy failure, or may cause cytochrome-c (cyt-c) release into the cytosol leading to caspase activation and apoptosis (Cardoso *et al.*, 2004).

1.8.2.3 Vulnerability of the brain to oxidative stress

Nervous tissue is especially vulnerable to oxidative stress due to the high rate of oxygen consumption, relatively low levels of antioxidant defences compared with liver or kidney and a high content of polyunsaturated fatty acids and iron (Dringen, 2000; Cardoso *et al.*, 2004). In addition, the loss of neurons in adult brain cannot generally be compensated by generation of new ones (Dringen *et al.*, 2000).

1.8.2.4 Protection of the nervous system against reactive oxygen species

Nervous system cells *in vivo* and *in vitro* must cope with the effect of reactive oxygen species generated by aerobic metabolism, or due to xenobiotics and other conditions. Therefore, neurons and astrocytes possess mechanisms that remove, or prevent the generation of ROS (see also section 1.8.3.2). In general, glial cells are more resistant than neurons to oxidative stress and play an important role in antioxidant defence mechanisms of the nervous system (Iwata-Ichikawa *et al.*, 1999). In neuron-astrocytic co-culture systems, astrocytes protect neuronal cells against H_2O_2 toxicity by maintaining neuronal GSH levels, by scavenging free radicals and perhaps also through pyruvate release (Iwata-Ichikawa *et al.*, 1999).

1.8.2.4.1 Pyruvate

The cytoplasmic enzymes catalase and glutathione peroxidase, can eliminate membrane permeable H_2O_2 intracellularly. However, extracellular H_2O_2 will be reduced to $^{\bullet}OH$ if not scavenged immediately (O'Donnell *et al.*, 1987). In this situation, pyruvate can contribute to the defence against H_2O_2 induced cytotoxicity by reacting non-enzymatically with the peroxide to liberate carbon dioxide, water and acetate (Desagher *et al.*, 1997). It has been suggested that pyruvate is a neuroprotective factor released from astrocytes (Shimizu *et al.*, 2004). Additionally, many cell culture media formulations include sodium pyruvate in addition to glucose, following the observation that pyruvate promotes cell survival, serving as an additional energy substrate and an extracellular H_2O_2 scavenger (O'Donnell *et al.*, 1987; Wang and Cynader, 2001).

1.8.3 Glutathione

In 1888, de Rey Pailhade discovered the substance 'hydrogénant le soufre', later determined by F. G. Hopkins in 1929 to be the sulfhydryl tripeptide glutathione (GSH), synthesised from L-glutamate, L-cysteine and glycine (Sies, 1999) (figure 1.1). Glutathione is a major cellular antioxidant, present at millimolar concentrations within most mammalian cells, including those of the brain and as such plays an important neuroprotective role (Clarke *et al.*, 1996).

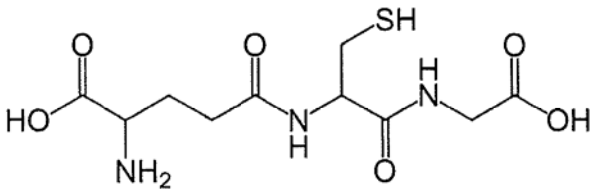

Figure 1.1 The structure of glutathione showing the thiol group (SH).

The functional importance of GSH lies in the presence of the thiol group (SH) on the cysteinyl residue which enables it to serve as both a reductant and a nucleophile (see figure 1.2, adapted from Wang and Ballatori, 1998). Along with reacting non-enzymatically with radicals, GSH is a substrate of glutathione peroxidase, and maintains intracellular, sulfhydryl-containing proteins in the reduced and active form through either thiol-disulfide exchange reactions or reduction of toxic peroxides

(Wullner *et al.*, 1999; Schuliga *et al.*, 2002). As a nucleophile, GSH functions as a substrate of glutathione-S-transferase to convert electrophilic centres of various potentially toxic compounds to thioether bonds, with the resulting conjugates being exported from the cell (Wang and Ballatori, 1998). Thus the activities of GSH facilitate the detoxification of xenobiotics and both endogenous and exogenously produced ROS, along with repair of damage induced by oxidative stress and continued efficient membrane function (Schuliga *et al.*, 2002; Takuma *et al.*, 2004).

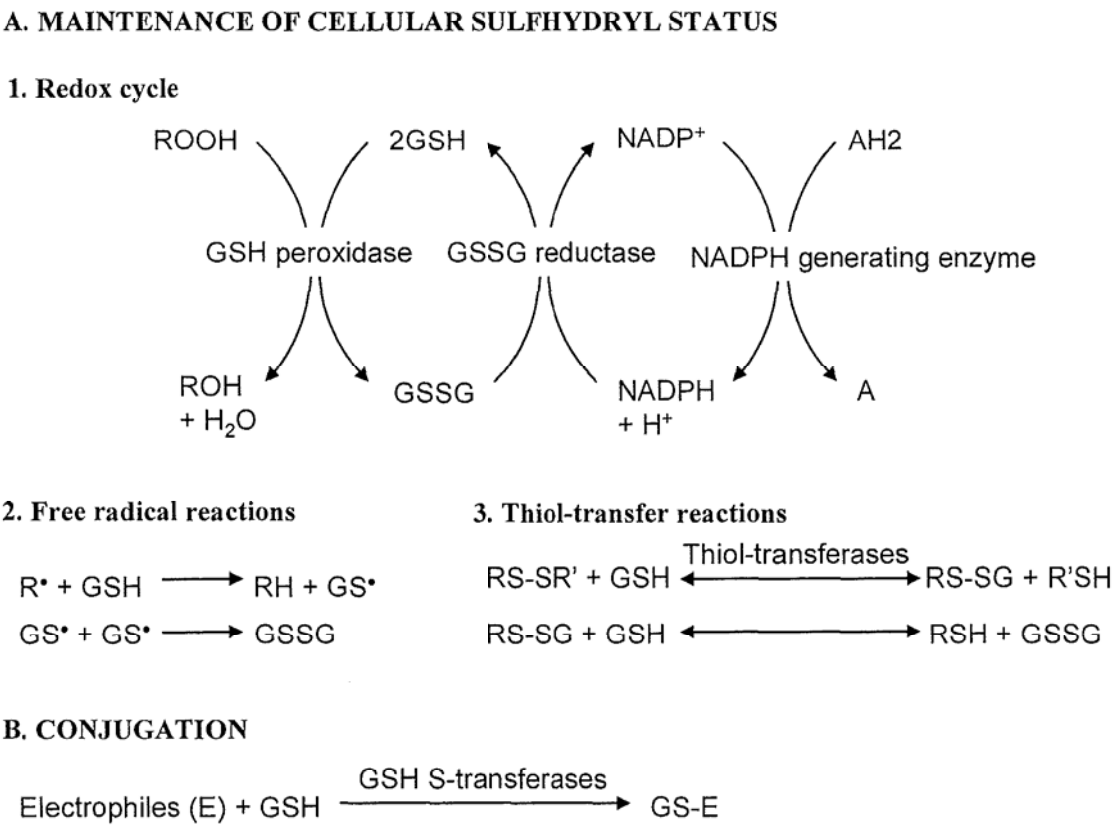

Figure 1.2 The detoxification functions of glutathione include the conjugation of electrophilic chemicals and maintenance of the cellular thiol redox status. AH2 and A are the reduced and oxidized forms respectively of compounds that participate in the synthesis of NADPH. RH and R are the reduced and oxidized forms respectively of some organic molecules. ROOH (hydroperoxide), ROH (alcohol), RS-SG (GSH thioester) and RS-SR' (mixed organic disulfide).

GSH is synthesised by the ATP-dependent enzymes glutamate-cysteine ligase and GSH synthetase and is present inside cells mainly in the reduced form. Oxidation leads to the formation of glutathione disulphide (GSSG) (Gegg *et al.*, 2003), which is recycled to the reduced form by glutathione reductase (GSR) using NADH as an electron donor

(Fujii *et al.*, 2003). In contrast, GSH is consumed during the generation of glutathione-S-conjugates by glutathione-S-transferases, thus lowering cellular glutathione levels. As an imbalance between rates of ROS production and antioxidant capacity results in oxidative stress, GSH consumed must be replaced via resynthesis from its constituent amino acids to maintain sufficient concentration of the antioxidant (Dringen *et al.*, 2000).

1.8.3.1 Role of glutathione in the brain

In mammalian cells, reactive oxygen species are generated continuously during aerobic metabolism and oxidative stress has been postulated to play a role in the action of various neurotoxins and neurodegenerative processes (Dringen *et al.*, 1999a). Due to the high oxygen consumption of the brain and the prevalence of polyunsaturated fatty acids, this organ must be well protected from oxidative damage (Watts *et al.*, 2005). In order to avoid damage such as lipid peroxidation and protein modification, the brain has developed an effective antioxidant system which disposes of, or prevents the generation of ROS (Makar *et al.*, 1994; Dringen, 2000). There is much evidence that glutathione plays a major role in this system and also in the conjugation of xenobiotics. Therefore, the determination of effects on cellular GSH protective capacity is an important endpoint in *in vitro* studies of neurotoxicity (Clarke *et al.*, 1996; Dringen *et al.*, 1999a).

Glutathione is present in high concentrations (1-3 mM) in human brain cells (Sagara *et al.*, 1996; Iwata-Ichikawa *et al.*, 1999) and the enzymes for its synthesis, catalysis of interconversion of GSH and GSSG and formation of GS-conjugates are all present in brain (Makar *et al.*, 1994). Virtually the entire glutathione pool in the brain cell is composed entirely of GSH with little GSSG (< 1 %) (Sagara *et al.*, 1996). Studies suggest that GSH in the CNS is more concentrated in astrocytes and they also possess high levels of GSH synthesising capacity, which might protect surrounding neurons that are poorer in GSH, against oxidative insults (Sagara *et al.*, 1996; Takuma *et al.*, 2004).

1.8.3.2 Response of astrocytes and neurons to hydrogen peroxide

Agents that deplete GSH will indirectly increase ROS levels and may induce cell death but it should be noted that the glutathione system is only part of the cellular defence system against ROS. As well as superoxide dismutase and catalase, exogenous antioxidants such as ascorbate and α-tocopherol, are also involved in ROS detoxification (Dringen, 2000). However, it is catalase and glutathione peroxidase (GPx) which are responsible for the enzymatic clearance of hydrogen peroxide, that is generated continuously in brain cells (Desagher *et al.*, 1996; Dringen, 2000).

H_2O_2 has been found to cause apoptotic cell death or necrosis of cultured neurons and to a lesser extent in cultured astrocytes. This may be due to the lower concentrations of GSH found in neurons compared with astrocytic cells (Wullner *et al.*, 1999) and GPx activity is also up to 4.5 times higher in astrocytes than neurons (Desagher *et al.*, 1996).

As H_2O_2 is the peroxide generated in the highest quantity in the brain, the protection by astrocytes of neurons against toxicity caused by it are an important consideration (Dringen *et al.*, 1999b). In enriched primary murine brain cultures even at a cellular ratio of 1:20 astrocytic:neuronal cells, a significant protection against H_2O_2 toxicity towards neurons was observed. However, the protective function of astrocytes was found to diminish when these cells were depleted of glutathione (Drukarch *et al.*, 1997). The ability of astroglial cells to protect neurons against H_2O_2 is considered to be related predominantly to the capacity of these cells to remove the peroxide using GSH as a substrate of glutathione peroxidase. Thus the enhanced H_2O_2 toxicity in GSH-depleted astrocytes is deemed most likely to be due to reduced availability of GSH substrate for GPx (Desagher *et al.*, 1996) but may also be in part due to the release of pyruvate from astroglial cells (Desagher *et al.*, 1997).

1.8.3.3 Support of neuronal GSH synthesis by astrocytes

There is evidence that an intensive metabolic exchange occurs between astrocytes and neurons which is important regarding the maintenance of optimal neuronal thiol status and protection of the brain against oxidative stress (Dringen *et al.*, 1999b; Dringen, 2000). Although, as mentioned above, glutathione is present at millimolar levels in both neurons and astrocytes, generally, astrocytes have a more efficient GSH synthesis systems and higher levels of GSH compared with neurons both *in vivo* and in

culture (Watts *et al.*, 2005). Indeed, primary murine neurons co-cultured with astrocytes approximately double their GSH concentration and are thought to be dependent on neighbouring astrocytes for maintenance of their GSH level via provision of cysteine, the rate-limiting substrate for GSH synthesis (Drukarch *et al.*, 1997; Gegg *et al.*, 2003).

The capacity of cells to maintain or even increase glutathione levels during a xenobiotic or oxidative challenge is important in the prevention of cell dysfunction and death (Dringen *et al.*, 2000). It has been suggested that transcriptional up-regulation of glutathione synthesis in astrocytes appears to mediate astrocytic resistance against oxidative stress, and enables astrocytes to protect neurons (Iwata-Ichikawa *et al.*, 1999). The importance of the function of astrocytic GSH metabolism that is evident at least for cell culture models, suggests that *in vivo* a compromised glutathione system may contribute to a lower defence capacity of the brain against ROS.

1.8.4 Apoptosis and necrosis

Cell death is conventionally classified as being apoptotic or necrotic, with both evolving as a sequence of structural events (Martin *et al.*, 1998) but which differ morphologically and biochemically (Ankarcrona *et al.*, 1995). Typically necrosis refers to rapid cell lysis (within 8 hours) in a process damaging to other cells, whereas apoptosis has been considered as a slower progression towards cell death (8-48 hours) and is less lethal to surrounding cells (Del Rio and Velez-Pardo, 2002).

Many xenobiotics can elicit apoptosis and/or necrosis in several cell types - including neurons - depending on the severity and nature of the insult. In general, toxicants tend to cause apoptosis at low levels and necrosis at higher levels (Ankarcrona *et al.*, 1995; Martin *et al.*, 1998). The modes of cell death may involve similar metabolic disturbances (Ca^{2+} overload, generation of ROS, depletion of antioxidants and ATP; section 1.8.1.3) and it is likely that cell death may take the form of necrosis if these processes are abrupt but apoptosis if they are protracted. Additionally, as discussed (section 1.8.1.4), availability of ATP may influence mode of cell death (Gregus and Klaassen, 2001). Whilst the distinction between the two types of cell death is obvious in certain cell systems, in others there is a co-existence of necrotic and apoptotic

cells, making it difficult to determine the predominant mechanism of cell death (Ankarcrona *et al.*, 1995).

1.8.4.1 Characteristics and causes of necrosis

Necrosis is a passive process of cell death characterised by cell and organelle swelling, with membrane rupture at an early phase of cell death, leading to release of intracellular debris that triggers an inflammatory reaction and injury to surrounding tissue (Ankarcrona *et al.*, 1995; McConkey, 1998). The cell dies as toxic insult causes overwhelming metabolic injury leading to huge perturbations in mitochondrial function, ion homeostasis, membrane permeability and cell volume (Martin *et al.*, 1998; Saito *et al.*, 2006). Degenerative processes such as oxidative and hydrolytic degradation of macromolecules and membranes, as well as disintegration of intracellular volume homeostasis, go to completion. This causes complete failure in cell structure maintenance and function, culminating in osmotic influx of water, swelling and cell lysis (Gregus and Klaassen, 2001).

1.8.4.2 Characteristics of apoptosis

The toxic chemicals that adversely affect cellular energy metabolism, Ca^{2+} homeostasis, redox state and ultimately cause necrosis, may also initiate apoptosis at an earlier stage of metabolic injury, which counteracts the progression of the toxic injury by preventing the consequential inflammatory response of necrosis. The term 'apoptosis' was originally proposed by Kerr *et al.,* (1972). It describes a pattern of morphological alterations associated with normal programmed cell death that occurs during embryonal development and facilitates the removal of extra, aged or damaged cells throughout life (Griffioen *et al.*, 2004). It has also been observed to be a feature of neuronal death occurring in both acute and chronic neurodegenerative disease such as Alzheimer's and Parkinson's diseases (Pong *et al.*, 2001; Kerr, 2002) and may be influenced by external inducers such as radiation and toxin exposure (Andersson *et al.*, 2000).

Apoptosis is an active and regulated process whereby the cell triggers special

metabolic, signal transduction and gene regulation pathways that systematically shut down the cell and disassemble its components. While the necrotic cell swells and lyses, the apoptotic cell shrinks, with loss of contact with neighbouring cells and compaction of nuclear and cytoplasmic materials (Verdaguer *et al.*, 2002; Griffioen *et al.*, 2004). Membrane enclosed particles containing intracellular material are produced ('apoptotic bodies') and are then sequestered in vivo by phagocytic cells, preventing inflammation and damage to nearby cells (McConkey, 1998; Ochu *et al.*, 1998). Morphologically, apoptosis usually leads to the formation of diagnostic oligonucleosomal DNA fragments (DNA ladders) (McConkey, 1998).

1.8.4.3 Induction and execution of apoptosis

1.8.4.3.1 Cytochrome c

Mitochondria are key mediators of apoptosis. Early in apoptosis, the essential electron transport chain intermediate cytochrome c (cyt-c) is released from the mitochondria into the cytosol where it initiates an irreversible cascade that activates programmed cell death (Pong *et al.*, 2001; Griffioen *et al.*, 2004). Once in the cytosol cyt-c forms a complex with apoptotic protease-activating factor-1 (Apaf-1), in a dATP or ATP dependent fashion and promotes a conformational change that allows procaspase-9 to join the complex, termed the 'apoptosome'. The structural alterations that follow caspase-9 binding result in its proteolytic cleavage via a mechanism that requires ATP hydrolysis, and once activated, caspase-9 can proteolytically activate other caspases (McConkey, 1998) (see below).

1.8.4.3.2 Caspases

The central component of the apoptosis machinery is a proteolytic system involving a family of cysteine dependent, aspartate directed, proteases called caspases (Del Rio and Velez-Pardo, 2002). Some caspases are necessary for the initiation of the apoptotic programme (including caspase-2, -8, -9 and -10), whilst others are critical for the execution of that programme (including caspase-3, -6, and -7) (Brecht *et al.*, 2001). Caspases are synthesised as inactive procaspases that are activated autocatalytically or by other proteases (Edelstein *et al.*, 1999; Andersson *et al.*, 2000). Activation of

initiator caspases causes cleavage of effector caspases, leading to amplification of the death signal via a caspase cascade (Belizario *et al.*, 2001; Nelson *et al.*, 2002), the overall function of which is to arrest the cell cycle, inactivate DNA repair and apoptosis inhibitors and dismantle the cytoskeleton (Hu, 2003; Jurkiewicz *et al.*, 2004).

1.8.4.3.3 Caspase-3

Among the caspases, caspase-3 has been implicated as a key executor protease that is activated during the early stages of apoptosis and effectively controls apoptosis (Verdaguer *et al.*, 2002; Hu, 2003). In the apoptotic cascade, once procaspase-9 is cleaved and activated, it subsequently initiates cleavage and activation of caspase-3 (Cardoso *et al.*, 2002). Once activated, caspase-3 proteolytically cleaves and activates other caspases and decomposes various proteins including cell cycle regulatory proteins as well as many other relevant targets in the nucleus and cytoplasm (Gabryel *et al.*, 2002). Caspase-3 is believed to cleave poly-(ADP-ribose)polymerase (PARP), which facilitates the degradation of cellular DNA during apoptosis (Andersson *et al.*, 2000; Saito *et al.*, 2006). Additionally, a caspase-3 activated deoxyribonuclease termed CAD (C activated domain) has been identified which causes the degradation of chromosomal DNA into nucleosomal units, which are a landmark of apoptosis (Gabryel *et al.*, 2002).

1.8.4.4 The switch between apoptosis and necrosis

As discussed, it is likely that cell death may take the form of necrosis if metabolic disturbances are abrupt but apoptosis if they are more protracted (see section 1.8.4). The following briefly summarises possible contributions to the switch between apoptosis and necrosis.

1.8.4.4.1 Calcium overload

It has been shown that xenobiotics may cause lethal Ca^{2+} overload that has been implicated in both apoptotic and necrotic cell death. The levels and/or nature of cytosolic Ca^{2+} increase may determine the mode of death. A low, sustained influx may lead to cyt-c release with activation of apoptosis if sufficient energy is maintained

during the critical phases of execution of the cell death programme. Whereas an uncontrolled, high influx may overwhelm cellular metabolism, deplete ATP and result in lysis (McConkey, 1998; Nicotera and Orrenius, 1998).

1.8.4.4.2 ATP depletion

As discussed in section 1.8.1.4, ATP levels can serve as a 'switch' between apoptosis and necrosis. It has been estimated that the depletion of 40-70 % of cellular ATP is sufficient to switch the mechanism of cell death from apoptosis to necrosis (McConkey, 1998).

1.8.4.4.3 Oxidative stress

As discussed in section 1.8.2, oxidative stress is defined as a disturbance in the oxidant-antioxidant balance in favour of reactive oxidative species (ROS). Moderate accumulation of ROS may cause DNA strand breakage and induction of apoptosis, whilst higher levels may inhibit caspase activation (Pong *et al.*, 2001) and have a more severe effect on cellular protein and lipid functions, causing necrosis (Geller *et al.*, 2001).

Hydrogen peroxide is one of the most abundant ROS and is produced directly or indirectly during cellular respiration. It has been reported that H_2O_2 can induce the release of cyt-c into the cytosol, followed by activation of caspase-9 and -3 leading to apoptosis. Alternatively, H_2O_2 may induce necrosis by inhibiting caspase activation or caspase activity, or by leading to ATP depletion (Gregus and Klaassen, 2001).

Saito *et al.*, (2006) observed that a moderate concentration of H_2O_2 (50 μM) triggered apoptosis, whilst an elevated concentration (500 μM) caused a marked decrease in intracellular ATP level and necrosis in a human T-lymphoma cell line. The group also demonstrated that that prevention of ATP loss using antioxidants resulted in caspase-3 activation and switched the mode of cell death to apoptosis (Saito *et al.*, 2006).

1.8.4.4.4 Role of antioxidants

Glutathione (GSH) has been implicated in the regulation of both apoptosis and necrosis. GSH may maintain thiol status critical to caspase activation, most likely because the caspase family possesses a potentially redox-sensitive cysteine residue within the active site (McConkey, 1998). Additionally, GSH may protect against ATP depletion, however excessive depletion of GSH tends to predispose cells to necrosis due to the effects of excessive oxidative stress (Piwocka *et al.*, 2001)

1.9 Range of test chemicals

In order to compare the sensitivity of the various cell systems, the test chemicals included two known human acute neurotoxins, one chronic neurotoxin and two non-neurotoxins, which are described in the following sections.

1.9.1 n-Hexane and 2,5-hexanedione

n-Hexane is a volatile organic solvent, widely used in the preparation of fabrics, glues, paints and varnishes for many years as it was considered to pose little hazard to health (Mayan *et al.*, 2002; Pei *et al.*, 2007). However, the compound has been withdrawn from use in many contexts following the discovery that chronic low-level exposure, occupationally or through solvent abuse, led to neurotoxicity in humans (Spencer *et al.*, 1980; Decaprio, 1987).

Metabolism studies *in vivo* and *in vitro* revealed that n-hexane is bioactivated by cytochromes P450 and cytoplasmic dehydrogenases to form the γ-diketone, 2,5-hexanedione (2,5-HD) (Zhu *et al.*, 1995). It is 2,5-HD that is the ultimate neurotoxic metabolite responsible for the neurological effects that accompany frequent exposure to n-hexane (Spencer *et al.*, 1980).

Occupational exposure to n-hexane causes a slow, progressive, sensory and motor dysfunction in the hands and feet, with distal muscle weakness and a more rapid, sub-acute course in solvent-sniffers (Couri and Milks, 1982). Similar effects were noted in animals exposed by oral or inhalation routes (Spencer *et al.*, 1980; Prieto *et al.*, 2003). The nerve damage induced by chronic exposure to high concentrations of n-hexane or

in experimental animals administered 2,5-HD, was originally characterised as a central-peripheral distal axonopathy. This referred to the apparent dying back process of the central nervous system (CNS) and peripheral nervous system (PNS) axons that accompanied the debilitating neuropathy (Couri and Milks, 1982). However, the underlying molecular mechanism whereby 2,5-HD causes neurotoxicity is still a subject of some debate.

1.9.1.1 Human exposure to n-hexane

The world-wide accepted threshold limit for airborne n-hexane in industry is 50 ppm (Couri and Milks, 1982). However, the majority of occupational cases of n-hexane neuropathy have occurred in small industrial concerns such as shoe manufacturers, where workers were exposed sub-chronically in badly ventilated rooms with ambient air levels of over 2500 ppm (Spencer *et al.*, 1980). The reported symptoms were numbness of toes and fingers, followed by a proximal progression of loss of sensory and motor function. Other early symptoms such as headache and dizziness have been reported following 10 minutes exposure to 1000-5000 ppm, with recovery following cessation of exposure (dos Santos *et al.*, 2002; Hernandez-Viadel *et al.*, 2003).

Free and conjugated 2,5-HD is identified in urine samples from n-hexane exposed workers and is used for biological monitoring (Mayan *et al.*, 2002; Prieto *et al.*, 2003). However, with a log P of -0.27, 2,5-HD is not readily lipid soluble (IPCS, 1991) and the 2,5-HD intra-neuronal and intra-axonal concentration following systemic exposure has not been determined (Sickles *et al.*, 1990).

1.9.1.2 Mechanism of 2,5-hexanedione neuropathy

Substantial effort has been made to understand the mechanism of action of 2,5-hexanedione neurotoxicity at a molecular level. Historically the neuropathy was pathologically characterised by multifocal, giant axonal swellings containing aggregations of neurofilaments (Selkoe *et al.*, 1978; Decaprio, 1987). It was considered that axonal regions below the swellings then underwent degeneration due to physical blockade of axonal nutrient flow, to give a dying back neuropathy of both motor and

sensory fibres in the peripheral and central nervous systems (Couri and Milks, 1982; Iwasaki and Tsuruta, 1984).

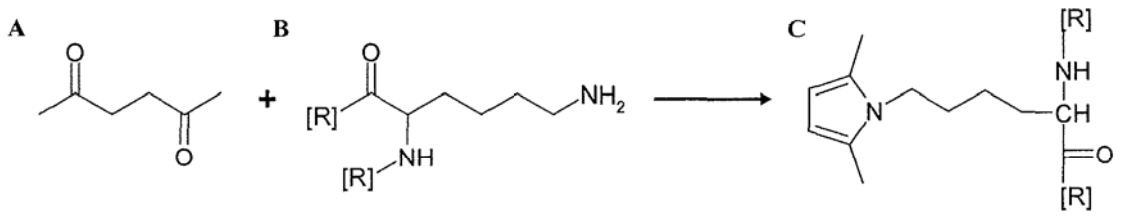

2,5-HD | Protein lysine residue | ε-N[2,5-dimethylpyrrolyl] norleucine adduct

Figure 1.3 Illustration of the formation of lysine protein adducts by 2,5-hexanedione. A) The γ-diketone electrophile, 2,5-hexanedione reacts covalently with B) nucleophilic lysine ε-amine groups to form C) 2,5-dimethylpyrrole adducts on neurofilament proteins.

Neurofilaments are the major intermediate filament type expressed in mature neurons and are composed of three polypeptide subunits (Hartley *et al.*, 1997). 2,5-HD is a soft electrophile and has been found to bind covalently to neurofilament lysine ε-amines *in vivo* and *in vitro*, to yield 2,5-dimethylpyrrole adducts which are considered critical to the mechanism of toxicity (figure 1.3) (Decaprio *et al.*, 1987; Zhu *et al.*, 1995; Heijink *et al.*, 2000). Pyrrole formation is proposed to result in physiochemical changes in the proteins, sufficient to cause neurofilament accumulation and swelling as they accumulate at the nodes of Ranvier (Zhu *et al.*, 1995).

1.9.1.3 Axonal atrophy

Most research in past twenty years has focused on elucidating the mechanism of neurofilament accumulation, axon swelling and presumed subsequent distal axonal degeneration (LoPachin, 2000). However, neurofilamentous swellings are now widely considered to be a non-essential phenomenon related only to long-term, low dose intoxication (LoPachin, 2000; LoPachin *et al.*, 2000; LoPachin and DeCaprio, 2004).

More recent studies have demonstrated axonal atrophy to be the morphological hallmark of 2,5-HD induced neuropathy. Atrophied axons in various 2,5-HD-exposed animal models have been characterised by a decrease in cross-sectional area with

maintenance of a relatively normal length. As the axon shrinks it becomes misshapen and crenated, with the onset of neurological deficits and electrophysiological dysfunction being observed to develop contemporaneously with loss of axon calibre (LoPachin, 2000). The actual mechanism of axonal atrophy is unknown. However, as neurofilaments are an important determinant of axon calibre, presumably the changes in neurofilament structure and/or function that follow 2,5-HD adduction mean they cannot interact appropriately with the cytoskeletal network, subsequently leading to atrophy (Lehning *et al.*, 1995; LoPachin and DeCaprio, 2004; LoPachin and DeCaprio, 2005).

1.9.1.4 2,5-Hexanedione toxicological studies

Although recognised as the chronic neurotoxic metabolite of n-hexane, 2,5-HD is not considered to be especially acutely toxic based on oral rat exposures (LD_{50} = 23.7 mmol/kg (Couri and Milks, 1982). Acute toxic effects *in vivo* consist of narcosis, dizziness and mucous membrane irritation (Couri and Milks, 1982).

Most 2,5-hexanedione neurotoxicological studies are chronic, observational animal experiments. However, a number of *in vitro* sub-acute and acute mechanistic studies have been carried out using primary, murine, neuronal and astrocytic cell cultures and human neuroblastoma cell lines, employing wide dose ranges, including unphysiologically high levels of the metabolite. These studies have examined the ability of 2,5-HD to adduct neurofilaments, other members of the intermediate filament family and other protein targets, in the compound's role as a soft electrophile (Boegner *et al.*, 1992; Heijink *et al.*, 2000; LoPachin and DeCaprio, 2005). Additionally, 2,5-HD has been observed to disrupt cellular energy supply (Schmuck *et al.*, 2000) and cause apoptosis (Ogawa *et al.*, 1996).

1.9.2 2,3- and 3,4-Hexanedione

In addition to 2,5-HD, two other hexanedione isomers are commercially available. Although not formed via n-hexane metabolism *in vivo*, the α-diketones 2,3-HD and 3,4-HD occur naturally in some foodstuffs and are used as synthetic flavouring and

fragrance agents. The alpha-spacing of the two carbonyl groups (figure 1.4) sterically hinders 2,3- and 3,4-HD from forming pyrrole adducts and they are accordingly reported to be non-neurotoxic (Iwasaki and Tsuruta, 1984). However, it has also been reported that the closer the proximity of two carbonyl groups within a diketone, the more electrophilic and cytotoxic it will be (Chen and Hee, 1995).

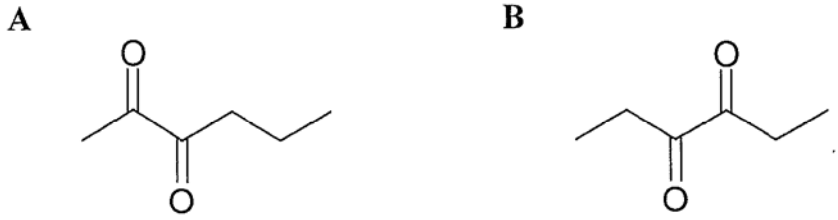

Figure 1.4 Illustration of the position of the carbonyl groups in the α-diketones, A) 2,3-hexanedione and B) 3,4-hexanedione.

1.9.2.1 Human exposure

2,3-Hexanedione (CAS number 3848-24-6) occurs naturally in beer, coffee and fermented soya beans and is used to give a buttery-cheesy taste in flavourings and some fragrances. 3,4-Hexanedione (CAS number 4437-51-8) occurs naturally in coffee and cauliflower and is used to give a sweet caramel-buttery odour and taste (FAO/WHO, 1999).

2,3- and 3,4-HD belong to a group of 22 flavouring agents evaluated by the Joint FAO/WHO Expert Committee on Food Additives (JECFA). They were subsequently classified in structural Class II, which means they are expected to be metabolised to innocuous products *in vivo* and pose no safety concern if the daily human intake does not exceed 540 μg. The estimated per capita intake of 2,3-HD and 3,4-HD in Europe is 13 and 33 μg/day respectively and thus neither compound exceeds the threshold level for class II at their current levels of intake as flavouring agents. For a 75 kg person, these levels correspond to an approximate human daily intake of 0.14 μmol and 0.33 μmol for 2,3-HD and 3,4-HD, respectively (FAO/WHO, 1999).

1.9.2.2 Toxicological studies

Studies regarding the toxic potency of 2,3- and 3,4-hexanedione are limited. Diketones such as 2,3- and 3,4-HD have been previously utilised as negative controls in *in vitro* studies of the neurotoxicity of γ-diketones in murine neuroblastoma cell lines (Selkoe *et al.*, 1978) and rat primary brain cells (Medrano and LoPachin, 1989), as they lack the 1,4 carbonyl group spacing. The α-diketones failed to show a toxic effect and in contrast to 2,5-HD (section 1.9.1), the effects of 2,3- and 3,4-HD had not previously been investigated *in vitro* in human neural or astrocytic cell lines. However, in recent studies within the laboratory, 2,3- and 3,4-HD were significantly more toxic towards the NT2 neural and SK-N-SH neuroblastoma cell lines compared with 2,5-HD, after 4- and 24-hours exposure (Woehrling *et al.*, 2006).

1.9.2.3 Interaction of α-diketones with the mitochondrial oxoglutarate carrier

The inner mitochondrial membrane contains a transport protein, the oxoglutarate carrier (OGC) which is important for several metabolic processes and catalyses a counter-exchange between 2-oxoglutarate and L-malate. The positively charged amino-acid arginine plays an essential role in binding and translocation of the negatively charged substrates oxoglutarate and malate and has been shown to be essential for OGC activity (Stipani *et al.*, 1996). Whereas pyrolle formation via adduction of lysine residues is unique to γ-diketones (section 1.9.1.2), α-diketones are stronger electrophiles than 2,5-HD owing to the closer α-spacing of the carbonyl groups. Such compounds are highly selective for modification of arginine residues in proteins, making them potential inhibitors of several anion transporters, including the OGC (Stipani *et al.*, 1996).

1.9.2.4 The importance of malate and oxoglutarate in the tricarboxylic acid cycle

Glycolysis is a metabolic pathway by which a glucose molecule is oxidised to two molecules each of pyruvate, NADH, H^+ and ATP, in the cytosol. The reducing equivalents are then carried into the mitochondria as malate through exchange for oxoglutarate (Griffin *et al.*, 2000). The bulk of ATP used by many cells to maintain homeostasis is produced by the oxidation of pyruvate in the tricarboxylic acid (TCA) cycle. The cycle generates NADH and reduced $FADH_2$, which are subsequently used to

drive ATP synthesis via oxidative phosphorylation (Stryer, 1995). In the TCA cycle, oxoglutarate is oxidatively decarboxylated by the α-oxoglutarate dehydrogenase complex, generating an equivalent of NADH. L-malate is the specific substrate for malate dehydrogenase, the final enzyme of the TCA cycle, with oxidation yielding a further equivalent of NADH (Stryer, 1995). The OGC therefore plays a number of major roles in the ultimate synthesis of ATP and 2,3- and 3,4-HD have the potential to disrupt this process.

1.9.3 Trimethyltin chloride

Approximately 35,000 tones of organotin compounds (organic derivatives of tetravalent tin) are produced annually worldwide and poisoning has occurred in industry, under experimental conditions and due to leaching from vessels whose production involved their use (Gunasekar *et al.*, 2001b). Of these compounds, trimethyltin (TMT) is characterised by the presence of covalent bonds between three methyl groups and a tin atom and has the general formula $(CH_3)_3Sn$-X, where X is an anion (Van-Heijst, 1999).

Trimethyltin chloride (RN: 1066-45-1; X=Cl) arises in industry through heat stabilisation of polyvinylchloride and production of other tin derivatives and is the TMT derivative most often used in experimental protocols (Karpiak and Eyer, 1999; Jenkins *et al.*, 2004).

TMT-Cl is primarily a CNS neurotoxin which causes a specific pattern of neuronal degeneration in the hippocampus and other parts of the limbic system after a single exposure, with symptoms reflecting injury in this area (Fiedorowicz *et al.*, 2001; Cristofol *et al.*, 2004). The hippocampus is the region of the limbic system which plays a part in memory and spatial navigation (Figiel and Fiedorowicz, 2002) and memory problems and disorientation appear among the first symptoms following TMT-Cl exposure (Van-Heijst, 1999).

1.9.3.1 Exposure and metabolism

TMT-Cl vaporises readily, augmenting its potential as inhalant toxicant in industrial workers (Van-Heijst, 1999). Accidental poisoning to the general population has occurred, with TMT-Cl being detected in drinking water due to significant leaching from PVC pipes and in alcoholic beverages due to its use as stabiliser in storage vessels (Karpiak and Eyer, 1999; Jenkins and Barone, 2004). TMT-Cl has also been detected in the urine of humans with no known acute exposure, suggesting the possibility of environmental exposure or methylation of other tin species *in vivo* (Jenkins and Barone, 2004).

Trimethyltin compounds are well absorbed through the skin, from the lungs and intestinal tract (Van-Heijst, 1999) and TMT-Cl has been found in brain of various animal species following neurotoxic exposures to levels of 5-18.5 μM (Eyer *et al.*, 2000). However, the regional toxic specificity observed is not thought to be due to preferential distribution to the limbic area of the brain (Viviani *et al.*, 1998b; Van-Heijst, 1999). Trisubstituted organotin compounds undergo dealkylation by the microsomal monooxygenase system, which is dependent on cytochrome P450 in the liver and other organs (Kimmel *et al.*, 1977; Doctor *et al.*, 1983). Results have indicated that TMT rapidly distributes and although water-soluble (log P = 0.28) (Doctor *et al.*, 1983), persists in tissues (10 day half life) and is slowly removed from brain (Maier *et al.*, 1995).

Following acute human inhalation intoxication, serum levels of 0.6 μM TMT and urine levels of 2.6 μM TMT have been measured (Van-Heijst, 1999). TMT-Cl levels were determined in various tissues of male mice at 1-16 hours after administration of 4.26 mg/kg; i.p., with penetration into the brain observed 6 hours following administration and by 16 hours the animals exhibited convulsions followed by death (Doctor *et al.*, 1983).

1.9.3.2 CNS effects following *in vivo* exposure

TMT-Cl causes a complex neurological syndrome. Reported symptoms in humans following acute, oral and inhalation toxicity include headache, disorientation, memory defects, seizures, fatigue and respiratory depression, with onset from a few hours up to

three days after exposure (Cristofol *et al.*, 2004; Jenkins and Barone, 2004). In a case where a woman drank a glass of contaminated wine of unknown TMT-Cl concentration, she rapidly displayed intermittent episodes of unresponsiveness and agitation, followed by death (Van-Heijst, 1999). Post-mortem of humans following fatal exposure has revealed neuronal necrosis and apoptosis in areas of the hippocampus, cerebral cortex and cerebellum, similar to that observed following TMT-Cl intoxication in rodents and *in vitro* exposure of primary hippocampal neurons (Van-Heijst, 1999; Cristofol *et al.*, 2004).

1.9.3.3 Investigation of acute toxicity

The acute potential TMT-Cl to induce an apoptotic or necrotic mode of cell death has been widely investigated in numerous cell systems. These include primary cultures of rodent derived, hippocampal and cerebral neurons and astrocytes and neuronal PC12 cell line (Gunasekar *et al.*, 2001b), human neuroblastoma cell lines and human foetal cerebral neurons (Cristofol *et al.*, 2004). Sensitivity to TMT-Cl was found to vary in between species and cell type in *in vitro* cell cultures. Generally, primary rodent cells are more sensitive than human derived cultures and as *in vivo*, cells from the hippocampal region demonstrate specific sensitivity. Additionally, specific astrocytic effects have been noted.

As discussed (section 1.3.2), astrocytes play a supportive and interactive role with neurons and whilst generally being considered to be less vulnerable towards TMT-Cl induced toxicity, several studies have linked TMT-Cl neurotoxicity to astrocytic cells (Aschner and Aschner, 1992; Karpiak and Eyer, 1999). Administration of both neuropathic and non-neuropathic doses of TMT-Cl to rats have been demonstrated to produce a distinct *in vivo* morphological response of astrocytes in several brain regions, with hypertrophy, swelling and GFAP and metabolic increase suggestive of astrogliosis (O'Callaghan, 1991; Maier *et al.*, 1995). Similar morphological alterations have been observed *in vitro*, in mixed and pure astrocytic cultures (Rohl *et al.*, 2001; Figiel and Fiedorowicz, 2002).

Whilst the toxicological effects of TMT compounds are well documented following

human and animal exposure, the possible mechanism and the factors determining the selective regional vulnerability of the CNS to TMT-Cl neurodegeneration have not been completely elucidated. Many hypotheses have been formulated regarding the possible necrotic or apoptotic mechanism of TMT-Cl induced neuronal death, including; astrocytic release of cytokines such as tumour necrosis factor alpha (TNF-α) (Viviani *et al.*, 1998a), calcium overload (Florea *et al.*, 2005), oxidative stress due to antioxidant depletion and/or an increase in ROS production (Viviani *et al.*, 2001) and caspase activation leading to apoptosis (Jenkins and Barone, 2004).

1.9.4 Tributyltin chloride

Similar to trimethyltin (TMT), tributyltin (TBT) compounds are organic derivatives of tetravalent tin but possessing three, 4-carbon alkyl chains and the general formula $(C_4H_9)_3Sn$-X, where X is an anion (IPCS, 1990).

Tributyltin compounds have been widely used as biocides; in wood preservation, industrial textiles, antifouling paints for boats and ships and disinfection of industrial cooling waters. Numerous tributyltin compounds have been found to be toxic to mammals. Subsequently, a European Union (EU) regulation which came into effect in 2003, restricts their use in marine anti-fouling paints but concern remains over their use in other applications (Corsini *et al.*, 1998; Appel, 2004; Jurkiewicz *et al.*, 2004). Historically, the tributyltin with X=chloride (TBT-Cl, RN: 1461-22-9) was the most widely used for marine applications and due to its long half life (> 2 years), the threat of ongoing contamination and adverse effects within environmental and biological systems exists (Nakatsu *et al.*, 2006a). Indeed, the World Wildlife Fund described TBT-Cl as "the most toxic chemical ever deliberately released into the seas" (von Ballmoos *et al.*, 2004).

1.9.4.1 Human exposure

Exposure to workers may occur during the manufacture of TBT-Cl products, in the application of paints and in wood preservation (Corsini *et al.*, 1998). EU regulation has greatly reduced marine pollution but exposure of the general population can take place

through consumption of contaminated fish and seafood (Corsini *et al.*, 1997; Appel, 2004). TBT-Cl has also been detected in meat and milk (Jurkiewicz *et al.*, 2004).

EU member states identified TBT-Cl contamination through its accumulation in various marine species, with muscles and fish found to contain approximately 40 and 20 nmol TBT-Cl/kg respectively (Appel, 2004). Shellfish in polluted areas of Japan have been found to contain up to 5 μmol TBT-Cl (Mizuhashi *et al.*, 2000a). The daily TBT-Cl intake for German males from freshwater fish has been estimated at ≤ 0.3 nmol (Appel, 2004) and in Japan was estimated through a market basket survey to be 7.1 nmol/day in 1997 (Okada *et al.*, 2000). The environmental dietary exposure of humans of no known acute contact has been confirmed by detection of dibutyltin-chloride (DBT-Cl), a metabolite of TBT-Cl that indicates bioavailability. DBT-Cl has been detected at levels of up to 0.6 nM in human urine (Jenkins *et al.*, 2004) and 2 – 90 nmol/kg in the liver of Danish males (Appel, 2004).

1.9.4.2 Metabolism

TBT-Cl is subject to cytochrome P450 dependent hydroxylation and dealkylation to di and monobutyltin, followed by tin, with clearance from the body expected to occur within a few days (IPCS, 1990; Appel, 2004). However, it is highly lipophilic (log P = 4.76) and thus has the potential to accumulate in lipid rich organs such as the brain and may target membranes. No data is available for TBT-Cl concentration in human brain but because of it lipophilicity it is speculated that it may accumulate, leading to concentrations in excess of those detected in human liver (Mizuhashi *et al.*, 2000b; Nakatsu *et al.*, 2006a). The BBB does not appear to prevent transfer of TBT-Cl into the CNS, with a single oral dose of 46 μmol TBT-Cl/kg in rabbits, leading rapidly to high concentrations in the cerebellum and frontal lobe (Appel, 2004).

1.9.4.3 Effects following *in vivo* exposure

Acute human exposure to TBT-Cl has been reported to cause skin and eye irritation and inflammation of the respiratory tract (IPCS, 1990). In experimental animals, TBT-Cl toxicity is associated with immunosupression via spleen and thymus atrophy, with the

deletion of immuno-competent cells such as lymphocytes, thymocytes and white blood cells (Lavastre and Girard, 2002; Jenkins *et al.*, 2004). Additionally, acute renal and hepatic damage (Karpiak and Eyer, 1999; Lavastre and Girard, 2002) and reproductive toxicity in both males and female rats, has been reported (Appel, 2004). Recently the neurotoxic potential of TBT-Cl has also become apparent, with a single experimental exposure observed to cause significant neurobehavioural changes in rats (Lavastre and Girard, 2002), a decrease in brain weight (Nakatsu *et al.*, 2006b) and an increase in the permeability of the BBB (Elsabbagh *et al.*, 2002).

1.9.4.4 Investigation of acute toxicity

Acute exposure to low micromolar amounts of TBT-Cl has been observed to induce apoptosis in a wide variety of cell types, including primary rat thymocytes (Okada *et al.*, 2000), human peripheral blood lymphocytes and the human Hut-78 and Jurkat T-lymohocyte cell lines (Stridh *et al.*, 1999b; Stridh *et al.*, 1999c). The acute neurotoxic effects of the organotin compound *in vitro* have also been investigated, predominantly in rodent derived cell-systems. These include hippocampal neurons using organotypic slice cultures from immature rats (Mizuhashi *et al.*, 2000a) and primary rat cortical neurons (Nakatsu *et al.*, 2006a). A limited number of studies have also shown astrocytes to be sensitive to low micromolar concentrations of TBT-Cl *in vitro*, in the absence of neurons.

A variety of mechanisms have been suggested to account for the acute cytotoxic potential of TBT-Cl. However, the most studied mode of cell death is the generation of apoptosis which is considered by many to be underlying mechanism for the immuno, hepatotoxic and neurotoxic effects of TBT-Cl (Appel, 2004). The precise apoptotic mechanism has not been fully established but is speculated to be mediated by an early intracellular Ca^{2+} elevation, followed by the release of ROS and cyt-c from mitochondria (Appel, 2004) and caspase-3 activation, resulting in DNA fragmentation (Gennari *et al.*, 2000; Jurkiewicz *et al.*, 2004). The involvement of ATP depletion (Stridh *et al.*, 1999a) and glutamate excitotoxicity (Nakatsu *et al.*, 2006a) has also been postulated.

1.10 Aims and objectives of the present study

The scope of this project is the pressing need for a relevant, tiered, *in vitro* test strategy for the prediction of acute neurotoxicity in humans. The aim of the research presented here is the preliminary development of a post-mitotic, human cell line based, neuronal-astrocytic cell system, for inclusion in a test battery for the first-tier, rapid screening of new and existing compounds for acute neurotoxic potential. The suitability of the NT2.N/A co-culture cell system to correctly predict acute neurotoxicity was appraised in comparison with a number of other human cell lines (NT2.N mono-, CCF-STTG1 astrocytoma and NT2.D1 neuronal precursor cultures), using a measure of basal cytotoxicity and a number of biochemical endpoints and test chemicals.

In summary the objectives of the study are;

i) To prepare differentiated human NT2.N mono-cultures and NT2.N/A co-cultures and briefly characterise them using neuronal and astrocytic phenotypic markers to ensure efficient adaptation of protocols from the literature has been achieved (Chapter 2). To culture all the cell populations (NT2.N, NT2.N/A, NT2.D1 and CCF-STTG1) in an appropriate format for the high-throughput screening of potential neurotoxins.

ii) To perform an evaluation of the sensitivity of the different cell systems following 4- or 24-hours exposure to cytotoxic concentrations of 2,5-HD (chronic neurotoxin), 2,3- and 3,4-HD (non-toxic), TMT-Cl and TBT-Cl (acute neurotoxins), via comparison of IC_{50} values. An estimation of the non-cytotoxic (NOAEL) concentration range at 4-hours will also be carried out (Chapter 3).

iii) To develop sensitive and relevant protocols for the rapid assessment of biochemical endpoints, including a measure of cellular energy (ATP levels) and oxidative status (hydrogen peroxide and glutathione levels) and caspase-3 levels as an indicator of apoptosis (Chapter 4). It is intended to employ these biochemical endpoints in order to compare the ability of the of the different cell populations to differentiate between the acute neurotoxic or cytotoxic potential of the test chemicals following 4-hours exposure at non-cytotoxic concentrations (Chapter 5).

Chapter 2 – Identification of suitable neuronal and astrocytic cell lines

2.1 Introduction

Regarding human hazard assessment, it was considered that the use of human cell lines in a first-tier *in vitro* neurotoxicity screen would offer the greatest degree of relevance to the *in vivo* situation. A reliable source of both post-mitotic neurons and astrocytes was required, as human cell lines that phenotypically reflect the heterogeneity and post-mitotic nature of the *in vivo* nervous system as closely as possible were deemed to be the most appropriate. Therefore, it was necessary to initially identify suitable human cell lines for use in, and/or comparison with, a neuronal and astrocytic co-culture cell system, culture them in an appropriate format for the high-throughput screening of potential human neurotoxins and briefly characterise them to ensure efficient adaptation of protocols from the literature had been achieved.

Embryonal carcinoma (EC) cell lines, among them the well characterised EC NT2.D1 cell line, may be induced to differentiate terminally *in vitro* into a mono-culture of post-mitotic neurons, or co-culture of post-mitotic neurons and astrocytes, in sufficient enough numbers for toxicity assessments. There is no evidence to date which suggests that human NT2.D1 derived neurons differentiate in an aberrant way and instead they have been found to express many key marker proteins typical of neurons *in vivo* and *in vitro*, including neuron-specific enolase (NSE), neurofilament 68 (NF68) and β-tubulin III. The post-mitotic NT2.A cells have been shown to express the astrocyte specific marker, glial fibrillary acidic protein (GFAP) (Bani-Yaghoub *et al.*, 1999; Stewart *et al.*, 2003). In addition to these terminally differentiated cell systems, the NT2.D1 neuronal precursor cell line was also employed, along with the GFAP positive CCF-STTG1 astrocytoma cell line as a comparative astrocytic mono-culture.

2.2 Materials and Methods

2.2.1 Materials

Standard solvents were obtained from Fisher (Loughborough, UK) and all gases from BOC Ltd (Guildford, UK). All reagents were of molecular biology grade (Sigma Chemical Company, Poole, UK) unless otherwise stated. Pen/strep (10,000 U penicillin-G and 10 mg streptomycin per ml), sodium pyruvate solution (100 mM), phosphate buffered saline (PBS; pH 7.4) and protease inhibitor cocktail (solution in DMSO for use with mammalian cell and tissue extracts) were also purchased from Sigma. All cell culture media, foetal bovine serum (FBS), L-glutamine (200 mM) and HANKS Balanced Salt Solution (HBSS) were obtained from Invitrogen (Paisley, UK). Deionised water used was of at least 18.3 MΩ.cm quality and produced using a Milli-Q Ultrapure Water System (Millipore, UK).

The CCF-STTG1 (Human astrocytoma cell line) cells (ECACC No. 90021502) were purchased from the European Collection of Cell Cultures (ECACC, Porton Down) and the NTERA-2 clone D1 (NT2.D1; Human teratocarcinoma cell line) cells (ECACC No. 01071221) were kindly donated by Professor P. W. Andrews (University of Sheffield).

Cell culture plastics, including CellBIND® 6-well plates and cryovials, were from Corning Costar (Schiphol-Rijk, Netherlands) unless otherwise stated. Clear 96-well multiplates provide the best signal to noise ratio for colorimetric reading and were also purchased from Corning Costar. Black multiwell plates show minimal plate phosphorescence for luminescence reading, also provide the best signal to noise ratio for fluorescence measurements and were purchased from Perkin Elmer LAS (UK).

2.2.2 Sub-culture of cell lines

The NT2.D1 and CCF-STTG1 cell lines were cultured as a monolayer in 75 cm^2 or 162 cm^2 flasks at 37 °C in a humid atmosphere containing 5 % CO_2, 95 % air. The NT2.D1 cells were maintained in Dulbecco's Modified Eagle Medium, high-glucose (4.5 g/L; 25 mM D-glucose) formulation (DMEM-HG) containing Glutamax™I (3.97 mM; a stable glutamine dipeptide that can be used in place of L-glutamine) and 1 mM sodium

pyruvate and supplemented with 10 % (v/v) FBS and 1 % (v/v) pen/strep. The CCF-STTG1 cells were cultured in RPMI 1640 (2 g/L; 11.11 mM D-glucose) media supplemented with 10 % (v/v) FBS, 1 % (v/v) pen/strep, 1 % (v/v; 1 mM) sodium pyruvate and 1 % (v/v; 2 mM) L-glutamine. In all cases, the media was pre-warmed to 37 °C before use.

All cultures were microscopically examined regularly for their level of confluence, morphological appearance and any signs of microbial contamination. Sub-culture (dilution 1 in 2) of the continuous NT2.D1 and CCF-STTG1 cell lines was carried out by gentle scraping when the cells had reached approximately 90 % confluence. If cultures were not confluent within three days of seeding, the medium was aspirated and replaced.

2.2.3 Cryopreservation of cells in liquid Nitrogen

In order to maintain long-term stocks of the NT2.D1 and CCF-STTG1 cell lines, cells were routinely frozen down at final concentration of approximately 2 x 10^6 cells/ml in freezing medium (FBS with 10 % dimethyl sulfoxide (DMSO) as a cryoprotectant) and stored under liquid Nitrogen.

2.2.4 Resuscitation of cells from liquid Nitrogen

The ampoule of cells required was removed from the liquid Nitrogen bank and placed in a waterbath at 37 °C to thaw. The cells were then suspended in fresh medium, centrifuged (179 g, 5 min) and the pellet transferred to a 75 cm^2 culture flask with an appropriate volume of medium. When confluent the cells were transferred to a 162 cm^2 flask.

2.2.5 Differentiation of the NT2.D1 cell line

NTera2 cl.D1 (NT2.D1) cells may be differentiated into several morphologically and biochemically distinct cell types upon treatment with all trans-retinoic acid (RA), followed by mitotic inhibitors. Cell types that may be obtained include terminally

differentiated, postmitotic neuronal NT2.N cells (Andrews, 1984) and astrocytic NT2.A cells (Bani-Yaghoub *et al.*, 1999), which resemble those of the human central nervous system. Several NT2.D1 cell differentiation methods have been developed. The following protocol for the differentiation of NT2.D1 cells into NT2.N mono-cultures is based on the plating method proposed by Andrews (1984) and further developed by Pleasure *et al.,* (1992). For the differentiation into NT2.N followed by NT2.A cells to give an integrated neural-astrocytic culture, a modification of the plating method first proposed by Bani-Yaghoub *et al.,*(1999) and further developed by Stewart *et al.,* (2003) was employed.

It has previously been found that differentiated neurons will only demonstrate neurite outgrowth on plates coated with the synthetic attachment factor poly-d-lysine and the basement membrane component laminin (pdl/lam), rather than on traditional cell culture plastic (Stewart *et al.*, 2003). This is consistent with neurite-outgrowth-promoting effects of laminin on a variety of PNS and CNS neuronal cells in culture (Manthorpe *et al.*, 1983; Rogers *et al.*, 1983). However, a new type of CellBIND® 6-well plate was obtained from Corning Costar (Netherlands). CellBIND plastics have a novel, non-biological, treated polymer surface that is designed to improve cell attachment and promote cell spreading and outgrowth. The plating method was adapted for antiproliferative treatment of cells within CellBIND 6-well plates following retinoic acid treatment (sections 2.3.1 and 2.3.2). This was a completely novel step and conferred the advantage of not having to chemically remove differentiated cells from the pdl/lam prior to carrying out certain experimental procedures that may be subject to interference by the attachment surface, e.g. laminin may cause over-estimation of sample protein levels.

2.2.5.1 Differentiation into a mono-culture of neuronal (NT2.N) cells

NT2.D1 cells were cultured as described in section 2.2.2 and seeded into 75 cm^2 flasks at a density of 2 x 10^6 cells/flask, in their usual medium. After overnight incubation in a humidified atmosphere at 37 °C, in 5 % CO_2, 95 % air, the medium was replaced with that containing 1 x 10^{-5} M retinoic acid (RA). The RA medium was changed twice a week, for four weeks and the cells were allowed to build up in layers without sub-culturing.

Following RA treatment, the cultures were replated into 75 cm^2 flasks, using RA free medium, at a dilution of 1:3 (replate #1) to allow the release of NT2.N cells buried in the midst of the cells layers. After two days incubation, striking the flasks sharply ten times on each side mechanically dislodged the NT2.N cells. The resulting disrupted cells were collected by centrifugation and replated onto CellBIND 6-well plates at a density of 22.5 x 10^5 cells/well (replate #2), in medium supplemented with the mitotic inhibitors (MI) 1 μM cytosine arabinoside (ARAC), 10 μM fluorodeoxyuridine (FDU) and 10 μM uridine, to reduce the proliferation of non-neuronal cell types. The MI medium was changed twice a week, for three weeks. ARAC was continued for the first seven days of culture, FDU and uridine for the total three weeks of culture. Following the differentiation procedure, the cells were maintained in normal DMEM-HG medium and usually utilised in experimental procedures within seven days. The cells were observed regularly for morphological changes and any signs of microbial contamination.

2.2.5.2 Differentiation into a co-culture of neuronal and astrocytic (NT2.N/A) cells

NT2.D1 cells were cultured in RA medium as described in section 2.2.5.1. Then, in order to obtain astrocytes in addition to neurons, after replate #2 cells were maintained in medium supplemented with 0.1 μM ARAC, 3 μM FDU and 5 μM uridine. The MI medium was changed twice a week, for four weeks. ARAC was continued for the first ten days of culture, FDU and uridine for the total four weeks of culture. Following the differentiation procedure the cells were maintained in normal DMEM-HG medium and usually utilised in experimental procedures within seven days. The cells were observed regularly for morphological changes and any signs of microbial contamination.

2.2.6 Growth of NT2.N and NT2.N/A cells on pdl/lam coverslips

Certain characterisation procedures (section 2.2.9) required the growth of cells on coverslips. As CellBIND coverslips are not yet available, 12 mm pdl/lam coated coverslips (BD Biocoat, Belgium) were employed. Prior to replate #2 (section 2.2.5.1), three coverslips were placed in a well of a CellBIND 6-well plate and the protocol for production of NT2.N or NT2.N/A cultures followed as usual (section 2.2.5).

2.2.7 Establishing post-mitotic status of the NT2.N and NT2.N/A cell cultures

In order to confirm the post-mitotic status of mono-cultures of NT2.N and co-cultures of NT2.N/A cells, following differentiation (section 2.2.5), cell density in consecutive wells of a 6-well plate was estimated every two weeks for eight weeks using the MTT reduction assay (section 3.2.2.1). The results are presented as the mean ± standard error of the mean (SEM) and were compared statistically with week zero using one-way ANOVA followed by the Dunnett's Post-test, using Graphpad prism software.

2.2.8 Characterisation of the NT2.N and NT2.N/A cell cultures using western blotting

Western blotting is a widely used technique for the detection and identification of protein antigens using antibodies. It can characterise cells and confirm their phenotype. The process involves isolation of proteins from a cell sample and separation of these proteins using polyacrylamide gel electrophoresis (PAGE), followed by transfer from the gel to a membrane. Detection of the protein of interest is achieved by the exposing the membrane to a specific primary antibody, which is then bound to a secondary antibody. The secondary antibody has directly conjugated to it a detection molecule such as horse radish peroxidase (HRP), which may be visualised by exposure of the membrane to photographic film (Harlow and Lane, 1998). Previous extensive characterisation has shown NT2.N cells to express a variety of neural markers, including neuron-specific enolase (NSE), neurofilament 68 (NF68) (Pleasure *et al.*, 1992) and β-tubulin III (Stewart *et al.*, 2003). The NT2.A cells have been shown to express glial fibrillary acidic protein (GFAP) (Bani-Yaghoub *et al.*, 1999; Stewart *et al.*, 2003). GFAP is reported to be present in 70-80 % of CCF-STTG1 cells (Barna *et al.*, 1985).

Protein samples were prepared from the NT2.D1, NT2.N, NT2.N/A and CCF-STTG1 cells, separated on sodium dodecyl sulfate (SDS)-polyacrylamide gels and immunoblotted, using a method previously optimised within the laboratory. The primary antibodies used to detect the protein markers and secondary antibody used to visualise them are described in table 2.1. A GFAP positive control from human brain

(46 kDa, Calibochem, UK, 345996) was run alongside some of the samples.

2.2.8.1 Cell lysis

In order to extract cellular protein, each well containing NT2.N or NT2.N/A cells (section 2.2.5), or each 75 cm^2 flask containing NT2.D1 or CCF-STTG1 cells (section 2.2.2), was first rinsed three times with PBS, then scraped into 1 ml PBS and centrifuged (5 min, 179 g). The supernatant was discarded and the cell pellet resuspended in 0.5 ml of RIPA (10 mM Tris HCl (pH 8.0), 100 mM NaCl, 1 mM EDTA, 1 % (v/v) NP40, 0.5 % (w/v) Sodium deoxycholate, 0.1 % (w/v) SDS and 1 Protease inhibitors tablet (Complete mini, Roche, UK)), on ice. The sample was then centrifuged (30 min, 4°C, 15000 g). The supernatant was removed and stored at -20 °C until protein level determination (section 2.2.8.2) and examination using SDS PAGE (section 2.2.8.3).

2.2.8.2 Protein analysis

Prior to examination by SDS PAGE (section 2.2.8.3), a 25 µl aliquot of cell protein lysate was taken for protein determination using the BCA protein assay reagent kit from Pierce (Rockford, USA), according to the manufacturer's guidelines for the 25 µl microplate procedure. Briefly, 25 µl of samples or bovine serum albumin (BSA) standards (125-2000 µg/ml, water acted as a BSA-free control) were added to a clear microplate together with 200 µl of the working reagent (50:1, Reagent A:B), incubated at 37 °C for 30 min and allowed to cool to room temperature. Then the A_{590} was measured using a Thermo Multiskan EX 96-well microplate spectrophotometer (Thermo Electron Corporation, USA) equipped with Ascent software.

2.2.8.3 SDS PAGE

Following protein analysis (section 2.2.8.2), samples underwent electrophoresis with SDS PAGE using the Mini Protean® 3 Cell with 10 % (w/v) SDS gels, cast according to the manufacturer's instructions (Biorad, UK). Sample buffer (5 % (v/v) glycerol, 12.5 mM Tris HCl (pH 6.8), 0.4 % (w/v) SDS, 0.002 % bromophenol blue (v/v) and 1

% (v/v) β-mercaptoethanol in deionised water) was used to prepare 10 μg samples of cell lysate, which were then loaded onto the gel along with broad range molecular weight markers (Biorad, UK). The gel was run at 200 V, 60 mA for 45 min.

2.2.8.4 Western blot transfer

Following separation of proteins by SDS PAGE, (Section 2.2.8.3), the plates were carefully separated and the gels were equilibrated in transfer buffer (25 mM Tris, 192 mM glycine and 10 % (v/v) methanol) for 15 min, before being laid upon pre-wetted (methanol) PVDF transfer membrane (Amersham Pharmacia, UK). The protein gels and PVDF were then sandwiched between four pieces of filter paper (Whatman, UK) and two pieces of sponge, pre-soaked in transfer buffer. Transfers were performed overnight using the mini trans-blot electrophoretic transfer cell (Biorad, UK) at 30 V, 90 mA.

2.2.8.5 Western blot analysis

Following western blot transfer, PVDF membranes (section 2.2.8.4) were blocked in TBS (136 mM NaCl, 2.7 mM KCl, 25 mM Tris-base in deionised water) with 0.01 % (v/v) Tween and 5 % (w/v) powdered milk for 2 hours at room temperature and then rinsed in TBS 0.01 % (v/v) Tween. The membranes were then transferred to TBS 0.01 % (v/v) Tween, 3 % (w/v) powdered milk, containing the appropriate primary antibody at the relevant dilution (table 2.1) and incubated at 4 °C overnight on a rolling platform. The next day the membranes were washed extensively (6 x 5 min) in TBS 0.01 % (v/v) Tween, in order to completely remove unbound antibody, before being placed in TBS 0.01 % (v/v) Tween, 3 % (w/v) powdered milk, containing the appropriate secondary antibody at the relevant dilution (table 2.1) for 1 hour at room temperature on a rolling platform. The membranes were then washed extensively in TBS 0.01 % (v/v) Tween and then TBS alone and placed in ECL detection reagent (Amersham Pharmacia, UK) for 5 min before being immediately sandwiched between acetates and exposed to photographic film (Amersham Pharmacia, UK) in a developing cassette. To visualise the bound antibody, exposed films were developed using developer (Sigma Chemical Company, UK) and after extensive washing fixed with fixer (Sigma Chemical

Company, UK) in a darkroom and then scanned.

Marker protein	Mass (KDa)	Primary antibody	Company/ Product code	Dilution	Secondary antibody	Company/ Product code	Dilution
GFAP	46	All Mouse Anti-Protein monoclonal IgG	AbCam, AB8975-1	1:1000	All Anti-mouse IgG, HRP-linked	Cell Signaling, #7076	1:5000
NSE	45		Chemicon, MAB324	1:2000			1:5000
β-tubulin III	55		Chemicon, MAB1637	1:500			1:1000
NF68	68		Sigma, N-5139	1:1000			1:5000

Table 2.1 The primary and secondary antibodies utilised in the western blotting procedure.

2.2.9 Characterisation of the NT2.N and NT2.N/A cell cultures using immunofluorescence microscopy

Proportions of neurons and astrocytes in a mixed population may be estimated by manual counting on slides after specific double immunostaining. Cells may be incubated simultaneously with two different primary antibodies, which may be distinguished with secondary antibodies conjugated to different fluorochromes. Specific antibodies against the intracellular markers β-tubulin III and GFAP have been previously successfully used to discriminate neurons from astrocytes in primary (Sergent-Tanguy *et al.*, 2003) and cell line derived co-cultures (Stewart *et al.*, 2003). The technique is also useful for the production of images of pure and mixed cell cultures.

2.2.9.1 Cell staining

Immunostaining of NT2.N and NT2.N/A cultures grown on pdl/lam coated coverslips in 6-well plates (section 2.2.6), was performed according to the method of Stewart *et al.*, (2003) with some modification. The coverslips were washed briefly in PBS and then the cells fixed by immersion in ice-cold methanol for 10 min, followed by three rinses with PBS. The cells were then covered with SBP (PBS containing 0.1 % (v/v) saponin and 0.3 % (w/v) BSA) and incubated at room temperature for 1 hour to

permeabilise the cells. A mixture of the primary antibodies was added to the coverslip in SBP, followed by incubation at room temperature for 2 hours. Goat anti-GFAP (N-18) polyclonal (diluted 1:100; SC-6171, Santa-Cruz, USA) and Mouse anti-β-tubulin III monoclonal IgG (diluted 1:500; MMS-435P, Covance, UK) primary antibodies were used as to detect the GFAP and β-tubulin III epitopes respectively. The primary antibodies were decanted and the coverslips were rinsed three times in SBP for 5 min each wash, to remove unbound antibody.

The secondary antibodies, Rhodamine (REDX)-conjugated Affinipure Rabbit anti-goat IgG (diluted 1:100; 305-295-003, Jackson Immunoresearch, USA) and fluoroscein (FITC)-conjugated Affinipure Rabbit anti-mouse IgG (diluted 1:100; 319-095-003, Jackson Immunoresearch, USA) were used to detect the anti-GFAP and anti-β-tubulin III primary antibodies respectively. The coverslips were incubated with the fluorochrome-conjugated secondary antibodies in SBP for 1 hour at room temperature. The secondary antibody mixture was then removed and the coverslips rinsed three times in SBP for 5 min each wash to remove unbound antibody. Each coverslip was then inverted onto a microscope slide containing Vectashield mounting medium with 4',6-diamidino-2-phenylindole (DAPI) fluorescent counterstain to visualise cell nuclei (Vector Laboratories, UK). The cells were then viewed and photographed using a an an Axioskop Microscope and AxioCam Camera with Axiovision software (Zeiss, Germany). Controls consisted of omitting the primary antibodies from the slides. A number of slides were also viewed according to the expertise of Dr Eric Hill (Aston University, UK), using a Zeiss LSM510 Confocal Microscope with Axioplan 2 Imaging MOT Upright Microscope and Zeiss Image Browser software (Zeiss, Germany).

2.2.9.2 Quantitative analysis of the NT2.N/A co-culture

The number of β-tubulin III and GFAP expressing cells and total cell nuclei were counted using the appropriate filters for the secondary antibodies and DAPI fluorochromes. Excitation/emission wavelengths were 546/590 nm (REDX; red), 450-490/515 nm (FITC; green) and 365/420 nm (DAPI; blue). Image overlays were done using Axiovision software and could be combined to make one image. The percentage

of cells was calculated as the number of each type of immunopositive cells reported to the total number of nuclei. Five hundred cells were examined in six random areas of each coverslip. The experiments were done in triplicate using three separate batches of cells.

2.3 Results

2.3.1 Cell culture

The NT2.D1 and CCF-STTG1 continuous cell lines were cultured as a monolayer using normal cell culture plastic. Both cell lines exhibited good growth rates, reaching confluence after a 1 in 2 split within 3-4 days. Resuscitation from liquid nitrogen gave a good yield of viable cells.

To induce the formation of a mono-culture of post-mitotic neurons (NT2.N), the pleuripotent NT2.D1 cell line was exposed to 10 μM retinoic acid (RA), followed by splitting, dissociation, reseeding and treatment with anti-proliferative agents as an adherent culture on CellBIND plastic or pdl/lam coverslips. Alternatively, the NT2.D1 cells were differentiated into a co-culture of both post-mitotic neurons and astrocytes (NT2.N/A) using a lower concentration of anti-proliferative agents over a longer period. NT2.N and NT2.N/A cultures were consistently produced at weekly intervals, with sufficient numbers of cells being readily generated in a 6-well plate format for toxicity experiments.

2.3.2 Establishing post-mitotic status of the NT2.N and NT2.N/A cell cultures

In order to confirm the post-mitotic status of mono-cultures of NT2.N and co-cultures of NT2.N/A cells, viable cell density in consecutive wells of a CellBIND 6-well plate was estimated every two weeks, for eight weeks, using the MTT reduction assay (section 3.2.2).

It can be seen in figure 2.1, that for both the NT2.N and NT2.N/A cultures, no statistical increase in cell number was detected over the first 6 weeks in normal mitotic inhibitor free medium ($P > 0.05$), suggesting that the cells were post-mitotic. Following 8 weeks in normal medium, cell density was statistically lowered compared with week zero (NT2.N, $P < 0.001$; NT2.N/A, $P < 0.05$) and the decrease in cell number was more pronounced in the NT2.N than the NT2.N/A cell line.

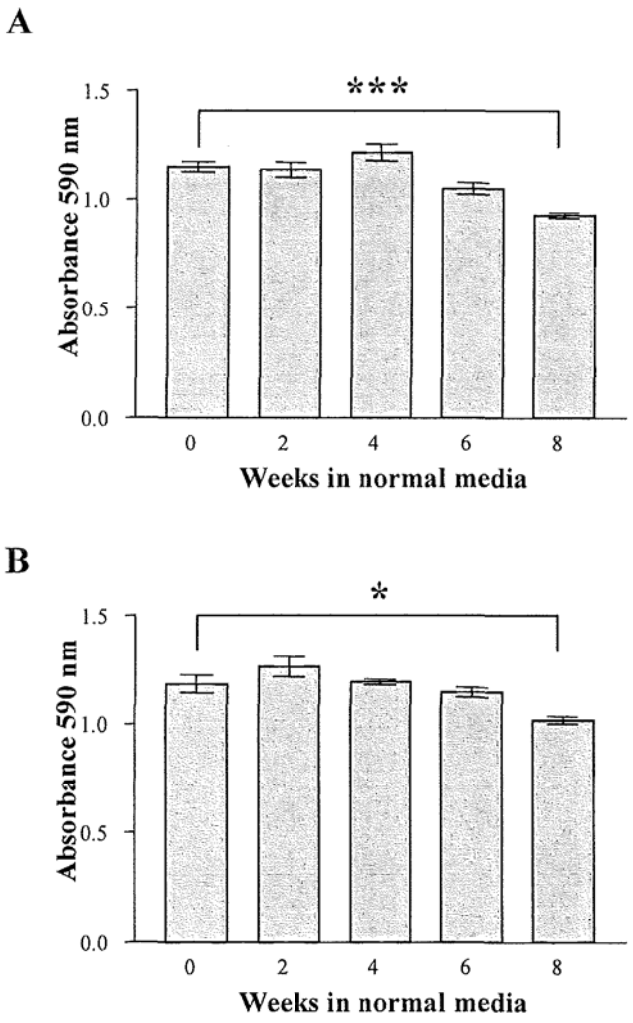

Figure 2.1 The density of viable A) NT2.N or B) NT2.N/A cells in consecutive wells of a CellBIND 6-well plate. Results are expressed as the A_{590} of cells assayed for viability as determined by MTT reduction every two weeks for eight weeks. Bars represent the mean ± SEM of octuplicate samples from a single experiment. Brackets indicate compared columns that differ statistically, *P<0.05, **P<0.01, ***P<0.001.

2.3.3 Cell characterisation using western blotting

Western blotting was routinely used with each batch of cells to confirm cell phenotype via the identification of protein antigens using antibodies. Cellular protein was extracted from the NT2.D1, CCF-STTG1, NT2.N and NT2.N/A cells and analysed by SDS PAGE and western blot using anti-GFAP, anti-β-tubulin III, anti-NSE or anti-NF68 primary antibodies to detect the protein of interest. The following show scans of representative western blots obtained.

2.3.3.1 Glial Fibrillary Acidic Protein (GFAP)

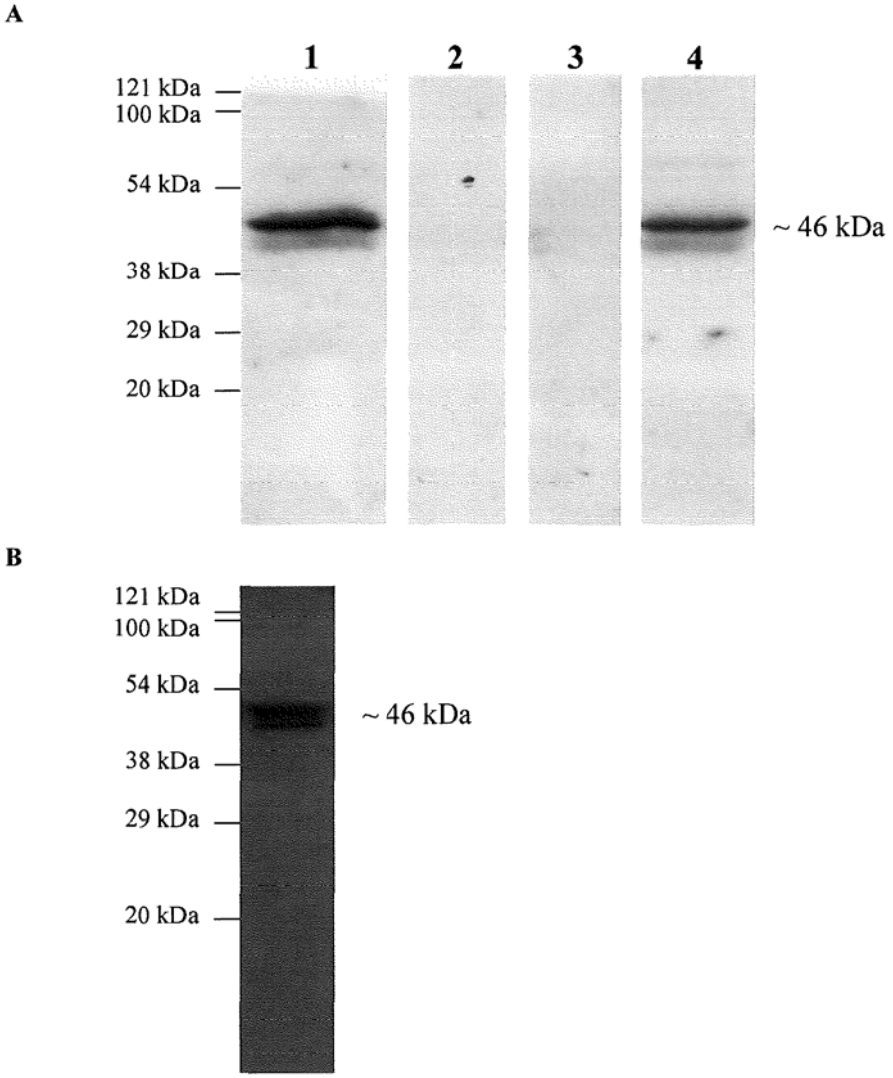

Figure 2.2 Analysis of Glial Fibrillary Acidic Protein (GFAP). Cell lysate proteins (prepared from one well from each batch of cells) and the GFAP positive control were analysed by SDS PAGE and western blot. Anti-GFAP immunoblot transferred from 10 % acrylamide SDS PAGE. (A) Lane 1) 10 ng GFAP positive control. Lane 2) 10 µg NT2.D1 protein lysate. Lane 3) 10 µg NT2.N protein lysate. Lane 4) 10 µg NT2.N/A protein lysate. (B) 10 µg CCF-STTG1 protein lysate. Following interpolation with pre-stained protein standards run alongside samples, the darker-band detected by the anti-GFAP antibody can be estimated at approximately 46 kDa.

Immunoblotting was carried out using the mouse anti-GFAP monoclonal IgG antibody to examine for the presence of GFAP in NT2.D1, NT2.N, NT2.N/A and CCF-STTG1 cell lysate proteins and a commercially available GFAP positive control.

It can be seen in figure 2.2 A that a double band was detected in lane 4 and similarly

for the GFAP positive control (lane 1). Comparison with molecular markers revealed the proteins in the darker band to have a molecular weight of approximately 46 kDa. This is consistent with the data provided with the positive control which estimated the GFAP molecular weight to be ~ 46 kDa and thus confirms the presence of astrocytes in the NT2.N/A co-culture (lane 4). The GFAP epitope was not detected in the lanes containing lysate proteins from NT2.D1 or NT2.N cells, therefore it appeared that antibody binding was specific to proteins of an astrocytic phenotype.

It can be seen in figure 2.2 B (CCF-STTG1 cells) that a double band was detected and comparison with molecular markers revealed the proteins in the darker band to have a molecular weight of approximately 46 kDa. This is consistent with the expected astrocytic phenotype of the CCF-STTG1 cell line.

2.3.3.2 Neuron-Specific Enolase (NSE)

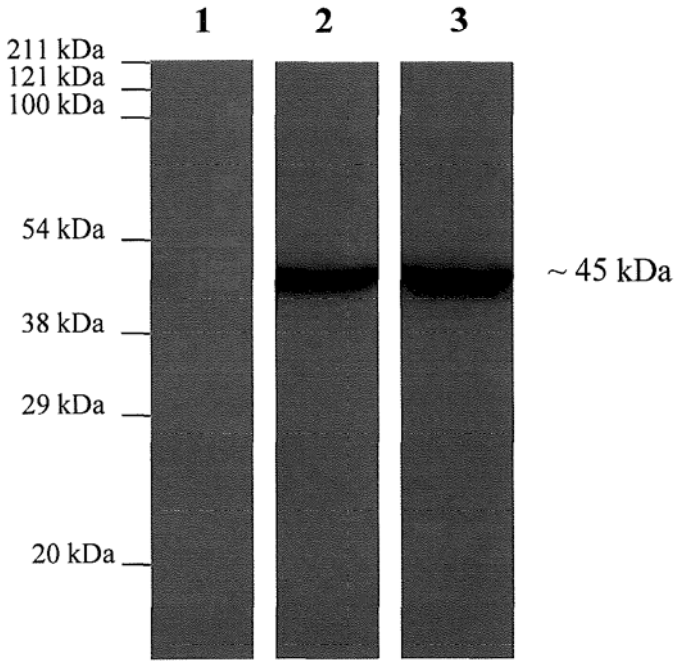

Figure 2.3 Analysis of Neuron-Specific Enolase (NSE) protein. Cell lysate proteins (prepared from one well from each batch of cells) were analysed by SDS PAGE and western blot. Anti-NSE immunoblot transferred from 10 % acrylamide SDS PAGE. Lane 1) 10 µg NT2.D1 protein lysate. Lane 2) 10 µg NT2.N protein lysate. Lane 3) 10 µg NT2.N/A protein lysate. Following interpolation with pre-stained protein standards run alongside samples, the band detected by anti-NSE antibodies can be estimated at approximately 45 kDa.

Immunoblotting was carried out using the mouse anti-NSE monoclonal IgG antibody to examine for the presence of NSE in NT2.D1, NT2.N and NT2.N/A cell lysate proteins. Comparison with molecular markers revealed the proteins to have a molecular weight of approximately 45 kDa (figure 2.3). This is consistent with the expected neuronal phenotype of the NT2.N mono-culture (lane 2) and confirms the presence of neurons in the NT2.N/A co-culture (lane 3). NSE was not detected in the lane containing lysate proteins from the NT2.D1 cells, which is consistent with the non-neuronal phenotype of this culture.

2.3.3.3 β-Tubulin III

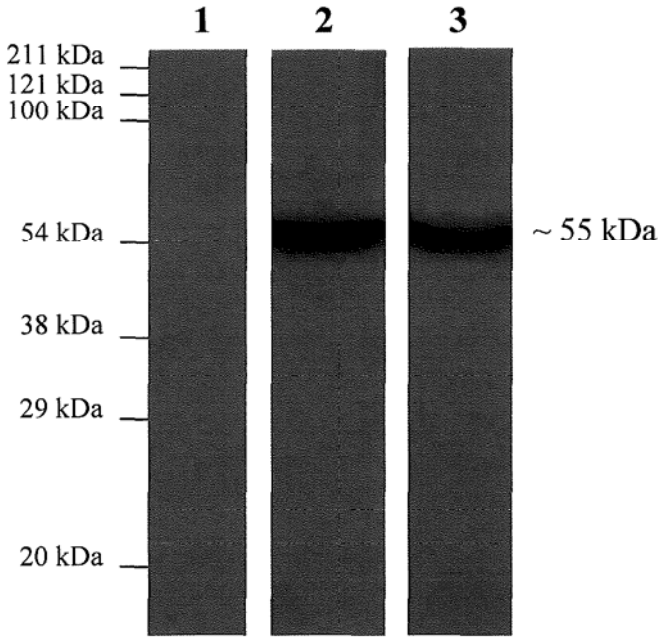

Figure 2.4 Analysis of β-tubulin III protein. Cell lysate proteins (prepared from one well from each batch of cells) were analysed by SDS PAGE and western blot. Anti-β-tubulin III immunoblot transferred from 10 % acrylamide SDS PAGE. Lane 1) 10 μg NT2.D1 protein lysate. Lane 2) 10 μg NT2.N protein lysate. Lane 3) 10 μg NT2.N/A protein lysate. Following interpolation with pre-stained protein standards run alongside samples, the band detected by anti-β-tubulin III antibodies can be estimated at approximately 55 kDa.

Immunoblotting was carried out using the mouse anti-β-tubulin III monoclonal IgG antibody to examine for the presence of β-tubulin III in NT2.D1, NT2.N and NT2.N/A cell lysate proteins. Comparison with molecular markers revealed the proteins to have a molecular weight of approximately 55 kDa (figure 2.4). This is consistent with the expected neuronal phenotype of the NT2.N mono-culture (lane 2) and

confirms the presence of neurons in the NT2.N/A co-culture (lane 3). β-Tubulin III was not detected in the lane containing lysate proteins from the NT2.D1 cells and therefore, antibody binding was specific to proteins of a neuronal phenotype.

2.3.3.4 Neurofilament 68 (NF68)

Immunoblotting was carried out using the mouse anti-NF68 monoclonal IgG antibody to examine for the presence of NF68 in NT2.D1, NT2.N and NT2.N/A cell lysate proteins. Comparison with molecular markers revealed the proteins to have a molecular weight of approximately 68 kDa (figure 2.5). This is consistent with the expected neuronal phenotype of the NT2.N mono-culture (lane 2) and confirms the presence of neurons in the NT2.N/A co-culture (lane 3). NF68 was not detected in the lane containing lysate proteins from the NT2.D1 cells, therefore it appeared that antibody binding was specific to proteins of a neuronal phenotype.

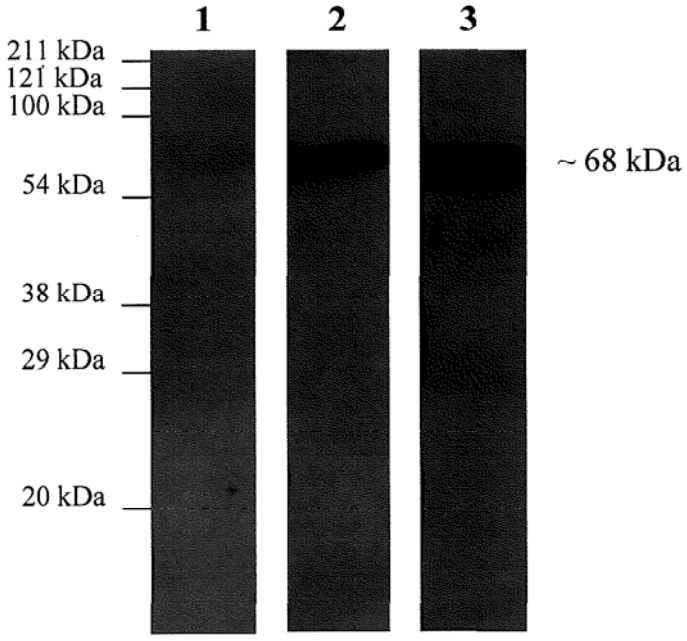

Figure 2.5 Analysis of Neurofilament 68 (NF68) protein. Cell lysate proteins (prepared from one well from each batch of cells) were analysed by SDS PAGE and western blot. Anti-NF68 immunoblot transferred from 10 % acrylamide SDS PAGE. Lane 1) 10 μg NT2.D1 protein lysate. Lane 2) 10 μg NT2.N protein lysate. Lane 3) 10 μg NT2.N/A protein lysate. Following interpolation with pre-stained protein standards run alongside samples, the band detected by anti-NF68 antibodies can be estimated at approximately 68 kDa.

2.3.3.5 Western blotting summary

The NT2.D1 cells were negative for GFAP, NSE, β-tubulin III and NF68 and the CCF-STTG1 cells were positive for GFAP. The NT2.N/A cells were positive for the pan-neuronal markers NSE, β-tubulin III and NF68 and the astrocytic marker GFAP. The NT2.N cells were also positive for NSE, β-tubulin III and NF68 and they were negative for GFAP.

2.3.4 Immunofluorescence microscopy

Specific immunostaining for the intracellular markers GFAP and β-tubulin III, distinguished with secondary antibodies conjugated to different fluorochromes, (GFAP positive astrocytes stained red, β-tubulin III positive neurons stained green) was used to produce images of the NT2.N mono- and NT2.N/A co-cultures (see section 2.2.9).

2.3.4.1 Images of the NT2.N mono-culture

Figures 2.6 A and B show images of an NT2.N mono-culture resulting from treatment of NT2.D1 cells with RA and anti-proliferative agents. Splitting, dissociation and reseeding of differentiated cultures onto pdl/lam coverslips appeared to release large numbers of neural cells. The neuronal cell bodies formed small, evenly dispersed aggregations (50-100 μm) with linking bundles of neurites that had frequent branches to thinner processes. The extensive interconnecting neuritic fascicles covered the entire surface of the coverslip. The vast majority of cells showed positive staining for the neuronal marker β-tubulin III, confirming their neural nature. Additionally, the NT2.N mono-culture was negative for GFAP staining.

Neurons typically have a single axon and multiple dendrites. Figure 2.6 C shows an example of an aggregation of neuronal cell bodies at higher magnification and the extending neurites may be clearly seen but they were not distinguishable as dendrites and axons.

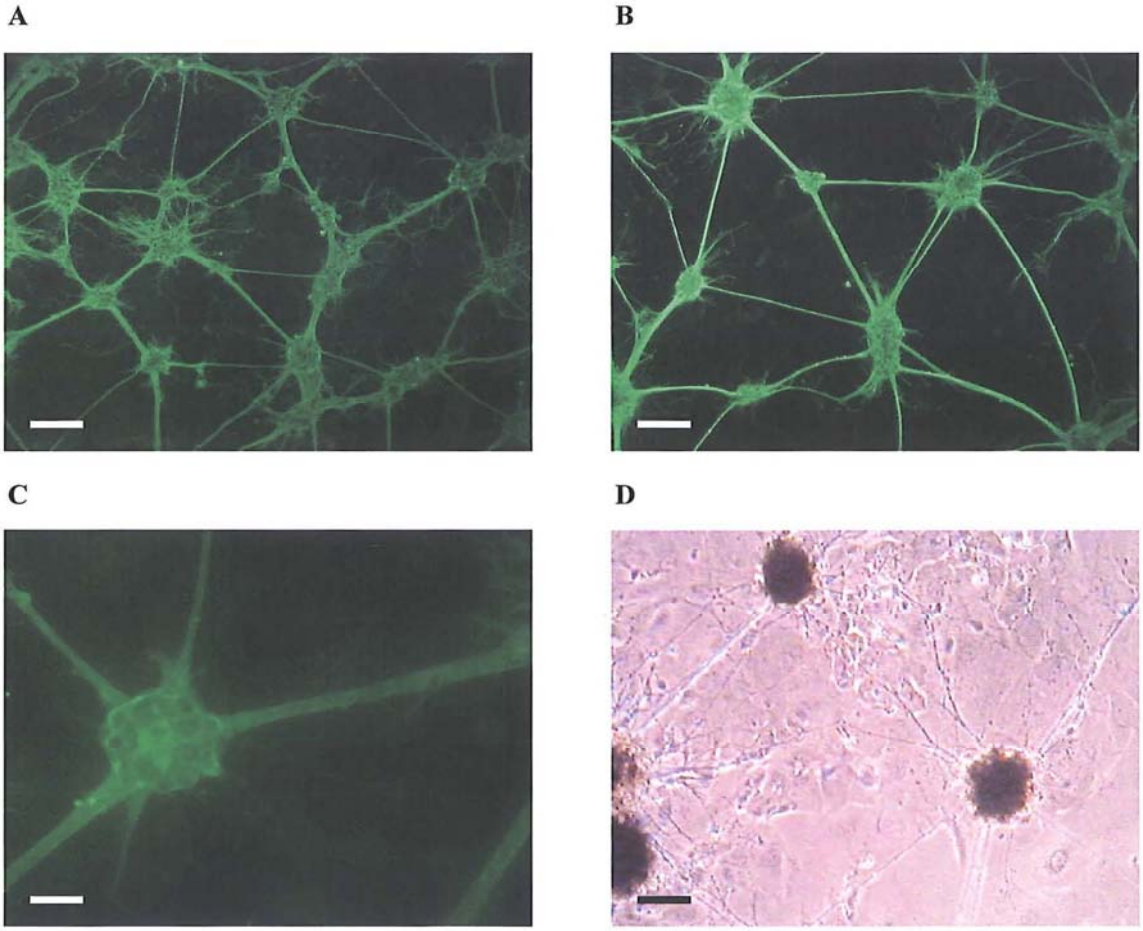

Figure 2.6 Immunostaining of the NT2.N mono-culture for β-tubulin III. A) and B) Interconnecting β-tubulin III positive, neuritic fascicles covering the surface of the pdl/lam coverslip. C) An aggregation of β-tubulin III neuronal cell bodies with extending neurites. D) Unstained NT2.N cells. Scale bar, A-B 100 μm, C 40 μm, D 75 μm.

As mentioned, the images in figure 2.6 A-C are of NT2.N cells grown on pdl/lam coverslips. However, the differentiation of the NT2.D1 cell line proceeded equally well when the differentiated cells were reseeded onto CellBIND 6-well plates prior to anti-proliferative treatment. Figure 2.6 D shows an example of unstained NT2.N cells, although these 6-well plates were difficult to photograph clearly. Despite the poor quality, the image demonstrates that aggregations of retinoic acid induced cells adhered to CellBIND plastic and showed evidence of neuritic network formation as significant as with the pdl/laminin substrate.

2.3.4.2 Images of the NT2.N/A co-culture

Alternatively, the use of a lower concentration of anti-proliferative agents over a longer period allowed for limited cell proliferation and the formation of colonies of GFAP positive cells to give a co-culture of both neurons and astrocytes. Images of the resulting NT2.N/A co-culture are shown in figures 2.7 A and B.

Similar to the images of NT2.N cells (figures 2.6 A and B), evenly dispersed aggregations of neuronal perikarya with linking bundles of neurites were visible. Confirmation of the neuronal nature of the cell bodies and large numbers of branching neurites was demonstrated by their positive staining for β-tubulin III. These neuronal structures appeared to form a network on a supporting monolayer of GFAP positive astrocytic cells, suggesting the neurons have an affinity for the astrocytes. It can be seen in the images taken at higher magnification (figures 2.7 C and D) that some of the astrocytes were obviously associated with the neurons, with clustering around the aggregations of neuronal cell bodies and between neurite outgrowths.

Figures 2.7 E and F show GFAP positive cells. These images demonstrate that some of these cells exhibit the stellate morphology and short processes expected of human astrocytes. Some of the GFAP positive cells were more rounded in shape with a large volume taken over by the cell nucleus (figure 2.7 F).

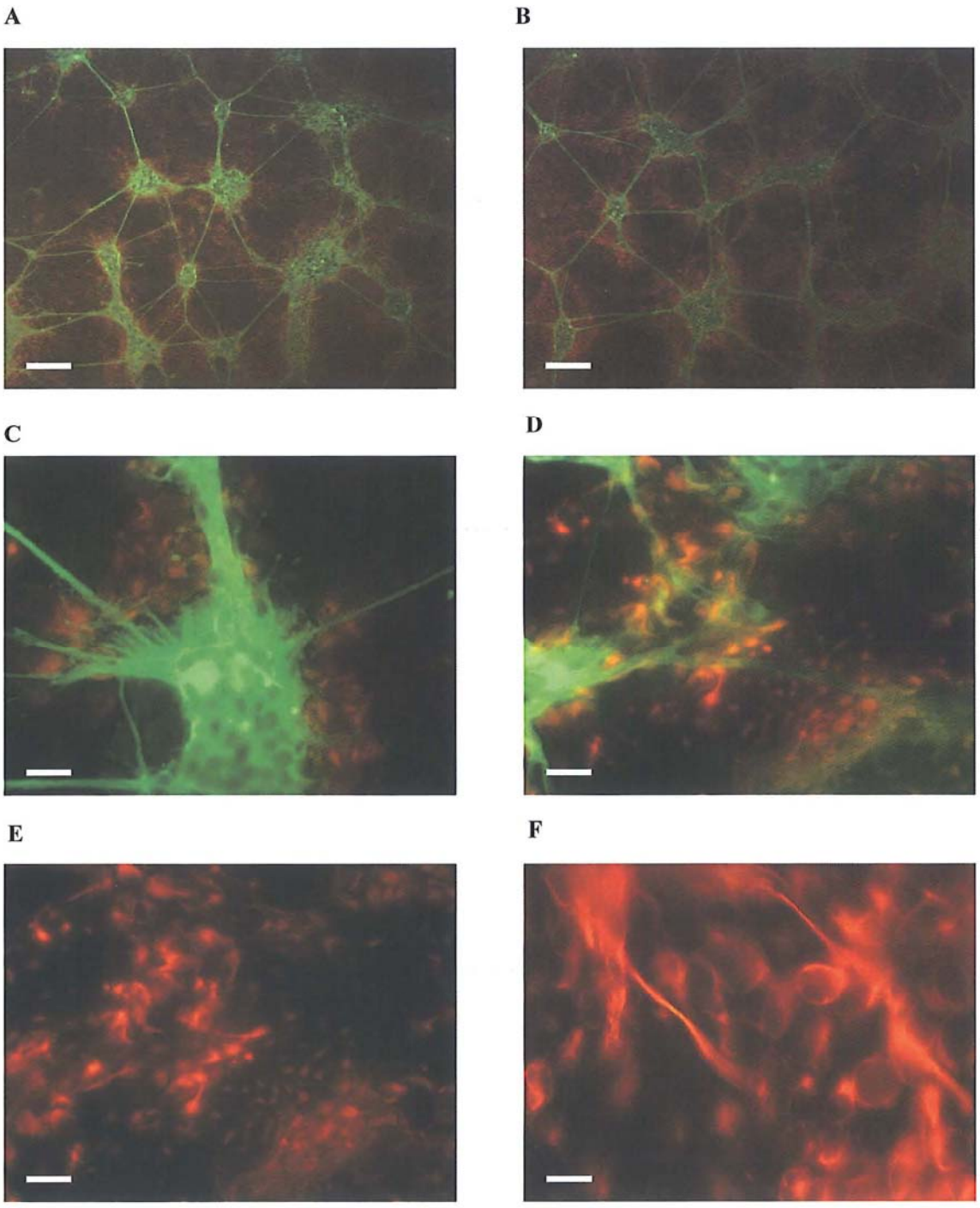

Figure 2.7 Immunostaining of the NT2.N/A co-culture for β-tubulin III and GFAP. A) and B) Aggregations of β-tubulin III positive neuronal perikarya with linking bundles of neurites, on a monolayer of GFAP positive astrocytic cells. C) and D) GFAP positive astrocytes clustering around the aggregations of β-tubulin III positive neuronal cell bodies and between neurite outgrowths. E) and F) GFAP positive astrocytic cells. Scale bar, A-B 100 μm, C-E 40 μm, F 15 μm.

2.3.4.3 Quantitative analysis

The proportion of neurons and astrocytes in three representative batches of NT2.N/A cells grown on pdl/lam coverslips were estimated by manual counting of β-tubulin III and GFAP expressing cells and total cell nuclei, using a fluorescent microscope after specific immunostaining (section 2.2.9). The percentage of cells was calculated as the number of each type of immunopositive cell reported to the total number of nuclei.

Figures 2.8 A-D show examples of the individual and layered images from which the different cell types were counted. The actual manual counting of each cell type (nuclei - DAPI (blue), GFAP positive - REDX (red) and β-tubulin III positive - FITC (green)) was carried out from the monitor with the aid of the software zoom function and a grid. Figures 2.8 E and F show an example of an image of the cell nuclei and GFAP positive cells respectively, at higher magnification.

The DAPI counter-staining was very clear and counting the total number of cell nuclei was relatively straightforward. The FITC fluoresced brightly but stained neurons within the cellular aggregates were at times difficult to count due to their close proximity. There was no REDX staining in these areas so it was assumed that the DAPI-stained cell nuclei were those of neurons. The REDX staining was less bright but with the zoom function it was possible to distinguish the astrocytes the majority of the time. Following these considerations, it was estimated that the NT2.N/A co-culture consisted of a large number of GFAP positive astrocytes (58 ± 7 %, n=3) along with Tuj1 positive neurons (27 ± 4 %, n=3). Therefore, the ratio of NT2 astrocytes to NT2 neurons was approximately 2:1.

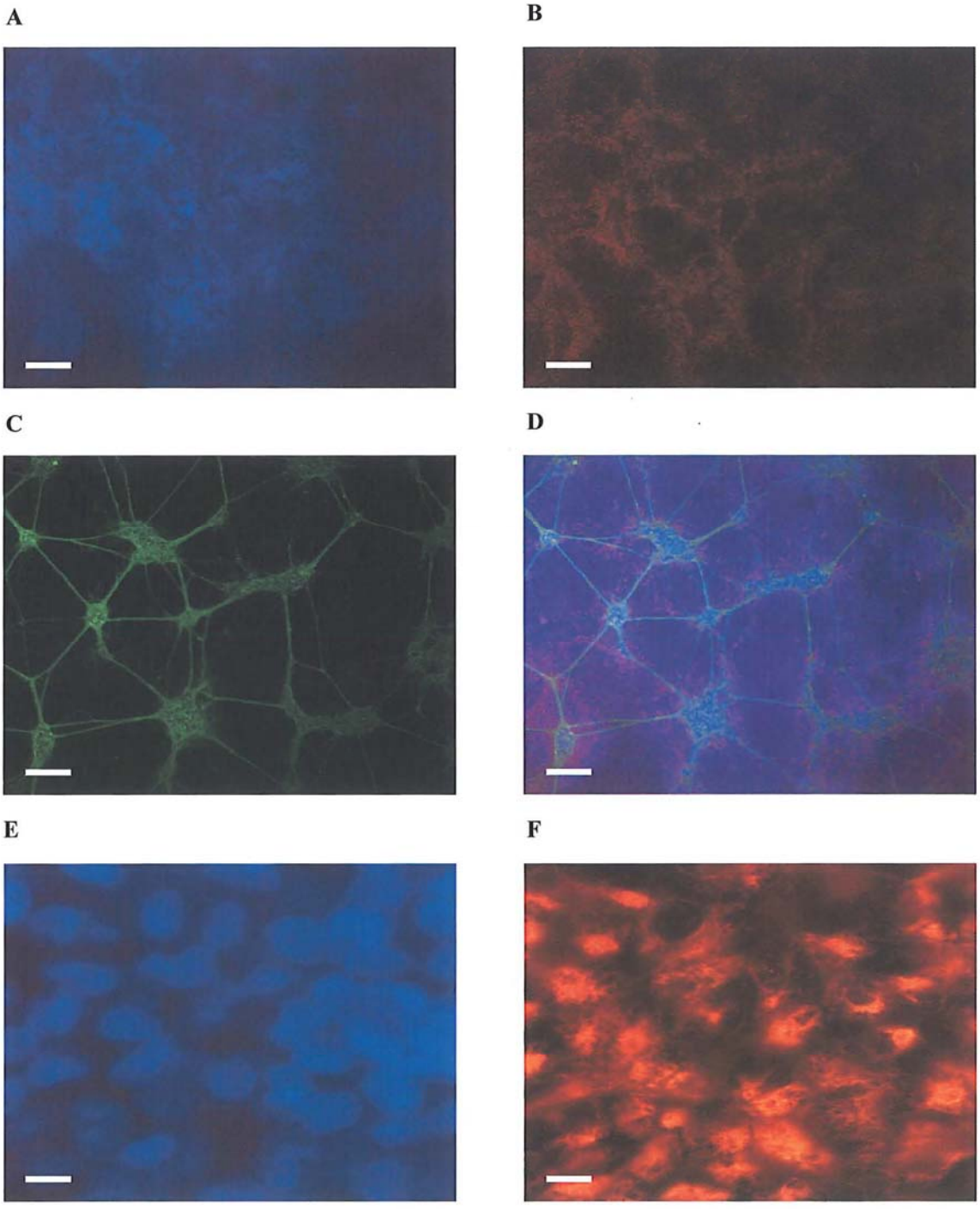

Figure 2.8 Immunostaining of the NT2.N/A co-culture for β-tubulin III and GFAP with DAPI counter stain for cell counting. A) GFAP positive astrocytic cells. B) Cell nuclei counterstained with DAPI. C) β-tubulin III positive neuronal cells. D) Collective layered image of A, B and C. E) Cell nuclei counterstained with DAPI. F) GFAP positive astrocytic cells. Scale bar, A-D 100 μm, E-F 15 μm.

2.3.5 Confocal microscopy

Some of the slides prepared in section 2.4.2 were also viewed using a confocal microscope, with visualisation of the GFAP (REDX - red) and β-tubulin III (FITC - green) markers but not the DAPI (blue) counter-stained nuclei.

Figures 2.9 A and B show examples of the NT2.N and NT2.N/A images, respectively. The FITC staining of β-tubulin III positive neurons was much clearer than that obtained using the fluorescent microscope and demonstrated that although grown in monolayer culture, the aggregations of neuronal bodies had a 3-D nature (figure 2.9 A). The REDX staining was also more highly visible using this microscope, again showing GFAP positive astrocytes clustering around the aggregations of neuronal bodies and between the linking bundles of neurites and neurite outgrowths (figure 2.9 B). The NT2.N mono-culture was negative for GFAP staining (figure 2.9 A).

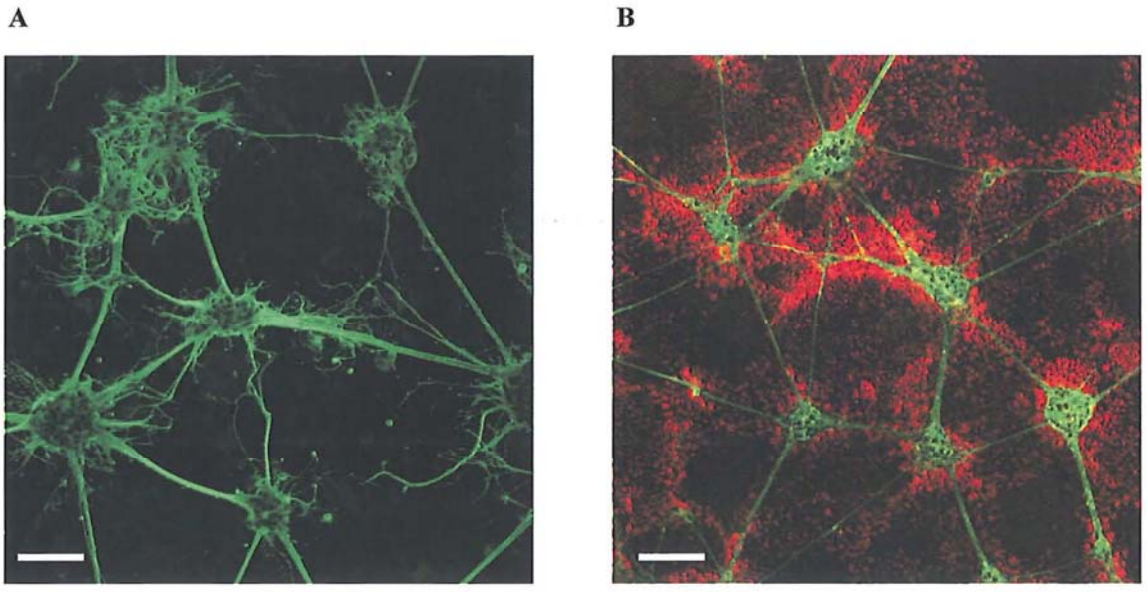

Figure 2.9 Immunostaining of the NT2.N mono- and NT2.N/A co-culture for β-tubulin III (green) and GFAP (red). A) NT2.N mono-culture. B) NT2.N/A co-culture. Scale bar, A-B 100 μm.

2.4 Discussion

In this study, the human NT2.D1 embryonal carcinoma (EC) cell line was differentiated into a mono-culture of post-mitotic neurons (NT2.N), or a co-culture of post-mitotic neurons and astrocytes (NT2.N/A), according to the published protocols of Pleasure *et al.*, (1992) and Bani-Yaghoub *et al.*, (1999) respectively, with some modifications. The cultures were produced at weekly intervals, yielding sufficient numbers of cells and allowing for comparison of the sensitivity to toxic insult of the post-mitotic NT2.N/A co-culture with a culture of NT2.N cells alone, as well as with the mitotic NT2.D1 neuronal precursor cell line and CFF-STTG1 astrocytoma cells.

Following retinoic acid treatment of the NT2.D1 cell line, traditionally the resulting differentiated neurons are plated onto petri-dishes coated with pdl/lam, to promote neurite outgrowth during mitotic inhibitor treatment (Manthorpe *et al.*, 1983). However, this method has the disadvantage of having to chemically remove differentiated cells from the coated surface prior to carrying out certain experimental procedures, which may disrupt vital cell-cell interactions. Therefore, the differentiation protocol was modified and differentiated neurons were instead plated onto CellBIND 6-well plates that possess an innovative polymer surface to promote cell attachment and spreading. This novel protocol modification conferred two main advantages over existing systems, in that experimental procedures could be carried out on cultures in situ and six different toxin concentrations could be examined in one inexpensive plate, allowing for high-throughput screening of compounds of interest.

Differentiation is the process leading to the expression of phenotypic properties characteristic of the functionally mature cell *in vivo*. For mature mammalian neurons, this includes loss of the ability to proliferate after they begin to form axons and dendrites. They thus become post-mitotic and any neurons within the CNS which are lost to toxic damage can not be replaced by the proliferation of surviving cells (Kleinsmith and Kish, 1995). It has been shown that *in vivo* and *in vitro*, retinoic acid induces growth arrest and terminal differentiation along a neuronal pathway (Bani-Yaghoub *et al.*, 1999; Baldassarre *et al.*, 2000). The post-mitotic status of the mono-cultures of NT2.N and co-cultures of NT2.N/A cells produced was confirmed using an

MTT assay. The cultures demonstrated no increase and rather a slight decrease in cell number over time (eight weeks), which was more pronounced in the NT2.N than the NT2.N/A culture and may be accounted for by a low-level of background apoptosis. From these observations the cultures were suggested to be post-mitotic but ideally a more sophisticated method to demonstrate the exit of the cells from the cell cycle is required.

Whilst transformed cell lines may not share the exact features of primary neural tissue, cell-cultures were successfully produced that demonstrated morphological characteristics of post-mitotic CNS neurons, following retinoic acid (1×10^{-5} M) and mitotic inhibitor treatment of the NT2.D1 cell line. Whether plated onto CellBIND plastic or pdl/lam coverslips, the NT2.N cells formed small, evenly dispersed aggregations that subsequently elaborated extensive and linking bundles of neuritic processes. Some processes bound together to form thick fascicles linking adjacent islands of neural perikarya, similar to those described by previous groups (Pleasure *et al.*, 1992; Younkin *et al.*, 1993; Marchal-Victorion *et al.*, 2003). Neurons typically have a single axon and multiple dendrites and NT2.N neuritic processes have previously been identified using molecular markers as dendrites or axons (Pleasure *et al.*, 1992) but this confirmation was not undertaken in the current study.

The neuronal phenotype of the NT2.N cultures produced was confirmed via immunochemical identification of a number of typical neuronal markers. Cells were shown to express β-tubulin III via immunofluorescence. β-tubulin III is a neuron-specific cytoskeleton component and should not identify the β-tubulin found in glial cells (Stewart *et al.*, 2003). Immunoblotting was carried out to compliment the fluorescence studies, yielding detectable amounts of neuron-specific enolase (NSE), the low molecular weight triplet protein NF68 and β-tubulin III. These correspond to markers detected following extensive characterisation of NT2.N cells by Pleasure *et al.*, (1992), from whom the mono-culture differentiation protocol was derived. It should be noted that in this study, the amounts of the expressed proteins were not quantified and thus absolute consistency of batch-to-batch expression was not confirmed.

The NT2.N cultures were deemed to be a purified population of neurons, as supported

by the lack of detectable expression of GFAP positive cells following examination by immuno-blot or fluorescence microscopy. Visually, there was no evidence of residual EC-like cells but this was not confirmed by negative expression for EC marker antigens, such as SSEA-3, SSEA-4 and TRA-1-60 (Andrews, 1988). NT2.N cells have also been shown to express many neuronal markers characteristic of CNS neurons, including a CNS specific 66 kDa neurofilament protein and NeuN, a protein specifically localised in the nucleus of terminally differentiated CNS neurons (Pleasure *et al.*, 1992; Younkin *et al.*, 1993; Megiorni *et al.*, 2005). Confirmation of the CNS nature of the NT2 neurons produced in this study was not undertaken. However, the phenotypic characterisation of the cells that was conducted suggests that efficient adaptation of the differentiation protocol from the literature was accomplished. Thus it was speculated that production of a population of CNS like neurons had been achieved.

In addition to a mono-culture of NT2 neurons, a co-culture of NT2 neurons and NT2 astrocytes (NT2.N/A) was also successfully produced. This was in agreement with Bani-Yaghoub *et al.*, (1999), who was the first to demonstrate that that the pleuripotent NT2.D1 cell line has the capacity to differentiate into an integrated population neurons and astrocytes and from whom the co-culture differentiation protocol was derived. Whether plated onto CellBIND plastic or pdl/lam coverslips, the NT2.N cells formed aggregations of neuronal perikarya linked by large numbers of branching neurites. These neuronal structures appeared to form a network on a supporting layer of NT2 astrocytes (NT2.A). Many of these astrocytic cells appeared to be clustered around the neuronal aggregations and between the neurite outgrowths. Astrocytes are star-shaped because of cytoplasmic processes that contain a large number of intermediate filaments composed of GFAP and many of the NT2.A cells appeared to exhibit such a characteristic stellate morphology. These observations were similar to those of previous groups who have described NT2.N/A co-cultures (Bani-Yaghoub *et al.*, 1999; Sandhu *et al.*, 2002; Stewart *et al.*, 2003).

As with the NT2.N mono-culture, the phenotype of the NT2.N cells in the co-culture was confirmed via immunochemical identification of detectable levels of β-tubulin III, NSE and NF68. The additional presence of NT2.A cells in the culture was established via detection of GFAP positive cells by immuno-blot and fluorescence microscopy and

thus the NT2.N/A cultures were deemed to be a population of neuronal cells in co-culture with astrocytes.

As was expected, the precursor EC cell line NT2.D1 was found to be negative for expression of the selected neuronal markers. Additionally, as suggested by the literature, the CCF-STTG1 astrocytoma cell line demonstrated detectable levels of GFAP (Barna *et al.*, 1985).

The proportion of NT2.A to NT2.N cells in the co-culture was estimated to be 2:1 by manual counting of cells using a fluorescent microscope, following specific immunostaining for neurons, astrocytes and total cell nuclei. This was a laborious process as the astrocytes stained less clearly than the neurons, thus the percentage of each cell type present should be regarded as an approximate figure. Additionally, the confocal images demonstrated the morphology of the co-culture more visibly than those obtained using the fluorescent microscope and it was evident that the aggregations of neuronal cell bodies had a 3D nature, which may have resulted in under-estimation of the number of NT2.N cells counted in 2D, using the fluorescent microscope. However, the quantification of each cell type was statistically consistent in three separate batches of cells and the 2:1 ratio of neurons to astrocytes was in good agreement with Bani-Yaghoub *et al.*, (1999), who also used this method of cell counting. *In vivo*, astrocytes outnumber neurons by at least 10:1 but *in vitro* astrocytes have been shown to provide a protective function over neurons at a ratio of 1:4 (Xu *et al.*, 1999; Gegg *et al.*, 2003). Thus, it was anticipated that the 2:1 ratio would provide adequate evidence of an astrocytic protective effect.

The morphology of the cultures produced and pattern of neuronal and astrocytic marker expression reported in this chapter indicates that the differentiation of the pleuripotent NT2.D1 cell line into post-mitotic neuronal and neuronal-astrocytic like cultures may be achieved in a convenient 6-well plate format, without the need for biological coatings. The results suggest that the NT2.N and NT2.N/A cultures may be useful *in vitro* as an alternative to human primary neural tissues for high throughput neurotoxicological testing. It was also found that sufficient numbers of the mitotic NT2.D1 and CCF-STTG1 cell lines and the post-mitotic NT2.N and NT2.N/A cultures

could be readily generated in sufficient numbers on a weekly basis for high-throughput screening. Following consideration of these results it was concluded that these four human cell systems were suitable for use in the preliminary development of an *in vitro* test battery for the rapid preliminary screening of compounds for acute neurotoxic potential in humans.

Chapter 3 – Determination of basal cytotoxicity

3.1 Introduction

As was stated eloquently by Paracelsus (1493-1541), '*What is there that is not a poison? All things are poison and nothing (is) without poison. Solely the dose determines that a thing is not a poison*'. As such, cytotoxicity is the cell-killing property of a chemical and is simply dependent on exposure to a high enough concentration of toxin. High levels of toxicity typically result in lethal cell injury such as necrosis or apoptosis, whereas the mechanisms underlying the toxic effect of a compound are often a result of a subtle disruption to basic biochemical processes. Whilst what practically distinguishes a neurotoxin from a cytotoxin is a nervous tissue specific response at a pharmacologically relevant concentration, a measure of basal cytotoxicity was first required for the stepwise assessment of the neurotoxic potential of the selected test chemicals.

In order to rapidly compare the basal cytotoxic potential of the test chemicals in each of the different cell systems, a range-finding study was conducted to establish the concentration at which 50 % of cell viability was affected following 4- and 24-hours exposure. This was done using the widely employed MTT reduction assay, which is a rapid, reliable and quantitative colorimetric method for determining mammalian cell viability *in vitro* (Tada *et al.*, 1986; Lamarche *et al.*, 2003). It was considered that development of 6-well plate MTT assay format would be appropriate for the high-throughput screening of the test chemicals for basal cytotoxicity. Additionally, the range-finding study allowed the estimation of the non-cytotoxic concentration range for each test chemical at the 4-hour timepoint, which was required later in the study.

3.2 Materials and methods

3.2.1 Materials

For materials, refer to Chapter 2, section 2.2.1.

3.2.2 MTT reduction assay

The MTT colorimetric reduction assay for determining mammalian cell viability, is based on the cleavage of the tetrazolium ring of MTT (3-(4,5-dimethylthazol-2-yl)-2,5-diphenyl tetrazolium bromide) by dehydrogenase enzymes in active mitochondria, to form a blue formazan product (Denizot and Lang, 1986; Lamarche *et al.*, 2003). Following solubilisation of the formazan crystals, the blue colour can be quantified by spectrophotometric means and is linearly proportional to metabolic activity present in culture up to an optical density of 1.2 (Mosmann, 1983). This reduction assay was originally developed by Mosmann (1983), and since then many variations of his method have arisen. The protocol that follows is based on that of Tada *et al.*, (1986) but with reagent volumes scaled to adapt the MTT assay from the traditionally used 96-well microplate to a 6-well CellBIND plate format. This gave the advantage of both toxin exposure and assay of cell viability in the same plate as the NT2.N and NT2.N/A cells were enriched following replate #2 (section 2.2.5), so cell-cell interactions were not disrupted by scraping and reseeding into 96-well plates.

3.2.2.1 Protocol

Following toxin exposure for 4- or 24-hours (section 3.2.3), cells were washed with fresh medium and 1 ml medium added to each well. To this were added 300 µl of MTT (5 mg/ml in PBS) and the plate was incubated in a humidified chamber at 37 °C in 5 % CO_2, 95 % air, for 4-hours, to allow for accumulation of formazan crystals. Following this, 1 ml of a 6.6 % (w/v) SDS solution in 0.01 N HCl was added and the plate incubated overnight to solubilise the formazan and give a homogeneous solution. A multipipette was used to transfer 230 µl of control and treated, solubilised samples (eight determinations per well) to a clear 96-well plate and the A_{590} read using a Thermo Multiskan EX, 96-well microplate spectrophotometer (Thermo Electron

Corporation, USA) with Ascent software. Change in MTT reduction with exposure to increasing concentration of toxin was expressed as a percentage decrease in the A_{590} below that of the untreated control value.

3.2.3 Exposure of cells to test chemicals

3.2.3.1 NT2.D1 and CCF-STTG1 cells

Cells were counted using a haemocytometer in conjunction with the vital stain neutral red, to distinguish between viable and non-viable cells. Cells were then plated out in their usual medium at a density of 5 x 10^5 viable cells per well of a 6-well plate and left in a humidified chamber overnight at 37 °C in 5 % CO_2, 95 % air. The medium was removed and the cells washed with fresh medium. The cells were then incubated in the presence of 2 ml of medium supplemented with increasing concentrations of test chemical (table 3.1). Nine to twelve wells were used in total per toxin, with one well utilised per toxin concentration and cells with medium only acted as an untreated control. Medium only without cells acted as a background control. The plates were then replaced in the humidified chamber at 37 °C in 5 % CO_2, 95 % air, for 4- or 24-hours, before carrying out the MTT assay as described in section 3.2.2.1.

3.2.3.2 NT2.N and NT2.N/A cells

Cultures of NT2.N or NT2.N/A cells were produced according to section 2.2.5. The medium was removed and the cells washed with fresh medium. The cells were then incubated in the presence of 2 ml of medium supplemented with increasing concentrations of test chemical (table 3.1 below). Nine to twelve wells were used in total per toxin, with one well utilised per toxin concentration and cells with medium only acted as an untreated control. Medium only without cells acted as a background control. The plates were then replaced in the humidified chamber at 37 °C in 5 % CO_2, 95 % air, for 4- or 24-hours, before carrying out the MTT assay as described in section 3.2.2.1.

Test chemical	Cell line	Concentration range		
		4-hours	24-hours	units
2,5-Hexanedione (2,5-HD)	NT2.D1	22-426	8-85	mM
	CCF-STTG1	43-552	8-117	
	NT2.N	43-636	8-85	
	NT2.N/A	43-636	8-117	
2,3-Hexanedione (2,3-HD)	NT2.D1	8-82	4-82	mM
	CCF-STTG1	8-82	8-82	
	NT2.N	4-82	8-82	
	NT2.N/A	8-98	4-98	
3,4-Hexanedione (3,4-HD)	NT2.D1	8-82	8-82	mM
	CCF-STTG1	8-82	8-82	
	NT2.N	8-82	8-82	
	NT2.N/A	8-82	8-98	
Trimethyltin chloride (TMT-Cl)	NT2.D1	0.25-5	0.01-1	mM
	CCF-STTG1	0.25-5	0.02-1.2	
	NT2.N	0.1-5	0.01-1.4	
	NT2.N/A	0.5-6	0.04-1.8	
Tributyltin chloride (TBT-Cl)	NT2.D1	1-25	0.2-6	μM
	CCF-STTG1	2-30	0.1-10	
	NT2.N	0.5-7.5	0.1-7.5	
	NT2.N/A	0.5-10	0.1-7.5	

Table 3.1 Concentration range of test chemical each cell line exposed to for 4- or 24-hours. Medium only acted as an untreated control.

3.2.4 Effect of test chemical pre-solubilisation on cell viability

All the test chemicals were readily soluble in cell culture medium, with the exception of tributyltin chloride (TBT-Cl) that required pre-solubilisation in ethanol before dilution using medium. In order to confirm that the concentration of ethanol required for TBT-Cl solubilisation was not itself toxic to cells, a simple MTT assay was used to assess its effects on the viability of cell line cultures. To a well containing 5 x 10^5 viable CCF-STTG1 or NT2.D1 cells, or NT2.N and NT2.N/A cells as prepared in section 2.2.5, were added 2 ml of appropriate medium, supplemented with 0.5 μM ethanol. Plates were incubated for 4- or 24-hours and the MTT assay was then carried out as detailed in section 3.2.2.1. Four determinations were made per well and the experiment was performed on two separate occasions.

3.2.5 Calibration of the MTT Assay

As the A_{590} measured in the MTT assay is linearly proportional to the number of metabolically active cells present in culture only up to an optical density of 1.2, the optimum seeding density was established for each cell line. Four determinations were made per well and the experiment was performed on two separate occasions.

3.2.5.1 NT2.D1 and CCF-STTG1 cells

Following counting using a haemocytometer in conjunction with the vital stain neutral red, to distinguish between viable and non-viable cells, increasing numbers of cells were seeded onto a 6-well plate in a 2 ml volume of the appropriate fresh medium. Medium only acted as a no cell control. The cells were then incubated overnight in a humidified chamber, at 37 °C in 5 % CO_2, 95 % air to allow for cell attachment and division. Then the MTT assay was carried out as described in section 3.2.2.1

3.2.5.2 NT2.N and NT2.N/A cells

Following replate #1 (section 2.2.5.1) and mechanical dislodging, the resulting floating cells were collected by centrifugation, washed with fresh medium and counted using a haemocytometer in conjunction with the vital stain neutral red. Cells were then seeded at increasing numbers onto CellBIND 6-well plates (replate #2) in a 2 ml volume of fresh medium supplemented with mitotic inhibitor media (MI) for three (NT2.N cells) or four (NT2.N/A cells) weeks (section 2.2.5.1-2). Medium only acted as a no cell control. The MTT assay was then carried out as described in section 3.2.2.1

3.2.6 Uniform growth of NT2.N and NT2.N/A cells in CellBIND 6-well plates

A simple MTT assay was used to confirm that each well of an individual 6-well plate and plates of the same batch of differentiated cells contained a statistically equivalent density of viable NT2.N or NT2.N/A cells following differentiation of the NT2.D1 cell line. Following the culture of NT2.N or NT2.N/A cells in CellBIND 6-well plates (section 2.2.5) cells were washed with fresh medium, 2 ml medium added to each well and the MTT assay was carried out as described in section 3.2.2.1. Four determinations were made per well and the experiment was performed for three separate plates from

the same batch.

3.2.7 Data analysis

The data analyses were carried out using GraphPad Prism software.

Each independent MTT experiment used eight determinations per toxin concentration and data are presented as the mean ± standard error of the mean (SEM) of four independent experiments, unless otherwise stated in the methods.

Log IC_{50} value = log concentration of chemical which resulted in a 50 % inhibition of MTT reduction, i.e. a 50 % decrease in cell viability below that of the untreated control. The mean log IC_{50} ± log SEM values of the four independent MTT experiments was determined using Graphpad Prism non-linear regression curve fit (variable slope) analysis. One-way ANOVA followed by the Tukey post-test was used to determine significant differences between the log IC_{50} values. Cell line and treatment related differences were considered significant at $P < 0.05$.

One-way ANOVA followed by the Tukey post-test was used to determine any significant differences between cell densities. One-way ANOVA followed by the Dunnett's multiple comparison test was used to determine significant increases in the A_{590} with increasing cell number, from the medium only control. Differences were considered significant at $P < 0.05$.

One-way ANOVA followed by the Dunnett's multiple comparison test was used to determine the No Observed Adverse Effect Level (NOAEL) at 4-hours, for each toxin. The NOAEL for each toxin was considered to be the highest concentration used at which the A_{590} was not significantly decreased below that of the untreated control ($P > 0.05$). Concentrations below the NOAEL were considered to encompass the non-cytotoxic range of a test chemical at 4-hours.

3.3 Results

3.3.1 Determination of test chemical IC_{50} values

The range-finding MTT assay was carried out as described in section 3.2.2.1 and the change in cell viability (as determined by MTT reduction) with exposure to increasing concentration of test chemical for 4- or 24-hours, was expressed as a percentage decrease in the A_{590} below that of the untreated control value. Following this, the corresponding log IC_{50} values were determined in order to compare the sensitivity of the NT2.N/A co-culture to the culture of NT2 neurons and CCF-STTG1 astrocytoma cells alone and with the undifferentiated non-neuronal NT2.D1 cell line, after acute exposure to cytotoxic concentrations to the various test chemicals. The log IC_{50} values and respective IC_{50} values generated by the MTT assay are summarised in tables 3.2a and 3.2b, section 3.3.1.7.

3.3.1.1 2,5-Hexanedione

As can be seen in Figure 3.1 A, increasing concentrations of 2,5-hexanedione (2,5-HD; 0-636 mM, table 3.1, section 3.2.3) reduced MTT turnover in all four cell cultures after a 4-hour exposure period. Log IC_{50} values (table 3.2, section 3.3.1.7) indicated that 2,5-HD was most toxic to the NT2.D1 cell line (2.0 ± 0.006 log mM) in comparison with the CCF-STTG1 (2.6 ± 0.01 log mM) and NT2.N (2.5 ± 0.009 log mM) cell lines, which demonstrated statistically equivalent sensitivity ($P > 0.05$). 2,5-HD was least toxic to the NT2.N/A cells (2.7 ± 0.001 log mM) and thus the co-culture was significantly less sensitive to the γ-diketone than was the NT2.N mono-culture ($P < 0.001$), which is evident from figure 3.1 A.

Similarly, increasing concentrations of 2,5-HD (0-117 mM, table 3.1, section 3.2.3) reduced MTT turnover in all four cell cultures after a 24-hour exposure period, as can be seen in figure 3.1 B. Log IC_{50} values indicated that 2,5-HD was again most toxic to the NT2.D1 cells (1.1 ± 0.04 log mM) followed by the NT2.N cells (1.6 ± 0.005 log mM) but was least toxic to the CCF-STTG1 (1.9 ± 0.002 log mM) and the NT2.N/A (1.9 ± 0.01 log mM) cells, which demonstrated statistically equivalent sensitivity ($P > 0.05$). Thus, as with 4-hours exposure, the co-culture was again significantly less

sensitive to the γ-diketone than was the NT2.N mono-culture ($P < 0.001$). This is evident from figure 3.1 B.

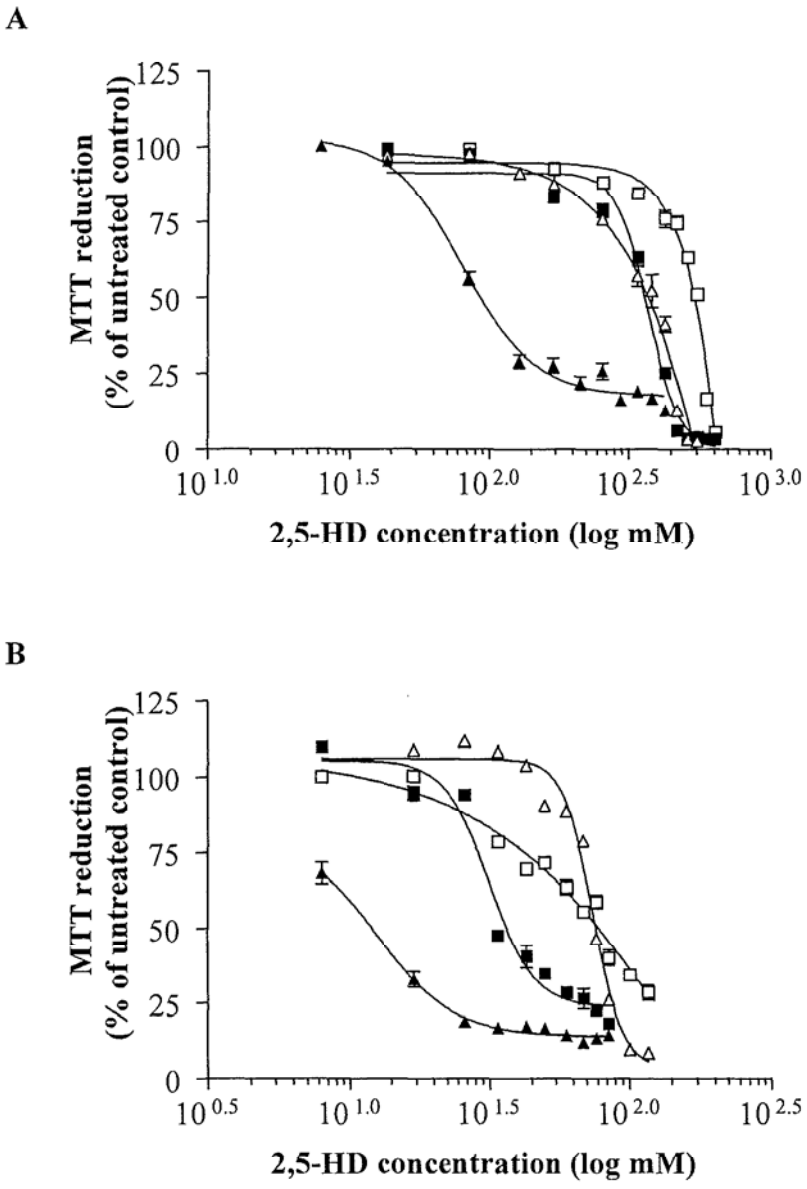

Figure 3.1 Cell viability as determined by MTT reduction following exposure to increasing concentrations of 2,5-hexanedione for 4 (A) or 24 (B) hours. Sigmoidal concentration-response curve (variable slope) for NT2.D1 (▲), CFF-STTG1 (△), NT2.N (■) and NT2.N/A (□) cells. The MTT assay was carried out and the plates read for absorbance at 590 nm. MTT reduction results are expressed as the A_{590} for the toxin treated sample as a percentage of the A_{590} for the untreated control sample. Data points represent the mean ± SEM of the sample means from four separate experiments.

3.3.1.2 2,3-Hexanedione

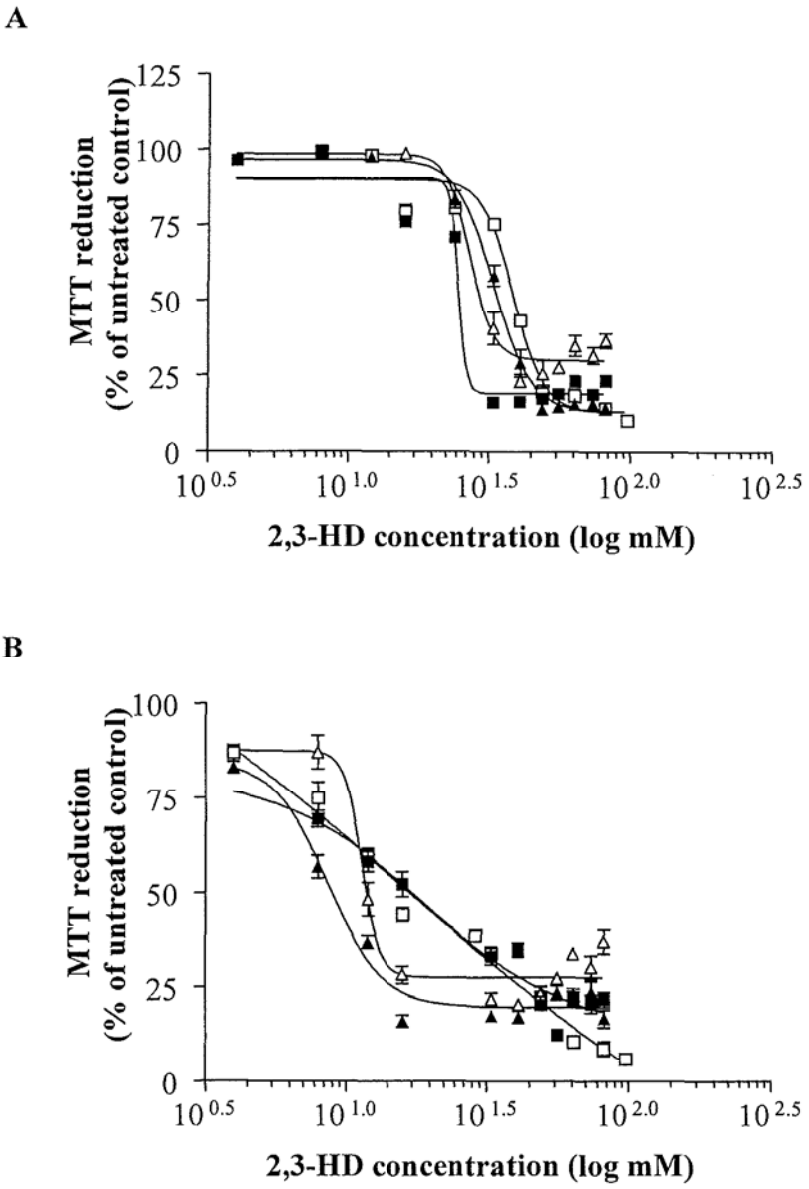

Figure 3.2 Cell viability as determined by MTT reduction following exposure to increasing concentrations of 2,3-hexanedione for 4 (A) or 24 (B) hours. Sigmoidal concentration-response curve (variable slope) for NT2.D1 (▲), CFF-STTG1 (△), NT2.N (■) and NT2.N/A (□) cells. The MTT assay was carried out and the plates read for absorbance at 590 nm. MTT reduction results are expressed as the A_{590} for the toxin treated sample as a percentage of the A_{590} for the untreated control sample. Data points represent the mean ± SEM of the sample means from four separate experiments.

As is evident from figure 3.2 A, increasing concentrations of 2,3-hexanedione (2,3-HD; 0-98 mM, table 3.1, section 3.2.3) reduced MTT turnover in all four cell cultures after a 4-hour exposure period. Log IC_{50} values (table 3.2, section 3.3.1.7) indicated that 2,3-HD was most toxic to the NT2.N mono-culture (1.4 ± 0.004 log mM) in comparison

with the NT2.D1 (1.5 ± 0.008 log mM) CCF-STTG1 (1.6 ± 0.007 log mM) and NT2.N/A (1.6 ± 0.003 log mM) cell lines, which demonstrated statistically equivalent sensitivity ($P > 0.05$). The difference in sensitivity of the mono-culture and co-culture towards the α-diketone was considered significant after 4-hours exposure ($P < 0.001$).

As can be seen in figure 3.2 B, increasing concentrations of 2,3-HD (0-98 mM, table 3.1, section 3.2.3) also reduced MTT turnover in all four cell cultures after a 24-hour exposure period. Log IC_{50} values indicated that 2,3-HD was significantly more toxic to the NT2.D1 cells (1.0 ± 0.01 log mM; $P < 0.01$) in comparison with the CCF-STTG1 (1.1 ± 0.05 log mM), NT2.N (1.2 ± 0.02 log mM) and NT2.N/A (1.2 ± 0.02 log mM) cell lines, which demonstrated statistically equivalent sensitivity ($P > 0.05$). As stated, the co-culture was equally sensitive to the α-diketone as was the NT2.N mono-culture ($P > 0.05$) and this may also be observed from figure 3.2 A.

3.3.1.3 3,4-Hexanedione

As can be observed from figure 3.3 A, increasing concentrations of 3,4-hexanedione (3,4-HD; 0-82 mM, table 3.1, section 3.2.3) reduced MTT turnover in all four cell cultures after a 4-hour exposure period. Log IC_{50} values (table 3.2, section 3.3.1.7) indicated that 3,4-HD was significantly more toxic to the CCF-STTG1 cell line (1.5 ± 0.01 log mM; $P < 0.001$) in comparison with the NT2.D1 (1.6 ± 0.007 log mM), NT2.N (1.6 ± 0.004 log mM) and NT2.N/A (1.6 ± 0.003 log mM) cell lines, which demonstrated statistically equivalent sensitivity ($P > 0.05$). As stated, the co-culture was equally sensitive to the α-diketone as was the NT2.N mono-culture ($P > 0.05$), which is evident from figure 3.3 A.

As can be seen in figure 3.3 B, increasing concentrations of 3,4-HD (0-98 mM, table 3.1, section 3.2.3) reduced MTT turnover in all four cell cultures after a 24-hour exposure period. Comparison of log IC_{50} values indicated that 3,4-HD was most toxic to the NT2.D1 (1.2 ± 0.02 log mM), CCF-STTG1 (1.2 ± 0.04 log mM) and NT2.N (1.3 ± 0.02 log mM) cells, which demonstrated statistically equivalent sensitivity ($P > 0.05$). 3,4-HD was least toxic to the NT2.N/A (1.5 ± 0.02 log mM) cells. Thus as stated, following 24-hours exposure, the neuronal mono-culture was significantly

more sensitive to the α-diketone than was the NT2.N/A co-culture ($P < 0.01$).

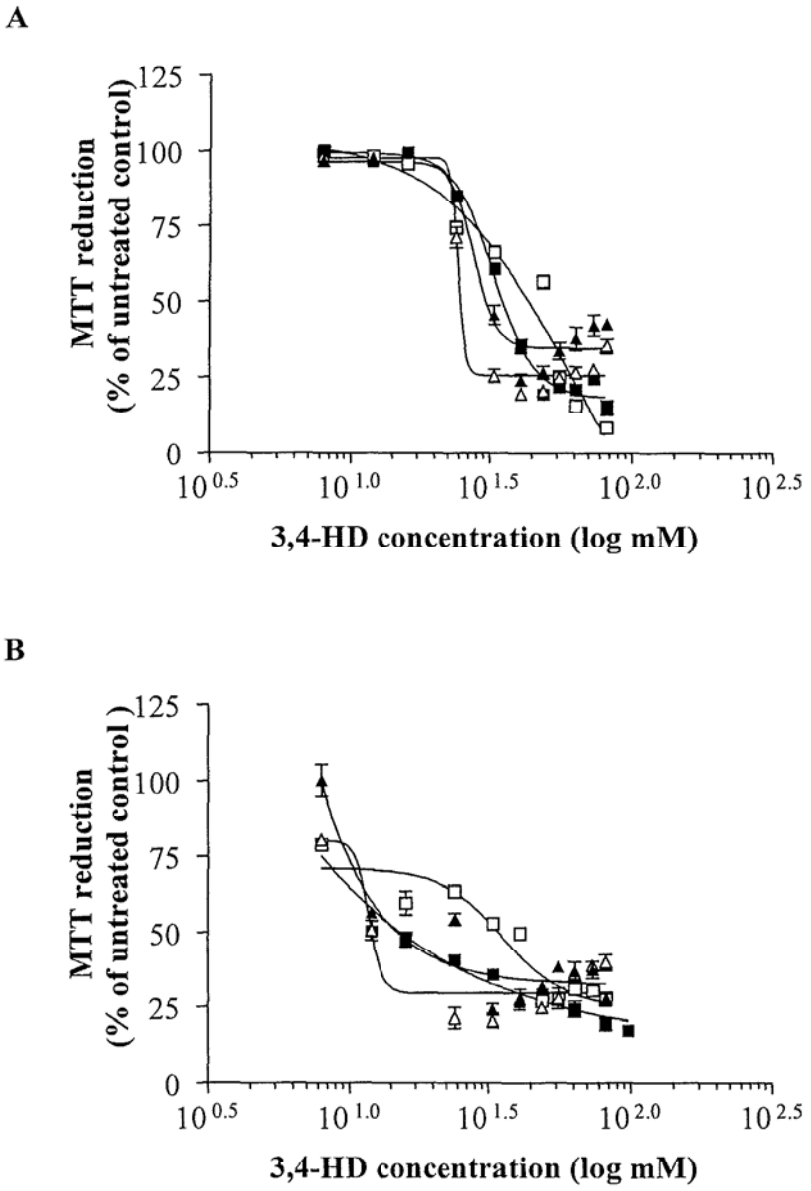

Figure 3.3 Cell viability as determined by MTT reduction following exposure to increasing concentrations of 3,4-hexanedione for 4 (A) or 24 (B) hours. Sigmoidal concentration-response curve (variable slope) for NT2.D1 (▲), CFF-STTG1 (△), NT2.N (■) and NT2.N/A (□) cells. The MTT assay was carried out and the plates read for absorbance at 590 nm. MTT reduction results are expressed as the A_{590} for the toxin treated sample as a percentage of the A_{590} for the untreated control sample. Data points represent the mean ± SEM of the sample means from four separate experiments.

3.3.1.4 Trimethyltin chloride

After a 4-hour exposure period, increasing concentrations of trimethyltin

chloride (TMT-Cl; 0-6 mM, table 3.1, section 3.2.3) reduced MTT turnover in all four cell cultures as is evident from figure 3.4 A. However, both the NT2.N/A and CCF-STTG1 cultures demonstrated an initial increase in MTT reduction above that of the control values. Formazan production reached 113.0 ± 1.3 % (0.5 mM) in the NT2.N/A co-culture and 109.3 ± 1.6 % (0.25 mM) in the CCF-STTG1 cells.

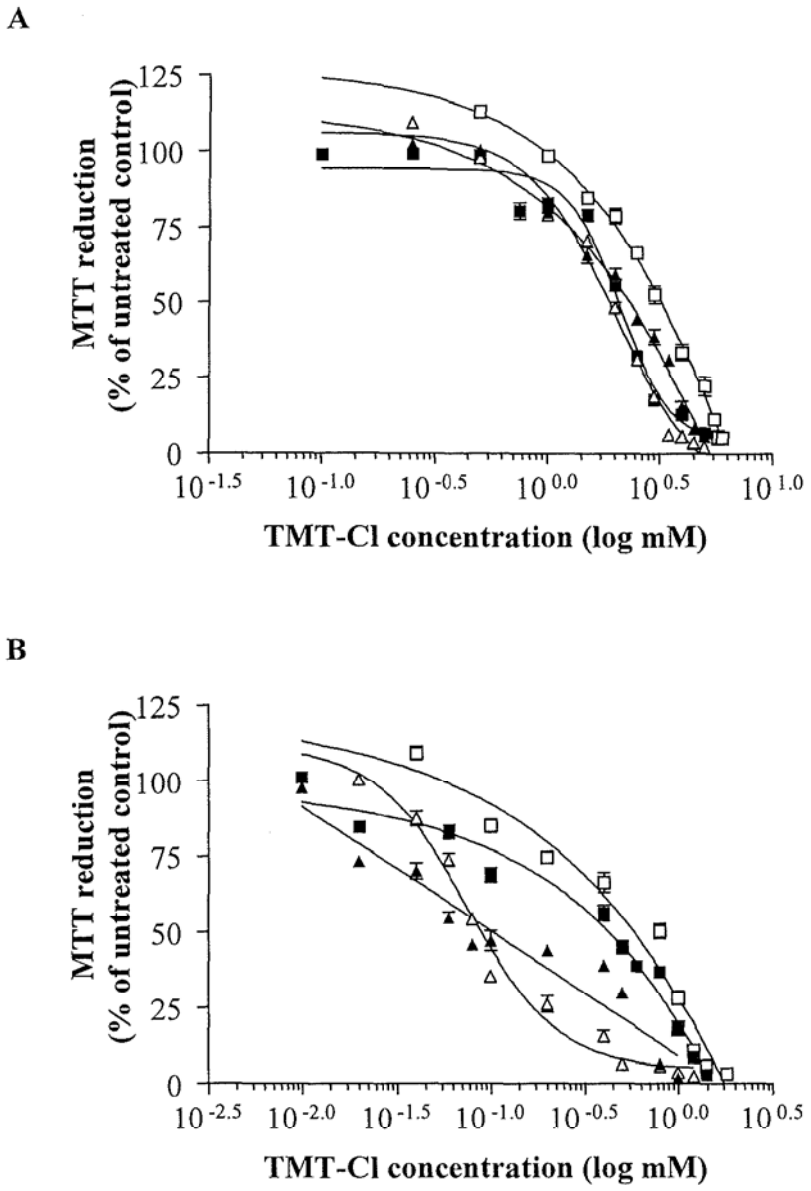

Figure 3.4 Cell viability as determined by MTT reduction following exposure to increasing concentrations of trimethyltin chloride for 4 (A) or 24 (B) hours. Sigmoidal concentration-response curve (variable slope) for NT2.D1 (▲), CFF-STTG1 (△), NT2.N (■) and NT2.N/A (□) cells. The MTT assay was carried out and the plates read for absorbance at 590 nm. MTT reduction results are expressed as the A_{590} for the toxin treated sample as a percentage of the A_{590} for the untreated control sample. Data points represent the mean ± SEM of the sample means from four separate experiments.

The log IC_{50} values (table 3.2, section 3.3.1.7) suggested that following 4-hours exposure, TMT-Cl was most toxic to the NT2.D1 (0.3 ± 0.004 log mM), CCF-STTG1 (0.3 ± 0.003 log mM) and NT2.N (0.3 ± 0.01 log mM) cell lines, which demonstrated statistically equivalent sensitivity ($P > 0.05$). In comparison, the NT2.N/A cell line was significantly less sensitive (0.5 ± 0.006 log mM; $P < 0.001$) at this timepoint ($P < 0.001$). As stated, the NT2.N mono-culture demonstrated greater sensitivity to the tin compound than did the NT2.N/A co-culture ($P < 0.001$), which can be seen from figure 3.4 A.

As can be seen in figure 3.4 B, increasing concentrations of TMT-Cl (0-1.8 mM, table 3.1, section 3.2.3) reduced MTT turnover in all four cell cultures after a 24-hour exposure period. However, in as with 4-hours exposure, the NT2.N/A culture initially demonstrated an increase in MTT reduction above that of the control value. Formazan production reached 109.2 ± 2.2 % (0.04 mM) in the NT2.N/A. There was no formazan increase above the control in the CCF-STTG1 cells at 24-hours.

Log IC_{50} values indicated that TMT-Cl was most toxic to the NT2.D1 (-1.0 ± 0.003 log mM) and CCF-STTG1 (-1.0 ± 0.008 log mM) cells, which demonstrated statistically equivalent sensitivity ($P > 0.05$). The NT2.N culture was statistically less sensitive than these cell lines (-0.5 ± 0.003 log mM; $P < 0.001$). TMT-Cl was least toxic to the NT2.N/A (-0.3 ± 0.02 log mM) culture and thus as with 4-hours exposure, the neuronal mono-culture was significantly more sensitive to the tin compound than was the co-culture ($P < 0.001$).

3.3.1.5 Tributyltin chloride

As is evident from figure 3.5 A, increasing concentrations of tributyltin chloride (TBT-Cl; 0-30 μM, table 3.1, section 3.2.3) reduced MTT turnover in all four cell cultures after a 4-hour exposure period. Log IC_{50} values (table 3.2, section 3.3.1.7) indicated that TBT-Cl chloride was most toxic to the NT2.N (-2.7 ± 0.006 log mM), followed by the NT2.N/A (-2.6 ± 0.004 log mM) and NT2.D1 (-2.3 ± 0.004 log mM) cell lines, with the CCF-STTG1 (-2.2 ± 0.005 log mM) cell line being significantly the least sensitive to TBT-Cl exposure for 4-hours ($P < 0.001$). The greater sensitivity of the NT2.N

mono-culture to the tin compound, compared with the NT2.N/A co-culture was statistically considered to be highly significant ($P < 0.001$). However, it is evident from figure 3.5 A that the cultures were similar in their response to 4-hours TBT-Cl exposure.

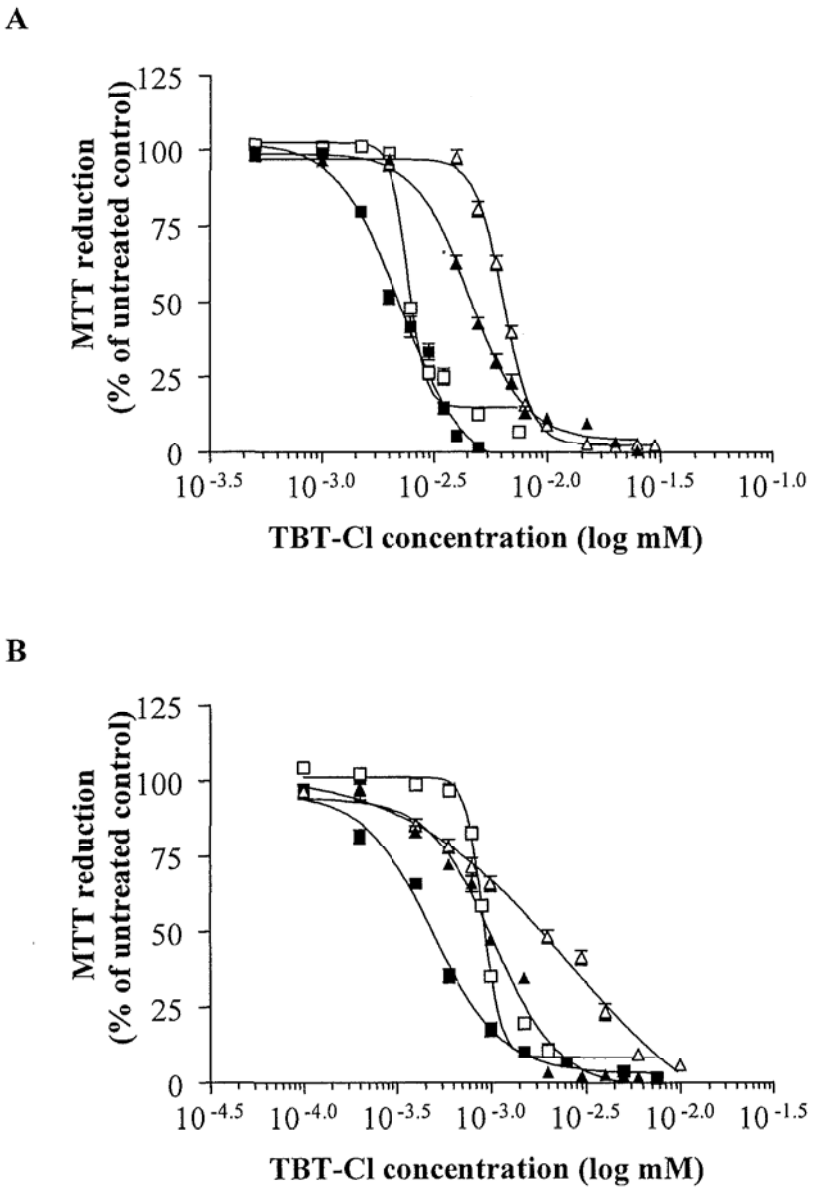

Figure 3.5 Cell viability as determined by MTT reduction following exposure to increasing concentrations of tributyltin chloride for 4 (A) or 24 (B) hours. Sigmoidal concentration-response curve (variable slope) for NT2.D1 (▲), CFF-STTG1 (△), NT2.N (■) and NT2.N/A (□) cells. The MTT assay was carried out and the plates read for absorbance at 590 nm. MTT reduction results are expressed as the A_{590} for the toxin treated sample as a percentage of the A_{590} for the untreated control sample. Data points represent the mean ± SEM of the sample means from four separate experiments.

As can be seen in figure 3.5 B, increasing concentrations of TBT-Cl (0-10 μM, table 3.1, section 3.2.3) reduced MTT turnover in all four cell cultures after a 24-hour exposure period. IC_{50} values indicated that TBT-Cl was again most toxic to the NT2.N (-3.3 ± 0.02 log mM) cells, followed by the NT2.N/A (-3.0 ± 0.006 log mM) and NT2.D1 (-3.0 ± 0.007 log mM) cells that demonstrated statistically equivalent sensitivity ($P > 0.05$). Thus, as stated, the neuronal mono-culture was significantly more sensitive to the tin compound than was the co-culture ($P < 0.001$). TBT-Cl was least toxic to the CCF-STTG1 cell line (-2.8 ± 0.02 log mM).

3.3.1.6 Summary of log IC_{50} values and IC_{50} values

The MTT reduction log IC_{50} values generated by the MTT assay are summarised in table 3.2a. The respective IC_{50} values are summarised in table 3.2b.

Test chemical	Cell line	4-hours exposure	24-hours exposure
		log IC_{50} ± log SEM (log mM)	log IC_{50} ± log SEM (log mM)
2,5-Hexanedione (2,5-HD)	NT2.D1	2.0 ± 0.006	1.1 ± 0.04
	CCF-STTG1	2.6 ± 0.01	1.9 ± 0.002
	NT2.N	2.5 ± 0.009	1.6 ± 0.005
	NT2.N/A	2.7 ± 0.001	1.9 ± 0.01
2,3-Hexanedione (2,3-HD)	NT2.D1	1.5 ± 0.008	1.0 ± 0.01
	CCF-STTG1	1.6 ± 0.007	1.1 ± 0.05
	NT2.N	1.4 ± 0.004	1.2 ± 0.02
	NT2.N/A	1.6 ± 0.003	1.2 ± 0.02
3,4-Hexanedione (3,4-HD)	NT2.D1	1.6 ± 0.007	1.2 ± 0.02
	CCF-STTG1	1.5 ± 0.01	1.2 ± 0.04
	NT2.N	1.6 ± 0.004	1.3 ± 0.02
	NT2.N/A	1.6 ± 0.003	1.5 ± 0.02
Trimethyltin chloride (TMT)	NT2.D1	0.3 ± 0.004	-1.0 ± 0.003
	CCF-STTG1	0.3 ± 0.003	-1.0 ± 0.008
	NT2.N	0.3 ± 0.01	-0.5 ± 0.003
	NT2.N/A	0.5 ± 0.006	-0.3 ± 0.02
Tributyltin chloride (TBT)	NT2.D1	-2.3 ± 0.004	-3.0 ± 0.007
	CCF-STTG1	-2.2 ± 0.005	-2.8 ± 0.02
	NT2.N	-2.7 ± 0.006	-3.3 ± 0.02
	NT2.N/A	-2.6 ± 0.004	-3.0 ± 0.006

Table 3.2a Summary of the log IC_{50} ± log SEM values obtained for each test chemical, in each cell system, using the MTT reduction assay.

Test chemical	Cell line	4-hours exposure	24-hours exposure
		IC_{50} ± SEM (mM)	IC_{50} ± SEM (mM)
2,5-Hexanedione (2,5-HD)	NT2.D1	100.0 ± 1.4	12.6 ± 1.2
	CCF-STTG1	398.1 ± 9.2	79.4 ± 0.4
	NT2.N	316.2 ± 6.6	39.8 ± 0.5
	NT2.N/A	501.2 ± 1.2	79.4 ± 1.8
2,3-Hexanedione (2,3-HD)	NT2.D1	31.6 ± 0.6	10.0 ± 0.2
	CCF-STTG1	39.8 ± 0.6	12.6 ± 1.5
	NT2.N	25.1 ± 0.2	15.8 ± 0.7
	NT2.N/A	39.8 ± 0.3	15.8 ± 0.7
3,4-Hexanedione (3,4-HD)	NT2.D1	39.8 ± 0.6	15.8 ± 0.7
	CCF-STTG1	31.6 ± 0.9	15.8 ± 1.5
	NT2.N	39.8 ± 0.4	20.0 ± 0.9
	NT2.N/A	39.8 ± 0.3	31.6 ± 1.5
Trimethyltin chloride (TMT)	NT2.D1	2.0 ± 0.02	0.1 ± 0.007
	CCF-STTG1	2.0 ± 0.01	0.1 ± 0.002
	NT2.N	2.0 ± 0.05	0.3 ± 0.002
	NT2.N/A	3.2 ± 0.04	0.5 ± 0.02
Tributyltin chloride (TBT)	NT2.D1	$(5.0 \pm 0.05) \times 10^{-3}$	$(1.0 \pm 0.02) \times 10^{-3}$
	CCF-STTG1	$(6.3 \pm 0.07) \times 10^{-3}$	$(1.6 \pm 0.07) \times 10^{-3}$
	NT2.N	$(2.0 \pm 0.03) \times 10^{-3}$	$(0.5 \pm 0.02) \times 10^{-3}$
	NT2.N/A	$(2.5 \pm 0.02) \times 10^{-3}$	$(1.0 \pm 0.01) \times 10^{-3}$

Table 3.2b Summary of the IC_{50} ± SEM values obtained for each test chemical, in each cell system, using the MTT reduction assay.

3.3.2 Determination of the NOAEL for each test chemical at 4-hours

The NOAEL for each toxin at four hours was considered to be the highest concentration at which the A_{590} was not significantly decreased below that of the untreated control ($P > 0.05$). Concentrations below the NOAEL value were considered to encompass the non-cytotoxic range. The results are summarised in table 3.3.

Compound	Cell line	NOAEL at 4-hours (mM)
2,5-Hexanedione (2,5-HD)	NT2.D1	50
	CCF-STTG1	85
	NT2.N	85
	NT2.N/A	85
2,3-Hexanedione (2,3-HD)	NT2.D1	12
	CCF-STTG1	16
	NT2.N	8
	NT2.N/A	12
3,4-Hexanedione (3,4-HD)	NT2.D1	12
	CCF-STTG1	12
	NT2.N	16
	NT2.N/A	16
Trimethyltin chloride (TMT)	NT2.D1	0.5
	CCF-STTG1	0.5
	NT2.N	0.5
	NT2.N/A	1
Tributyltin chloride (TBT)	NT2.D1	2×10^{-3}
	CCF-STTG1	4×10^{-3}
	NT2.N	1×10^{-3}
	NT2.N/A	2×10^{-3}

Table 3.3 Summary of NOAEL determined for each test chemical after exposure of each cell system for 4-hours.

3.3.3 Effect of test chemical vehicle on cell viability

A simple MTT assay was carried out in order to confirm that that the 5 μM of ethanol required to solubilise tributyltin chloride in medium was not itself toxic to cells. Ethanol at 5 μM in normal medium was found to cause no statistical decrease in cell viability (as determined by MTT reduction) of the NT2.D1, CCF-STTG1, NT2.N or NT2.N/A cells after 4 or 24-hours exposure ($P > 0.05$). The data is not presented graphically.

3.3.4 Calibration of the MTT assay

As can be seen in figure 3.6, MTT turnover as measured by absorbance at 590 nm, increased with increasing cell number, for all cell lines. For the NT2.D1 cell line, no significant difference was evident by increasing cell number until above ~7813 cells/well ($P < 0.001$). However, a significant difference was evident for the CCF-

STTG1 cell line above ~1953 cells/well ($P < 0.05$). An absorbance reading of ~1 was achieved for both continuous cell lines at a density of ~500,000 cells/well.

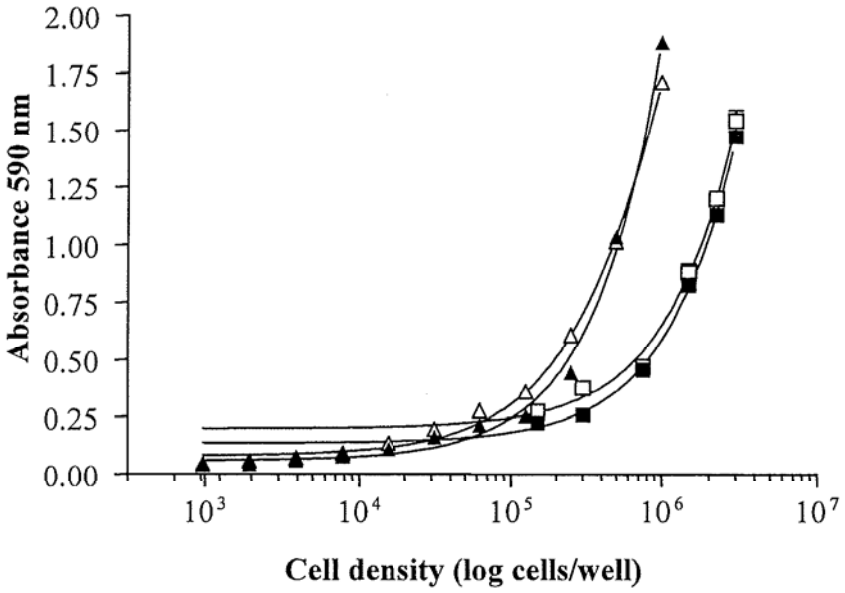

Figure 3.6 MTT escalation study on increasing numbers of NT2.D1 (▲), CFF-STTG1 (△), NT2.N (■), or NT2.N/A (□) cells. Viable cells were plated into 6-well plates at increasing densities up to 10 x 10^5 (NT2.D1 and CCF-STTG1 cells) or 30 x 10^5 (NT2.N and NT2.N/A cells following replate #2) cells/well. Sigmoidal density-response curve after overnight incubation in the case of the NT2.D1 and CCF-STTG1 cells and following mitotic inhibitor treatment in the case of the NT2.N and NT2.N/A cells. Results are expressed as the A_{590} of cells assayed for MTT reduction. Data points represent the mean ± SEM of the sample means from two separate experiments.

For the NT2.N and NT2.N/A cell systems, very low cell densities were not examined; thus, for both cultures a significant difference was evident between the medium only control and the first well, which contained 150,000 cells/well following replate #2 ($P < 0.001$). An absorbance reading of ~1.15 and ~1.20 was achieved for the NT2.N and the NT2.N/A cultures respectively at a density of ~2,250,000 cells/well.

3.3.5 Uniform growth of NT2.N and NT2.N/A cells in 6-well plates

3.3.5.1 Wells of individual 6-well plates

The density of NT2.N and NT2.N/A cells in each well of an individual 6-well plate was estimated by MTT reduction for three separate plates of the same batch. As is

demonstrated by figure 3.7, for each of the plates 1 to 3, both the NT2.N and NT2.N/A cell-cultures contained a statistically equivalent density of viable cells in each well following replate #2 and mitotic inhibitor treatment ($P > 0.05$).

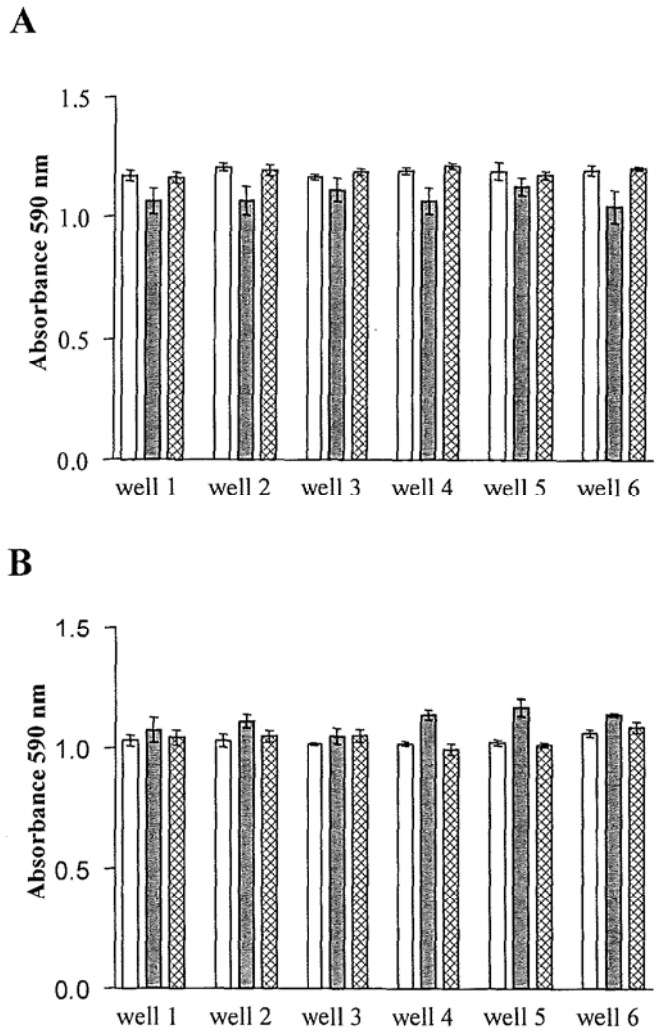

Figure 3.7 MTT 6-well plate study on uniform growth of NT2.N (A) and NT2.N/A (B) cells. Different shaded bars represent three separate plates of cells of the same batch. The MTT assay was carried out following the culture of NT2.N or NT2.N/A cells in 6-well plates and the A_{590} determined. Individual bars represent the mean ± SEM of quadruplicate samples from a single experiment.

3.3.5.2 6-Well plates of the same batch

As can be seen in figure 3.8, the mean cell density of NT2.N and NT2.N/A cells per well was estimated by MTT turnover via absorbance at 590 nm for three separate plates of the same batch. Both the NT2.N and NT2.N/A cell-cultures contained a statistically equivalent density of viable cells in each of the three plates following replate #2 and

mitotic inhibitor treatment ($P > 0.05$).

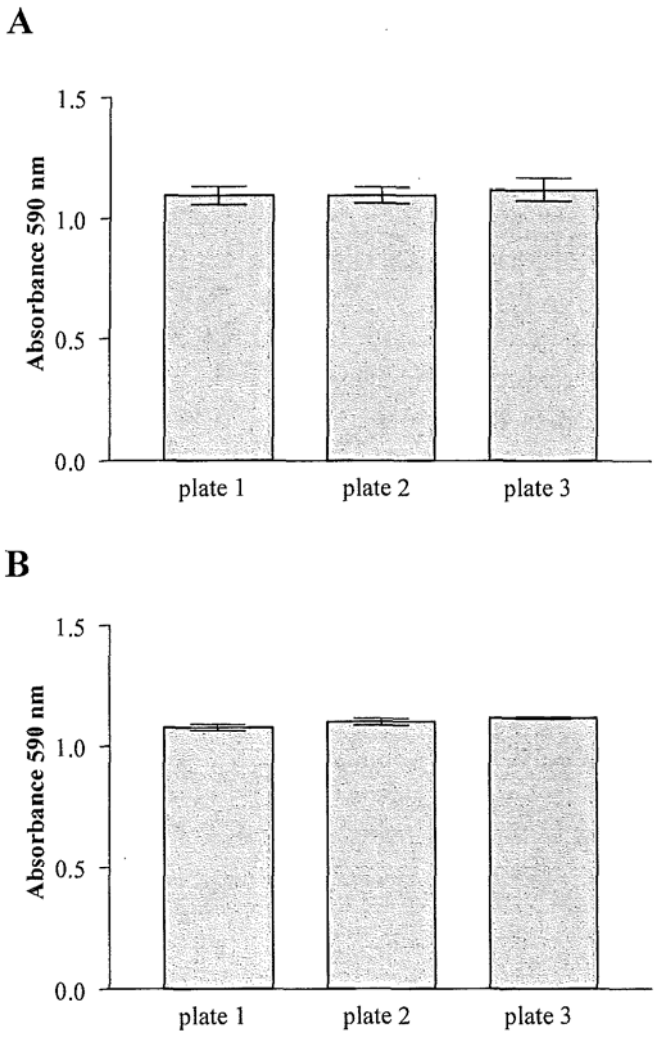

Figure 3.8 MTT 6-well plate study on uniform growth of NT2.N (A) and NT2.N/A (B) cells. The MTT assay was carried out following the culture of NT2.N or NT2.N/A cells in 6-well plates and the A_{590} determined. Individual bars represent the mean number of cells/well ± SEM, in three separate 6-well plates of cells of the same batch.

3.4 Discussion

It was considered that a 6-well plate format would be appropriate for the high-throughput screening of potential neurotoxins using both basal cytotoxicity and biochemical endpoints. This gave the advantage of cell growth and test chemical exposure in the same plate as the NT2.N and NT2.N/A cells were enriched following differentiation, so cell-cell interactions were not disrupted by scraping and reseeding into 96-well plates. It was also convenient to grow the NT2.D1 and CCF-STTG1 cells as a monolayer and reseed them into 6-well plates prior to screening experiments.

Regarding the MTT reduction assay, the most accurate results are obtained when the absorbance is within the range of linearity, with the A_{590} being determined by Mosmann (1983) to be linearly proportional to the number of metabolically active cells up to an optical density of 1.2. The optimum 6-well plate seeding density for the CCF-STTG1 and NT2.D1 cell lines prior to overnight incubation was established as being approximately 500,000 cells per well. At this density an absorbance reading of ~ 1 was achieved for both cell lines, with both cell cultures appearing confluent following overnight incubation. The optimal 6-well plate seeding density for the NT2.N and NT2.N/A for replate #2 was established as being approximately 2250,000 cells. This seeding density gave an absorbance reading of between 1.15 and 1.20 and yielded a dense but identifiable network of cells following mitotic inhibitor treatment.

For the majority of endpoint assays, nine to twelve wells and thus two separate 6-well plates, were required in total per toxin. Therefore, the MTT assay was used to confirm that following replate #2 and mitotic inhibitor treatment, each well of an individual 6-well plate and plates of the same batch of differentiated cells contained a statistically equivalent density of viable NT2.N or NT2.N/A cells. Both the mono- and co-culture were indeed found to demonstrate such uniform growth when comparing three separate plates of the same batch and between wells of a single plate.

A concentration-range finding study was conducted using the MTT assay, with cells seeded at the appropriate densities in 6-well plates. The resulting concentration-response curves were used to determine the log IC_{50} values at 4- and 24-hours (log

concentration of toxin which resulted in a 50 % inhibition of MTT turnover), for each toxin, in each cell system. These log IC_{50} values and the resulting IC_{50} values were then used to evaluate the quantitative response of the NT2.N/A co-culture in comparison with the culture of NT2.N and CCF-STTG1 cells alone and with the undifferentiated non-neuronal NT2.D1 cell line, to the test chemicals.

Additionally, where the data was available, LD_{50} mmol/kg values for the set of test chemicals were compared with the mean IC_{50} values obtained following 24-hours exposure, to observe if the *in vitro* cell systems were predictive of the *in vivo* cytotoxic response. However, a number of factors may lead to discrepancies in such an *in vitro/in vivo* comparison. For example, generally only experimental animal LD_{50} values are available, thus presenting the problem of species differences. Additionally, it has been reported that *in vitro* basal cytotoxicity IC_{50} values measured following 72-hours exposure is predictive of the acute oral rodent LD_{50} values, rather than exposure for 24-hours (Gartlon *et al.*, 2006).

When comparing IC_{50} values obtained in the different cell systems, it may be expected that i) neurotoxicants would be more toxic to the cell systems with greater rather than fewer neuronal properties and ii) due to the metabolic and protective support offered by astrocytes to neurons, the NT2.N/A co-culture may show increased tolerance to cytotoxic insult compared with the NT2.N mono-culture. However, the levels of overt toxicity measured by IC_{50} values could potentially mask specific neurotoxic mechanistic actions.

3.4.1 2,5-Hexanedione

The industrial solvent n-hexane is bioactivated to 2,5-hexanedione (2,5-HD), which is an established chronic neurotoxin (Spencer *et al.*, 1980; Couri and Milks, 1982). The γ-diketone has been found to form pyrrole adducts at neurofilament ε-lysine residues *in vivo* and *in vitro* (Heijink *et al.*, 2000) with subsequent axonal atrophy and development of predominantly PNS neurological deficits (LoPachin and DeCaprio, 2004). The 2,5-HD intra-neuronal and intra-axonal concentration following systemic exposure has not been determined (Sickles *et al.*, 1990) and how exactly the functional

consequences of atrophy relate to the development of chronic neurological deficits is unknown. However, 2,5-HD is not considered to be acutely toxic based on experimental animal exposures and no toxic effects from acute human exposure have been reported (Couri and Milks, 1982).

After 4-hours exposure, high millimolar concentrations of 2,5-HD (100.0 – 501.2 mM) were required to induce a decrease in cell viability in all four cell lines. From comparison of the IC_{50} values, the order of decreasing sensitivity was NT2.D1 > NT2.N = CCF-STTG1 > NT2.N/A. Lower millimolar concentrations were required to induce cytotoxicity after 24-hours exposure (IC_{50} values 5-10 fold lower compared with 4-hours), with the order of decreasing sensitivity NT2.D1 > NT2.N > CCF-STTG1 = NT2.N/A. Following 24-hours exposure, the IC_{50} values obtained (12.6 – 79.4 mM) were of comparable magnitude with the acute oral LD_{50} value of 2,5-hexanedione in rat, which has been established as being 23.7 mmol/kg (Opdyke, 1979).

There are a small number of *in vitro* studies utilising both neuronal and non-neuronal cells and an acute 2,5-HD exposure period. Hartley *et al.,* (1997) examined the effects in the human neuroblastoma cell line SH-SY5Y, after retinoic acid differentiation. 2,5-HD (25 mM) caused neurofilament accumulations after 24-hours but did not affect cell viability. In the present study, this concentration of 2,5-HD was sufficient to induce approximately a 75 % reduction in cell viability in the NT2.D1 cell line (IC_{50} = 12.6 mM) and approximately a 25 % decrease in the NT2.N cell line (IC_{50} = 39.8 mM) following 24-hours exposure. Thus the terminally differentiated NT2.N cell line demonstrated an increased vulnerability compared with the less phenotypically neuronal-like, neuroblastoma cell line.

As 2,5-HD is an established neurotoxin it may be hypothesised that it would be more toxic towards the cell systems with the most neuronal features, therefore the NT2.N and NT2.N/A cultures. However, 2,5-HD acts chronically and the current study examined acute cytotoxicity. Additionally, 2,5-HD neurodegenerations are characterised by primary destruction of the axon of neuronal cells without affecting the cell body. Cell viability as an endpoint will detect the basal cytotoxic potential only of such axonopathic chemicals and will not be sufficient to detect axon specific effects

that would differentiate neuronal from non-neuronal systems. Thus, it may be expected that the cell systems would demonstrate similar vulnerability to acute cytotoxic concentrations of the chronic neurotoxin 2,5-HD. Indeed, millimolar levels of the chronic toxin were required to produce an acute affect in all cell lines, suggesting acutely, 2,5-HD behaves as a cytotoxin, not a neurotoxin. Additionally, whilst 2,5-HD did significantly differentiate the cell system responses, the significant differences could not consistently be attributed to the presence or absence of neuronal features.

2,5-HD added to dorsal root ganglia from 8-day-old chick embryos at a concentration of 88 mM caused a loss in neuronal cell viability after 36-hours but astrocytic cell viability was not affected until after 48-hours exposure (Boegner *et al.*, 1992). This is consistent with the results of the present study in that a greater concentration of 2,5-HD was required to induce cytotoxicity in the astrocyte containing NT2.N/A and CCF-STTG1 cultures, than in the neuronal NT2.N culture, following 24-hours exposure. Indeed, the NT2.N/A co-culture demonstrated an increased resistance towards 2,5-HD exposure than did the NT2.N mono-culture, at both time points.

3.4.2 2,3- and 3,4-Hexanedione

Although not formed via hexane metabolism *in vivo*, the α-diketones 2,3-hexanedione (2,3-HD) and 3,4-hexanedione (3,4-HD) are used as synthetic flavouring and fragrance agents and are considered to be non-toxic if the daily human intake does not exceed 540 μg (4.74 μmol) (FAO/WHO, 1999).

Studies regarding the acute toxic potency of 2,3- and 3,4-HD *in vitro* are limited. The α-diketones have been previously utilised as negative controls during *in vitro* studies of the neurotoxicity of γ-diketones in murine neuroblastoma cell lines (Selkoe *et al.*, 1978) and rat primary brain cells (Medrano and LoPachin, 1989) and were reportedly non-toxic. There has been no investigation in human neural or astrocytic cell lines by other groups and in the present study it was expected that the cell systems would all demonstrate similar vulnerability and that high levels of the compounds would be required to induce a cytotoxic effect.

As expected, no consistent vulnerability of neuronal or non-neuronal cell types towards either of the α-hexanediones was demonstrated by comparison of the IC_{50} values generated by the MTT assay (2,3-HD; 25.1-39.8 mM at 4-hours, 10.0-15.8 mM at 24-hours. 3,4-HD; 31.6-39.8 mM at 4-hours, 15.8-31.6 mM at 24-hours). Additionally, millimolar amounts of compound were required to induce a cytotoxic effect. This basal cytotoxicity data suggests that the α-hexanediones are not acutely neurotoxic and rather demonstrate similar toxic potential and are only expected to be cytotoxic if unphysiologically high levels of the compounds are achieved.

For both compounds, at both time points, millimolar IC_{50} values were obtained for all cell lines (ranging from 10.0 – 39.8 mM). These are of comparable magnitude with the acute oral LD_{50} value of 2,3-hexanedione in rat, which has been established as being in excess of 44 mmol/kg (Opdyke, 1979). The acute oral LD_{50} value of 3,4-hexanedione is unavailable. The millimolar IC_{50} values obtained in this chapter are also obviously far in excess of the estimated approximate human daily intake for a 75 kg person (0.14 μmol, 2,3-HD; 0.33 μmol, 3,4-HD) and also the maximum safe recommended daily human intake of 540 μg (4.74 μmol) (FAO/WHO, 1999). Thus a cytotoxic response should not be apparent under normal human exposure conditions.

Whilst the cell viability IC_{50} values generated by the MTT assay demonstrate the α-diketones to be similarly and weakly cytotoxic at best, they were still approximately 3-14 fold more toxic than 2,5-HD after 4-hours exposure and also approximately 2-6 fold more toxic after 24-hours exposure, with the exception of the NT2.D1 cell line. Whereas pyrolle formation via adduction of lysine residues is unique to γ-diketones, α-diketones are also soft-electrophiles. It has been reported that the closer the two carbonyl groups in a diketone, the more cytotoxic it will be (Chen and Hee, 1995). Although it is uncertain exactly how the geometry around the carbonyl groups modulates toxicity, 2,3-HD 3,4-HD are stronger electrophiles than 2,5-HD owing to the closer α-spacing of the carbonyl groups (relative H-bond acceptor values, 2,3- and 3,4-HD = 0.47; 2,5-HD = 0.39) and this may contribute to their increased cytotoxic potential after acute exposure periods.

3.4.3 Trimethyltin chloride

Trimethyltin chloride (TMT-Cl) produces acute neurotoxic sequelae, with poisoning in humans and experimental animals primarily causing a specific pattern of neuronal necrosis and apoptosis in areas of the hippocampus, cerebral cortex and cerebellum. TMT-Cl has also been shown to be acutely toxic *in vitro*, in rodent and human primary neuronal and astrocytic cultures and human neuronal cell lines. Neuronal cells are considered to be more sensitive towards this tin compound than are astrocytes (Karpiak and Eyer, 1999; Fiedorowicz *et al.*, 2001; Cristofol *et al.*, 2004). Trimethyltin compounds are well absorbed via most routes of exposure (Van-Heijst, 1999) and although water-soluble (log P = 0.28), TMT-Cl has been found in brain of various animal species at levels of 5-18.5 μmol following acute neurotoxic exposures (Eyer *et al.*, 2000).

Astrocytes are thought to play a key role in the metabolic regulation and protection of neurons during toxic insult. Additionally, reactive astrogliosis is a frequently observed reaction to chemical insults to the brain, including TMT-Cl exposure (Richter-Landsberg and Besser, 1994). Administration of both neuropathic and non-neuropathic doses of TMT-Cl to rats have been demonstrated to produce an astrocytic response in several brain regions, with hypertrophy and swelling, along with amplified protein synthesis and enhanced metabolic status (Cookson and Pentreath, 1994; Karpiak and Eyer, 1999).

In this study, formazan production exceeded 100 % in treated NT2.N/A (113.0 ± 1.3 %; 0.5 mM) and CCF-STTG1 (109.3 ± 1.6 %; 0.25 mM) cells, following 4-hours exposure to TMT-Cl and in NT2.N/A cells only (109.2 ± 2.2 %; 0.04 mM), following 24-hours exposure. This increase in MTT reduction above that of the control cells is thought to reflect an initial enhancement of metabolic activity above that of control cultures, due to an astrogliotic response induced by TMT-Cl, rather than as a result of proliferation. Cookson *et al.*, (1995) also showed that primary astrocytic cultures exhibited an early burst of MTT reduction that preceded a later decline, upon exposure to TMT-Cl.

Micromolar to millimolar amounts (2000-3200 μM, 4-hours; 100-500 μM, 24-hours) of TMT-Cl were required to induce half maximal cytotoxicity in the investigated cell systems. The LD_{50} value in rat (oral) has been determined to be 63 μmol/kg (Van-

Heijst, 1999). Using the IC_{50} value of 500 μM obtained in the NT2.N/A co-culture as an example, it be seen that the LD_{50} value in rat was approximately 8-fold lower. This may reflect the problem of extrapolation between the *in vivo-in vitro* situation or between species. It may also simply be due to different time points being compared. For example, between 4- and 24-hours exposure, the IC_{50} value was reduced 6-fold in the NT2.N/A culture and it may thus be hypothesised that at 72-hours, the IC_{50} value may be reduced to the magnitude of the LD_{50} value determined in rat.

Interestingly, sensitivity to TMT-Cl has been seen to vary in between species and cell type in *in vitro* cell cultures. For example, primary neuronal cultures from rat hippocampus have been found to have an IC_{50} value of approximately 1.5 μM (24-hours) whereas, rat cortical neurons were found to have a higher IC_{50} value of 44 μM (24-hours) by Cristofol *et al.,* (2004), demonstrating the increased sensitivity of cells from the hippocampal region. However, primary cultures of cerebral cortical neurons and astrocytes from human foetal tissue yielded much higher IC_{50} values of 335.5 ± 90.5 μM and 619.7 ± 8.8 μM, respectively, after 24-hours exposure. Similarly, the human neuroblastoma cell line SH-SY5Y was estimated to have an IC_{50} value of 547 ± 46.3 μM after 24-hours exposure. This demonstrates that in that particular study, astrocytes were less sensitive towards TMT-Cl exposure than were neurons and human neurons were less sensitive than rat neurons but similarly sensitive as were SH-SY5Y neuroblastoma cells (Cristofol *et al.*, 2004). In the current chapter, the IC_{50} value obtained for the NT2.N (300 μM) mono-culture at 24-hours was very similar to that obtained in human foetal neurons. Additionally, the IC_{50} value obtained for the NT2.N/A (500 μM) co-culture at 24-hours, was similar to but slightly less than that obtained in human foetal astrocytes by Cristofol *et al.*, (2004), reflecting the presence of the more vulnerable neuronal cell type in the co-culture cell system.

A number of groups have examined the sensitivity of primary cultures of neonatal rat cortical astrocytes to TMT-Cl, with the resulting IC_{50} values following 24-hours exposure seen to vary widely, from as low as 2.5 μM (Richter-Landsberg and Besser, 1994) to 500 μM (Cookson *et al.*, 1995). Differences in media composition, the cytotoxicity assay used and in particular age and confluency of the cell culture may account for difference in sensitivity to TMT-Cl. For example, the cultures that

demonstrated the lowest IC_{50} values were seeded at low density and exposed to toxins 24-hours after plating and so may have still demonstrated a proliferative status. The cultures that demonstrated IC_{50} values more similar to those seen in the present study following 24-hours exposure (90-500 μM), were confluent and exposed 14-21 days after plating. The NT2.N and NT2.N/A cultures used in this study were also confluent and used 28-35 days after replate #2.

It has been postulated that species differences may account for the seemingly low sensitivity of human foetal neurons in the study conducted by Cristofol *et al.*, (2004) and the NT2 neurons used in the current study. For example, Almaas *et al.*, (2002) reported that human foetal neurons and NT2.N cells have a larger capacity for intracellular calcium buffering than do cortical rat neurons. It is generally accepted intracellular Ca^{2+} overload due to extracellular entry or release from intracellular stores may activate cell death via apoptosis or may cause necrotic disintegration of cells through the activity of Ca^{2+} sensitive digesting enzymes (Cristofol *et al.*, 2004; Florea *et al.*, 2005). This strengthens the argument that in general the use of relevant human cell lines may lead to easier extrapolation from *in vitro* models to the *in vivo* situation and facilitate the accuracy of human risk assessment. However, it is unknown whether NT2 neurons are able to reflect the hippocampal sensitivity to TMT-Cl observed *in vivo*.

As TMT-Cl is a known acute CNS toxin and neurons are considered to be more sensitive than astrocytes, it was expected that TMT-Cl would be more toxic towards the NT2.N and NT2.N/A cultures and too a lesser extent the CCF-STTG1 cells, than the non-neuronal NT2.D1 cells. Following 4-hours exposure, cell viability IC_{50} values generated by the MTT assay demonstrated the order of decreasing sensitivity to TMT-Cl to be NT2.N = CCF-STTG1 > NT2.D1 > NT2.N/A. Following 24-hours exposure, the order of sensitivity was CCF-STTG1 = NT2.D1 > NT2.N > NT2.N/A. Thus, at both time points it appears that the NT2.N mono-culture was more vulnerable towards TMT-Cl in comparison with the NT2.N/A co-culture, which may be suggestive of an astrocytic protective against TMT-Cl induced neurotoxicity. Gunasekar *et al.*, (2001b) also provided evidence that cell death following TMT-Cl exposure in rat cerebellar neurons was ameliorated when astrocytes were also present in the culture.

3.4.4 Tributyltin chloride

Tributyltin chloride (TBT-Cl) is acutely immunotoxic (Snoeij *et al.*, 1987) and has also been shown to be an acute CNS toxin *in vivo* in rodents (Lavastre and Girard, 2002) and *in vitro* in primary cultures and human cell lines (Karpiak and Eyer, 1999). TBT compounds have been widely used as biocides and have been found to be toxic to exposed mammals and marine organisms and also humans following occupational exposure or the consumption of contaminated fish and seafood (Mizuhashi *et al.*, 2000a; Appel, 2004). Shellfish in polluted areas of Japan have been found to contain up to 5 μmol TBT-Cl (Mizuhashi *et al.*, 2000a) and the daily intake in Japan was estimated to be 7.1 nmol TBT-Cl/day in 1997 (Okada *et al.*, 2000).

In the present study, cell viability IC_{50} values generated by the MTT assay produced significant differences between the cell system responses and only low micromolar amounts (2.5-6.3 μM, 4-hours; 0.5-1.6 μM, 24-hours) of TBT-Cl were required to induce half maximal cytotoxicity in the investigated cell lines. As TBT-Cl is highly lipophilic (log P = 4.76), and therefore able to cross and increase the permeability of the BBB (Elsabbagh *et al.*, 2002), it is expected to accumulate in lipid rich organs such as the brain at levels in excess of 90 nmol (Mizuhashi *et al.*, 2000b; Nakatsu *et al.*, 2006a). Therefore, it may be hypothesised that the low micromolar IC_{50} values obtained in this study may reflect physiologically relevant levels that may be attained in areas of high TBT-Cl pollution such as Japan. However, there are no reliable *in vivo* reports for human neurotoxicity (Appel, 2004).

The low micromolar IC_{50} values obtained are much reduced in comparison with the rat oral LD_{50} value for TBT-Cl, which is approximately 375 μmol/kg (IPCS, 1990), which may be suggestive of species differences. However, numerous groups have obtained IC_{50} values of similar magnitude to this study using cells obtained from rat nervous tissue following 24-hours TBT-Cl exposure. For example, the IC_{50} value of TBT-Cl was found to be 0.5 μM in rat primary cortical neuronal cultures (Nakatsu *et al.*, 2006a), whereas rat primary cortical astrocytes were found to be less sensitive with an IC_{50} value of 6-7 μM (Karpiak and Eyer, 1999). Therefore, the IC_{50} values of 0.5 and 1 μM obtained in the current study at 24-hours for the NT2.N mono-culture and

NT2.N/A co-culture respectively, were very comparable with the rat primary cortical neuronal cultures.

As TBT-Cl has previously demonstrated acute toxicity in neurons and astrocytes, it might have been expected to be more toxic towards the NT2.N, NT2.N/A and CCF-STTG1 cells, than the NT2.D1 cells. TBT-Cl was indeed most toxic towards the NT2.N and NT2.N/A cell systems following 4- and 24-hours exposure. However, the third most sensitive culture was the NT2.D1 cell line, with the astrocytic like CCF-STTG1 cells demonstrating the least sensitivity towards the tin compound at both time points. The NT2.N mono-culture was more sensitive than the NT2.N/A co-culture towards TBT-Cl induced cytotoxicity at both time points, though it was more readily apparent following 24-hours rather than 4-hours exposure. This increased tolerance of the NT2.N/A cell system may be suggestive of an astrocytic protective effect or simply the reduced sensitivity of astrocytic cells towards TBT-Cl.

3.4.5 Summary

In summary, two distinct, terminally differentiated, NT2.N and NT2.N/A *in vitro* cell systems, along with the mitotic precursor NT2.D1 cell line and mitotic CCF-STTG1 astrocytoma cell line, were used to study the basal cytotoxicities of several test chemicals reflecting different potencies and specificities. It was found that the measurement of basal cytotoxicity using different cell systems could differentiate between acute cytotoxicants and neurotoxicants, in that much lower micromolar concentrations of TMT-Cl and TBT-Cl were required to induce cell-death in comparison with the millimolar concentrations of 2,5-, 2,3- and 3,4-HD. However, the significant differences could not consistently be attributed to the presence or absence of neuronal features, as known neurotoxicants were not consistently more toxic to the differentiated neuronal cell systems in comparison with the continuous CCF-STTG1 and NT2.D1 cell lines. Thus, whilst the MTT reduction assay was found to be a useful estimation of the basal cytotoxic effects of the tested compounds, it could not establish their overall neurotoxic potential.

IC_{50} values obtained were generally in good agreement with those in the literature and

with the exception of TBT-Cl, acute oral rodent LD_{50} values correlated with cytotoxicity IC_{50} values. Factors such as species differences, *in vivo* CNS levels and compound kinetics were not generally considered. However, as mentioned, when initially screening a compound, it is advantageous to examine the intrinsic toxicity of the chemical in a controlled defined system without *in vivo* complicating factors. These factors are considered more critical when results from neurospecific endpoints from a later testing stage are evaluated.

Regarding the differentiated cell systems only, it appeared that the NT2.N mono-culture demonstrated a different vulnerability compared with the NT2.N/A co-culture in response to the neurotoxins 2,5-HD, TMT-Cl and TBT-Cl after both 4- and 24-hours exposure. That the NT2.N/A cell system was consistently more tolerant towards the toxins than the NT2.N culture may be due to the protective mechanisms of astrocytes limiting neurotoxic damage. However, it must be considered that as NT2.A cells outnumber NT2.N cells in the co-culture, insensitive astrocytic cells may at times simply be masking the cytotoxic effect. Thus in future a mono-culture of NT2 astrocytes may provide a useful comparison as the CCF-STTG1 did not provide consistent data for this purpose. Nevertheless, the basal cytotoxicity data obtained provides preliminary evidence of the value of astrocytes in cytotoxicity assays and the greater degree of relevance to the heterogeneous nervous system situation offered by an *in vitro* integrated population of human neurons and astrocytes.

The concentration-response curves were also used estimate the non-cytotoxic range (between zero and the highest concentration of toxin at which the A_{590} was not significantly decreased below that of the untreated control (NOAEL)) after 4-hours exposure to each toxin. This concentration range was employed for the biochemical endpoint assays (Chapter 5), as the various mechanisms inducing toxicity according to differing cell system properties may be more apparent at non-cytotoxic levels.

The NOAEL was estimated using only the first 3-5 points of each concentration-response curve. With hindsight, a more accurate estimation may have been obtained by focusing on this area of the curve with a further MTT assay following the IC_{50} value range finding study. However, the different mechanistic actions of the chemicals

should still be more apparent over this estimated non-cytotoxic range, with any alterations in biochemical parameters measured being due to toxin induced changes in cellular levels rather than due to a decrease in cell number.

Chapter 4 – Biochemical endpoint protocol development

4.1 Introduction

Numerous toxicants interfere with cellular biochemical functions in the central nervous system (CNS) and the resulting dysfunction can ultimately compromise cell survival (Gregus and Klaassen, 2001). Mitochondria are at the crossroads of several biochemical activities which may crucially affect cellular maintenance and the nervous system is particularly susceptible to toxicants that disrupt mitochondrial function and metabolism. It has been hypothesised that a number of key mitochondrial related disorders are involved in apoptotic or necrotic neuronal cell death inflicted by toxins, including an increase in intracellular reactive oxygen species (ROS) commensurate with impaired antioxidant function and a decrease in energy levels (Gregus and Klaassen, 2001; Gartlon *et al.*, 2006; Van Houten *et al.*, 2006). Therefore, whilst they have the limited ability to detect neural-specific effects, biochemical endpoints concerning changes to the energy and oxidative status of the cell have been recommended for inclusion in screening systems for detecting neurotoxicity. The mitochondrially related biochemical endpoints chosen for use in this study were a measure of cellular ATP, GSH and H_2O_2 levels and estimation of caspase-3 activation was included to indicate an apoptotic mode of cell death.

The MTT reduction assay was used to provide information on the basal cytotoxic potential of each test compound and also to estimate the non-cytotoxic concentration range for the test chemicals in each of the cell systems. It was hypothesised that the various subtle biochemical changes induced by the test chemicals according to differing cell system properties, such as differentiation level or inclusion of more than one cell type, may be more apparent at such non-cytotoxic levels when not masked by overt cytotoxic effects. So this process may provide a more sensitive assessment of the suitability of a particular cell system for detecting the acute neurotoxic potential of new and existing chemicals.

The methods to measure changes in such biochemical parameters that follow toxin exposure need to be rapid and inexpensive to match needs of the pharmaceutical and chemical industries, as well as in response to the REACH strategy. Accordingly, in the

present chapter, reliable and sensitive procedures were developed for the rapid collection and accurate quantification of the above biochemical endpoints. As with the measurement of basal cytotoxicity, it was considered that a 6-well plate format would be appropriate for the high-throughput screening of potential neurotoxins using biochemical endpoints. Thus, the protocols required that following toxin exposure, the cells be handled in such a way that endpoint analyte levels could be quantified in a 96-well plate, using the appropriate multiwell plate reader. The steps this involved were dependent on the factor being measured.

4.2 Materials and Methods

4.2.1 Materials

For materials, refer to Chapter 2, section 2.2.1.

4.2.2 Exposure of cells to test chemicals

The same optimum cell density as that determined by the MTT calibration assay (section 3.3.4) was used, as this was not contraindicated by any of the biochemical endpoint assay protocols.

4.2.2.1 NT2.D1 and CCF-STTG1 cells

Cells were counted using a haemocytometer in conjunction with the vital stain neutral red, to distinguish between viable and non-viable cells. Cells were then plated out in their usual medium, at a density of 5 x 10^5 viable cells per well of a 6-well plate and left in a humidified chamber overnight at 37 °C in 5 % CO_2, 95 % air. The medium was removed and the cells washed with fresh medium. The cells were then incubated in the presence of 2 ml of the appropriate medium (as described in individual biochemical endpoint protocols) supplemented with increasing non-cytotoxic concentrations of test chemical up to the NOAEL as determined using the MTT assay (see table 4.1 below and also section 3.3.2). Six to twelve wells were used in total per toxin, with one well utilised per toxin concentration and medium only acted as an untreated no-toxin control. The plates were then replaced in the humidified chamber at 37 °C in 5 % CO_2, 95 % air, for 4-hours, before utilising the cells in one of the biochemical endpoint assays as described in sections 4.2.3-6.

4.2.2.2 NT2.N and NT2.N/A cells

Cultures of NT2.N or NT2.N/A cells were produced as previously described (section 2.2.5). The medium was removed and the cells washed with fresh medium. The cells were then incubated in the presence of 2 ml of the appropriate medium (as described in individual biochemical endpoint protocols) supplemented with increasing non-

cytotoxic concentrations of test chemical up to the NOAEL as determined using the MTT assay (see table 4.1 below and also section 3.3.2). Six to twelve wells were used in total per toxin, with one well utilised per toxin concentration and medium only acted as an untreated control. The plates were then replaced in the humidified chamber at 37 °C in 5 % CO_2, 95 % air, for 4-hours, before utilising the cells in one of the biochemical endpoint assays as described in sections 4.2.3-6

Test chemical	Cell line	Concentration / Units	
2,5-Hexanedione (2,5-HD)	NT2.D1	5-50	mM
	CCF-STTG1	10-85	
	NT2.N	10-85	
	NT2.N/A	10-85	
2,3-Hexanedione (2,3-HD)	NT2.D1	0.5-12	mM
	CCF-STTG1	1-16	
	NT2.N	0.5-8	
	NT2.N/A	0.5-12	
3,4-Hexanedione (3,4-HD)	NT2.D1	0.5-12	mM
	CCF-STTG1	0.5-12	
	NT2.N	1-16	
	NT2.N/A	1-16	
Trimethyltin chloride (TMT)	NT2.D1	25-500	μM
	CCF-STTG1	25-500	
	NT2.N	25-500	
	NT2.N/A	50-1000	
Tributyltin chloride (TBT)	NT2.D1	0.2-2	μM
	CCF-STTG1	0.2-4	
	NT2.N	0.1-1	
	NT2.N/A	0.2-2	

Table 4.1 Non-cytotoxic concentration range of test chemical each cell line exposed to for 4-hours. Medium only acted as a no-toxin control.

4.2.3 Determination of adenosine triphosphate (ATP) levels

The luciferin-luciferase ATP detection assay was first proposed by Lemasters and Hackenbrock (1973) in order to measure mitochondrial ATP production, then it underwent further development as a cell viability assay by Lundin *et al.,* (1986), followed by utilisation for chemosensitivity testing (Petty *et al.,* 1995; Cree and Andreotti, 1997). Examination of the non-cytotoxic concentration-response of ATP levels to toxic agents can be used to assess the role of energetic stress in the mediation of toxic effects. Indeed, ATP levels are often depressed as a consequence of exposure

to neurotoxins (Marcaida *et al.*, 1997).

The ATPlite 1-step 96-well microplate assay is a quantitative ATP monitoring system based on the production of visible light (emission maximum 560 nm) caused by the reaction of ATP with added firefly luciferase and its substrate D-luciferin (figure 4.1).

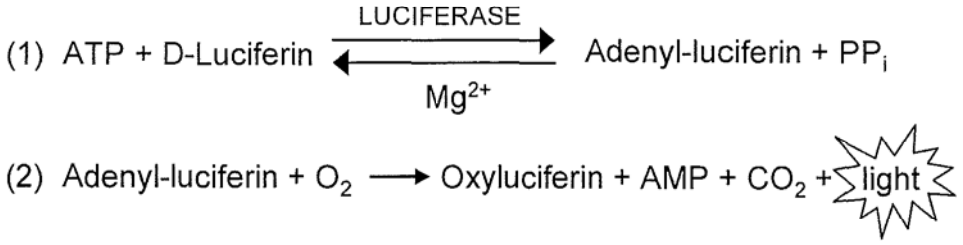

Figure 4.1 Reaction scheme utilised by the ATPlite 1-step assay.

In figure 4.1, reaction (1) is reversible and the equilibrium lies far to the right. Reaction (2) is cssentially irreversible. The light emitted is linearly proportional to the ATP present up to an ATP concentration of 10 μM so long as the cell number does not exceed 5 x 10^4 cells per 96-well and luminescence is measured within 30 min after ATPlite reagent addition.

The ATPlite assay guidelines recommend that the 1-step assay reagent be directly added to a suspension of cells and toxin, rather than following removal of the medium containing toxin and rinsing of the cells. Phenol red does not interfere with the luciferin/luciferase reaction but has been found to physically absorb some of the emitted light, resulting in lower assay signals and therefore, the usual cell culture medium was substituted with the phenol red free equivalent. FBS free medium was also desirable (see section 4.2.3.5). Other medium supplements such as L-glutamine and sodium pyruvate are not reported to interfere with the luminescence response.

4.2.3.1 Protocol

Cellular ATP levels were determined using the ATPlite 1-step assay kit (601673) from Perkin Elmer (Beaconsfield, UK), according to the manufacturer's guidelines (the exact constitution of kit contents is patent protected). Briefly, a vial of lyophilised

luciferin/luciferase based reagent solution was reconstituted using 10 ml assay buffer and mixed by inversion to give a clear homogeneous solution. A multipipette was used to add 100 µl reconstituted reagent to each well containing 100 µl cell suspension (section 4.2.3.2) or standard (4.2.3.4). This 1-step reagent both lyses the cells and starts the luminescence reaction. The plate was shaken gently for two min in order to mix the components thoroughly and the luminescence was measured using a SpectraMAX GeminiXS microplate luminometer (Molecular Devices, UK) and SoftMaxPro software. ATP levels were calculated using a standard curve (section 4.2.3.4), corrected for sample protein content (section 4.2.3.3) and expressed as a percentage decrease below the untreated control value.

4.2.3.2 Sample preparation

Cells were exposed to a range of non-cytotoxic concentrations of test chemical for 4-hours as described in section 4.2.2, using phenol red and FBS free RPMI or DMEM-HG medium as appropriate, both supplemented with 1 % (v/v) pen/strep, 1 % (v/v) sodium pyruvate and 1 % (v/v) L-glutamine. Following this the cells were carefully scraped and pipetted up and down a number of times with a multipipette to create a uniform cell suspension. Following this, 100 µl each of control and treated samples (eight determinations per well) were transferred into individual wells of a black 96-well microplate. The ATP assay was then carried out as described in section 4.2.3.1. A standard curve was run along with each new set of samples.

4.2.3.3 Protein determination using the BCA protein assay test tube procedure

Following luminescence detection, 100 µl aliquots of cell lysate (produced in section 4.2.3.1) were taken for sample protein estimation using the BCA protein assay reagent kit from Pierce (Rockford, USA), according to the manufacturer's guidelines for the test tube procedure. Briefly, 100 µl of samples or BSA standards (125-2000 µg/ml, water acted as a BSA-free control) were added to a test-tube together with the 2 ml of the working reagent (50:1, Reagent A:B), incubated at 37 °C for 30 min and allowed to cool to room temperature. The resulting solution was transferred to a cuvette and the A_{562} was measured using a Boeco SS-22 UV/Vis spectrophotometer (Boeco Company,

Germany).

4.2.3.4 Preparation of ATP standard curve

The lyophilised ATP standard provided with the assay kit was diluted with deionised water to produce a 10 μM standard which was diluted using phenol red and FBS free RPMI or DMEM-HG culture medium as appropriate, to produce ATP concentrations between 10 μM and 1 nM. Medium only acted as an ATP-free background control. 100 μl of standards (in duplicate) were loaded into individual wells of a black 96-well microplate and the ATP assay was then carried out as described in section 4.2.3.1.

4.2.3.5 Effect of serum free medium on cell viability

As protein measurements were determined directly from sample cell lysates produced as a result of the ATPlite 1-step procedure (section 4.2.3.1), serum free medium was desirable so that it did not elevate the protein levels of the samples being determined.

A simple MTT assay was used to assess for effects of serum free medium on the viability of cell cultures. To a well of a 6-well plate containing 5 x 10^5 viable CCF-STTG1 or NT2.D1 cells, or NT2.N and NT2.N/A cells as prepared in section 2.2.5, were added 2 ml of phenol red free RPMI or DMEM-HG medium, supplemented as in section 4.2.3.2 but with or without 10 % (v/v) FBS as appropriate. Plates were incubated for 4-hours and the MTT assay was then carried out as detailed in section 3.2.2.1. Four determinations were made per well and the experiment was performed on two separate occasions.

4.2.3.6 Examination for interference of test chemicals or medium with the ATPlite 1-step reagent

As the ATPlite 1-step reagent was combined directly with medium containing test chemical, it was determined whether any of the test chemicals or the medium itself interfered with ATP assay and subsequently the luminescent signal. Briefly, for each test chemical, aliquots of 100 μl of the highest non-cytotoxic concentration used (table

4.1, section 4.2.2) were prepared using phenol red free RPMI or DMEM-HG media, supplemented as in section 4.2.3.2 and were placed into individual wells of a black 96-well microplate. The ATP assay was carried out as described in section 4.2.3.1. Background controls consisted of medium only, PBS only or an aliquot of 200 µl toxin without the ATPlite 1-step reagent added. Four determinations were made per well and the experiment was performed on two separate occasions.

4.2.3.7 Examination for interference of test chemical and ATPlite 1-step reagent with BCA protein assay

As protein measurements were determined from cell lysates resulting from combination of the ATPlite reagent and medium containing test chemical, it was determined whether these agents interfered with the BCA protein assay. Luminescence examination of medium containing toxin combined with the ATPlite reagent was carried out as described in section 4.2.3.6 above. Following this, a 100 µl aliquot of the resulting solution from each well of row A of the microplate was taken for protein estimation using the BCA protein assay reagent kit from Pierce (Rockford, USA), according to the manufacturer's guidelines for the test tube procedure as detailed in section 4.2.3.3. The absorbance was compared with that of a 100 µl deionised water control or medium alone. Four determinations were made per well and the experiment was performed on two separate occasions.

4.2.4 Determination of caspase-3 levels

Caspases are a family of proteases thought to be the key initial effectors in the induction of apoptosis. During this process, cyt-c is released from the mitochondria and activates caspase-9, which in turn activates caspase-3 (Andersson *et al.*, 2000).

Caspase-3 plays a central role in the apoptotic cascade and an established method for detecting apoptosis induction involves the incorporation of a caspase-3 recognition-sequence peptide into a coumarin based fluorescent compound such as aminomethylcoumarin (AMC) (Betz *et al.*, 2003). Active caspase-3 recognises substrates with the sequence asp-glu-val-asp (DEVD) (Nobel *et al.*, 1997; Talanian *et*

al., 1997) and specifically cleaves at the c-terminal side of the aspartate residue of the substrate Ac-DEVD-AMC to release the fluorophore AMC (Yu *et al.*, 2001). The fluorescent substrate accumulates over time with a signal which is detectable at 1 hour and is proportional to caspase-3 activity present within a cell lysate sample (Betz *et al.*, 2003). Comparison of the fluorescence of AMC from an apoptotic sample with an uninduced control allows determination of the percentage increase in caspase-3 activity.

Caspase-3 activation occurs early in the apoptotic cascade. Cells incubated with 1 μM of the apoptotic inducer staurosporine showed substantial increase in caspase-3 activity after 3-hours but no evidence of apoptotic nuclei until after 8-hours exposure (Andersson *et al.*, 2000). Therefore, the assay is a useful tool for detecting apoptosis induction in cells exposed to toxins for 4-hours.

4.2.4.1 Protocol

Caspase-3 enzymic activity was determined via cleavage of the fluorogenic substrate Ac-DEVD-AMC using a protocol adapted from that kindly provided by Dr M. Grant (Birmingham Dental School, personal communication). Supernatent lysate samples (section 4.2.4.2) were incubated with 32 μl assay buffer (20 mM HEPES (pH 7.8), 10 % glycerol, 2 mM DTT), along with 20 μl of a 0.071 mM solution of the substrate Ac-DEVD-AMC in assay buffer and 38 μl water, for 1 hour at 37 °C. The 10 μl standards (section 4.2.4.4) were incubated without the substrate (32 μl assay buffer and 58 μl water). The fluorescence was then measured using SpectraMAX GeminiXS microplate fluorimeter (Molecular Devices, UK) with SoftMaxPro software and with excitation and emission set at 355 nm and 460 nm respectively. The amount of AMC released was calculated using a standard curve generated using known amounts of AMC (section 4.2.4.4), corrected for sample protein content (section 4.2.4.3) and expressed as a percentage increase above the untreated control value.

4.2.4.2 Sample preparation

Cells were to a range of non-cytotoxic concentrations of toxins for 4-hours as described

in section 4.2.2, using the usual RPMI or DMEM cell culture media as appropriate. Following toxin exposure the medium was removed, the cells were rinsed in PBS and then scraped into a 15 ml tube, centrifuged (450 g, 10 min) and 100 µl lysis buffer (10 mM Tris-HCl (pH 7.5), 130 mM NaCl, 1 % (v/v) Triton X 100 and 1 % (v/v) protease inhibitor cocktail) was added. After incubation on ice for 10 min and centrifugation (13000g, 5 min), 10 µl of supernatent lysate (eight determinations per well) was placed in a black 96-well microplate. The caspase-3 assay was then carried out as described in section 4.2.4.1. A standard curve was run along with each new set of samples. Cells treated with 1 µM of the apoptotic inducer staurosporine provided a positive control.

4.2.4.3 Protein determination using the BCA protein assay microplate procedure

A 10 µl aliquot of cell protein lysate was taken for protein determination using the BCA protein assay reagent kit from Pierce (Rockford, USA), according to the manufacturer's guidelines for the 10 µl microplate procedure. Briefly, 10 µl of samples or BSA standards (125-2000 µg/ml, water acted as a BSA-free control) were added to a clear microplate together with the 200 µl of the working reagent (50:1, Reagent A:B), incubated at 37 °C for 30 min, allowed to cool to room temperature and the A_{590} was measured using a Thermo Multiskan EX 96-well microplate spectrophotometer (Thermo Electron Corporation, USA) with Ascent software.

4.2.4.4 Preparation of AMC standard curve

A 100 µM AMC standard was prepared in, as well as diluted using DMSO, to give AMC concentrations between 100 µM and 0.1 µM. A 10 µl aliquot of each standard was then loaded in duplicate into individual wells of a black 96-well microplate, with DMSO only acting as a no AMC control. The caspase-3 assay was then carried out as described in section 4.2.4.1.

4.2.5 Determination of glutathione (GSH) levels

The most widely used and convenient method for the determination of total glutathione (GSH + GSSG) in a biological sample is a kinetic enzymatic-recycling assay first

reported by Owens and Belcher (1965). The method is based on the oxidation of GSH by 5,5'-dithiobis(2-nitrobenzoic) acid (DTNB), to produce the chromophore 5-thio-2-nitrobenzoic acid (TNB), which has maximal absorbance at 412 nm. Tietze (1969) developed the method to recycle GSH using the catalyst glutathione reductase (GSR) and NADPH, to improve specificity and sensitivity (figure 4.2) and Clarke *et al.,* (1996) adapted the assay from cuvette to a high-throughput microplate method. The colorimetric response is linear up to 170 μM and proteins should be precipitated prior to assay as they may falsely elevate GSH values. The assay was further modified by Schuliga *et al.,* (2002) and it is this communication upon which the following protocol is based, with additional examination of the optimum concentration of the GSR catalyst for use in our laboratory.

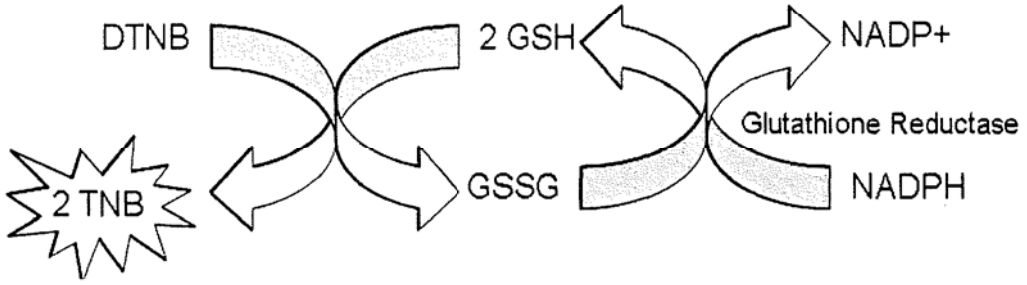

Figure 4.2 Schematic (non-stoichiometric) showing the enzymatic-recycling of GSH using the catalyst glutathione reductase (GSR) and NADPH to produce the chromophore 5-thio-2-nitrobenzoic acid (TNB) from 5,5'-dithiobis(2-nitrobenzoic) acid (DTNB).

4.2.5.1 Protocol

A working solution of 0.2 mM NADPH and 0.52 mM DTNB was prepared in sodium dihydrogen phosphate assay buffer (0.1 M sodium dihydrogen phosphate, pH 7.5 with 0.15 mM EDTA). A 5 U/ml GSR enzyme solution was prepared by dilution of glutathione reductase from bakers yeast (500 U in 3.6 M ammonium sulphate, pH 7) with assay buffer. The reaction was begun by adding 165 μl of NADPH/DTNB working solution to the standards and samples (prepared in sections 4.2.5.4 and 4.2.5.2) in each microplate well. The plate was protected from light and incubated at 37 °C for 15 min. GSR enzyme solution at 40 μl was then added and the plate incubated at room temperature for 5 min whilst protected from light. The A_{405} was then measured using a

Thermo Multiskan EX 96-well microplate spectrophotometer (Thermo Electron Corporation, USA) with Ascent software. Glutathione levels were calculated using a standard curve generated using known amounts of GSH (section 4.2.5.4), corrected for sample protein content (section 4.2.5.3) and expressed as a percentage decrease below the untreated control value.

4.2.5.2 Sample preparation

Cells were exposed to a range of non-cytotoxic concentrations of toxins for 4-hours as described in section 4.2.2 using the usual RPMI or DMEM-HG cell culture medium as appropriate. Nine to twelve wells were used in total per toxin, with the first well containing medium only, to act as an untreated control. The cells were then washed with 1 ml PBS. Cells from each well were scraped into 1 ml PBS, transferred to labelled microcentrifuge tubes and centrifuged (600 g, 10 min). The supernatent was removed and 100 µl 5 % (w/v) sulphosalicylic acid (SSA) solution added to deproteinise the samples. Following a duplicate freeze/thaw cycle using liquid nitrogen/waterbath (37 °C), the samples were centrifuged (10,000 g, 10 min) to give a protein pellet plus supernatent. The pellets were assayed for protein content as described in section 4.2.5.2. A repeat pipettor was used to load 10 µl of supernatent from control and treated samples (eight determinations per well) into individual wells of a clear 96-well microplate. The total glutathione assay was then carried out as described in section 4.2.5. A standard curve was run alongside each new set of samples.

4.2.5.3 Protein determination using the DC protein assay

The protein content of the protein pellet (section 4.2.5.2) was determined using the DC protein assay reagent kit (Bio-Rad, UK), according to the manufacturer's guidelines for the test tube procedure. Briefly, 127 µl working reagent A' was added to the protein pellet, which was then vortexed intermittently for 10 min to solubilise. Working reagent A' at 127 µl was also added to 100 µl of BSA standards (125-2000 µg/ml, water only acted as a no BSA control) and vortexed. To correct for volume difference between samples and standard curve, 100 µl water was added to the solubilised pellet. The resulting samples or standard solutions were added to a test-tube together with the

1 ml of reagent B, vortexed and incubated at room temperature for 15 min. The resulting solution was transferred to a cuvette and the A_{750} was measured using a Boeco SS-22 UV/Vis spectrophotometer (Boeco Company, Germany).

4.2.5.4 Preparation of glutathione (GSH) standard curve

A 50 μM glutathione standard solution was prepared in 5 % (w/v) SSA solution and 1 in 2 serially diluted using SSA to give glutathione concentrations between 50 μM and 1.56 μM. SSA only acted as a GSH-free background control. 10 μl of standards (in duplicate) were loaded into individual wells of a clear 96-well microplate and the total glutathione assay was then carried out as described in section 4.2.5.

4.2.5.5 Optimum concentration of glutathione reductase (GSR)

The protocol uses the catalyst GSR along with NADPH to recycle glutathione. The optimum concentration of GSR and recycling time for use in the GSH assay was determined. A 5, 10 and 14 U/ml GSR enzyme solution was prepared by dilution of glutathione reductase from bakers yeast (500 U in 3.6 M ammonium sulphate, pH 7) with assay buffer (0.1 M sodium dihydrogen phosphate, pH 7.5, with 0.15 mM EDTA). A 100 μM glutathione standard solution was prepared in 5 % (w/v) SSA solution and 1 in 2 serially diluted using SSA to give glutathione concentrations between 100 μM and 1.56 μM. SSA only acted as a GSH-free control. 10 μl of standards (in duplicate) were loaded into individual wells of a clear 96-well microplate. The total glutathione assay was then carried out as described in section 4.2.5 using each of the three GSR enzyme solutions in turn and with the A_{405} measured at 1, 2, 3, 4, 5, 7.5 and 10 min after GSR addition.

4.2.6 Determination of hydrogen peroxide (H_2O_2) levels in medium

As hydrogen peroxide is membrane permeable and is more stable than other reactive oxygen species (e.g. $O2^{-\bullet}$, $^{\bullet}OH$, singlet oxygen), it is often chosen to quantitate the extracellular release into solution of reactive oxygen species (ROS) produced by cells (Zhou *et al.*, 1997; Votyakova and Reynolds, 2004).

The Amplex® red (AR) assay for hydrogen peroxide was devised by Zhou *et al.*, (1997) for the *in vitro* quantification of hydrogen peroxide released by stimulated neutrophils and Mohanty *et al.,* (1997) for the determination of hydrogen peroxide generated by activated leukocytes. It has since been used successfully to measure H_2O_2 released into the culture medium by toxin exposed lung fibroblasts (Ingram *et al.*, 2003) and as a measure of oxidative stress in NT2.N/A co-cultures subjected to glutamate excitotoxicity (Sandhu *et al.*, 2003).

The AR assay uses the sensitive non-fluorescent probe N-acetyl-3,7,-dihydroxyphenoxazine (Amplex red). Amplex red itself reacts in a 1:1 stoichiometry with hydrogen peroxide in solution in the presence of the catalyst horseradish peroxidase (HRP), to produce the red, strongly fluorescent, stable, de-acetylated oxidation product 7-hydroxy-^{3}H-phenoxazine-3-one (resorufin) (Mohanty *et al.*, 1997) (see figure 4.3). HRP is a hemoprotein capable of catalysing the oxidation by hydrogen peroxide of a wide variety of substrates including ascorbate, cytochrome C and Amplex red, via a mechanism involving free radical formation (Votyakova and Reynolds, 2004) (figure 4.3). Resorufin has fluorescence absorption in the range of 530-560 nm and emission maxima of 590 nm and the Amplex red (AR) assay has been determined to be linear in the range 100 nM to 10 μM hydrogen peroxide (Zhou *et al.*, 1997).

$$HRP + H_2O_2 \rightarrow \text{Compound I}$$

$$\text{Compound I} + AH_2 \rightarrow \text{Compound II} + AH^{\bullet}$$

$$\text{Compound II} + AH_2 \rightarrow HRP + AH^{\bullet} + 2H_2O$$

$$AH^{\bullet} + AH^{\bullet} \rightarrow A + AH_2$$

$$\text{Overall reaction: } AH_2 + H_2O_2 \rightarrow A + 2H_2O$$

Figure 4.3 Scheme for the reaction of Amplex red with hydrogen peroxide, in the presence of the catalyst horse radish peroxidase (HRP), to produce the fluorescent product resorufin. AH_2 is the oxidisable substrate (in this case Amplex red) and A is the oxidised product (in this case resorufin). Compound II contains a one-electron oxidised iron ion Fe(IV). Compound I also has a one-electron oxidised $[heme]^{+\bullet}$. Thus, one two-electron oxidation equivalent of H_2O_2 is traded for two subsequent one-electron transfers from the substrate, resulting in the production of two $AH^{\bullet}$ radicals.

The AR assay is considered to be more reliable than the commonly used 2',7'-dichlorofluorescein fluorometric assay for reactive oxygen species determination, which is dependent on endogenous peroxidase and subject to artefacts of autooxidation (Ingram *et al.*, 2003). With the AR assay, further oxidation of resorufin to non-fluorescent resazurin only occurs significantly if the concentration of H_2O_2 exceeds the concentration of AR. Additionally, NADH and GSH can interact potentially with the HRP/Amplex red system by promoting the formation of resorufin. However, when mitochondria and cell membranes remain intact during an experiment, interference should be negligible.

4.2.6.1 Protocol

The Amplex red, hydrogen peroxide assay kit A22188, was purchased from Invitrogen Molecular Probes (Paisley, UK) and contained Amplex red reagent (AR), sodium phosphate reaction buffer (50 mM, pH 7.4) and horseradish peroxidase (10 U). A working solution of 100 μM AR and 0.2 U/ml HRP was prepared in reaction buffer. The reaction was begun by the addition of 50 μl of the AR/HRP working solution to the standards and samples (prepared in sections 4.2.6.3 and 4.2.6.2) in each microplate well. The plate was protected from light, shaken gently for 1 min and incubated at room temperature for 30 min. The fluorescence was then measured using a SpectraMAX GeminiXS microplate fluorimeter (Molecular Devices, UK) with SoftMaxPro software, with the excitation/emission wavelength filters set at 544 nm and 590 nm respectively. Hydrogen peroxide levels were calibrated using a standard curve constructed using known hydrogen peroxide concentrations and expressed as a percentage increase above the untreated control value.

4.2.6.2 Sample preparation

Cells were exposed to a range of non-cytotoxic concentrations of test chemicals for 4-hours as described in section 4.2.2 using HANKS BSS (HBSS) medium supplemented with 1 % L-glutamine (v/v) and an additional 1 mg/ml (CCF-STTG1 cells) or 3.5 mg/ml D-glucose (NT2.D1 derived cells) as appropriate (see section 4.2.6.4). Following this, a multipipette was used to load 50 μl of medium from control and

treated wells (eight determinations per well) into individual wells of a black 96-well microplate. The Amplex red assay was carried out as described in section 4.2.6.1. A standard curve prepared using the same medium was run alongside each new set of samples.

4.2.6.3 Preparation of hydrogen peroxide standard curve

A 10 μM H_2O_2 standard was prepared using HANKS BSS medium supplemented with 1 % L-glutamine (v/v) and 1 or 3.5 mg/ml D-glucose as appropriate and was 1 in 2 serially diluted to give H_2O_2 concentrations between 10 μM and 78 nM. A multipipette was used to load 50 μl of standards (in duplicate) into individual wells of a black 96-well microplate, with medium only acting as a no H_2O_2 control. The Amplex red assay was then carried out as described in section 4.2.6.1.

4.2.6.4 Effect of medium type on sensitivity of Amplex Red assay

The kit protocol suggested preparing a H_2O_2 standard curve in the sodium phosphate reaction buffer provided. However, as H_2O_2 levels released into the medium by toxin exposed cells were to be quantified, it seemed preferable to prepare the standards in the same medium as that of the exposed cells.

Phenol red is known to quench the fluorescent signal and serum may need to be avoided due to catalase activity that is capable of preventing the oxidation of AR. The essential amino acid L-glutamine often included in culture medium should not affect the sensitivity of the AR assay. However, the energy source supplement pyruvate is able to degrade H_2O_2 released into the medium through non-enzymatic oxidative decarboxylation, to carbon dioxide, water and acetate (Desagher *et al.*, 1997), resulting in the determination of reduced extracellular H_2O_2 levels. Due to these considerations, it has been reported that hydrogen peroxide may be detected with greater sensitivity in defined medium such as HANKS Balanced Salt Solution (HBSS) (Votyakova and Reynolds, 2004; Mandavilli *et al.*, 2005), which was developed for use in tissue culture to maintain cells in a viable state, at physiological pH and osmotic pressure for short periods of time, rather than to promote growth (Hanks, 1975).

4.2.6.4.1 Preparation of hydrogen peroxide standard curve using different medium formulations

In order to investigate effects of various types of medium on the sensitivity of the AR assay, a hydrogen peroxide standard curve was constructed using several combinations of phenol red free medium and supplements as detailed in table 4.2. HBSS is formulated with 1mg/ml D-glucose and was supplemented with a further 1mg/ml or 3.5 mg/ml to resemble the usual levels found in RPMI and DMEM-HG medium respectively.

Media	Total D-glucose (mg/ml)	Serum (10%)	Sodium Pyruvate (1%)	L-Glutamine (1%)
RPMI	**2**	+	+	+
RPMI	**2**	-	+	+
DMEM	**4.5**	+	+	+
DMEM	**4.5**	-	+	+
HANKS	**4.5**	-	-	+
HBSS	**4.5**	-	+	+
HBSS	**2**	-	-	-
HBSS	**2**	-	-	+
HBSS	**2**	-	+	-
HBSS	**2**	-	+	+
HBSS	**0**	-	-	-
Reaction buffer	**0**	-	-	-

Table 4.2 Preparation of hydrogen peroxide standard curve using different medium formulations. Phenol red free RPMI, DMEM or HBSS medium was supplemented with D-glucose and also supplemented with (+), or remained free of (-) serum, sodium pyruvate and L-glutamine, as detailed in the table.

A 5 μM H_2O_2 standard was prepared using each medium in turn and was 1 in 2 serially diluted to give H_2O_2 concentrations between 5 μM and 78 nM. A multipipette was used to load 50 μl of standards (in duplicate) into individual wells of a black 96-well microplate, with medium only acting as a no H_2O_2 control. The Amplex red assay was then carried out as described in section 4.2.6.1.

4.2.6.5 Effects of HANKS BSS on cell viability

As HBSS does not contain all the components usually included in cell culture medium

to aid efficient cell metabolism, a simple MTT assay was used to assess its effects on the viability of cultures of the cell lines. To a well containing 5 x 10^5 viable CCF-STTG1 or NT2.D1 cells, or NT2.N neurons and NT2.N/A neurons astrocytes as prepared in section 2.2.5, were added 3 ml of appropriate medium, supplemented as detailed in tables 4.3 and 4.4. Plates were incubated for 4-hours and the MTT assay was then carried out as detailed in section 3.2.2.1. Four determinations were made per well and the experiment was performed on two separate occasions.

Media	Total D-glucose (mg/ml)	Serum (10%)	Sodium Pyruvate (1%)	L-Glutamine (1%)
1 RPMI	**2**	+	+	+
2 RPMI	**2**	-	+	+
3 HBSS	**1**	-	-	-
4 HBSS	**2**	-	-	-
5 HBSS	**2**	-	-	+
6 HBSS	**2**	-	+	-

Table 4.3 Effects of HANKS BSS on CCF-STTG1 cell viability. Phenol red free RPMI or HBSS medium for use with the CCF-STTG1 cell line was supplemented with D-glucose and also supplemented with (+), or remained free of (-) serum, sodium pyruvate and L-glutamine as detailed.

Media	Total D-glucose (mg/ml)	Serum (10 %)	Sodium Pyruvate (1%)	L-Glutamine (1%)
1 DMEM-HG	**4.5**	+	+	+
2 DMEM-HG	**4.5**	-	+	+
3 HBSS	**1**	-	-	-
4 HBSS	**4.5**	-	-	-
5 HBSS	**4.5**	-	-	+
6 HBSS	**4.5**	-	+	-

Table 4.4 Effects of HANKS BSS on NT2.D1, NT2.N and NT2.N/A cell viability. Phenol red free DMEM or HBSS medium for use with the NT2.D1, NT2.N and NT2.N/A cell lines was supplemented with D-glucose and also supplemented with (+), or remained free of (-) serum, sodium pyruvate and L-glutamine as detailed.

4.2.6.6 Interference of test chemicals with the Amplex red reagent

As hydrogen peroxide levels were determined directly from medium containing the test chemicals, it was determined whether any of these toxins interfered with the Amplex red oxidation process and subsequently the fluorescence signal. Briefly, for each toxin, aliquots of 50 µl of the highest concentration (Cmax) used for non-cytotoxic exposure

(see table 4.1, section 4.2.2) and a 1 in 2 dilution (Cmax/2) were prepared using HBSS supplemented with 1 % (v/v) L-glutamine and a total of 4.5 mg/ml D-glucose. These aliquots were placed into individual wells of a black 96-well microplate and the Amplex red assay was carried out as described in section 4.2.6.1. An aliquot of 50 µl HBSS was used as a no toxin control.

The procedure was repeated for the Cmax of the α-diketones, 2,3- and 3,4-hexanedione only, with the omission of either the Amplex red or HRP from the AR/HRP working solution (section 4.2.6.1). Two determinations were made per aliquot and the experiment was performed on two separate occasions.

4.2.7 Untreated control analyte levels

Untreated control values for each cell line were determined for each of the assays (average of one replicate control value for each test chemical; therefore, N = 5 for the ATP, GSH and caspase assays and N = 3 for the hydrogen peroxide assay) and expressed in nmol analyte/mg protein in the case of the ATP, GSH and caspase-3 assays and nmol H_2O_2/µl medium in the case of the hydrogen peroxide assay.

4.2.8 Data analysis

The data analyses were carried out using GraphPad Prism software. Data are presented as the mean ± standard error of the mean (SEM), with N as detailed in the methods section for each experiment.

One-way ANOVA followed by Dunnett's multiple comparison test was used to assess for differences between treated compared with control values. Students unpaired t-test or one-way ANOVA followed by the Tukey post-test was used to assess for differences between mean responses at specific points or toxin concentrations. Groups of data were considered to be significantly different if $P < 0.05$.

4.3 Results

The following results section refers to the protocol development, sensitivity and data quantification aspects of the biochemical endpoint assays. Results concerning the analyte levels measured using the biochemical endpoint assays, following exposure of the cell systems to non-cytotoxic levels of test chemical, may be found in Chapter 5.

4.3.1 Determination of adenosine triphosphate (ATP) levels

Cells were exposed to a range of non-cytotoxic concentrations of test chemical for 4-hours as described in section 4.2.2 and then assayed using an ATPlite 1-step luminescent assay (section 4.2.3.1). ATP levels were then calculated using a 10 μM to 100 nM ATP standard curve (section 4.2.3.4), corrected for sample protein content (section 4.2.3.3) and expressed as a percentage decrease below the untreated control value.

4.3.1.1 Calibration curve

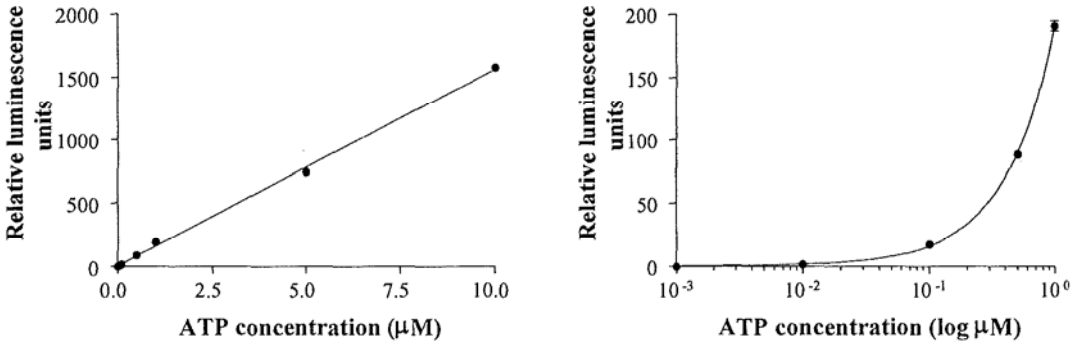

Figure 4.4 Representative ATP calibration curve. Concentration-response curve in response to increasing concentrations of ATP. A) linear regression or B) sigmoidal curve (variable slope). Results are expressed as the relative luminescence units of standards assayed for ATP levels by the ATPlite 1-step luminescent assay. Data points represent the mean ± SEM of duplicate standards from a single experiment.

Figure 4.4 shows a representative standard curve, one of which was analysed for ATP levels along with each new set of samples. As can be seen in figure 4.4 A, luminescent output increased linearly with increasing ATP concentration, with linear regression analysis yielding an R^2 value of 0.99. No significant difference was evident

between the luminescent signal for the no ATP standard and the 1 and 10 nM ATP standards ($P > 0.05$). However, a significant difference was evident for the 100 nM ATP standard ($P < 0.001$) and thus 100 nM ATP was considered to be the limit of detection. This may be more easily observed from figure 4.4 B which shows the log concentration-response at the lower end.

4.3.1.2 Effect of serum free medium on cell viability

FBS free medium was desirable in order that sample protein levels were not falsely elevated (see section 4.2.3.5). Thus a simple MTT assay was carried out in order to assess for effects of FBS free DMEM-HG or RPMI on cell viability after 4-hours exposure. Neither medium type was found to cause a statistical decrease in cell viability of the NT2.D1, NT2.N, NT2.N/A (DMEM-HG) or CCF-STTG1 (RPMI) cells after a 4-hour incubation period ($P > 0.05$). The data are not presented graphically.

4.3.1.3 Interference of test chemical or culture medium with ATPlite 1-step reagent

It was determined whether any of the test chemicals themselves interfered with the ATPlite assay luminescent signal (see section 4.2.3.6). Aliquots of the highest non-cytotoxic concentration of each toxin used were prepared in phenol red free medium and assayed using the ATPlite kit. None of the toxins were found to cause a statistical change in the luminescent signal compared with that of medium alone or toxin aliquots without the ATPlite working reagent added ($P > 0.05$). Medium alone was also not found to cause to cause a statistical change in the luminescent signal compared with that of PBS ($P > 0.05$). The data are not presented graphically.

4.3.1.4 Interference of test chemical and ATPlite 1-step reagent with BCA protein assay

Following luminescence examination of medium containing toxin combined with the ATPlite reagent (see section 4.2.3.7), an aliquot was taken to examine for any interference of toxin or assay reagent with the BCA protein assay (section 4.2.3.3).

None of the toxin/ATP assay reagent combinations were found to cause a statistical change in the luminescent signal compared with that of medium alone or deionised water ($P > 0.05$). The data are not presented graphically.

4.3.2 Determination of caspase-3 levels

Cells were exposed to a range of non-cytotoxic concentrations of toxin for 4-hours as described in section 4.2.2 and then assayed for caspase-3 activity via cleavage of the substrate Ac-DEVD-AMC to release the fluorophore AMC (section 4.2.4.1). Caspase levels were then calculated via a 100 μM to 100 nM AMC standard curve (section 4.2.4.4), corrected for sample protein content (section 4.2.4.3) and expressed as a percentage increase above the untreated control value.

4.3.2.1 Calibration curve

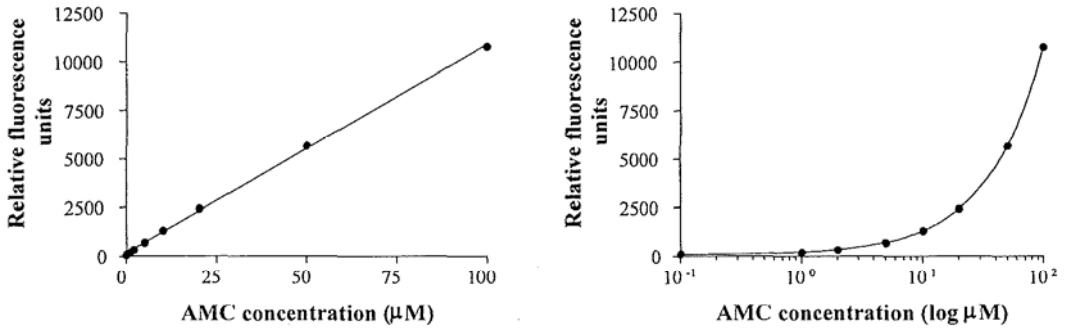

Figure 4.5 Representative AMC calibration curve. Concentration-response curve in response to increasing concentrations of AMC. A) linear regression or B) sigmoidal curve (variable slope). Results are expressed as the relative fluorescence units of standards assayed for AMC levels by the caspase assay. Data points represent the mean ± SEM of duplicate standards from a single experiment.

Figure 4.5 shows a representative standard curve, one of which was analysed for AMC levels along with each new set of samples. As can be seen in figure 4.5 A, fluorescent output increased linearly with increasing AMC concentration with linear regression analysis yielding an R^2 value of 0.99. A significant difference was evident between the fluorescent signal for the no AMC standard and the lowest 100 nM standard ($P < 0.001$) and thus 100 nM AMC was considered to be the limit of detection. This may be more easily observed from figure 4.5 B which shows the log concentration-response at

the lower end.

4.3.2.2 Staurosporine induced positive control

The staurosporine (1 μM) induced positive control cellular levels of caspase as determined in section 4.2.4.2, are shown in figure 4.6.

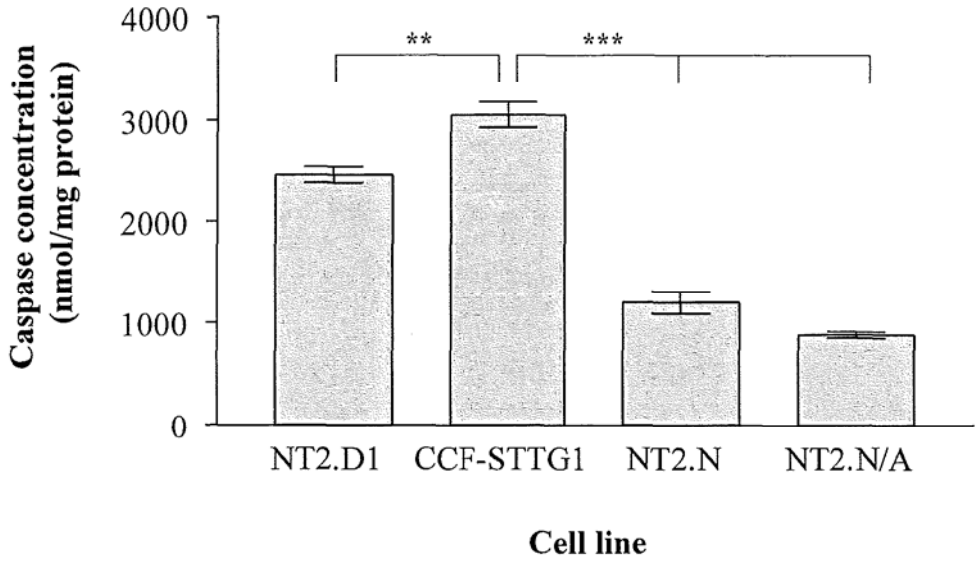

Figure 4.6 Caspase positive control values induced by 1 μM staurosporine were determined for each cell line. Bars represent the average of one replicate control value for each toxin ± SEM (N=5) and are expressed in nmol analyte/mg protein. Brackets indicate compared samples; *P<0.05, **P<0.01, ***P<0.001.

The positive control values indicated that caspase-3 levels were highest in cells from the CCF-STTG1 (3061.2 ± 124.1 nmol/mg) and NT2.D1 (2469.1 ± 80.4 nmol/mg) continuous cell lines, whose levels were significantly different ($P < 0.01$). In comparison with the continuous cell lines, cells from the post-mitotic NT2.N (1205.7 ± 111.0 nmol/mg) and NT2.N/A (889.5 ± 30.11 nmol/mg) cultures demonstrated significantly lower control levels of caspase activation ($P < 0.001$). As is evident from figure 4.6, the co-culture and mono-culture were found to have statistically equivalent control levels of caspase-3 ($P > 0.05$).

4.3.3 Determination of glutathione (GSH) levels

Cells were exposed to a range of non-cytotoxic concentrations of toxin for 4-hours as described in section 4.2.2 and then total cellular glutathione estimated using a colorimetric assay (section 4.2.5.1). Glutathione levels were calculated using a 50 μM to 3.13 μM GSH standard curve (section 4.2.5.4), corrected for sample protein content (section 4.2.5.3) and expressed as a percentage decrease below the untreated control value.

4.3.3.1 Calibration curve

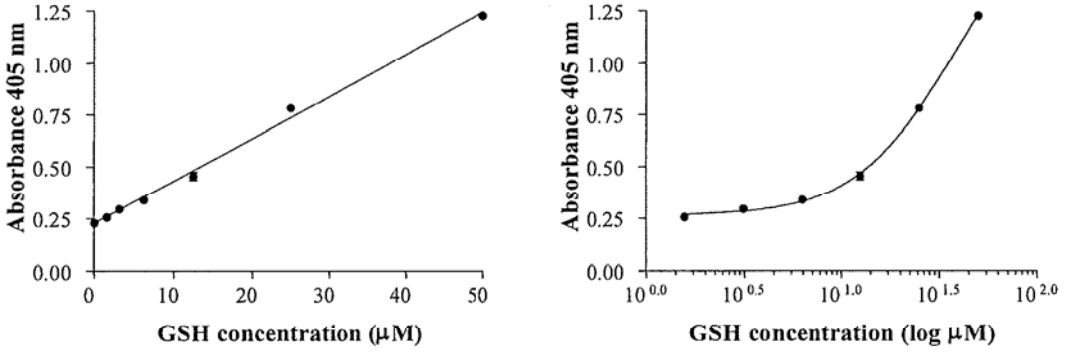

Figure 4.7 Representative glutathione calibration curve. Concentration-response curve in response to increasing concentrations of GSH. A) linear regression or B) sigmoidal curve (variable slope). Results are expressed as the A_{405} of standards assayed for GSH levels by the glutathione colorimetric assay. Data points represent the mean ± SEM of duplicate standards from a single experiment.

Figure 4.7 shows a representative standard curve, one of which was analysed for GSH levels along with each new set of samples. As can be seen in figure 4.7 A, absorbance at 405 nm increased linearly with increasing GSH concentration with linear regression analysis yielding an R^2 value of 0.99. There was no significant difference between the A_{405} for the no GSH standard and the 1.56 μM standard ($P > 0.05$). However, a significant difference was evident for the 3.13 μM GSH standard ($P < 0.05$) and thus 3.13 μM GSH was considered to be the limit of detection. This is may also be observed from the log concentration-response curve shown in figure 4.7 B.

4.3.3.2 Optimisation of glutathione reductase (GSR) concentration and recycling time

The optimum concentration of the GSR catalyst and recycling time for use in the GSH assay was determined using 5, 10 and 14 U/ml GSR enzyme solutions in turn and with the A_{405} measured at 1, 2, 3, 4, 5, 7.5 and 10 min after GSR addition (see section 4.2.5.5). The goodness of fit R^2 values obtained from linear regression analysis are summarised in table 4.5

Figure 4.8 A-C shows the standard curves obtained using the 5, 10 and 14 U/ml GSR enzyme solutions respectively following the various recycling time points. As can be seen in figure 4.8 A, absorbance at 405 nm increased linearly with increasing GSH concentration at 1, 2, 3, 4, 5 and 7.5 min following GSR addition. However, at 10 min after GSR addition, the fit following linear regression analysis was less good. Linear regression analysis gave an R^2 value of 1.0 for the 5 min time point and thus 5 min was considered to be the optimum recycling time for an enzyme concentration of 5 U/ml GSR (table 4.5).

As can be seen in figure 4.8 B, absorbance at 405 nm increased linearly with increasing GSH concentration at 1, 2, 3, 4 min following GSR addition. However, at 5, 7.5 and 10 min after GSR addition, the fit following linear regression analysis was less good. Linear regression analysis gave the highest R^2 value for the 2 min time point (0.998) and thus 2 min was considered to be the optimum recycling time for an enzyme concentration of 10 U/ml GSR (table 4.5).

As can be seen in figure 4.8 C, absorbance at 405 nm increased linearly with increasing GSH concentration at 1, 2, 3 minutes following GSR addition. However, at 4, 5, 7.5 and 10 min after GSR addition, the fit following linear regression analysis was less good. Linear regression analysis gave an R^2 value of 1.0 for the 1 minute time point and thus 1 minute was considered to be the optimum recycling time for an enzyme concentration of 14 U/ml GSR (table 4.5).

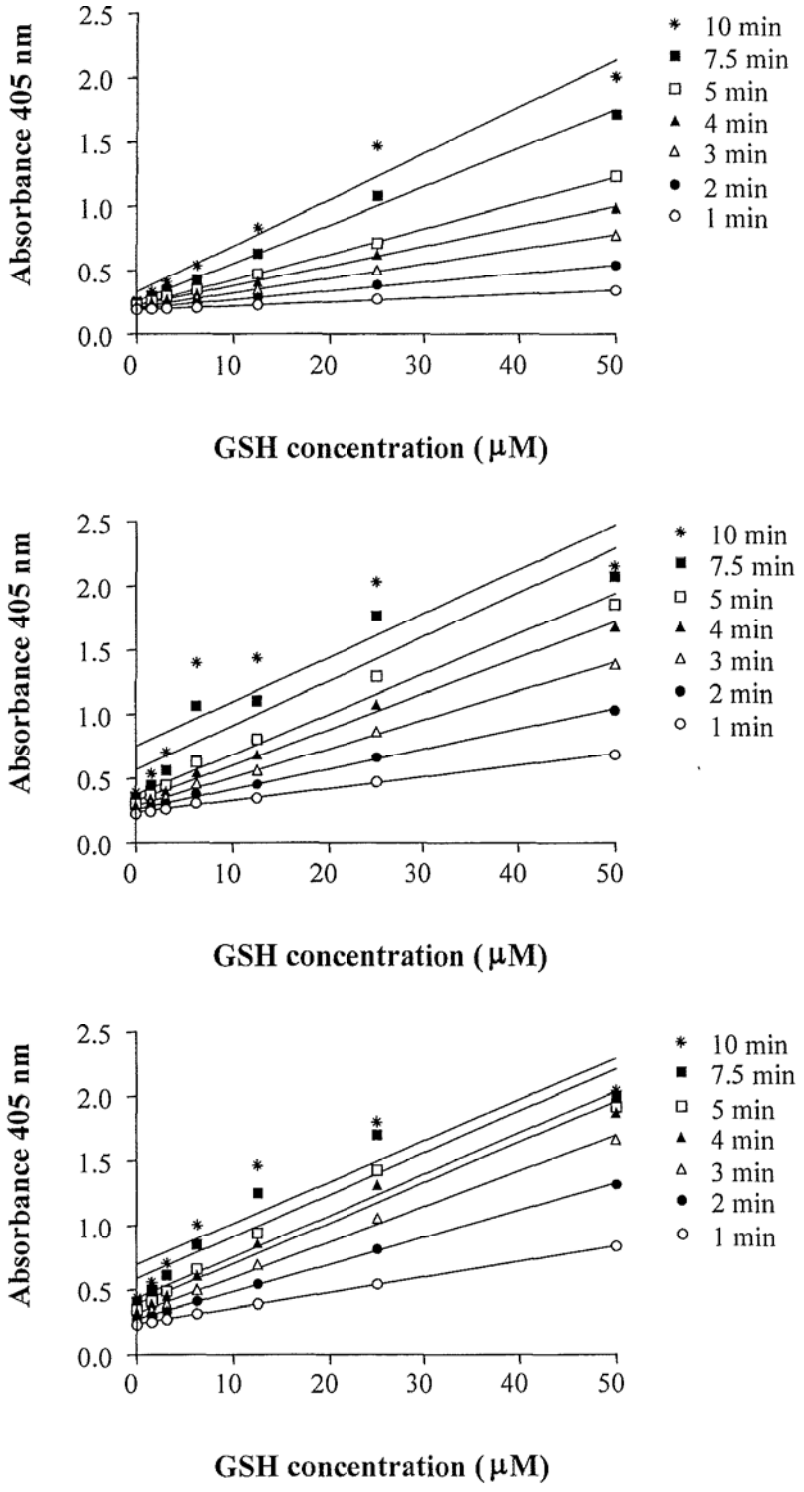

Figure 4.8 Determination of the optimum concentration of GSR catalyst and recycling time for use in the glutathione assay. A) 5, B) 10 and C) 14 U/ml GSR enzyme solutions were employed, with the A_{405} measured at 1 o, 2 ●, 3 △, 4 ▲, 5 □, 7.5 ■ and 10 * min after GSR addition. Data points represent the mean ± SEM of duplicate standards from a single experiment.

As 5 U/ml GSR was the most cost-effective concentration of enzyme solution and gave a good linear fit at a convenient recycling time of 5 minutes, this combination was employed in the glutathione assay protocol.

GSR (U/ml)	Linear regression R^2						
	1 min	2 min	3 min	4 min	5 min	7.5 min	10 min
5	0.997	0.998	0.999	0.999	1.000	0.995	0.968
10	0.996	0.998	0.997	0.994	0.980	0.869	0.751
14	1.000	0.999	0.996	0.979	0.963	0.884	0.826

Table 4.5 Summary of R^2 values. Goodness of fit R^2 values were obtained from glutathione concentration-response curves (linear regression) in response to increasing concentrations of glutathione, with variation in the concentration of GSR catalyst and recycling time as detailed in the table.

4.3.4 Measurement of hydrogen peroxide (H_2O_2) levels

Cells were exposed to a range of non-cytotoxic concentrations of toxin for 4-hours as described in section 4.2.6.2 and then the H_2O_2 released from cells into the medium determined using an Amplex red fluorimetric assay kit (section 4.2.6.1). H_2O_2 levels were then calculated using a 5 μM to 156 nM H_2O_2 standard curve (section 4.2.6.3) and expressed as a percentage increase above the untreated control value.

4.3.4.1 Calibration curve

Figure 4.9 shows a representative standard curve for HBSS with 2 or 4.5 mg/ml glucose in total, one of which was analysed for H_2O_2 levels along with each new set of samples. As can be seen in figure 4.9 A, fluorescent output increased linearly with increasing H_2O_2 concentration for both medium formulations with linear regression analysis yielding an R^2 value of 0.99 in both cases.

In the case of HBSS with 2 mg/ml glucose, no significant difference was evident between the fluorescent signal for the no H_2O_2 standard and 78 nM H_2O_2 standard ($P > 0.05$). However, a significant difference was evident for the 156 nM H_2O_2 standard ($P < 0.001$) and thus 156 nM H_2O_2 was considered to be the limit of detection. This may

be more easily observed from figure 4.9 B which shows the log concentration-response at the lower end.

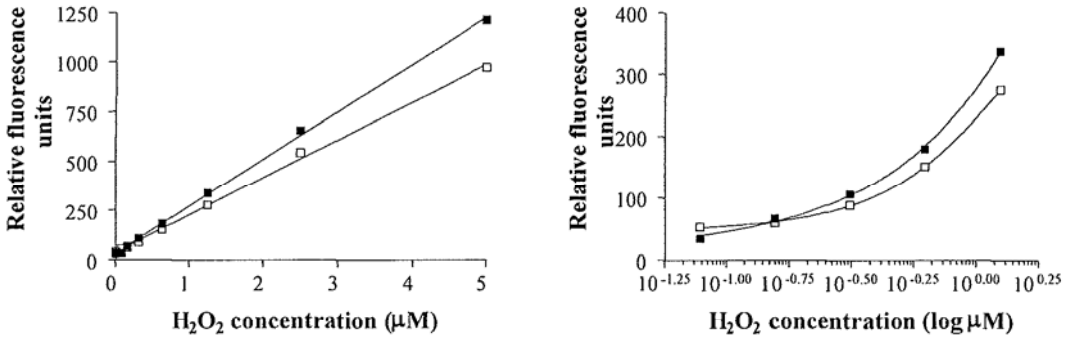

Figure 4.9 Representative H_2O_2 calibration curve. Concentration-response curve in response to increasing concentrations of H_2O_2 prepared in ■ HBSS with 2.0 mg/ml glucose and L-glutamine, or □ HBSS with 4.5 mg/ml glucose and L-glutamine. A) linear regression or B) sigmoidal curve (variable slope). Results are expressed as the relative fluorescence units of standards assayed for H_2O_2 levels by the Amplex red fluorimetric assay. Data points represent the mean ± SEM of duplicate standards from a single experiment.

In the case of HBSS with 4.5 mg/ml D-glucose, a significant difference was evident between the fluorescent signal for the no H_2O_2 standard and 78 nM H_2O_2 standard ($P < 0.001$). Thus 78 nM H_2O_2 was considered to be the limit of detection. This is may be more easily observed from figure 4.9 B.

4.3.4.2 Effect of medium on calibration curve

A hydrogen peroxide standard curve was constructed using several combinations of phenol red free medium and HBSS with supplements (table 4.2, section 4.2.6.4.1). These standard curves were compared with that constructed using the reaction buffer provided with the Amplex red kit. The effect of medium type on the sensitivity of the assay due to inhibition of the accumulation of the fluorescent product resorufin was then examined.

As can be seen from figure 4.10 A and B, the H_2O_2 concentration-response curves using the normal RPMI and DMEM media, both with and without FBS were significantly different from that obtained using reaction buffer ($P < 0.001$), with the order of sensitivity being reaction buffer >> medium without FBS > medium with FBS.

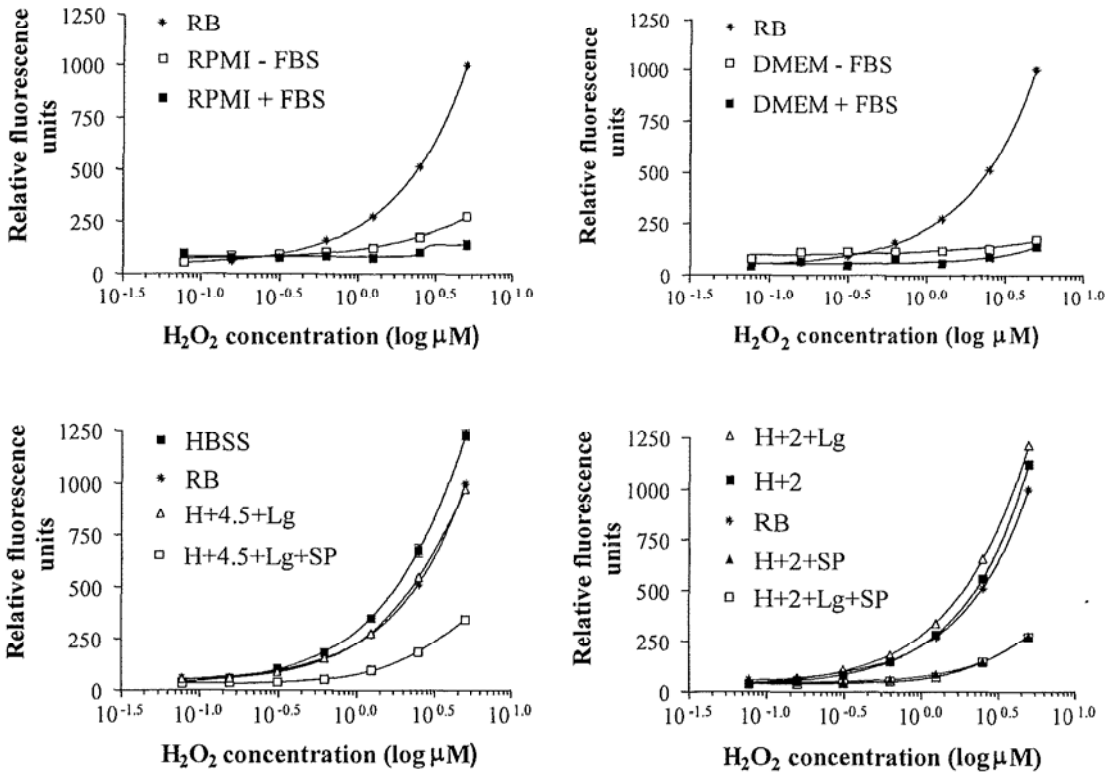

Figure 4.10 Hydrogen peroxide standard curves were constructed using several combinations of phenol red free medium, HBSS (H) with supplements and the Amplex red kit reaction buffer (RB). Sigmoidal concentration-response curve (variable slope) in response to increasing concentrations of H_2O_2 prepared in **A)** Reaction buffer *, RPMI without FBS □, RPMI with FBS ■, **B)** Reaction buffer *, DMEM without FBS □, DMEM with FBS ■, **C)** HBSS ■, Reaction buffer *, HBSS with 4.5 mg/ml glucose and L-glutamine (Lg) △, HBSS with 4.5 mg/ml glucose, L-glutamine and sodium pyruvate (SP) □ and **D)** HBSS with 2 mg/ml glucose and L-glutamine △, HBSS with 2 mg/ml glucose ■, Reaction buffer *, HBSS with 2 mg/ml glucose and sodium pyruvate ▲, HBSS with 2 mg/ml glucose, L-glutamine and sodium pyruvate □. Results are expressed as the relative fluorescence units of standards assayed for H_2O_2 levels by the Amplex red fluorimetric assay. Data points represent the mean ± SEM of duplicate standards from a single experiment.

It can be seen from figure 4.10 C, that the fluorescent signal increased most strongly with increasing H_2O_2 concentration when the standards were prepared in HBSS alone. In comparison, the standard curves prepared in reaction buffer or HBSS supplemented with glucose and L-glutamine were significantly less sensitive ($P < 0.001$) and the curves prepared in these media were not significantly different ($P > 0.05$). The fluorescent signal increased least strongly with increasing H_2O_2 concentration when the standards were prepared in HBSS with sodium pyruvate included in the formulation.

Figure 4.10 D shows that when the standards were prepared in HBSS supplemented with sodium pyruvate (and glucose, with or without L-glutamine), the fluorescent signal increased least strongly with increasing H_2O_2 concentration and the curves prepared in these media were not significantly different ($P > 0.05$). Sensitivity was increased significantly when the standards were prepared in reaction buffer or HBSS without sodium pyruvate ($P < 0.001$ in all cases) and the order of sensitivity was HBSS with glucose and L-glutamine > HBSS with glucose > reaction buffer.

4.3.4.3 Effects of HANKS BSS (HBSS) on cell viability

The effect of 4-hours exposure to HBSS substituted with various culture components (tables 4.3 and 4.4, section 4.2.6.5) on the viability of cells was compared with that of normal cell culture medium, using a simple MTT reduction assay.

As is demonstrated by figures 4.11 A-C, there was no significant difference in cell viability following exposure of the NT2.D1, CCF-STTG1 and NT2.N/A cells respectively to 1) normal medium with FBS, than there was following 4-hours culture in 2) normal medium without FBS, 5) HBSS with added glucose and L-glutamine and 6) HBSS with added glucose and sodium pyruvate ($P > 0.05$ in all cases). For all three cultures there was a significant decrease in cell viability following 4-hours exposure to 3) HBSS alone or 4) HBSS with added glucose only, than to normal medium with FBS ($P < 0.001$ in all cases). However, MTT reduction was significantly increased following exposure of the three different cell cultures to HBSS with added glucose than to HBSS alone (NT2.D1, $P < 0.05$; CCF-STTG1 and NT2.N, $P < 0.001$).

As is demonstrated by figure 4.11 D, there was no significant difference in cell viability following exposure of the NT2.N/A cells to normal medium with FBS than there was following 4-hours culture in any of the other medium formulations with the exception of HBSS alone ($P > 0.05$ in all cases). There was a significant decrease in cell viability following 4-hours exposure to HBSS alone than to normal medium with FBS ($P < 0.001$).

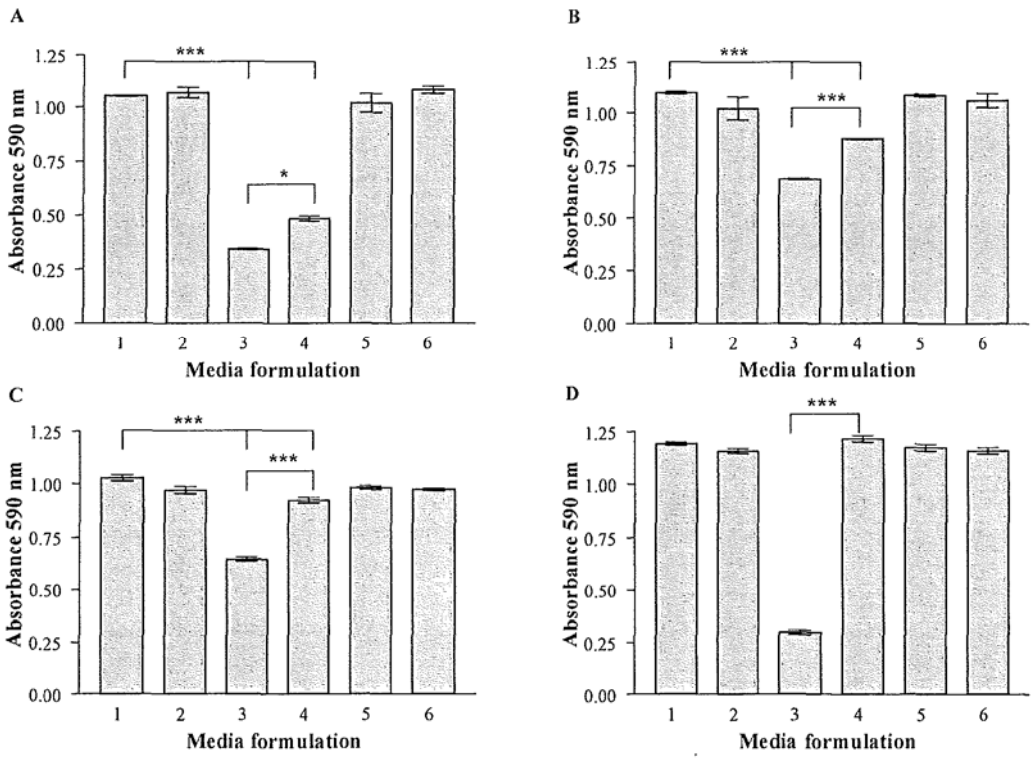

Figure 4.11 MTT study on the effect of 4-hours exposure to HBSS substituted with various culture components on the viability of each cell system in comparison with normal cell culture medium. Cell system A) NT2.D1, B) CCF-STTG1, C) NT2.N and D) NT2.N/A; Medium formulation 1) normal medium with FBS, 2) normal medium without FBS, 3) HBSS, 4) HBSS with added glucose, 5) HBSS with added glucose and L-glutamine and 6) HBSS with added glucose and sodium pyruvate. Results are expressed as the A_{590} of cells assayed for MTT turnover. Bars represent the mean ± SEM of the sample means from two separate experiments. Brackets indicate compared samples, *P<0.05, **P 0.01, ***P<0.001.

4.3.4.4 Interference of the test chemicals with the Amplex red reagent

It was determined whether the highest and half highest concentrations (Cmax and Cmax/2 respectively) of any of the toxins interfered with the Amplex red oxidation process and subsequent fluorescent signal. This was repeated for the α-hexanediones (Cmax only) without the presence of the HRP catalyst in the Amplex red working solution.

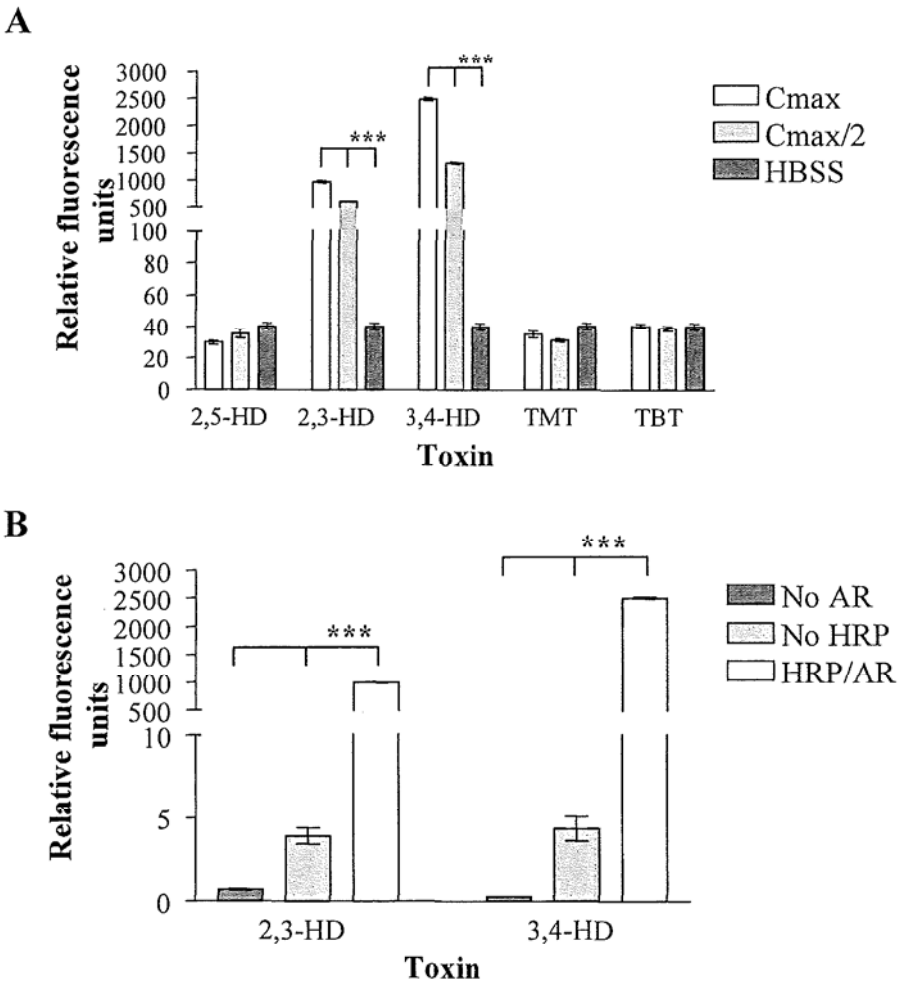

Figure 4.12 Determination of whether there was interference of the test chemicals with the Amplex red reagent. A) Investigation of the possible interference of the maximum and half maximum concentrations (Cmax and Cmax/2 respectively) of the test chemicals with the Amplex red oxidation process and subsequent fluorescent signal. B) Investigation of the necessity of Amplex red and/or the HRP catalyst for the interference of the α-hexanediones Cmax with the Amplex red oxidation process. The different shaded bars represent the use of A) the Cmax and Cmax/2 concentrations of test chemical and HBSS and B) a working solution of both Amplex red reagent and HRP or with the omission of either Amplex red or HRP. Results are expressed as the relative fluorescence units of samples assayed for using the Amplex red fluorimetric assay. Bars represent the mean ± SEM of the sample means from two separate experiments. Brackets indicate compared samples; *P<0.05, **P<0.01, ***P<0.001.

As can be seen from figure 4.12 A, there was no significant difference between the fluorescent signal obtained from HBSS only and the Cmax and Cmax/2, for the 2,5-HD, TMT-Cl and TBT-Cl containing media ($P > 0.05$ in all cases). However, for both the α-hexanedione compounds there was an extremely significant increase in the fluorescent signal for the Cmax and Cmax/2 compared with HBSS alone ($P < 0.001$ in

all cases). There was an approximately 25-fold increase for the Cmax and a 15-fold increase for the Cmax/2 in the case of 2,3-hexanedione and an approximately 60-fold increase for the Cmax and a 30-fold increase for the Cmax/2 in the case of 3,4-hexanedione.

As can be seen from figure 4.12 B, there was no significant difference between the fluorescent signal obtained for the 2,3-HD, compared with the 3,4-HD Cmax when Amplex red or HRP was omitted from the reagent solution ($P > 0.05$ in both cases). Additionally, for both α-hexanediones, there was no significant difference between the fluorescent signals obtained for the absence of Amplex red or HRP from the reagent solution ($P > 0.05$ in both cases). However, when both Amplex red and the HRP enzyme were included in the reagent solution, there was a significant difference between the Cmax fluorescent signals obtained for 2,3-HD and 3,4-HD ($P < 0.001$). Indeed, the fluorescence obtained from 3,4-HD was approximately 2.5-fold higher than with 2,3-HD.

4.3.5 Untreated control analyte levels

The untreated control cellular levels of ATP, glutathione, caspase and hydrogen peroxide as determined in section 4.2.7 (expressed in nmol analyte/mg protein in the case of the ATP, GSH and caspase assays and nmol H_2O_2/µl medium in the case of the Amplex red assay), are shown in figure 4.13 and summarised in table 4.6.

All of the cell lines demonstrated statistically equivalent levels of ATP in untreated cells, of approximately 27- 30 nmol ATP/mg protein and this is evident from figure 4.13 A ($P > 0.05$). The untreated control values indicated that caspase-3 activity (as estimated from AMC levels) was highest in cells from the CCF-STTG1 (101.6 ± 4.1 nmol/mg) and NT2.D1 (84.4 ± 2.1 nmol/mg) continuous cell lines, whose levels were significantly different ($P < 0.01$). Cells from the post-mitotic NT2.N (24.8 ± 2.5 nmol/mg) and NT2.N/A (19.4 ± 1.2 nmol/mg) cultures demonstrated significantly lower control levels of caspase activation in comparison with the continuous cell lines ($P < 0.001$). As is evident from figure 4.13 C, the co-culture and mono-culture were found to have statistically equivalent control levels of caspase-3 ($P > 0.05$).

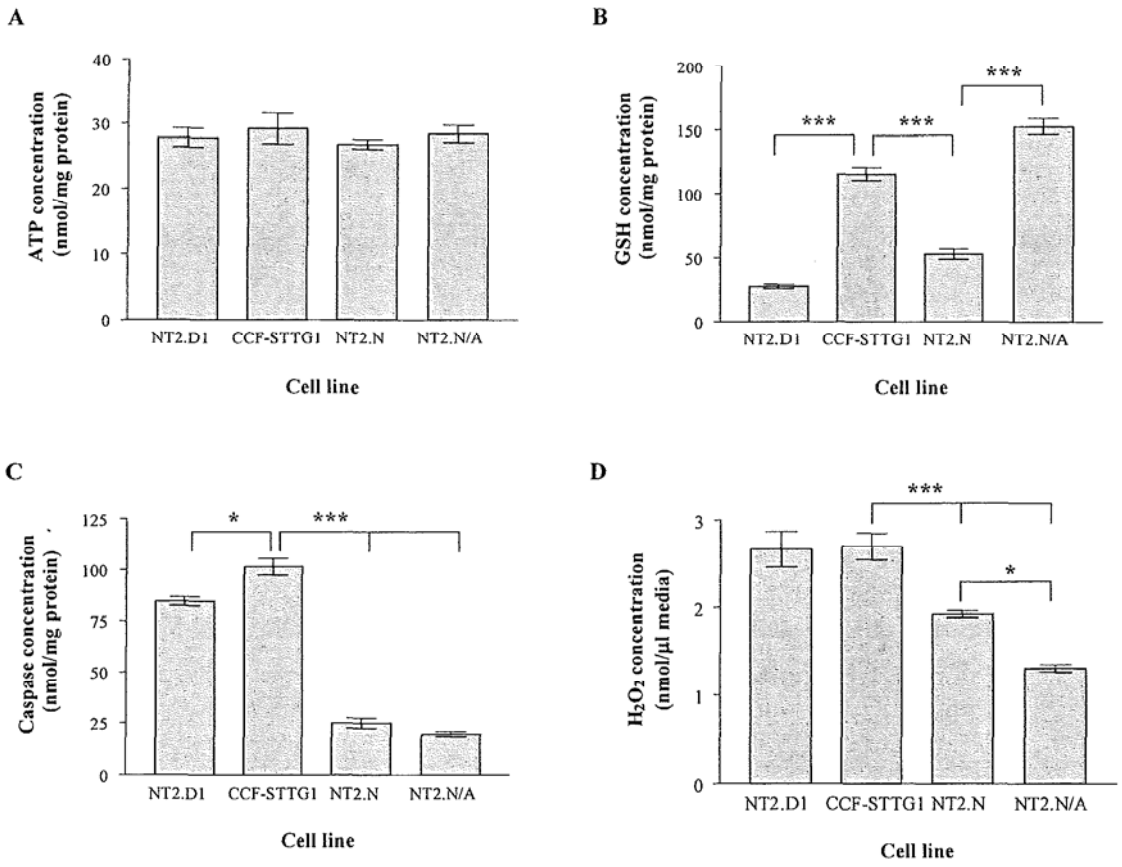

Figure 4.13 Untreated control analyte levels for each cell line were determined for each of the assays and expressed in nmol analyte/mg protein in the case of the A) ATP, B) GSH and C) caspase (AMC) assays and nmol H_2O_2/µl medium in the case of the D) Amplex red assay. Bars represent the mean ± SEM of five control values from separate plates. Brackets indicate compared samples; *P<0.05, **P<0.01, ***P<0.001.

Control levels of the antioxidant glutathione were found to be highest in the untreated astrocytic-neuronal NT2.N/A co-culture (152.6 ± 6.2 nmol/mg) followed by the astrocytic CCF-STTG1 cells (115.6 ± 5.1 nmol/mg), whose levels were statistically different ($P < 0.001$). In comparison, glutathione levels were statistically lower in the neuronal NT2.N mono-culture (52.8 ± 4.1 nmol/mg; $P < 0.001$) and lowest in the NT2.D1 cells (27.8 ± 1.6 nmol/mg), as is evident from figure 4.13 B. As stated, the NT2.N/A co-culture demonstrated statistically higher control levels of glutathione than did the NT2.N mono-culture ($P < 0.001$).

The untreated control values indicated that H_2O_2 levels were highest in cells from the NT2.D1 (2.7 ± 0.2 nmol/µl) and CCF-STTG1 (2.6 ± 0.2 nmol/µl) continuous cell lines, whose levels were statistically equivalent ($P > 0.05$). As is evident from figure 4.13 D,

cells from the post-mitotic NT2.N (1.9 ± 0.04 nmol/μl) and NT2.N/A (1.3 ± 0.04 nmol/μl) cultures demonstrated significantly lower H_2O_2 control levels in comparison with the continuous cell lines $P < 0.01$). Additionally, the co-culture was found to demonstrate slightly statistically lower control levels of H_2O_2 than the mono-culture ($P < 0.05$). However, it must be noted that control levels in medium are more difficult to compare accurately than levels corrected for protein as they are not corrected for inter-assay variability in cell density.

Cell line	Assay			
	ATP (nmol/mg protein)	Caspase-3 (nmol/mg protein)	GSH (nmol/mg protein)	H_2O_2 (nmol/μl medium)
NT2.D1	27.8 ± 1.5	84.4 ± 2.1	27.8 ± 1.6	2.7 ± 0.2
CCF-STTG1	29.2 ± 2.4	101.6 ± 4.1	115.6 ± 5.1	2.6 ± 0.2
NT2.N	26.8 ± 0.7	24.8 ± 2.5	52.8 ± 4.1	1.9 ± 0.04
NT2.N/A	28.4 ± 1.3	19.4 ± 1.2	152.6 ± 6.2	1.3 ± 0.04

Table 4.6 The untreated control analyte levels of ATP, caspase-3, GSH and H_2O_2 determined for each cell system (N=5).

4.4 Discussion

4.4.1 Adenosine triphosphate (ATP)

ATP levels are often depressed as a consequence of exposure to neurotoxins. Therefore, a luciferin-luciferase based ATP detection kit was utilised in order to sensitively assess for energetic stress induced by exposure of the cell systems to the selected test chemicals.

As phenol red may quench the ATP assay signal and serum may interfere with sample protein determination, phenol red and FBS free medium was utilised for the exposure of the cell systems to the test chemicals. The use of FBS free medium did not affect cell viability in any of the four cell systems over this 4-hour exposure period and was thus considered suitable for routine application in the ATP assay. Additionally, when the ATP standards were prepared in this medium, the range of linearity for ATP measurement was found to be between 100 nM and 10 μM ATP. The toxin treated samples all fell within this range, as did the control samples, with all of the cell systems demonstrating statistically equivalent baseline levels of ATP of approximately 27- 30 nmol ATP/mg protein. Thus, the ATPlite assay was considered sensitive enough for the examination of ATP effects in control cells and following exposure of the different cell systems to non-cytotoxic levels of toxin for 4-hours.

As the protocol required that cells grown and treated with toxin in 6-well plates be transferred to a 96-well plate for ATP quantification, it was required that the ATP reagent be combined directly with medium containing toxins and subsequently the resulting solution was combined with protein assay reagents. Thus, it was also determined whether any of the toxins themselves, or the culture medium, interfered with the ATP assay luminescent signal or the resulting solution with the protein assay absorbance measurement. None of the toxins or media were found to interfere with the ATP assay and none of the resulting toxin/assay reagent combinations were found to interfere with the protein assay that followed. Therefore, it was considered that the ATPlite assay was suitable for use with a 6-well plate format. This allowed for the culture of NT2.N and NT2.N/A cells and subsequent toxin treatment in situ, which permitted high-throughput screening of compounds without the disruption of vital cell-

cell interactions.

The ATPlite 1-step assay has been developed by the manufacturer so that analyte levels may be rapidly determined directly in toxin exposed cells without prior removal of the test chemical. In the present study, no interference of the test chemicals or culture medium with the luminescent signal or protein assay was observed. However, as this procedure entails prolonged handling of test chemical containing samples, depending on the nature of the toxin in question, it may be considered safer to remove the toxin from the well following cell exposure and rinse and scrape the cells into PBS, prior to transfer to the 96-well plate for ATP determination.

4.4.2 Caspase-3

Caspases are thought to be key effectors in the induction of apoptosis, with caspase-3 playing a central role in the apoptotic cascade. A caspase-3 assay was developed in order to assay the test chemical exposed cell systems for caspase-3 activity, via measurement of liberated AMC resulting from caspase-3 specific cleavage of Ac-DEVD-AMC.

It was observed that the baseline caspase-3 activation (untreated control values) was significantly lower in cells from the post-mitotic NT2.N (24.8 ± 2.5 nmol/mg) and NT2.N/A (19.4 ± 1.2 nmol/mg) cultures in comparison with the continuous CCF-STTG1 (101.6 ± 4.1 nmol/mg) and NT2.D1 (84.4 ± 2.1 nmol/mg) cell lines. Similarly, the staurosporine (1 μM) induced positive control values indicated that caspase-3 levels were also highest in cells from the CCF-STTG1 (3061.2 ± 124.1 nmol/mg) and NT2.D1 (2469.1 ± 80.4 nmol/mg) continuous cell lines, with cells from the post-mitotic NT2.N (1205.7 ± 111.0 nmol/mg) and NT2.N/A (889.5 ± 30.11 nmol/mg) cultures demonstrating significantly lower levels of caspase activation. This suggests that the dividing cell lines were more vulnerable to caspase-3 activation and induction of apoptosis than the terminally differentiated cell systems. This is in agreement with the general observation that the control of apoptosis is tied to the cell cycle and the greater the rate at which a population of cells proliferates, the greater the need for apoptotic control to prevent damaging changes being inherited by the daughter cells.

Whilst the intracellular factors that determine vulnerability to staurosporine-induced apoptosis are largely unknown (Inna Kruman, 1998), as *in vivo* CNS cells are post-mitotic, these observations may have important implications for *in vitro/in vivo* extrapolations. For example, the use of terminally differentiated *in vitro* cell systems may be more relevant to the *in vivo* situation when considering toxin induced and baseline caspase-3 activation.

As the medium was removed and cells rinsed prior to lysis, it was not considered that serum would interfere with protein measurement. Lysate could then be added to a 96-well plate for caspase-3 determination and therefore, the assay was suitable for use following toxin treatment of cells within 6-well plates. The range of linearity for caspase-3 estimation was found to be between 100 nM and 100 μM AMC and the untreated control, toxin treated samples and staurosporine induced positive controls, all fell within this range. Thus the caspase-3 assay was considered sensitive enough for the examination of caspase-3 activation induced by exposure of the different cell systems to non-cytotoxic levels of test chemical for 4-hours.

4.4.3 Glutathione (GSH)

Glutathione is a major cellular antioxidant present at 1-3 mM within cells of the nervous system, which plays a number of neuroprotective roles including prevention of oxidative stress and conjugation of xenobiotics. As GSH levels may become depleted due to toxic insult, a colorimetric enzymatic-recycling assay was developed for estimating total cellular glutathione following exposure of the cell systems to the test chemicals.

The optimum concentration of the GSR catalyst for use in the GSH assay was determined to be 5 U/ml GSR, with a recycling time of 5 minutes, which proved to be both cost-effective and convenient. With employment of these parameters, the range of linearity for total glutathione estimation was found to be between 3.13 μM and 50 μM GSH and the untreated control and toxin treated samples all fell within this range. Thus, the total glutathione assay was considered sensitive enough for the determination of effects on cellular GSH protective capacity resulting from exposure of the different

cell systems to non-cytotoxic levels of test chemical for 4-hours.

As the medium was removed and the cells rinsed in PBS prior to deproteinisation, it was not considered that serum would interfere with protein measurement of the resulting protein pellet. The supernatent could then be added to a 96-well plate for caspase-3 determination and therefore the assay was suitably adapted for use following toxin treatment of the cell systems within a 6-well plate format.

Control levels of the antioxidant glutathione were found to be highest in the untreated astrocytic-neuronal NT2.N/A co-culture (152.6 ± 6.2 nmol/mg) followed by the astrocytic CCF-STTG1 cells (115.6 ± 5.1 nmol/mg). In comparison, glutathione levels were statistically lower in the neuronal NT2.N mono-culture (52.8 ± 4.1 nmol/mg), followed by the NT2.D1 cells (27.8 ± 1.6 nmol/mg). This is agreement with studies of the relative GSH levels found *in vivo*, which suggest that GSH in the CNS is more concentrated in astrocytes and that astrocytes also possess a higher level of GSH synthesising capacity (Sagara *et al.*, 1996; Takuma *et al.*, 2004). These findings in culture advocate that, as astrocytes may be important in combating the effects of ROS and potentially harmful xenobiotics, NT2 astrocytes and neurons in co-culture may provide a convenient cell system for investigating the effects of toxic insults on antioxidant status.

4.4.4 Hydrogen peroxide (H_2O_2)

Toxic insult may lead to oxidative stress by causing an increased production of reactive oxygen species (ROS). The Amplex red fluorimetric assay for hydrogen peroxide was developed as a measure of ROS released into the medium by the cell systems following exposure to the test chemicals.

With standards prepared in HBSS, the range of linearity for H_2O_2 estimation was found to be between 156 nM and 5 μM H_2O_2 and between 78 nM and 5 μM H_2O_2 for the 2 mg/ml glucose and 4.5 mg/ml glucose formulations, respectively. The relevant untreated control and test chemical treated samples all fell within this range. Therefore, the Amplex red assay was considered sensitive enough for the determination of

elevation of ROS levels resulting from exposure of the different cell systems to non-cytotoxic concentrations of test chemical for 4-hours.

The untreated control values indicated that H_2O_2 levels were highest in cells from the NT2.D1 (2.7 ± 0.2 nmol/μl) and CCF-STTG1 (2.6 ± 0.2 nmol/μl) continuous cell lines, with cells from the post-mitotic NT2.N (1.9 ± 0.04 nmol/μl) and NT2.N/A (1.3 ± 0.04 nmol/μl) cultures demonstrating significantly lower H_2O_2 control levels. Regarding the terminally differentiated cell systems, the control data is in agreement with reports that cultured astrocytes are more capable than neurons of disposing of H_2O_2 (Dringen *et al.*, 1999a). It is thought that this may be due to the lower concentrations of GSH and GPx activity found in neurons compared with astrocytic cells (Wullner *et al.*, 1999). As discussed above, control GSH levels in the co-culture were indeed found to be higher than in the mono-culture. However, GSH levels were also found to be higher in the CCF-STTG1 astrocytic culture than in the NT2.N mono-culture, yet the baseline production of H_2O_2 was higher in the CCF-STTG1 cells than in the NT2.N cells. The NT2.N cell line may possess comparatively higher levels of other defences for the enzymatic clearance of H_2O_2, such as catalase.

Many cell culture medium formulations include sodium pyruvate to serve as an extracellular H_2O_2 scavenger (O'Donnell *et al.*, 1987; Wang and Cynader, 2001). Externally applied antioxidants provide more protection against extracellular radicals than against intracellular radicals. Therefore, the possibility exists that despite its GSH content, the continuous CCF-STTG1 cell line is dependent on sodium pyruvate in culture for antioxidant defence and that, due to the absence of pyruvate from the HANKS BSS formulation, these cells are thus rendered less capable of extracellular H_2O_2 detoxification. Indeed, when either the NT2.D1 or CCF-STTG1 continuous cell lines were incubated for 4-hours in medium without sodium pyruvate or L-glutamine, cell viability was reduced compared with control cells cultured in normal medium. However, addition of either L-glutamine or sodium pyruvate maintained cell viability at control levels. The NT2.N/A co-culture did not demonstrate any decrease in cell viability when L-glutamine and sodium pyruvate were removed from the medium, suggesting this culture is less dependent on these components during a 4-hour culture period.

Additionally, it must be noted that control levels in medium are more difficult to compare accurately than levels corrected for protein as they are not corrected for inter-assay variability in cell density, which may affect the relative levels of H_2O_2 estimated in the cell systems.

Phenol red is known to quench the Amplex red fluorescent signal, so the use of serum may need to be avoided due to catalase activity which can prevent the oxidation of AR. Additionally, the energy source supplement pyruvate is able to degrade H_2O_2 released into the medium, resulting in the determination of reduced extracellular H_2O_2 levels. Due to these considerations and reports that hydrogen peroxide may be detected with greater sensitivity in HBSS, a hydrogen peroxide standard curve was constructed using several combinations of phenol red free medium or HBSS with supplements and compared with that constructed using the reaction buffer provided with the Amplex red kit. It was found that inclusion of pyruvate and serum did indeed inhibit the accumulation of the fluorescent product resorufin. Moreover, additional factors present in RPMI and DMEM-HG medium (without serum or pyruvate supplementation) were also found to greatly reduce assay sensitivity. Following consultation of each of the medium formulation components it is not readily obvious what factors may have contributed to this situation, thus highlighting the importance of such considerations when medium is not removed or cells rinsed prior to endpoint quantification.

Incorporation of L-glutamine and L-glucose into the HBSS only slightly compromised assay sensitivity compared with unsupplemented HBSS. This slight decrease in sensitivity was deemed acceptable when considered along with examination of effects of medium type on cell viability. As mentioned above, inclusion of L-glutamine in the HBSS enhanced cell viability to levels measured in normal cell culture medium when NT2.D1 and CCF-STTG1 cells were incubated for 4-hours. L-glutamine also marginally improved cell viability in the NT2.N culture. Maintenance of HBSS glucose levels to those found in the normal culture medium also improved cell viability in all the cell systems, to a greater extent in the NT2.N and in particular the NT2.N/A cultures, than in the NT2.D1 and CCF-STTG1 cultures. This may suggest that the differentiated culture systems are more glucose dependent compared with the continuous cell lines. This may reflect their neuronal phenotype and thus high

metabolic requirements, as the majority of the normal ATP to meet CNS demand comes from oxidative metabolism of glucose to water and CO_2 (Gabryel *et al.*, 2002; Seyfried and Mukherjee, 2005). Removal of serum from the medium was not found to affect cell viability in any of the cell systems following 4-hours exposure. Therefore, the use of HBSS without serum supplementation was considered to be acceptable for exposure of the cell systems to the selected toxins for this time period.

The Amplex red assay is intended to quantitate the extracellular release of hydrogen peroxide into the medium containing the toxin, with subsequent transfer of this medium to a 96-well plate. Thus it was necessary to determine whether any of the toxins interfered with the Amplex red oxidation process and subsequent fluorescent signal. No such interference was caused by 2,5-hexanedione, trimethyltin chloride or tributyltin chloride. However, both the α-hexanedione compounds were found to greatly increase the fluorescent signal obtained, compared with toxin-free HBSS. This increase was approximately 25-fold in the case of 2,3-hexanedione and 60-fold in the case of 3,4-hexanedione, for the highest concentration of toxin employed. Both Amplex red and the HRP catalyst were required in the working solution to obtain a significant difference between the fluorescent signals obtained for 2,3-hexanedione and 3,4-hexanedione and that of HBSS alone. Therefore, it is not simply that the compounds themselves are capable of emitting a fluorescent signal upon excitation. This suggests that HRP is capable of catalysing the oxidation of Amplex red by the α-hexanediones in a similar way to the mechanism by which it catalyses the reaction between Amplex red and hydrogen peroxide. Thus 2,3-HD and 3,4-HD appear to be substrates of HRP, capable of oxidising the non-fluorescent Amplex red to produce the fluorescent product resorufin. Whether the reaction proceeds via the same free radical mechanism as when H_2O_2 is the substrate is unknown. However, as the kit did not highlight the potential of such toxins to interfere with the Amplex red assay, the importance of assessing kit suitability for each particular laboratory requirement is emphasised.

Therefore, as it was considered that the Amplex red assay was unsuitable for use with 2,3- or 3,4-HD, in future an alternative method for the quantification of oxidative species arising from such toxic insult, would be required. In fact, although this assay was found to be a very rapid method for measuring H_2O_2 levels, it required a number of

considerations that may render it inappropriate for the reliable and sensitive quantification of reactive oxygen species produced as a result of exposure of a cell system to a new compound of unknown neurotoxic potential.

Following quantification of biochemical endpoint levels using the relevant calibration curve, with the exception of hydrogen peroxide, sample levels were then corrected for protein content. Whilst the MTT assay showed 6-well plates within a batch to have a consistent cell-density, correction for protein content accounted for possible discrepancies such as inter-batch variability in density and incomplete sample transfer from 6- to 96-well plate format.

Cells were all cultured in medium containing FBS, sodium pyruvate and L-glutamine prior to test chemical exposure. However, according to the endpoint assay, they were then exposed to toxins in medium of varying composition. For example, FBS free medium in the ATP assay and FBS and pyruvate free HBSS in the Amplex red assay. Although these media compositions did not affect overall cell viability as determined by the MTT assay, they may have had more subtle effects on cell behaviour which may have affected resulting levels of analyte measured. Thus, following correction for protein, analyte levels were then expressed as a percentage decrease below the untreated control value. It was hoped that correcting sample values for the control values would minimise effects due to variations in medium used and thus allow comparison of the different endpoints when examining the response of the cell systems to a particular test chemical.

Chapter 5 – The use of biochemical endpoints to detect acute neurotoxicity

5.1 Introduction

It was hypothesised that the various subtle biochemical changes induced by toxins according to differing cell system properties, for example, level of differentiation or inclusion of more than one cell type, may be more apparent at non-cytotoxic levels when not masked by overt cytotoxic effects. This process should provide a more sensitive assessment of the suitability of a particular cell system for detecting the acute neurotoxic potential of new and existing chemicals.

Mitochondria play a key role in cellular maintenance and the nervous system is particularly susceptible to toxicants that disrupt mitochondrial function and metabolism. Thus, sensitive protocols were developed for the rapid measurement of several mitochondrial related biochemical endpoints, including cellular energy (ATP), glutathione (GSH) and hydrogen peroxide (H_2O_2) levels and additionally caspase-3 activity as an indicator of apoptosis (Chapter 4).

Following estimation of their basal cytotoxicity using the MTT assay (Chapter 3), the toxicity profiles of the five test chemicals at non-cytotoxic concentrations were obtained using the above biochemical endpoints, in order to appraise the ability of the selected cell systems to distinguish acute neurotoxicants and cytotoxicants. The resulting compound toxicity profiles were then used to determine the suitability of the inclusion of this combination of biochemical endpoints and in particular the NT2 neuronal and astrocytic co-culture cell system, in a preliminary test battery for the screening of compounds for acute neurotoxic potential in humans.

5.2 Materials and methods

5.2.1 Materials

For materials, refer to Chapter 2, section 2.2.1.

5.2.2 Methods

Cells were exposed to a range of non-cytotoxic concentrations of the test chemicals; 2,5-HD, 2,3-HD, 3,4-HD, TMT-Cl or TBT-Cl for 4-hours as described in Chapter 4, section 4.2.2. The resulting samples were then assayed for levels of ATP, caspase-3, GSH or H_2O_2 as developed and described in Chapter 4, sections 4.2.3-6, in order to compare the different cell lines for compromised cell function. 2,3-Hexanedione and 3,4-hexanedione were not assessed using the Amplex red assay for hydrogen peroxide.

5.2.3 Data analysis

Data analyses were carried out using GraphPad Prism software.

Each independent experiment used eight determinations per toxin concentration and data are presented as the mean ± standard error of the mean (SEM) of three independent experiments, unless otherwise stated.

The change in cellular response with exposure to increasing concentration of toxin was expressed as a percentage decrease below that of the untreated control value (ATP and GSH), or percentage increase above that of the untreated control value (caspase and H_2O_2). The resulting curves were log concentration-response curves and thus neither the 0 % nor 100 % toxin-free control points were represented. The respective nmol analyte/mg protein (ATP, GSH and caspase-3 assays) or nmol analyte/µl medium (H_2O_2 assay) values were used where it was necessary to compare toxin-exposed responses with the untreated control response.

Two-way ANOVA was employed to determine the significance of the impact of cell line type on the results (such as determination of significant differences between

concentration-response curves) and the impact of toxin concentration on the results (whether the concentration-response curves are horizontal), using GraphPad Prism.

The NOAEL range at 4-hours determined for each toxin varied for each cell line due to differing respective sensitivities in the MTT assay (table 4.1, section 4.2.2). However, two-way ANOVA may only be used to compare concentration-response curves over the portion where the toxin concentrations are identical (the common concentration range). As a result, some differences had to be compared by visual inspection.

5.3 Results

The following results section refers to the analyte levels measured using the biochemical endpoint assays, following exposure of the cell systems to non-cytotoxic levels of each test chemical in turn. Results concerning the protocol development, sensitivity and data quantification aspects of the biochemical endpoint assays, may be found in Chapter 4.

5.3.1 2,5-Hexanedione

The non-cytotoxic (NOAEL) range after a 4-hour exposure period for the NT2.D1 cells was 0-50 mM and 0-85 mM for the CCF-STTG1, NT2.N and NT2.N/A cells (table 4.1, section 4.2.2).

5.3.1.1 ATP

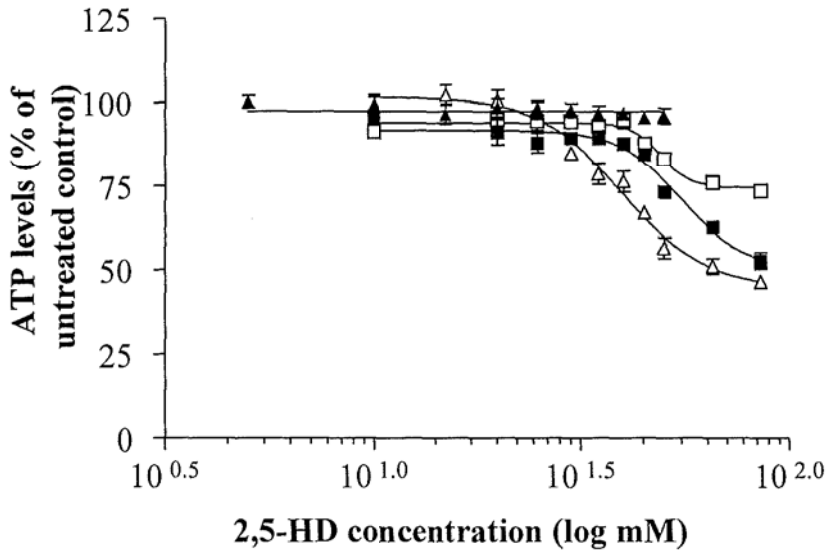

Figure 5.1 Percentage decrease in cellular ATP following exposure to increasing concentrations of 2,5-hexanedione for 4-hours. Sigmoidal concentration-response curve (variable slope) for NT2.D1 (▲), CFF-STTG1 (△), NT2.N (■) and NT2.N/A (□) cells. The ATP assay was carried out, the plates read for luminescence and ATP levels were calculated using a standard curve and corrected for sample protein content. Results are expressed as ATP (nmol/mg protein) for the toxin treated sample as a percentage of the ATP (nmol/mg protein) for the untreated control sample. Data points represent the mean ± SEM of the sample means from three separate experiments.

Figure 5.1 shows that increasing concentrations of 2,5-hexanedione were associated with a progressive decrease in cellular ATP levels in the CCF-STTG1, NT2.N and NT2.N/A cultures after a 4-hour exposure period. However, there was no statistically significant decrease in cellular ATP in the NT2.D1 cell line over the non-cytotoxic range ($P > 0.05$).

Two-way ANOVA analysis over the 10-85 mM range (NT2.D1 data excluded) indicated the concentration-response curves for the CCF-STTG1 cells as well as the NT2.N and NT2.N/A cell systems, were significantly different ($P < 0.001$) and that increasing concentration significantly affected the response ($P < 0.001$). Thus, from analysis of figure 5.1 it may be concluded that with increasing concentration, 2,5-hexanedione led to the greatest reduction in ATP levels in the CCF-STTG1, followed by the NT2.N and then the NT2.N/A culture.

At the highest common 2,5-hexanedione concentration used (85 mM) the NT2.N/A co-culture maintained significantly greater levels of ATP (73.7 ± 1.8 %) compared with the NT2.N mono-culture (52.7 ± 2.4 %; $P < 0.001$).

5.3.1.2 Caspase-3

Figure 5.2 indicates that increasing concentrations of 2,5-hexanedione caused no statistically significant difference in caspase-3 activity compared with the untreated control in the NT2.D1, CCF-STTG1 or NT2.N cultures over the non-cytotoxic range ($P > 0.05$). However, the NT2.N/A co-culture showed an initial progressive increase in caspase-3 activity, with a maximum significant increase above the untreated control of 105.9 ± 2.2 % at a concentration of 50 mM 2,5-HD ($P < 0.001$). Caspase-3 levels then declined to 15.1 ± 3.5 % by 85 mM 2,5-HD.

Two-way ANOVA analysis of the concentration-response curve for the NT2.N/A cells over the 5-85 mM range indicated that increasing 2,5-HD concentration significantly affected the caspase-3 response ($P < 0.001$). However, as there was no statistical change in caspase-3 activity over the non-cytotoxic range, the curve for the NT2.N culture was statistically horizontal ($P > 0.05$).

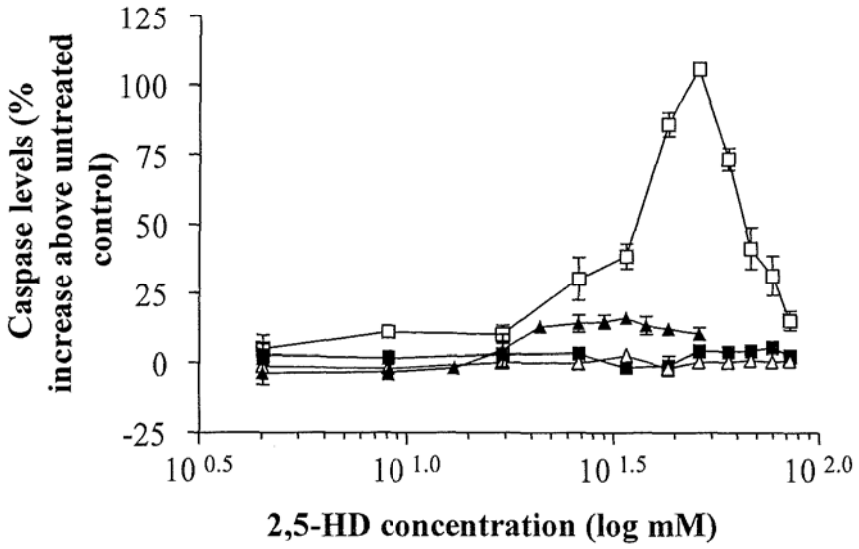

Figure 5.2 Percentage increase in cellular caspase-3 activity following exposure to increasing concentrations of 2,5-hexanedione for 4-hours. Concentration-response curve (points joined, not curve fit) for NT2.D1 (▲), CFF-STTG1 (△), NT2.N (■) and NT2.N/A (□) cells. The caspase-3 assay was carried out, the plates read for fluorescence (355/460 nm ex/em) and caspase-3 levels were calculated using a standard curve and corrected for sample protein content. Results are expressed as caspase-3 (nmol/mg protein) for the toxin treated sample as a percentage increase above the caspase-3 (nmol/mg protein) for the untreated control sample. Data points represent the mean ± SEM of the sample means from three separate experiments.

5.3.1.3 Glutathione

With figure 5.3, increasing concentrations of 2,5-hexanedione were associated with a progressive decrease in cellular glutathione levels in the NT2.D1, NT2.N and NT2.N/A cultures after a 4-hour exposure period. Interestingly, there was no statistically significant decrease in cellular GSH in the CCF-STTG1 cell line over the non-cytotoxic range ($P > 0.05$).

Two-way ANOVA analysis over the common 10-50 mM range indicated the concentration-response curves for the NT2.D1, NT2.N and NT2.N/A cells were significantly different ($P < 0.001$) and that increasing 2,5-HD concentration significantly affected the response ($P < 0.001$). Thus, from analysis of figure 5.3 it may be concluded that with increasing concentration, 2,5-hexanedione led to the greatest reduction in GSH levels in the NT2.D1, followed by the NT2.N and then the NT2.N/A

culture.

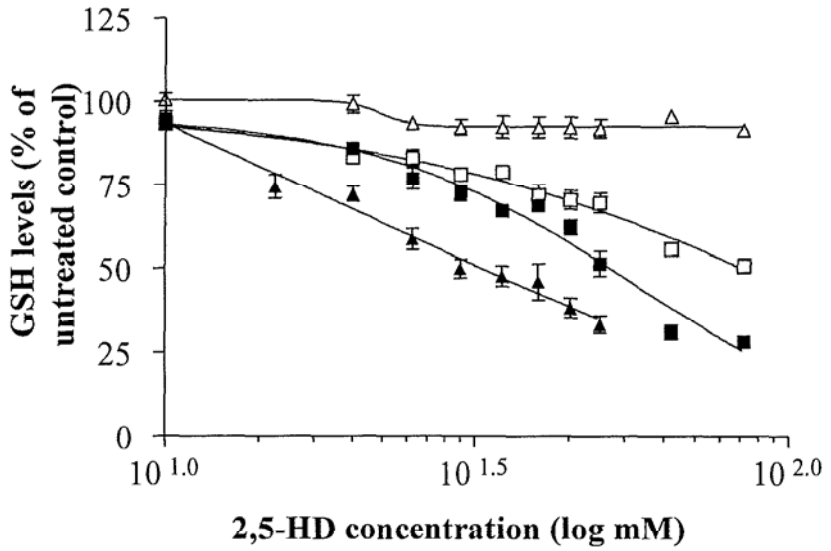

Figure 5.3 Percentage decrease in cellular GSH following exposure to increasing concentrations of 2,5-hexanedione for 4-hours. Sigmoidal concentration-response curve (variable slope) for NT2.D1 (▲), CFF-STTG1 (△), NT2.N (■) and NT2.N/A (□) cells. The GSH assay was carried out, the plates read for absorbance at 405 nm and GSH levels were calculated using a standard curve and corrected for sample protein content. Results are expressed as GSH (nmol/mg protein) for the toxin treated sample as a percentage of the GSH (nmol/mg protein) for the untreated control sample. Data points represent the mean ± SEM of the sample means from three separate experiments.

At the highest common 2,5-hexanedione concentration used (85 mM) the NT2.N/A co-culture maintained significantly greater levels of GSH (50.7 ± 2.1 %) compared with the NT2.N mono-culture (28.2 ± 0.5 %; $P < 0.001$).

5.3.1.4 Hydrogen peroxide

Figure 5.4 shows that increasing concentrations of 2,5-hexanedione were associated with a progressive increase in H_2O_2 levels in the medium of all four cell cultures after a 4-hour exposure period.

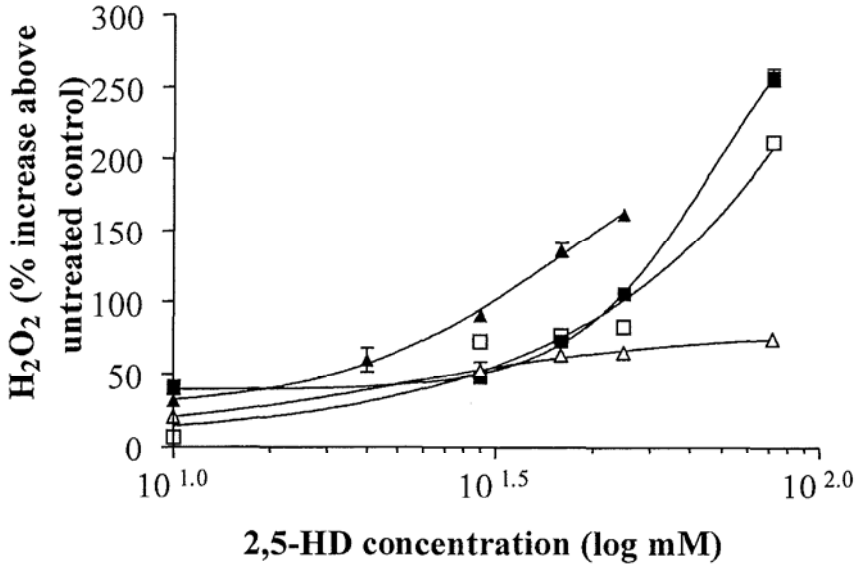

Figure 5.4 Percentage increase in H_2O_2 in culture media following cellular exposure to increasing concentrations of 2,5-hexanedione for 4-hours. Sigmoidal concentration-response curve (variable slope) for NT2.D1 (▲), CFF-STTG1 (△), NT2.N (■) and NT2.N/A (□) cells. The Amplex red assay was carried out, the plates read for fluorescence (544/590 nm ex/em) and H_2O_2 levels were calculated using a standard curve. Results are expressed as H_2O_2 (nmol/μl medium) for the toxin treated sample as a percentage increase above the H_2O_2 (nmol/μl medium) for the untreated control sample. Data points represent the mean ± SEM of the sample means from three separate experiments.

Two-way ANOVA analysis over the common 10-50 mM range indicated that for all four cell lines, increasing concentration significantly affected the response ($P < 0.001$). The concentration-response curves for the NT2.D1 and CCF-STTG1 cells were significantly different from each other and those of the NT2.N and NT2.N/A cells ($P < 0.001$). However, the concentration-response curves for the NT2.N and NT2.N/A cells showed only a slight significant difference ($P < 0.05$). Additionally, at the highest common 2,5-HD concentration used (85 mM) the NT2.N/A co-culture maintained only moderately lower levels of H_2O_2 (211.9 ± 1.9 %) than did the NT2.N mono-culture (257.5 ± 6.0 %; $P < 0.05$). Thus, from analysis of figure 5.4 it may be concluded that with increasing concentration, 2,5-hexanedione (0-50 mM) most increased H_2O_2 levels in the NT2.D1, followed by the NT2.N and NT2.N/A cultures and least in the CCF-STTG1 culture.

5.3.1.5 2,5-Hexanedione summary

Increasing concentrations of 2,5-HD were associated with a progressive decrease in glutathione that was reflected by an increase in H_2O_2 levels in all four cultures, after a 4-hour exposure period. The order of sensitivity of the cell lines to 2,5-HD regarding these two components correlated well in terms of the decreases in glutathione and increases in hydrogen peroxide; from most to least sensitive, the order of the lines was as follows NT2.D1 > NT2.N > NT2.N/A > CCF-STTG1. Conversely, the CCF-STTG1 cell line was the most sensitive with regards to ATP levels, with the NT2.D1 cell line sustaining no effect and the co-culture a lesser effect than the neuronal mono-culture. 2,5-hexanedione caused a significant change in caspase-3 activity in the NT2.N/A co-culture only, which reached its maximum at 50 mM and then declined.

The NT2.N/A co-culture maintained significantly greater levels of ATP and GSH and sustained a smaller significant increase in H_2O_2 levels compared with the NT2.N mono-culture. However, the mono-culture showed no significant increase in caspase-3 activity, whereas the maximum response of the co-culture was 105.9 ± 2.2 % (50 mM) increase above control levels.

5.3.2 2,3-Hexanedione

The non-cytotoxic (NOAEL) range was 0-8 mM for the NT2.N cells, 0-12 mM for the NT2.D1 and NT2.N/A cells and 0-16 mM for the CCF-STTG1 cells (table 4.1, section 4.2.2).

5.3.2.1 ATP

Figure 5.5 illustrates that increasing concentrations of 2,3-hexanedione were associated with an immediate decrease in cellular ATP levels in the CCF-STTG1 cell line and a decrease in the NT2.N cell line at the higher concentration end after a 4-hour exposure period. However, there was no statistically significant decrease in cellular ATP in the NT2.D1 or NT2.N/A cell lines over the non-cytotoxic range ($P > 0.05$).

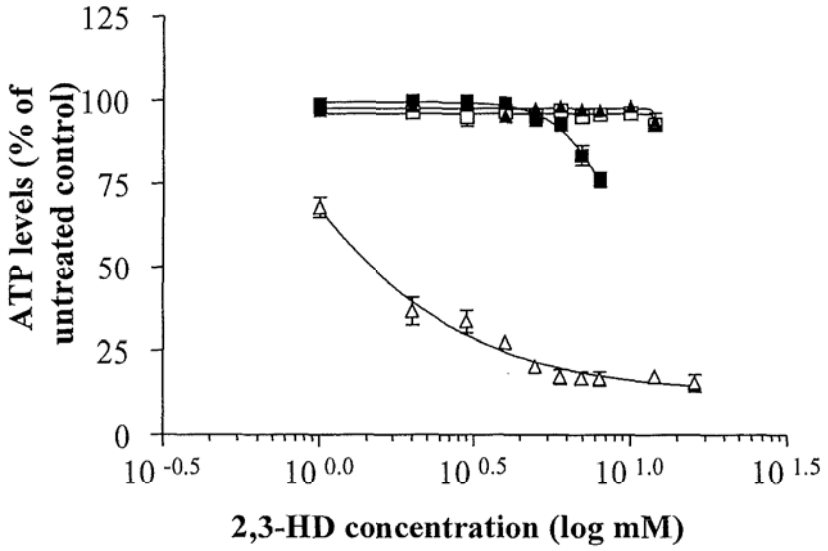

Figure 5.5 Percentage decrease in cellular ATP following exposure to increasing concentrations of 2,3-hexanedione for 4-hours. Sigmoidal concentration-response curve (variable slope) for NT2.D1 (▲), CFF-STTG1 (△), NT2.N (■) and NT2.N/A (□) cells. The ATP assay was carried out, the plates read for luminescence and ATP levels were calculated using a standard curve and corrected for sample protein content. Results are expressed as ATP (nmol/mg protein) for the toxin treated sample as a percentage of the ATP (nmol/mg protein) for the untreated control sample. Data points represent the mean ± SEM of the sample means from three separate experiments.

Two-way ANOVA analysis over the common 2-8 mM range indicated the concentration-response curves for the CCF-STTG1 and NT2.N cells were significantly different ($P < 0.001$) and that increasing concentration significantly affected the response ($P < 0.001$). This is also evident from figure 5.5 and it may be seen that with increasing concentration, 2,3-hexanedione greatly reduced ATP levels in the CCF-STTG1 cell line to only 16.6 ± 2.0 % at 8 mM.

At the highest common 2,3-hexanedione concentration used (8 mM) the NT2.N/A co-culture maintained significantly superior levels of ATP (95.9 ± 0.5 %) than did the NT2.N mono-culture (76.3 ± 2.2 %; $P < 0.001$).

5.3.2.2 Caspase-3

As can be seen in figure 5.6, increasing concentrations of 2,3-hexanedione caused a

small but statistically significant difference in caspase-3 activity in the NT2.D1 and CCF-STTG1 cultures compared with the untreated control ($P < 0.001$), with a maximum significant increase above the untreated control of 32.1 ± 0.7 % (3 mM) and 22.7 ± 0.4 % (4 mM), respectively ($P < 0.001$ in both cases). Caspase levels in both cultures then declined to the equivalent of control values at the highest concentration of 2,3-HD used ($P > 0.05$).

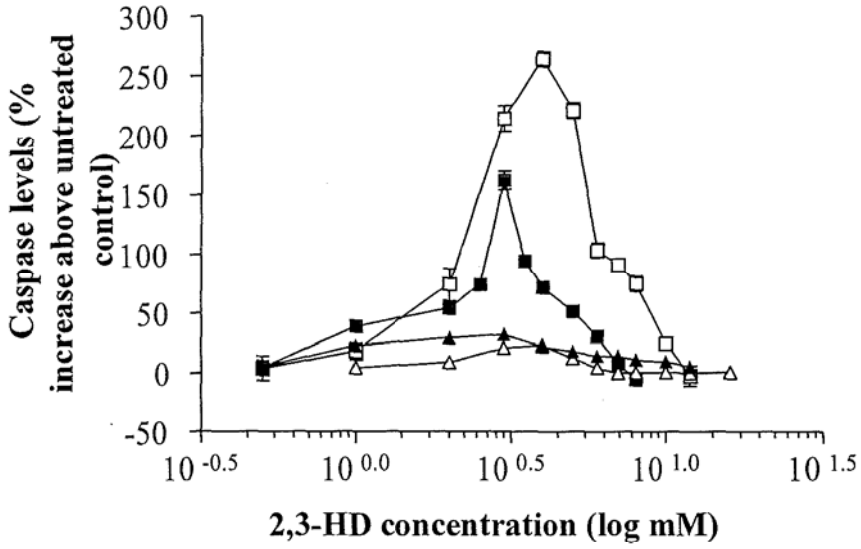

Figure 5.6 Percentage increase in cellular caspase-3 activity following exposure to increasing concentrations of 2,3-hexanedione for 4-hours. Concentration-response curve (points joined, not curve fit) for NT2.D1 (▲), CFF-STTG1 (△), NT2.N (■) and NT2.N/A (□) cells. The caspase-3 assay was carried out, the plates read for fluorescence (355/460 nm ex/em) and caspase-3 levels were calculated using a standard curve and corrected for sample protein content. Results are expressed as caspase-3 (nmol/mg protein) for the toxin treated sample as a percentage increase above the caspase-3 (nmol/mg protein) for the untreated control sample. Data points represent the mean ± SEM of the sample means from three separate experiments.

The NT2.N and NT2.N/A cultures showed a much greater progressive increase in caspase-3 activity with a maximum significant increase above the untreated control of 162.2 ± 7.9 % (3 mM) and 263.7 ± 6.4 % (4 mM) respectively. Caspase-3 levels in both cultures then declined to the equivalent of control values at the highest concentration of 2,3-HD used ($P > 0.05$).

Two-way ANOVA analysis over the common 0.5-8 mM range indicated the concentration-response curves for the NT2.N and NT2.N/A cells were significantly

different ($P < 0.001$) and that increasing 2,3-HD concentration significantly affected the caspase-3 response ($P < 0.001$). As is visible from figure 5.6 at concentrations above 2 mM, caspase-3 activity was significantly greater in the NT2.N/A co-culture than in the NT2.N mono-culture ($P < 0.001$).

5.3.2.3 Glutathione

Figure 5.7 shows increasing concentrations of 2,3-hexanedione were associated with a progressive decrease in cellular GSH to a level of < 25 % in the NT2.D1, NT2.N and NT2.N/A cultures after a 4-hour exposure period. However, GSH levels in the CCF-STTG1 cell line reaching a plateau at approximately 50 % of the untreated control.

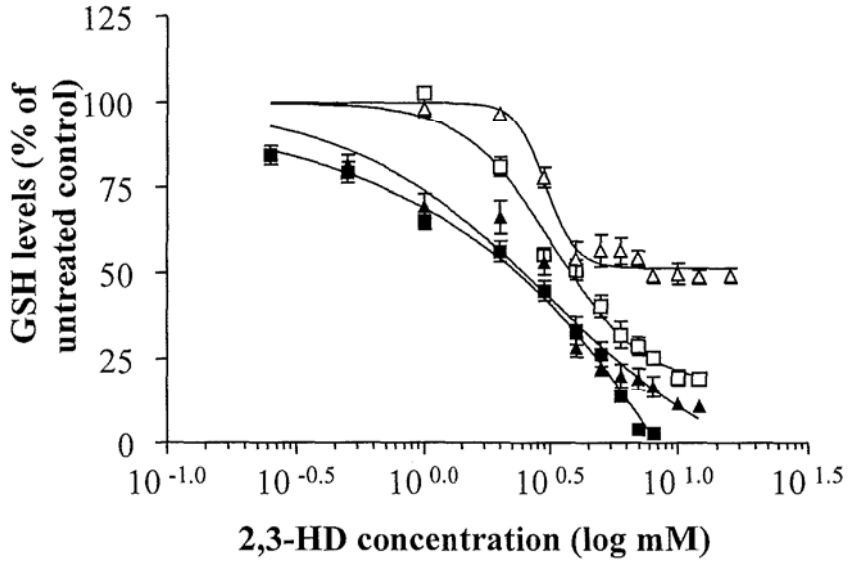

Figure 5.7 Percentage decrease in cellular GSH following exposure to increasing concentrations of 2,3-hexanedione for 4-hours. Sigmoidal concentration-response curve (variable slope) for NT2.D1 (▲), CFF-STTG1 (△), NT2.N (■) and NT2.N/A (□) cells. The GSH assay was carried out, the plates read for absorbance at 405 nm and GSH levels were calculated using a standard curve and corrected for sample protein content. Results are expressed as GSH (nmol/mg protein) for the toxin treated sample as a percentage of the GSH (nmol/mg protein) for the untreated control sample. Data points represent the mean ± SEM of the sample means from three separate experiments.

At the highest common 2,3-hexanedione concentration used (8 mM) the NT2.N/A co-culture maintained significantly higher levels of GSH (24.4 ± 1.9 %) compared with the NT2.N mono-culture (2.8 ± 0.9 %; $P < 0.001$).

Two-way ANOVA analysis over the common 1-8 mM range indicated the concentration-response curves for all four cell cultures were significantly different ($P < 0.001$) and that increasing concentration significantly affected the response ($P < 0.001$). Thus, from analysis of figure 5.7 it may be concluded that with increasing concentration, 2,3-hexanedione had the greatest impact in reducing GSH levels in the NT2.N, followed by the NT2.D1 and then the NT2.N/A culture, with the CCF-STTG1 culture maintaining the highest residual level of GSH.

5.3.2.4 2,3-Hexanedione summary

Increasing concentrations of 2,3-hexanedione caused a steep decrease in ATP levels in the CCF-STTG1 culture following exposure for 4-hours. However, the NT2.N culture showed only a small decrease compared with the untreated control (~ 25 %) and the NT2.D1 and NT2.N/A cultures showed no effect. Conversely, the CCF-STTG1 cell line was the least sensitive with regards to GSH response, with levels in the remaining cell lines declining to below 25 % (order of sensitivity, CCF-STTG1 < NT2.NA < NT2.D1 < NT2.N).

2,3-hexanedione caused only a small increase in caspase-3 activity in the NT2.D1 and CCF-STTG1 cultures, with a much larger effect in the neuronal containing NT2.N and NT2.N/A cell systems (maximum level: 162.2 ± 7.9 % (NT2.N, 3 mM) and 263.7 ± 6.4 % (NT2.N/A, 4 mM).

The NT2.N/A co-culture maintained significantly superior levels of GSH and ATP compared with the NT2.N mono-culture. Both cultures showed evidence of caspase activation but at concentrations above 2 mM 2,3-HD, the co-culture maintained significantly higher levels of caspase-3 activity overall.

5.3.3 3,4-Hexanedione

The non-cytotoxic (NOAEL) range after a 4-hour exposure period was 0-12 mM for the NT2.D1 and CCF-STTG1 cells and 0-16 mM for the NT2.N and NT2.N/A cells (table 4.1, section 4.2.2).

5.3.3.1 ATP

As can be seen in figure 5.8, increasing concentrations of 3,4-hexanedione were associated with an immediate decrease in cellular ATP levels in the CCF-STTG1 cell line and a progressive decrease in the NT2.N and NT2.N/A cultures, after a 4-hour exposure period. However, there was no statistically significant decrease in cellular ATP in the NT2.D1 cell line over the non-cytotoxic range ($P > 0.05$).

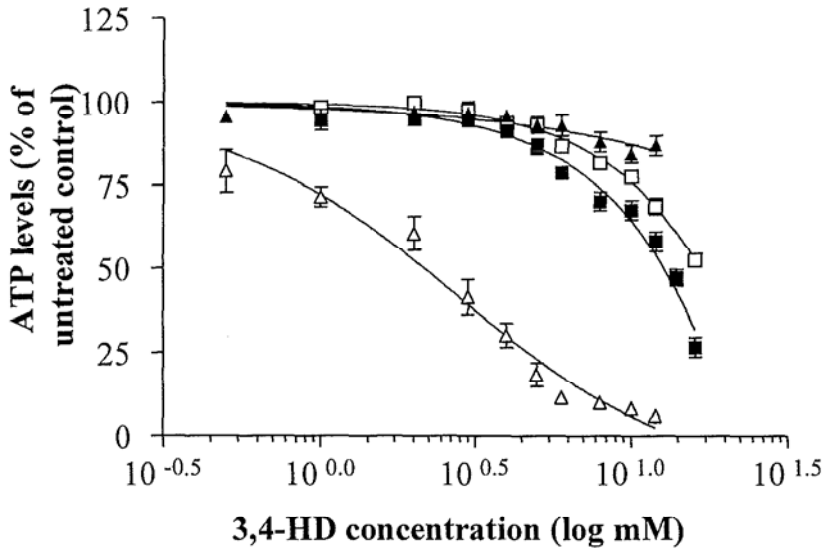

Figure 5.8 Percentage decrease in cellular ATP following exposure to increasing concentrations of 3,4-hexanedione for 4-hours. Sigmoidal concentration-response curve (variable slope) for NT2.D1 (▲), CFF-STTG1 (△), NT2.N (■) and NT2.N/A (□) cells. The ATP assay was carried out, the plates read for luminescence and ATP levels were calculated using a standard curve and corrected for sample protein content. Results are expressed as ATP (nmol/mg protein) for the toxin treated sample as a percentage of the ATP (nmol/mg protein) for the untreated control sample. Data points represent the mean ± SEM of the sample means from three separate experiments.

Two-way ANOVA analysis over the common 1-12 mM range indicated the concentration-response curves for the CCF-STTG1, NT2.N and NT2.N/A cell lines were significantly different from each other ($P < 0.001$) and that increasing concentration significantly affected the response ($P < 0.001$). This is also evident from figure 5.8 and it may be concluded that with increasing concentration, 3,4-hexanedione had the least effect on ATP levels in the NT2.N/A, followed by the NT2.N and then the CCF-STTG1 culture, whose ATP levels were vastly reduced to only 7.7 ± 1.1 % of

control values at 12 mM.

At the highest common 3,4-hexanedione concentration used (16 mM) the NT2.N/A co-culture maintained significantly superior levels of ATP (52.6 ± 1.6 %) than did the NT2.N mono-culture (26.6 ± 2.9 %; $P < 0.001$).

5.3.3.2 Caspase-3

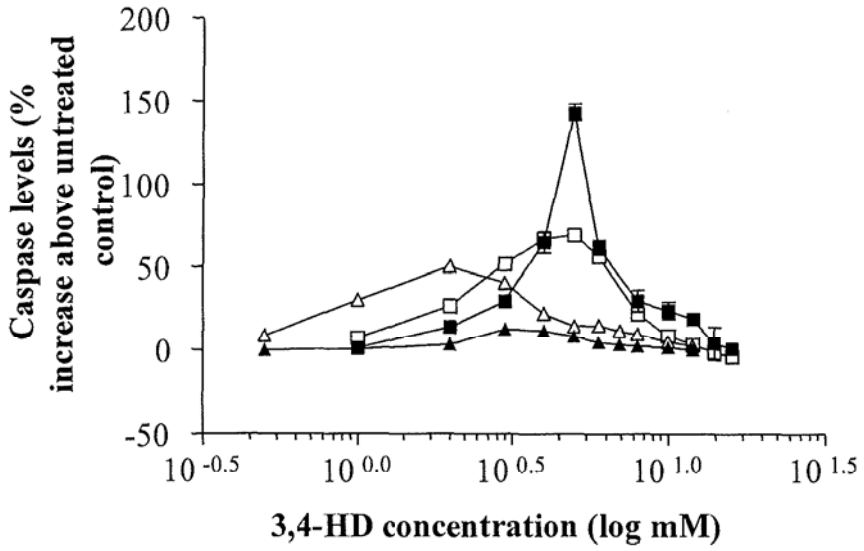

Figure 5.9 Percentage increase in cellular caspase-3 activity following exposure to increasing concentrations of 3,4-hexanedione for 4-hours. Concentration-response curve (points joined, not curve fit) for NT2.D1 (▲), CFF-STTG1 (△), NT2.N (■) and NT2.N/A (□) cells. The caspase-3 assay was carried out, the plates read for fluorescence (355/460 nm ex/em) and caspase-3 levels were calculated using a standard curve and corrected for sample protein content. Results are expressed as caspase-3 (nmol/mg protein) for the toxin treated sample as a percentage increase above the caspase-3 (nmol/mg protein) for the untreated control sample. Data points represent the mean ± SEM of the sample means from three separate experiments.

Figure 5.9 indicates that increasing concentrations of 3,4-hexanedione caused no overall significant difference in caspase-3 activity compared with the untreated control in the NT2.D1 culture over the non-cytotoxic range ($P > 0.05$). The CCF-STTG1 and NT2.N/A cultures showed an initial progressive increase in caspase-3 activity with a maximum significant increase above the untreated control of 50.5 ± 2.2 % (2 mM) and 69.2 ± 3.3 % (5 mM), respectively ($P < 0.001$ in both cases). Caspase levels in both cultures then declined to the equivalent of control values at levels above 10 mM 2,3-

HD ($P > 0.05$). The NT2.N culture showed the highest maximum significant increase in caspase-3 activity of 143.3 ± 5.2 % (5 mM), with caspase-3 levels then declining to control levels.

Two-way ANOVA analysis over the common 1-12 mM range indicated that the concentration-response curves for the CCF-STGG1, NT2.N and NT2.N/A cells were significantly different ($P < 0.001$) and that increasing 3,4-HD concentration significantly affected the caspase-3 response ($P < 0.001$). As is visible from figure 5.9 the concentration-response curves for the NT2.N and NT2.N/A cultures were similar with the exception of the maximum response at 5 mM. At this 3,4-HD concentration, caspase-3 activity was significantly greater in the NT2.N mono-culture than in the NT2.N/A co-culture ($P < 0.001$).

5.3.3.3 Glutathione

As can be seen in figure 5.10, increasing concentrations of 3,4-hexanedione were associated with a progressive decrease in cellular GSH levels in the NT2.D1 and NT2.N cultures to below 25 % after a 4-hour exposure period and a steeper decline in the CCF-STTG1 culture. There was also a decline in GSH levels in the NT2.N/A cell line but this reached a plateau at approximately 70 % of the untreated control.

Two-way ANOVA analysis over the common 1-12 mM range indicated the concentration-response curves for all four cell cultures were significantly different ($P < 0.001$) and that increasing concentration significantly affected the response ($P < 0.001$). Thus, from analysis of figure 5.10 it may be concluded that overall, with increasing concentration, 3,4-hexanedione caused the greatest reduction in GSH levels in the CCF-STTG1, followed by the NT2.D1 and then the NT2.N culture, with the NT2.N/A culture maintaining the highest level of GSH. However, at concentrations above 5 mM, the GSH levels in the NT2.D1 and CCF-STTG1 cell lines were statistically equivalent ($P > 0.05$).

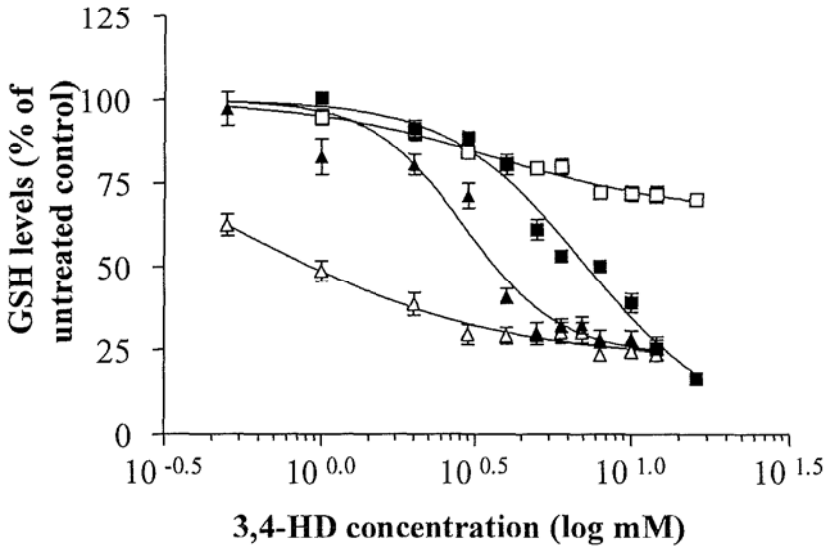

Figure 5.10 Percentage decrease in cellular GSH following exposure to increasing concentrations of 3,4-hexanedione for 4-hours. Sigmoidal concentration-response curve (variable slope) for NT2.D1 (▲), CFF-STTG1 (△), NT2.N (■) and NT2.N/A (□) cells. The GSH assay was carried out, the plates read for absorbance at 405 nm and GSH levels were calculated using a standard curve and corrected for sample protein content. Results are expressed as GSH (nmol/mg protein) for the toxin treated sample as a percentage of the GSH (nmol/mg protein) for the untreated control sample. Data points represent the mean ± SEM of the sample means from three separate experiments.

At the highest common 3,4-hexanedione concentration used (16 mM) the NT2.N/A co-culture maintained significantly greater levels of GSH (70.1 ± 1.3 % of control values) than did the NT2.N mono-culture (16.6 ± 1.4 %; $P < 0.001$).

5.3.3.4 3,4-Hexanedione summary

As with 2,3-hexanedione, increasing concentrations of 3,4-hexanedione caused a steep decrease in ATP levels in the CCF-STTG1 culture following exposure for 4-hours, with the NT2.D1 culture showing no effect. The neuron containing NT2.N and NT2.N/A cultures showed a progressive decrease. The CCF-STTG1 cell line also showed a step decline in glutathione and levels in the NT2.D1 and NT2.N cell lines also declined to below 25 %. The NT2.N/A cell line was the least sensitive regarding the GSH response.

3,4-hexanedione caused no change in caspase-3 activity in the NT2.D1 culture, with the CCF-STTG1 culture showing a moderate effect (maximum level: 50.5 ± 2.2 %, 2 mM). The neuron containing NT2.N and NT2.N/A cultures showed the highest levels of caspase-3 activation and similar concentration-response curves but with differing maximum levels (143.3 ± 5.2 % and 69.2 ± 3.3 %, respectively at 5 mM).

The NT2.N/A co-culture maintained significantly greater levels of GSH and ATP compared with the NT2.N mono-culture. Both cultures showed evidence of caspase-3 activation, with similar concentration-response curves but it was the mono-culture which had the highest maximum level of caspase-3 activity.

5.3.4 Trimethyltin chloride

The non-cytotoxic (NOAEL) range after a 4-hour exposure period was 0-500 μM for the NT2.D1, CCF-STTG1 and NT2.N cell lines and 0-1000 μM for the NT2.N/A cell line (table 4.1, section 4.2.2).

5.3.4.1 ATP

With figure 5.11, increasing concentrations of trimethyltin chloride were associated with a progressive decrease in cellular ATP levels in the NT2.N and CCF-STTG1 cell lines after a 4-hour exposure period. However, there was no statistically significant decrease in cellular ATP in the NT2.D1 cell line over the non-cytotoxic range ($P > 0.05$). Interestingly, the NT2.N/A co-culture showed evidence of increasing astrocytic activation with a maximum increase in ATP of 46.2 ± 2.3 % above the untreated control (500 μM TMT-Cl; $P < 0.001$). ATP levels then declined progressively to 79.2 ± 2.8 % (1000 μM TMT).

Two-way ANOVA analysis over the common 50-500 μM range indicated the concentration-response curves for all four cell lines were significantly different from each other ($P < 0.001$) and that increasing concentration significantly affected the response ($P < 0.001$). This is also evident from figure 5.11 and it may be concluded that with increasing concentration, TMT-Cl had least effect on ATP levels in the NT2.N/A,

followed by the NT2.D1 and then the CCF-STTG1 and NT2.N cultures.

At the highest common trimethyltin chloride concentration used (500 μM) the NT2.N/A co-culture maintained significantly superior levels of ATP (146.2 ± 2.8 %) than did the NT2.N mono-culture (51.9 ± 2.0 %; $P < 0.001$).

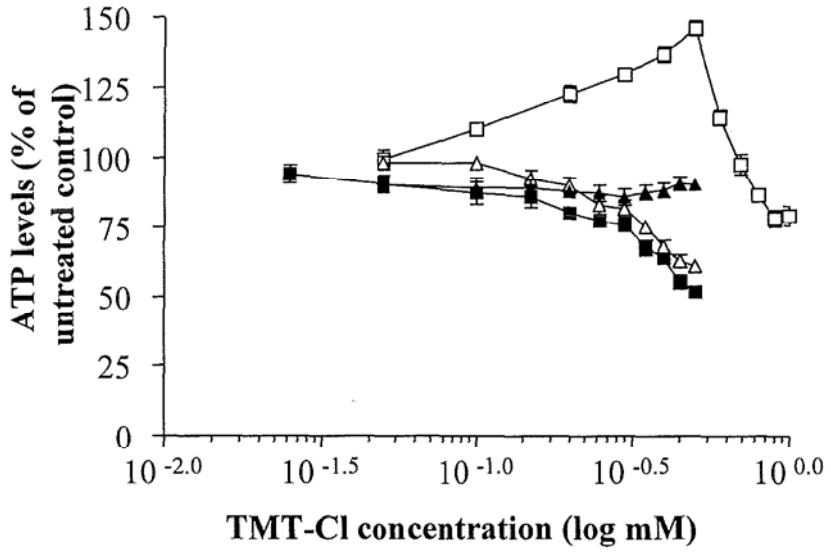

Figure 5.11 Percentage decrease in cellular ATP following exposure to increasing concentrations of trimethyltin chloride for 4-hours. Concentration-response curve (points line connected) for NT2.D1 (▲), CFF-STTG1 (△), NT2.N (■) and NT2.N/A (□) cells. The ATP assay was carried out, the plates read for luminescence and ATP levels were calculated using a standard curve and corrected for sample protein content. Results are expressed as ATP (nmol/mg protein) for the toxin treated sample as a percentage of the ATP (nmol/mg protein) for the untreated control sample. Data points represent the mean ± SEM of the sample means from three separate experiments.

5.3.4.2 Caspase-3

As can be seen in figure 5.12, increasing concentrations of trimethyltin chloride caused no statistically significant difference in caspase-3 activity compared with the untreated control in the NT2.N mono-culture over the non-cytotoxic range ($P > 0.05$). However, the NT2.N/A co-culture showed an initial progressive increase in caspase-3 activity, followed by a steep rise with a maximum significant increase above the untreated control of 278.2 ± 5.5 % (800 μM TMT-Cl; $P < 0.001$). Caspase-3 levels then declined steeply to 46.6 ± 8.4 % by 1000 μM TMT-Cl.

The NT2.D1 and CCF-STTG1 cultures showed a small overall change in caspase-3 activity with a maximum significant increase above the untreated control of 44.91 ± 1.8 % (200 μM TMT) and 32.7 ± 1.8 % (400 μM TMT), respectively.

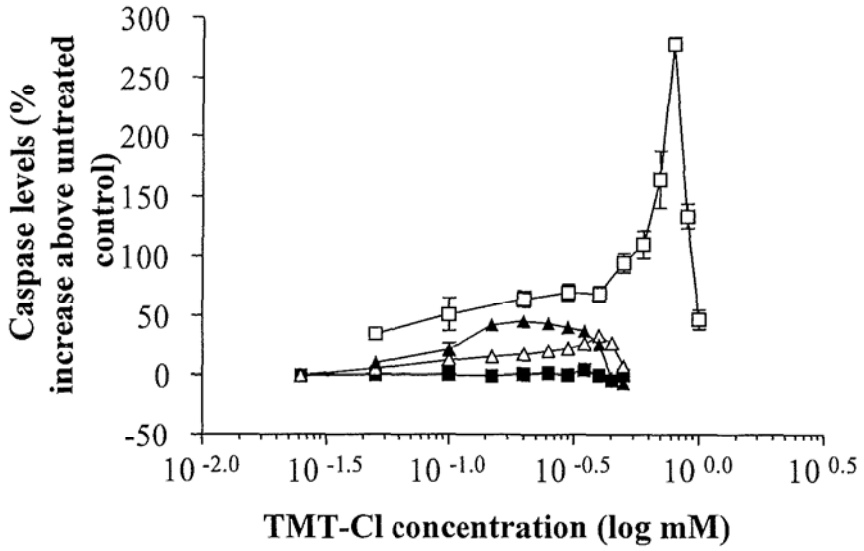

Figure 5.12 Percentage increase in cellular caspase-3 activity following exposure to increasing concentrations of trimethyltin chloride for 4-hours. Concentration-response curve (points joined, not curve fit) for NT2.D1 (▲), CFF-STTG1 (△), NT2.N (■) and NT2.N/A (□) cells. The caspase assay was carried out, the plates read for fluorescence (355/460 nm ex/em) and caspase-3 levels were calculated using a standard curve and corrected for sample protein content. Results are expressed as caspase-3 (nmol/mg protein) for the toxin treated sample as a percentage increase above the caspase-3 (nmol/mg protein) for the untreated control sample. Data points represent the mean ± SEM of the sample means from three separate experiments.

Two-way ANOVA analysis over the common 50-500 μM range indicated the concentration-response curves for the NT2.D1, CCF-STTG1 and NT2.N/A cell lines were significantly different from each other ($P < 0.001$) and that increasing concentration significantly affected the caspase-3 response ($P < 0.001$). By visual inspection of figure 5.12 it can be seen that overall, caspase-3 activation was greatest in the NT2.N/A culture and that the level reached its maximum at a concentration above the common NOAEL range.

5.3.4.3 Glutathione

As can be seen in figure 5.13, increasing concentrations of trimethyltin chloride were

associated with an immediate decrease in cellular GSH levels in the NT2.D1 culture and a progressive decline in GSH in the NT2.N culture after a 4-hour exposure period.

Interestingly, the NT2.N/A co-culture and CCF-STTG1 cell line showed evidence of astrocytic activation, with a maximum GSH level significant increase above the untreated control of 43.4 ± 1.8 % (200 μM TMT) and 24.2 ± 2.3 % (50 μM TMT), respectively ($P < 0.001$). Glutathione levels declined to below control levels in the CCF-STTG1 cell line at 200 μM TMT. Glutathione levels declined in the NT2.N/A co-culture also but did not decrease below control levels.

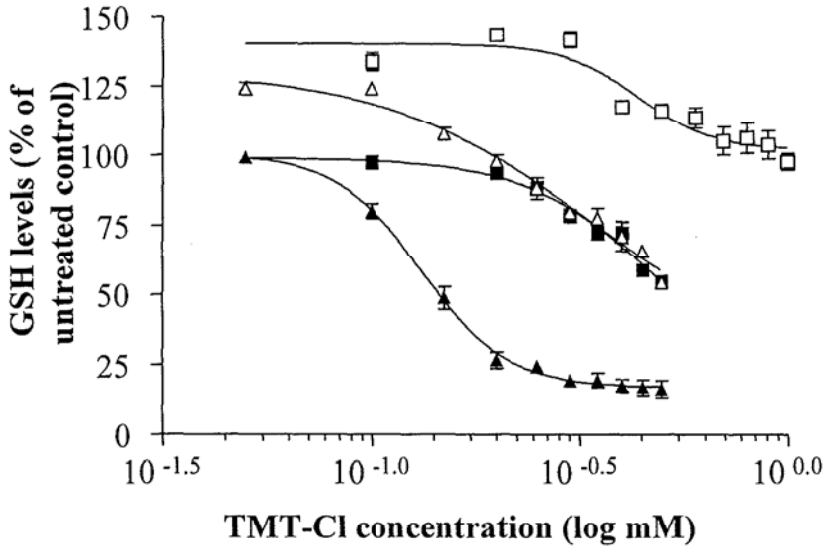

Figure 5.13 Percentage decrease in cellular GSH following exposure to increasing concentrations of trimethyltin chloride for 4-hours. Sigmoidal concentration-response curve (variable slope) for NT2.D1 (▲), CFF-STTG1 (△), NT2.N (■) and NT2.N/A (□) cells. The GSH assay was carried out, the plates read for absorbance at 405 nm and GSH levels were calculated using a standard curve and corrected for sample protein content. Results are expressed as GSH (nmol/mg protein) for the toxin treated sample as a percentage of the GSH (nmol/mg protein) for the untreated control sample. Data points represent the mean ± SEM of the sample means from three separate experiments.

Two-way ANOVA analysis over the common 100-500 μM range indicated the concentration-response curves for the NT2.N and CCF-STTG1 cells were not significantly different ($P > 0.05$). However, the NT2.N and CCF-STTG1 curves were significantly different from the NT2.D1 and NT2.N/A curves ($P < 0.001$) and increasing concentration significantly affected the response in all four cultures

($P < 0.001$). Thus, from analysis of figure 5.13 it may be concluded that with increasing concentration, trimethyltin chloride most reduced GSH levels in the NT2.D1, followed by the NT2.N and CCF-cultures and that levels were not decreased overall in the NT2.N/A culture.

At the highest common trimethyltin chloride concentration used (500 μM) the NT2.N/A co-culture maintained significantly greater levels of GSH compared with the control (116.1 ± 2.3 %) than did the NT2.N mono-culture (54.7 ± 1.4 %; $P < 0.001$).

5.3.4.4 Hydrogen peroxide

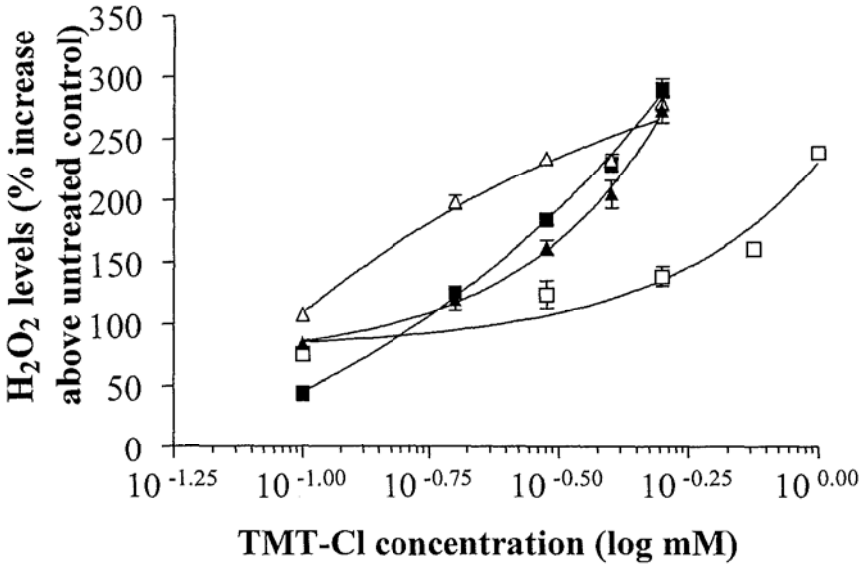

Figure 5.14 Percentage increase in H_2O_2 in culture media following cellular exposure to increasing concentrations of trimethyltin chloride for 4-hours. Sigmoidal concentration-response curve (variable slope) for NT2.D1 (▲), CFF-STTG1 (△), NT2.N (■) and NT2.N/A (□) cells. The Amplex red assay was carried out, the plates read for fluorescence (544/590 nm ex/em) and H_2O_2 levels were calculated using a standard curve. Results are expressed as H_2O_2 (nmol/μl medium) a percentage increase above the H_2O_2 (nmol/μl medium) for the untreated control sample. Data points represent the mean ± SEM of the sample means from three separate experiments.

Figure 5.14 shows increasing concentrations of TMT-Cl were associated with a progressive increase in H_2O_2 levels in the medium of all four cell cultures after a 4-hour exposure period.

Two-way ANOVA analysis over the common 100-400 μM range (500-1000 μM excluded) indicated that concentration-response curves for the NT2.D1 and NT2.N cells were not significantly different from each other ($P > 0.05$). However, over this concentration range the NT2.D1 and NT2.N curves were significantly different from the CCF-STTG1 and NT2.N/A curves ($P < 0.001$) and increasing concentration significantly affected the response in all four cultures ($P < 0.001$). Thus, from analysis of figure 5.14 it may be concluded that with increasing concentration, TMT-Cl (0-400 μM) caused the greatest increase in H_2O_2 levels overall in the CCF-STTG1, followed by the NT2.N and NT2.D1 cultures and least effect in the NT2.N/A culture. However, at 500 μM, H_2O_2 levels were statistically equivalent in the NT2.D1, CCF-STTG1 and NT2.N cell lines.

At the highest common TMT-Cl concentration used (500 μM) the NT2.N/A co-culture maintained significantly lower levels of H_2O_2 (138.8 ± 7.9 % increase over control values) compared with the NT2.N mono-culture (291.0 ± 7.7 %; $P < 0.001$).

5.3.4.5 Trimethyltin chloride summary

Increasing concentrations of TMT-Cl were associated with a progressive decrease in glutathione in the NT2.D1 and NT2.N cells and also the CCF-STTG1 cell line after an initial increase, which was reflected by an increase in H_2O_2 levels in all three cultures, after a 4-hour exposure period. The NT2.N/A culture also showed evidence of astrocytic activation with a > 40 % initial increase in GSH above control levels, with levels remaining above 100 % over the whole concentration range. This was reflected by H_2O_2 levels, which were lowest in the NT2.N/A cell line.

The NT2.N/A co-culture also showed an initial > 40 % maximum increase in ATP levels, which then declined to ~ 80 % of control levels. The NT2.D1 cells showed no decline in ATP levels and the NT2.N and CCF-STTG1 cell lines a moderate decrease. These levels correlated with changes in caspase-3, with the cultures that maintained the highest levels of ATP sustaining the largest significant change in caspase-3 activity. The NT2.N/A co-culture showed the greatest maximum increase of 278.2 ± 5.5 % increase over control values (800 μM), the NT2.D1 and CCF-STTG1 cells a much

lower increase (maximum < 45 %) and the NT2.N mono-culture showed no evidence of caspase-3 activation.

The NT2.N/A co-culture showed evidence of astrocytic activation and maintained significantly superior levels of ATP and GSH compared with the NT2.N mono-culture. The co-culture also sustained a smaller significant increase in H_2O_2 levels compared with the mono-culture, however, the mono-culture showed no significant increase in caspase-3 activity, whereas the maximum response of the co-culture was a 278.2 ± 5.5 % (800 μM) over control levels.

5.3.5 Tributyltin chloride

The non-cytotoxic (NOAEL) range after a 4-hour exposure period was 0-1 μM for the NT2.N cell line, 0-2 μM for the NT2.D1 and NT2.N/A cell lines and 0-4 μM for the CCF-STTG1 cell line (table 4.1, section 4.2.2).

5.3.5.1 ATP

As can be seen in figure 5.15, increasing concentrations of tributyltin chloride were associated with a progressive decrease in cellular ATP levels in all four cultures after a 4-hour exposure period. However, the decline was least steep in the NT2.N/A cell line.

Two-way ANOVA analysis over the common 0.2-1 μM range indicated the concentration-response curves for all four cell lines were significantly different from each other ($P < 0.01$) and that increasing concentration significantly affected the response ($P < 0.001$). This is also evident from figure 5.15 and it may be concluded that with increasing concentration (0.2-1 μM), TBT-Cl had least effect on ATP levels in the NT2.N/A, followed by the CCF-STTG1 and then the NT2.N and NT2.D1 cultures.

At the highest common TBT-Cl concentration used (1 μM) the NT2.N/A co-culture maintained significantly superior levels of ATP (82.0 ± 3.2 % of control values) than did the NT2.N mono-culture (30.6 ± 3.6 %; $P < 0.001$).

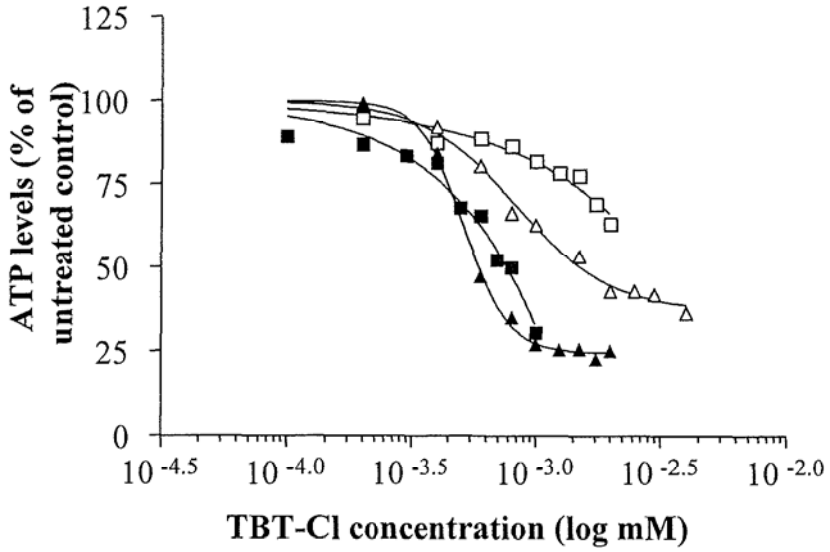

Figure 5.15 Percentage decrease in cellular ATP following exposure to increasing concentrations of tributyltin chloride for 4-hours. Sigmoidal concentration-response curve (variable slope) for NT2.D1 (▲), CFF-STTG1 (△), NT2.N (■) and NT2.N/A (□) cells. The ATP assay was carried out, the plates read for luminescence and ATP levels were calculated using a standard curve and corrected for sample protein content. Results are expressed as ATP (nmol/mg protein) for the toxin treated sample as a percentage of the ATP (nmol/mg protein) for the untreated control sample. Data points represent the mean ± SEM of the sample means from three separate experiments.

5.3.5.2 Caspase-3

Figure 5.16 illustrates that increasing concentrations of tributyltin chloride over the non-cytotoxic range caused an initial progressive increase in caspase-3 activity, which peaked and then declined to ≤ control levels, in all four cell cultures. The maximum significant increase above the untreated control for each cell line was 129.5 ± 4.7 % (NT2.D1, 0.4 μM), 158.2 ± 6.0 % (NT2.N, 0.3 μM), 223.3 ± 4.9 % (NT2.N/A, 0.6 μM) and 359.8 ± 6.6 % (CCF-STTG1, 2 μM) ($P < 0.001$ in all cases).

Two-way ANOVA analysis over the common 0.1-1 μM range indicated the concentration-response curves for the NT2.D1, NT2.N and NT2.N/A cell lines were significantly different from each other ($P < 0.001$; CCF-STTG1 data excluded) and that increasing concentration significantly affected the response ($P < 0.001$). By visual inspection of figure 5.16 it can be seen that caspase-3 activation was greatest in the

CCF-STTG1 cell line.

As is visible from figure 5.16 the maximum response in the NT2.N/A cell line (223.3 ± 4.9 %, 0.6 μM) was significantly greater and occurred at a higher TBT-Cl concentration compared with the NT2.N cell line (158.2 ± 6.0 %, 0.3 μM) ($P < 0.001$).

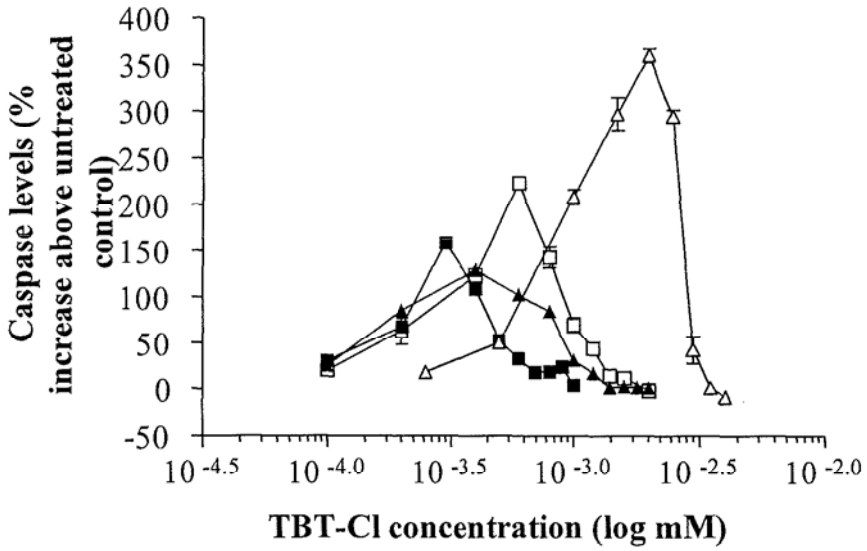

Figure 5.16 Percentage increase in cellular caspase-3 activity following exposure to increasing concentrations of tributyltin chloride for 4-hours. Concentration-response curve (points joined, not curve fit) for NT2.D1 (▲), CFF-STTG1 (△), NT2.N (■) and NT2.N/A (□) cells. The caspase-3 assay was carried out, the plates read for fluorescence (355/460 nm ex/em) and caspase-3 levels were calculated using a standard curve and corrected for sample protein content. Results are expressed as caspase-3 (nmol/mg protein) for the toxin treated sample as a percentage increase above the caspase-3 (nmol/mg protein) for the untreated control sample. Data points represent the mean ± SEM of the sample means from three separate experiments.

5.3.5.3 Glutathione

Figure 5.17 shows that increasing concentrations of tributyltin chloride were associated with an immediate decrease in cellular GSH levels in the NT2.D1 cell line after a 4-hour exposure period. There was a progressive decrease in cellular GSH levels in the CCF-STTG1 cell line and a moderate decrease in the NT2.N cell line to approximately 60 % of the control culture level. However, there was no statistically significant decrease in cellular GSH in the NT2.N/A cell line over the non-cytotoxic range ($P > 0.05$).

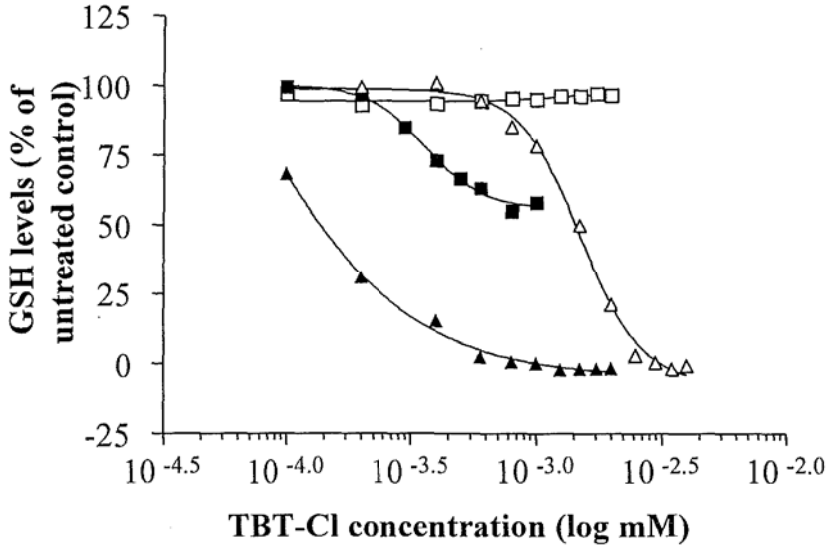

Figure 5.17 Percentage decrease in cellular GSH following exposure to increasing concentrations of tributyltin chloride for 4-hours. Sigmoidal concentration-response curve (variable slope) for NT2.D1 (▲), CFF-STTG1 (△), NT2.N (■) and NT2.N/A (□) cells. The GSH assay was carried out, the plates read for absorbance at 405 nm and GSH levels were calculated using a standard curve and corrected for sample protein content. Results are expressed as GSH (nmol/mg protein) for the toxin treated sample as a percentage of the GSH (nmol/mg protein) for the untreated control sample. Data points represent the mean ± SEM of the sample means from three separate experiments.

Two-way ANOVA analysis over the common 0.2-1 μM range indicated the concentration-response curves for the NT2.D1, CCF-STTG1 and NT2.N cells were significantly different ($P < 0.001$) and that increasing concentration significantly affected the response ($P < 0.001$). Thus, from analysis of figure 5.17 (0.2-1 μM) it may be concluded that overall, with increasing concentration, TBT-Cl reduced GSH levels least in the NT2.N/A, followed by the CCF-STTG1 and then the NT2.N cultures and finally the NT2.D1 culture. Visual inspection revealed that at concentrations above 1 μM, there was a steep decline in GSH levels in the CCF-STTG1 cultures to ~ 0 % those of the control.

At the highest common 2,5-hexanedione concentration used (1 μM) the NT2.N/A co-culture maintained significantly greater levels of GSH (95.1 ± 2.6 % of control values) than the NT2.N mono-culture (58.0 ± 3.0 %; $P < 0.001$).

5.3.5.4 Hydrogen peroxide

Figure 5.18 indicates increasing concentrations of tributyltin chloride were associated with a progressive increase in H_2O_2 levels in the medium of all four cell cultures after a 4-hour exposure period.

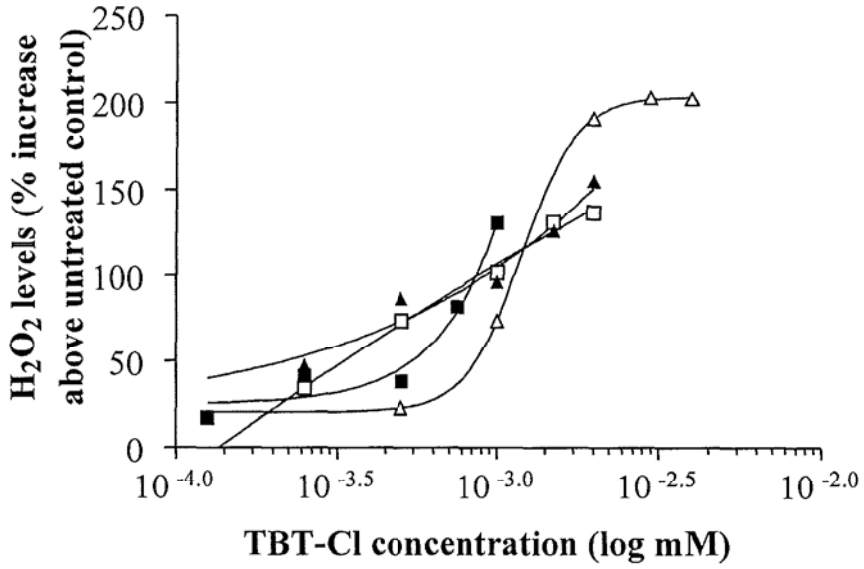

Figure 5.18 Percentage increase in H_2O_2 in culture media following cellular exposure to increasing concentrations of tributyltin chloride for 4-hours. Sigmoidal concentration-response curve (variable slope) for NT2.D1 (▲), CFF-STTG1 (△), NT2.N (■) and NT2.N/A (□) cells. The Amplex red assay was carried out, the plates read for fluorescence (544/590 nm ex/em) and H_2O_2 levels were calculated using a standard curve. Results are expressed as H_2O_2 (nmol/µl medium) a percentage increase above the H_2O_2 (nmol/µl medium) for the untreated control sample. Data points represent the mean ± SEM of the sample means from three separate experiments.

Two-way ANOVA analysis over the common 0.25-1 µM range showed the concentration-response curves for the NT2.D1, NT2.N and NT2.N/A cell lines were not significantly different ($P > 0.05$; CCF-STTG1 data excluded) but that increasing concentration significantly affected the response ($P < 0.001$). However, at the highest common 2,5-hexanedione concentration used (1 µM) the NT2.N/A co-culture maintained moderately lower levels of H_2O_2 (96.6 ± 2.1 % increase over control values) than did the NT2.N mono-culture (131.1 ± 0.9 %; $P < 0.01$). At 1 µM the CCF-STTG1 cell line sustained the smallest significant increase in H_2O_2 levels compared with the other three cell lines (73.6 ± 0.6 %; $P < 0.01$). However, visual inspection of

figure 5.18 shows that at concentrations above 1 μM, there was a steep increase in H_2O_2 levels in the CCF-STTG1 culture to over 200 % of control levels.

5.3.5.5 Tributyltin chloride summary

Increasing concentrations of tributyltin chloride were associated with a steep decrease in glutathione levels in the NT2.D1 cell line, a progressive decrease in the CCF-STTG1 cell line and a moderate decrease in the NT2.N cell line that was reflected by an increase in H_2O_2 levels in all three cultures, after a 4-hour exposure period. The NT2.N/A co-culture showed no decrease in GSH levels but did show an increase in H_2O_2 levels comparative with those of the NT2.D1 and NT2.N cell lines.

There was a progressive decrease in ATP levels in the NT2.D1 and NT2.N cell lines, with the NT2.N/A followed by the CCF-STTG1 cell line maintaining higher levels of ATP. Tributyltin chloride caused a significant change in caspase-3 activity in all four cultures, with the astrocytic containing CCF-STTG1 and NT2.N/A cultures showing the highest maximum levels of caspase-3 activation.

The NT2.N/A co-culture maintained significantly greater levels of ATP and GSH but sustained a similar increase in H_2O_2 levels compared with the NT2.N mono-culture and a higher maximum increase in caspase-3 activity.

5.4 Discussion

Changes in levels of ATP, GSH, H_2O_2 and caspase-3 caused by 4-hours exposure of the cell systems to non-cytotoxic levels of the selected test chemicals were measured in relation to an untreated control. The resulting concentration-response curves were then used to evaluate the quantitative response of the NT2.N/A co-culture in comparison with the culture of NT2.N and CCF-STTG1 cells alone and with the undifferentiated NT2.D1 cell line, regarding test chemical induced effects on the biochemical endpoints.

5.4.1 2,5-Hexanedione

2,5-Hexanedione (2,5-HD) is an established chronic neurotoxin (Couri et al., 1978; Spencer et al., 1978), found to form pyrrole adducts specifically at neurofilament ε-lysine residues within the axon (Heijink et al, 2000), with subsequent axonal atrophy and development of predominantly PNS neurological deficits (LoPachin and DeCaprio, 2004). Thus, it may be expected that the biochemical endpoints would demonstrate the diketone to be more toxic towards the cell systems with the most neuronal features. However, 2,5-HD is not considered to be acutely neurotoxic (Couri and Milks, 1982). Indeed the cell viability IC_{50} values generated by the MTT assay demonstrated that the chronic neurotoxin was acutely cytotoxic only at millimolar concentrations after 4- and 24-hours exposure. Generally, the order of sensitivity of the cell systems was NT2.D1 > NT2.N > CCF-STTG1 ≥ NT2.N/A.

The actual mechanism of axonal atrophy is unknown. However, 2,5-HD is a soft electrophile, thought to act through the formation of adducts with soft nucleophilic centres on protein lysine residues (LoPachin and DeCaprio, 2005). Intermediate filaments are typically the most stable part of the cytoskeleton. As such, neurofilaments are an important determinant of axon calibre and presumably their adduction disrupts the structure and/or function sufficient in magnitude to result in axonal atrophy.

2,5-HD chronic neurodegenerations are primarily characterised by destruction of the axon of neuronal cells without affecting the cell body. However, it is possible that 2,5-HD also causes acute dysfunction *in vitro* via adduction of sites within the perikaryon.

Indeed, Hartley *et al.,* (1997) found that 2,5-HD (25 mM) caused neurofilament accumulations in the cell body of the retinoic acid differentiated human neuroblastoma SH-SY5Y cell line, after 24-hours. Additionally, GFAP aggregations have been observed in astrocytes from dissociated cultures of foetal mouse dorsal root ganglia following three weeks exposure to 4 mM 2,5-HD (Durham, 1988). More acute effects were obtained when 88 mM 2,5-HD added to dorsal root ganglia from chick embryos resulted in a number of astrocytes with GFAP aggregations, reduced processes and vacuolisation of cytoplasm and swelling, followed by astrocytic cell death at 48 hrs (Boegner *et al.*, 1992). It is possible therefore, that aggregation of important structural intermediate filaments by 2,5-HD may compromise the integrity of various cell types (Anthony *et al.*, 2001), which may in part explain the cell system sensitivity observed in the present study. Indeed, soft electrophiles can cause a wide variety of cytotoxicity through reaction with nucleophilic sites that are common to many proteins across tissues (LoPachin and DeCaprio, 2005). Recently, 2,5-HD has also been demonstrated to form reaction products with β-alanine and glycine *in vitro* (Pei *et al.*, 2007). The consequences of such a generalised toxic mechanism may be more serious for CNS tissue, as post-mitotic neurons within the CNS which are lost to toxic damage can not be replaced by the proliferation of surviving cells (Kleinsmith and Kish, 1995; Harris and Blain, 2004).

2,5-HD (52 μM) caused a 50 % sub-acute decrease in cellular ATP following 7 days exposure of primary cultures of embryonal rodent cerebral tissue (Schmuck *et al.*, 2000). These cultures contain mature differentiated neurons and a minor number of astrocytes. Sickles *et al.*, (1990) demonstrated that 30 minute exposure to 4 mM 2,5-HD produced a 20 % decrease in endogenous ATP content in isolated rat neural mitochondria. This suggests that at higher concentrations, 2,5-HD is also able to affect cellular energy supply acutely. With the exception of the NT2.D1 cell line, data from this chapter are in broad agreement, in that there was a progressive decrease in cellular ATP levels in the cultures following exposure to non-cytotoxic concentrations of 2,5-HD (0-85 mM) over 4-hours. The order of decreasing sensitivity was CCF-STTG1 > NT2.N > NT2.N/A, with the NT2.D1 cell line maintaining its ATP levels.

Due to the high energy consumption necessary for normal CNS function, neuronal cell

health is highly dependent on the production and utilisation of ATP (Massicotte *et al.*, 2005). That the NT2.N/A co-culture maintained significantly greater levels of ATP than the NT2.N mono-culture, may be evidence of an astrocytic protective effect and a reflection of previous observations that at least chronically, neurons are more vulnerable than astrocytes towards the diketone compound. Conversely, the CCF-STTG1 cell line was more vulnerable than the NT2.N/A culture. However, this cell line was found to be generally one of the most sensitive to ATP effects following exposure to the other test chemicals.

Chronic 2,5-HD exposure has previously been shown to cause apoptosis in neuronal cells of mouse dorsal root ganglia exposed to 8.8 mM 2,5-HD for 6 days (Ogawa *et al.*, 1996). Acutely, 33.5 mM 2,5-HD was demonstrated to disturbance calcium homeostasis in the Vsc4.1 motor neuron cell line, with an increase in the intracellular Ca^{2+} level occurring after 10 minutes (Zhang *et al.*, 2006). Those authors considered that intracellular calcium increase may have been involved in the mechanism of acute 2,5-HD toxicity and alterations in intracellular Ca^{2+} homeostasis have been implicated in both apoptotic and necrotic cell death. Relatively high Ca^{2+} levels may overwhelm the cell via activation of calcium dependent enzymes including proteases, lipases and nucleases and the production of ROS, leading to necrosis (Garcia and Massieu, 2003). However, certain Ca^{2+} concentration ranges promote cytochrome c release and caspase activation followed by apoptosis, if sufficient ATP levels are maintained during the critical phases of execution of the cell death programme (Nicotera and Orrenius, 1998; Saito *et al.*, 2006).

In the present study, only the NT2.N/A culture showed evidence of increased caspase-3 activation as a result of 2,5-HD exposure and the co-culture also maintained a high level of ATP that may have supported an apoptotic mode of cell death. This might suggest that the remaining cell lines were more vulnerable to necrosis by millimolar concentrations of 2,5-HD, despite the NT2.D1 cell line also maintaining high ATP levels. In the future, a measure of effects of non-cytotoxic concentrations of 2,5-HD on calcium homeostasis would provide a useful indication of possible involvement of Ca^{2+} in apoptotic cascade initiation or alternatively a necrotic mode of cell death.

Cultured neurons have been reported to be more vulnerable than cultured astrocytes to cell death caused by oxidative species, postulated to be due at least in part to the lower concentrations of GSH found in neurons compared with astrocytic cells (Wullner *et al.*, 1999). This is in good agreement with the observation in this chapter that the CCF-STTG1 cell line maintained its levels of GSH following exposure to non-cytotoxic concentrations of 2,5-HD for 4-hours. Additionally, whilst 2,5-HD progressively depleted GSH levels in the remaining cultures, the NT2.N/A co-culture maintained superior levels of the antioxidant compared with the NT2.N mono-culture. Indeed, in neuron astrocytic co-culture systems, astrocytes have been demonstrated to protect neuronal cells against ROS induced toxicity by maintaining neuronal GSH levels (Iwata-Ichikawa *et al.*, 1999).

As discussed, 2,5-HD acts chronically via the formation of pyrrole adducts specifically at neurofilament ε-lysine residues, resulting in axonal atrophy (Heijink et al, 2000). It has been postulated that mechanisms which indirectly involve adduct formation, most notably oxidative stress, can also play a role in neurotoxicity (LoPachin and DeCaprio, 2005). Soft electrophiles that adduct thiol groups can significantly decrease cellular reducing agents such as GSH, with a decrease in GSH indirectly leading to an increase in oxidative species. It is possible therefore, that such electrophilic reactions contributed to the depletion in GSH observed in the cell systems in this study.

The neuroprotective ability of astrocytes against H_2O_2 is considered to be related predominantly to their capacity to remove the peroxide using GSH as a substrate of glutathione peroxidase (Drukarch *et al.*, 1997). Increasing concentrations of 2,5-hexanedione were associated with a progressive increase in H_2O_2 levels in all four cell cultures after a 4-hour exposure period, which correlated well with the order of sensitivity regarding GSH depletion. This suggests that following acute 2,5-HD exposure, the enhanced levels of H_2O_2 observed are due to reduced availability of GSH as a substrate for GPx (Desagher *et al.*, 1996). This disturbance in the oxidant-antioxidant balance may leave the cell systems vulnerable to oxidative stress. H_2O_2 can react with metal ions to create hydroxyl radicals ($^{\bullet}OH$) that react and damage proteins, lipids, membranes and inactivate thiol dependent Ca^{2+} pumps, which can severely compromise cellular function culminating in cell death by necrosis or apoptosis

(Dringen, 2000; Saito *et al.*, 2006).

Thus 2,5-HD, an established chronic neurotoxin, was broadly capable of inducing acute effects on ATP, GSH and H_2O_2 in all of the cultures and caspase-3 activation in the NT2.N/A cell system, at millimolar, non-cytotoxic concentrations. With the exception of caspase-3 activation, the metabolic endpoints examined were generally able to differentiate between the cell system responses but not in a manner consistent with specific acute neurotoxicity. The neuronal NT2.N and NT2.N/A cultures did demonstrate particular vulnerability regarding GSH depletion, commensurate with an increase in H_2O_2 oxidative species, which may have been an indirect result of 2,5-HD electrophilic adduct formation. However, specific mechanistic studies would be required to confirm this, which are outside the scope of the development of a preliminary neurotoxicity screen.

The NT2.N/A co-culture was able to maintain superior levels of ATP and GSH and sustained a smaller increase in H_2O_2 levels compared with the NT2.N mono-culture, which may be indicative of astrocytic protective capabilities. In contrast to the co-culture, the mono-culture showed no significant increase in caspase-3 activity. It is not possible to quantify this from the current data but the quantity of cells undergoing death by necrosis may be greater in the NT2.N culture, perhaps as a consequence of the greater depletion in ATP and GSH and increase in H_2O_2 levels.

5.4.2 2,3- and 3,4-Hexanedione

As mentioned, studies regarding the acute toxic potency of 2,3- and 3,4-hexanedione are limited. In the present study, at almost identical concentrations, the cell viability IC_{50} values generated by the MTT assay demonstrated both 2,3- and 3,4-hexanedione to be only weakly cytotoxic and not acutely neurotoxic. Additionally, no consistent vulnerability of neuronal or non-neuronal cell types was demonstrated by comparison of the IC_{50} values at 4- or 24-hours, with all cell systems being equally or very similarly sensitive towards the α-hexanediones. Thus, it may be expected that following 4-hours exposure to non-cytotoxic concentrations of 2,3-HD (0-16 mM), or 3,4-HD (0-16 mM), the different cultures would demonstrate similar responses to the

biochemical endpoints. Thus the two compounds are discussed together here.

To be a target, an endogenous molecule must possess the appropriate reactivity and/or steric configuration to allow the toxin to interact and cause dysfunction (Gregus and Klaassen, 2001). α-Diketones are electrophilic and 2,3- and 3,4-HD have been found to be highly selective for modification of arginine residues in proteins, including those associated with the oxoglutarate carrier (OGC) of the inner mitochondrial membrane. The OGC catalyses a counter-exchange between 2-oxoglutarate and L-malate and arginine specific reagents have been shown to inactivate the OGC, with 2,3- and 3,4-HD causing an almost complete inhibition of oxoglutarate and malate transport. 2,5-HD which does not interact with arginine residues, had no significant effect on the activity of the OGC (Stipani *et al.*, 1996). Malate and oxoglutarate play a number of important roles in the ultimate synthesis of ATP, including generation of NADH equivalents in the tricarboxylic acid (TCA) cycle (Stryer, 1995). Inhibition of the OGC and thus malate and oxoglutarate transport by α-hexanediones has the potential to deplete cellular ATP levels.

In the present study, such inhibition of the OGC may account for the steep decrease in ATP levels demonstrated by the CCF-STTG1 cell line following exposure to both α-diketones. It may also account for the decline seen in the NT2.N and NT2.N/A cultures upon exposure to 3,4-HD and to a much lesser extent in the NT2.N culture upon exposure to 2,3-HD. However, this potential inhibition of the TCA cycle did not seem to impact on the NT2.D1 cells in either case, or when the NT2.N/A cells were exposed to 2,3-HD. With the exception of TBT-Cl, ATP levels were not generally depleted in the NT2.D1 cells by the test chemicals. This may suggest an overall low metabolic demand of the non-neuronal cell line. Additionally, the NT2.N/A culture was also generally insensitive regarding ATP depletion in response to toxin exposure, which may suggest the co-culture has the ability to maintain its ATP levels when under oxidative pressure, perhaps through glycolysis. Why the CCF-STTG1 cell line was so vulnerable to 2,3- and 3,4-HD induced ATP depletion is unclear, though this cell line demonstrated high vulnerability to ATP modulation overall. Perhaps the CCF-STTG1 cell line is incapable of invoking glycolysis under toxic pressure, possibly inferring a lack of phenotypic closeness to what would be considered a crucial *in vivo* astrocytic

response.

Exposure of the cell systems to non-cytotoxic concentrations of 2,3-HD for 4-hours caused only a small change in caspase-3 activity in the NT2.D1 and CCF-STTG1 cultures, with a much larger effect being observed in the neuronal containing cell systems. 3,4-HD exposure caused a moderate difference in caspase-3 activity in CCF-STTG1 and NT2.N/A cultures. The NT2.N culture showed the highest maximum increase in caspase-3 activity but overall the concentration-response curves for the NT2.N and NT2.N/A cell systems were similar. These results suggest that concentrations of 2,3-HD of 3,4-HD that are non-cytotoxic at 4-hours, have the potential to cause cell death by apoptosis at a later time point, particularly in the differentiated cell systems. However it was not possible to consistently rank the sensitivity of the cell systems to 2,3-HD or 3,4-HD, regarding apoptotic response.

There have been no previous studies regarding the potential of 2,3-HD or 3,4-HD to induce an apoptotic mode of cell death and it is not clear why the differentiated cell systems may be more vulnerable to caspase-3 induction by the α-diketone compounds. Many xenobiotics can elicit both apoptosis and necrosis depending on the severity and nature of the insult and it is widely considered that cellular ATP content constitutes a switch between necrotic and apoptotic mode of cell death (Gregus and Klaassen, 2001; Saito *et al.*, 2006). As upon exposure to 2,3-HD the NT2.N/A cell system maintained its ATP levels at 100 %, this may have contributed to the higher overall level of capase-3 activation achieved, in comparison with the lower level in the NT2.N culture that experienced an ATP decrease. In addition this may explain the very low level of capase-3 activation demonstrated by the CCF-STTG1 culture upon exposure to 2,3-HD, which experienced a severe ATP depletion. Interestingly, comparatively higher levels of caspase-3 activation were experienced by the CCF-STTG1 cells following 3,4-HD exposure. The maximum level of a 50.5 ± 2.2 % increase compared with the control was achieved at 2 mM and at this concentration the CCF-STTG1 culture maintained ATP levels at ~60 %, which may have been adequate to support apoptosis. However, the NT2.D1 culture maintained its ATP levels upon exposure to both the α-hexanediones but demonstrated only an extremely low level of caspase-3 activation in comparison with the differentiated systems. It has been postulated that necrosis may

intervene before the apoptotic programme has a chance to develop fully and the NT2.D1 cell line may be more vulnerable to this mode of cell death (Ankarcrona *et al.*, 1995).

With increasing concentration, 2,3-hexanedione had the greatest impact in depleting GSH levels in the NT2.N cells, followed by the NT2.D1 and then the NT2.N/A culture. In contrast with the observed steep decline in ATP levels, the CCF-STTG1 cell line was the least sensitive with regards to GSH response, maintaining a residual level of ~ 50 %. In comparison, 3,4-hexanedione had the greatest initial impact in depleting GSH levels in the CFF-STTG1 culture. However, 3,4-HD was associated with a progressive decrease in cellular GSH levels in the NT2.D1 and NT2.N cultures also, with all three cultures showing levels below 25 % at the highest concentration used. There was also a decline in GSH levels in the NT2.N/A cell line but this reached a plateau at approximately 70 % of control cells.

Generally, astrocytes have a more efficient GSH synthesis system and higher levels of GSH compared with neurons both *in vivo* and in culture (Watts *et al.*, 2005). As such, neurons are thought to be dependent on neighbouring astrocytes for maintenance of their GSH level via provision of synthesis precursors (Drukarch *et al.*, 1997; Gegg *et al.*, 2003). This is obviously important regarding maintenance of optimal thiol status of neurons and protection of brain against oxidative stress (Dringen *et al.*, 1999b; Dringen, 2000). This may explain why the NT2.N/A co-culture was able to maintain higher levels of GSH in comparison with the NT2.N mono-culture, in response to both diones. The importance of astrocytes in combating the effects of ROS resulting from potentially harmful xenobiotics, highlights the need for their inclusion in a relevant cell system for the investigation of nervous system metabolic insult.

Methylglyoxal is a reactive dicarbonyl byproduct resulting from sugar modifications that can mediate protein and DNA damage if not detoxified. It is also known as a 'ketal' because it has an aldehydic and ketonic carbonyl group (Wondrak *et al.*, 2002) and the first step in its detoxification of methylglyoxal is reduction by GSH to produce the ketol 1-hydroxy acetone (figure 5.19) and glutathione disulphide (GSSG) (Wondrak *et al.*, 2002). The GSSG may then be recycled back to its reduced form.

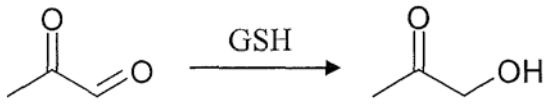

Figure 5.19 Reduction of methylglyoxal to 1-hydroxy acetone by glutathione

As previously mentioned, 2,3- and 3,4-HD are electrophiles and thus have the potential to react with nucleophiles. It is anticipated that *in vivo* both these α-diketones are initially metabolised principally by reduction to the corresponding α-diol (FAO/WHO, 1999). It may be hypothesised that GSH may reduce 2,3- and 3,4-HD in a similar way to the reduction of methylglyoxal and this may account for the reduction in GSH observed in all four cell systems. Agents that deplete GSH will indirectly increase ROS levels and may induce cell death. Levels of GSH may eventually be recovered through the recycling of GGSG and via resynthesis from its constituent amino acids. In the meantime depletion of antioxidant capacity would render the cell more vulnerable to oxidative damage and this may account for the cytotoxicity of the compounds at high concentrations. However, in order to be reduced by glutathione, a toxin must possess the appropriate reactivity and/or steric configuration to allow the GSH to interact with it (Gregus and Klaassen, 2001). GSH reacts with the carbonyl group of methylglyoxal rather than the ketone group. In reality, reaction with the ketone groups of the α-hexanediones may not proceed. Further investigation would be required to establish this and any other potential harmful electrophilic reactions, for example, protein modification.

Thus in general, both the α-hexanediones were capable of inducing effects on ATP, GSH and capase-3 in most of the cell systems at non-cytotoxic compound concentrations. The NT2.N/A co-culture was capable of maintaining overall superior ATP and GSH levels in comparison with the NT2.N mono-culture, in response to both α-hexanedione compounds, which may be indicative of astrocytic protective functions. No such consistent effect was observed regarding caspase-3 activation and in general the specific cell system responses did not differentiate either 2,3- or 3,4-HD as

neurotoxic.

Following examination of the cell viability IC_{50} values generated by the MTT assay it was expected that 2,3- and 3,4-hexanedione would demonstrate similar effects on the biochemical endpoints but this was not the case. For example, generally, 2,3-HD had an affect on GSH levels at lower concentrations, whereas 3,4-HD was more capable of eliciting an effect on ATP levels. Additionally, it was not possible to consistently rank the sensitivity of the cell systems to 2,3-HD and 3,4-HD regarding their response to the biochemical endpoints. A clear difference in the acute cytotoxic potential of these two compounds may be more apparent through the examination of effects at a later timepoint, such as 72-hours, or by the employment of a wider selection of endpoints.

As mentioned, to be a target, an endogenous molecule must possess the appropriate reactivity and/or steric configuration to allow the toxin to enter into covalent or non-covalent interactions (Gregus and Klaassen, 2001). Similarly, a toxin must be sterically able to interact with the endogenous molecule in order to cause dysfunction. Whilst 2,3- and 3,4-HD have the same electrophilic potential (relative H-bond acceptor value = 0.47), the identity of the carbon chains around the ketone groups differs. 2,3-HD possesses a methyl (1C) group and a propyl (3C) group and 3,4-HD possess two ethyl (2C) groups. A degree of steric hindrance may result from the larger propyl group of 2,3-HD that may affect the degree of dysfunction observed. Conversely, in some situations steric hindrance of 2,3-HD may actually be alleviated by the presence of the smaller methyl group, in comparison with the ethyl groups of 3,4-HD but this would require investigation too specific for a rapid screen of neurotoxic potential.

5.4.3 Trimethyltin chloride

In humans and experimental animals, trimethyltin chloride (TMT-Cl) behaves primarily as an acute CNS neurotoxin, causing necrosis and apoptosis specifically in areas of the hippocampus, cerebral cortex and cerebellum. TMT-Cl has also been shown to be acutely toxic *in vitro*, demonstrating species dependent potency and with neuronal cells exhibiting greater vulnerability than astrocytes. Thus, it may be expected that in the present study, the organotin would demonstrate specific neurotoxicity rather

than generalised cytotoxicity and as such the order of decreasing sensitivity of the cultures would be NT2.N > NT2.N/A > CCF-STTG1 > NT2.D1. However, the cell viability IC_{50} values generated by the MTT assay showed that following both 4- and 24-hours exposure, TMT-Cl was the least cytotoxic towards the NT2.N/A co-culture, with the order sensitivity of the remaining cell lines varying between the time-points.

Whilst the neurological effects of TMT compounds are well documented, the cellular mechanisms involved have not been completely elucidated. However, postulated causes of TMT-Cl induced necrotic or apoptotic death, include calcium overload (Florea *et al.*, 2005), astrocytic activation and release of cytokines (Viviani *et al.*, 1998a), caspase activation (Jenkins and Barone, 2004) and oxidative stress (Viviani *et al.*, 2001). Thus, it was hypothesised neurospecific toxicity may be more evident from examination of some of these biochemical endpoints following exposure of the cell systems to non-cytotoxic concentrations of TMT-Cl (0-1000 μM).

Administration of both neuropathic and non-neuropathic doses of TMT-Cl to rats have been demonstrated to produce a distinct *in vivo* morphological response of astrocytes in several brain regions, with hypertrophy, swelling and GFAP and metabolic increase suggestive of astrogliosis (O'Callaghan, 1991; Maier et al., 1995). Similar morphological alterations have been observed *in vitro*, in mixed and pure astrocytic cultures (Rohl et al., 2001; Figiel and Fiedorowicz, 2002). As such, in the current chapter, following exposure to non-cytotoxic concentrations of TMT-Cl for 4-hours, the NT2.N/A co-culture showed an initial increase in ATP levels above that of the untreated control (46.2 ± 2.3 %; 500 μM). This apparent metabolic increase may be suggestive of astrocytic activation. The CCF-STTG1 cell line and the NT2.N mono-culture demonstrated a moderate, progressive decrease in cellular ATP, suggesting TMT-Cl is able to affect high energy phosphate production in these cultures. Depletion of ATP by the tin compound may have been due to impairment of oxidative phosphorylation by ROS, or increased ATP consumption, for example due to Ca^{2+}-ATPases working to eliminate excess intracellular Ca^{2+}. However, the NT2.D1 cell line maintained ATP levels at control values.

Effects of TMT-Cl on Ca^{2+} homeostasis were not examined in this study. However,

exposure of the human neuroblastoma SH-SY5Y cell line to TMT-Cl concentrations identical to those examined in this chapter (500 μM), caused a sustained concentration dependent increase in intracellular Ca^{2+} due to release from internal stores (Florea *et al.*, 2005). Similarly, TMT-Cl was found to significantly increase intracellular Ca^{2+} in human, foetal, cerebral cortical neuronal cultures at 500 μM and to a lesser extent in astrocytes (Cristofol *et al.*, 2004). TMT-Cl has also been demonstrated to cause oxidative stress, which will be discussed later.

That the NT2.N/A co-culture maintained significantly superior levels of ATP than did the NT2.N mono-culture is in agreement with previous observations that astrocytes are less vulnerable than neurons towards the tin compound. This may be due to smaller Ca^{2+} perturbations in astrocytes and may also be a reflection of the increased metabolic rate induced in the co-culture. Indeed, it is considered that if sufficient levels of cellular ATP are maintained, repair processes may have the opportunity to delay or prevent cell death (Saito *et al.*, 2006).

A number of authors have explored the possibility that TMT-Cl induces an apoptotic cascade involving caspases in *in vitro* and *in vivo* studies. Jenkins and Barone (2004) found that exposure of neuronal like PC12 cells to 8 μM TMT-Cl for up to 20 hours, lead to the activation of caspase-3, followed by apoptosis, with caspase inhibition preventing apoptotic cell death. Geloso *et al.,* (2002) observed that following *in vivo* exposure (2.5 mg/kg; i.p.) in rats, the cells from the hippocampal region demonstrated caspase-3 activation closely associated with apoptotic nuclear morphology. However, it is also postulated that TMT-Cl induced cell death may include necrotic pathways. For example, Fiedorowicz *et al.,* (2001) investigated primary mixed cultures from rat hippocampus (50 % neurons, 32 % astrocytes and 15 % microglia) and found that TMT-Cl (10 μM) induced apoptosis in hippocampal neurons but not astrocytes or microglia following 24-hours exposure. However, in the absence of astrocytes and microglia, the neuronal cells underwent a necrotic mode of cell death. Additionally, the mode of cell death has been postulated to be dependent on the concentration of TMT-Cl utilised (Gunasekar *et al.*, 2001a).

In the current study, exposure of the cell systems to non-cytotoxic concentrations of

TMT-Cl for 4-hours caused no difference in caspase-3 activity compared with the untreated control in the NT2.N mono-culture and a only small overall change in caspase-3 activity in the continuous NT2.D1 and CCF-STTG1 cell lines. This may suggest that these cultures were more vulnerable to a necrotic mode of cell death induced by millimolar concentrations of TMT-Cl, despite the NT2.D1 cell line maintaining control levels of ATP. A much larger effect was observed in the NT2.N/A co-culture, which showed a progressive, then steep increase in caspase-3 activity (278.2 ± 5.5 %; 800 μM), followed by a rapid decline.

A complex interdependency exists between neurons and glial cells in the nervous system that is essential for the efficient function and survival of both cell types. Additionally, there is evidence that astrocytes may be necessary for the expression of certain neuronal toxic effects, particularly via the release of cytokines (Harry *et al.*, 1998; Viviani *et al.*, 2000). Indeed, the activation of astrocytes and microglia that follows exposure to TMT-Cl both *in vivo* and *in vitro* has been associated with the upregulation of cytokines, including TNF-α (Viviani *et al.*, 2001). Viviani *et al.*, (1998a), found both primary rat cerebral astrocytes and microglia to release TNF-α in approximately equal quantities upon exposure to 1 μM TMT-Cl for 24-hours. Additionally, TNF-α mRNA has been found to be induced within hours after TMT-Cl administration (Maier *et al.*, 1995). TNF-α is a diffusible cytokine demonstrated to affect a wide range of biological activities in many cell types, including mediating the inflammatory response, immune function and triggering apoptosis in certain cells (Hu, 2003). TNF-α has been reported to have neurotoxic potential, with the apoptotic signal being triggered by binding of TNF-α to the TNF-α receptor and initiating caspase activation (Maier *et al.*, 1995; Eskes *et al.*, 2003).

As mentioned, in the current study, the increase in caspase-3 activation was largest in the NT2.N/A co-culture, whilst no caspase-3 increase was measurable in the NT2.N mono-culture. It is possible that this pattern of caspase-3 activation is related to astrocytic TNF-α release and indeed this observation is in agreement with a number of previous studies. For example, Viviani *et al.*, (1998a) used pure or sandwich co-cultures of primary rat hippocampal neurons and cerebral glia (97 % astrocytes and 3 % microglia) to characterise the role of glial cells in TMT-Cl induced neurodegeneration.

Exposure to 0.1-1 μM TMT-Cl for 24-hours caused primarily necrotic cell death in pure neuronal cultures, with no release of TNF-α. Glial cell viability in pure cultures was not affected at these concentrations but these cells did release significant amounts of TNF-α. However, neuronal apoptosis and glial TNF-α release were vastly increased when the two cell types were exposed together, suggesting a synergistic response. Treatment of the co-culture with TNF-α antibody prevented neuronal apoptosis and TNF-α administration induced neuronal apoptosis, suggesting glial cells are able to modulate the mode of TMT-Cl induced neuronal death via TNF-α production.

Thus the present chapter, along with previous findings, suggests that the presence of both astrocytes and neurons is required for TNF-α release and subsequent initiation of the apoptotic cascade, with the mode of cell death switching to necrosis in the absence of astrocytic cells. However, the 4-hour exposure timepoint utilised in this chapter may be of too short a duration for astrocytic TNF-α release to induce measurable biochemical effects at the protein level. It must be considered that a number of other factors may ultimately be involved in the mode of cell death observed. Nevertheless, that an increase in caspase-3 activation was only measurable in the presence of astrocytes highlights their importance regarding the accurate screening of compounds for potential neurotoxicity.

Regarding TMT-Cl effects on glutathione levels, both the CCF-STTG1 and NT2.N/A cultures showed evidence of astrocytic activation, with a maximum GSH increase above the untreated control of ~24 % (50 μM) and ~43 % (200 μM), respectively. Following this, the NT2.N/A culture maintained its GSH content at control levels and the CCF-STTG1 cell line sustained a progressive moderate decrease to ~54 % of the control value. With increasing concentration, TMT-C1 depleted GSH levels immediately in the NT2.D1 cell line to ~16 % and more progressively in the NT2.N cells to ~55 % of the control value.

The capacity of cells to maintain or even increase glutathione levels during a xenobiotic or oxidative challenge is important in the prevention of cell dysfunction and death (Dringen *et al.*, 2000). As such, cultured neurons have been reported to be more vulnerable than cultured astrocytes to apoptotic or necrotic cell death caused by

oxidative stress. This may be due to the lower concentrations of GSH found in neurons compared with astrocytic cells (Wullner *et al.*, 1999). Indeed, the cell viability IC_{50} values generated by the MTT assay demonstrated that at both time points the NT2.N mono-culture was more vulnerable towards TMT-Cl induced cell death than the NT2.N/A co-culture. No such pattern was observed for the CCF-STTG1 and NT2.D1 cell lines. However, the rapid decline in GSH may have contributed to the sensitivity of the non-neuronal NT2.D1 cell line towards TMT-Cl induced cytotoxicity.

As discussed, it has been suggested that TMT-Cl has direct effects on astrocytes which are important for mediating toxicity in neurons through the release of TNF-α (Maier *et al.*, 1995). There is evidence that astrocytes also protect neurons upon exposure to TMT-Cl. The sensitivity of primary rat cerebellar neurons to 10 μM TMT-Cl following 24-hours exposure was attenuated during co-culture with astrocytes. This was thought to be due to increased antioxidant protection (Gunasekar *et al.*, 2001b) and indeed these authors found that the quantity of ROS produced after TMT-Cl exposure was reflected by a greater GSH depletion in neuronal cells than in astrocytes or mixed cultures. In the present study, the observed GSH levels also correlate somewhat with the H_2O_2 levels measured in the medium of all four cell cultures. The final levels of H_2O_2 attained were similar in the NT2.D1, CCF-STTG1 and NT2.N cultures (~ 270-290 %). These cultures also experienced GSH depletion to varying degrees. At 500 μM TMT-Cl, the NT2.N/A co-culture sustained lower increases in release of H_2O_2 (139 % above control values), which rose to 240 % when exposed to the higher concentration of 1 mM TMT-Cl. However, the co-culture maintained its cellular GSH at control levels or higher over this TMT-Cl concentration range. Pre-treatment with glutathione, superoxide dismutase or catalase has been shown to protect cells from TMT-Cl induced cell death (Gunasekar *et al.*, 2001a; Gunasekar *et al.*, 2001b). This suggests mechanisms involving oxidative stress are a factor in TMT-Cl induced cell destruction and that a variety of oxidative species may be responsible. It has been postulated that catalase plays a predominant protecting role against H_2O_2 within astrocytes (Desagher *et al.*, 1996). It is possible therefore; that the increase in H_2O_2 observed in the NT2.N/A culture was as a result of catalase depletion rather than reduction of intracellular GSH.

In summary, TMT-Cl was capable of inducing effects on ATP, GSH, capase-3 and

H_2O_2 in all of the cell systems at micromolar, non-cytotoxic concentrations, with the exception of the maintenance of ATP and caspase-3 at control levels by the NT2.D1 and NT2.N cell lines, respectively. The metabolic endpoints examined were generally able to differentiate between the cell system responses but it is not clear if the cell systems responses were consistent with specific neurotoxicity. Whilst the NT2.N/A co-culture did demonstrate the characteristic astrogliotic response to TMT-Cl, this culture was generally the least sensitive to sub-cytotoxic perturbations, with the exception of the observed caspase-3 activation. Additionally, the NT2.N mono-culture was not consistently observed to be the most vulnerable cell-type. However, whilst TMT-Cl was shown to affect the biochemical endpoints in all the cell systems at micromolar concentrations, it may be considered that due to their irreplaceable nature, neurons would prevail as the most vulnerable cell-type. Also, additional factors regarding the uniqueness of neuronal cells may render them more susceptible to TMT-Cl induced toxicity and this is considered further below.

The NT2.N/A co-culture demonstrated evidence of astrocytic activation with a > 40 % initial increase in GSH and ATP above control levels and overall maintained significantly superior levels of ATP and GSH and lower levels of H_2O_2 compared with the NT2.N mono-culture. This may be indicative of astrocytic protective capabilities, for example, through the provision of glutathione. Indeed, neurons are regarded as being more sensitive than are glial cells towards TMT-Cl and as mentioned previously, the cell viability IC_{50} values generated by the MTT assay demonstrated that TMT-Cl decreased cell viability more in the NT2.N than the NT2.N/A cultures after 4- and 24-hours exposure. However, it appeared that the presence of NT2 astrocytes was required to induce an increase in caspase-3 activity. This importance of astrocytes in modulating the response of neurons via TNF-α release following TMT-Cl exposure has been reported by several other groups. It could be speculated that the quantity of cells undergoing death by necrosis in this chapter may be greater in the NT2.N mono-culture than in the co-culture and in the co-culture it is possible that it is the neurons rather than the astrocytes which demonstrate an increase in caspase-3 activity. For comparison purposes, the examination of the ability of TMT-Cl to induce caspase-3 activation in future NT2 astrocytic mono-culture studies would be instructive.

As previously discussed, sensitivity to TMT-Cl has been seen to vary in between species and cell type. Generally, rodent derived cells such as rat primary hippocampal neurons and the PC12 cell line demonstrate up to a 1000-fold greater vulnerability towards TMT-Cl than do human based systems, including human foetal cerebral neurons, the SH-SY5Y neuroblastoma cell line and the cell systems employed in the current study. However, the pattern of neurotoxic effects observed seems to be conserved between species and in all species TMT-Cl is considered to demonstrate a regional specific neurotoxicity towards the hippocampus. It has been postulated that factors including intracellular calcium buffering may account for such differences in species sensitivity, with the capacity of human foetal neurons and NT2.N cells being larger than that of cortical rat neurons (Almaas *et al.*, 2002). Thus, in such cases the use of relevant human cell lines may facilitate the accuracy of human risk assessment. It is unknown whether NT2 neurons reflect the hippocampal, cerebral and cerebellar sensitivity to TMT-Cl observed *in vivo*. Interestingly, NT2-neuronal sensitivity to TMT-Cl in this chapter was found to occur at similar concentrations as human foetal, cerebral cortical neuronal cultures and astrocytes (~ 500 μM) (Cristofol *et al.*, 2004).

5.4.4 Tributyltin chloride

Historically, the most important property of TBT-Cl in mammals was considered to be its immunotoxic potential via spleen and thymus atrophy (Lavastre and Girard, 2002; Jenkins *et al.*, 2004). However, TBT-Cl has also previously been demonstrated to cross the blood brain barrier (BBB), have neurotoxic effects *in vivo* and is expected to accumulate in lipid rich organs such as the brain at levels ≥ 90 nM (Mizuhashi *et al.*, 2000b; Nakatsu *et al.*, 2006a). Accordingly, TBT-Cl has also been shown to cause acute neurotoxicity *in vitro*, with neurons demonstrating greater vulnerability than astrocytes. Thus, it may be expected the order of decreasing sensitivity of the cultures towards the organotin would be NT2.N > NT2.N/A > CCF-STTG1 > NT2.D1 cells. Indeed the cell viability IC_{50} values generated by the MTT assay demonstrated that TBT-Cl decreased cell viability at micromolar amounts, with the NT2.N followed by the NT2.N/A cultures showing the most sensitivity following 4- and 24-hours exposure. This may demonstrate a neurotoxic specificity of TBT-Cl rather than general cytotoxicity and may be suggestive of an astrocytic protective effect. The NT2.D1 cell

line was more sensitive than the CCF-STTG1 cell line towards the tin compound. TBT-Cl has been shown to generate apoptosis in a wide variety of cells in culture, including those derived from the immune, hepatic and nervous systems, which may account for the vulnerability of the non-neuronal NT2.D1 cell line. The precise apoptotic mechanism has not been fully established but is speculated to involve intracellular Ca^{2+} elevation, ROS release (Appel, 2004) and caspase-3 activation (Gennari *et al.*, 2000; Jurkiewicz *et al.*, 2004), with the additional involvement of ATP depletion (Stridh *et al.*, 1999a) and glutamate excitotoxicity (Nakatsu *et al.*, 2006a) being postulated. Thus, neurospecific toxicity may be more evident from examination of some of these biochemical endpoints following exposure of the cell systems to non-cytotoxic concentrations of TBT-Cl (0-4 μM).

Following exposure to non-cytotoxic concentrations of TBT-Cl for 4-hours, the NT2.D1 and NT2.N cultures demonstrated a steep decrease in ATP levels. The CCF-STTG1 cells showed a moderate ATP decline with the NT2.N/A co-culture appearing to be the least vulnerable regarding this metabolic endpoint. The high metabolic rate of neurons is known to render them particularly sensitive to changes to the energy status of the cell and indeed the NT2 neurons were one of the most sensitive cultures. That the NT2.N/A co-culture maintained significantly superior levels of ATP than did the NT2.N mono-culture, may be evidence of an astrocytic protective effect and a reflection of previous observations that neurons are more vulnerable than astrocytes towards the tin compound. The CCF-STTG1 cell line was more vulnerable than the NT2.N/A culture but as previously mentioned, this cell line was found to be one of the most sensitive to chemical induced ATP effects.

Mitochondrial oxidative metabolism is the preferred method of pyruvate breakdown from glycolysis. However, if there is drop in cellular ATP due to the inhibition of oxidative metabolism by mitochondrial toxins, it is postulated that some cells can respond with an increase in glucose consumption and glycolytic activity to supplement ATP levels. As such, in response to mitochondrial toxins, primary rat cortical astrocytes but not neurons were found to prevent ATP depletion via stimulation of the glycolytic pathway (Almeida *et al.*, 2001). Thus, it is considered that generally astrocytes will demonstrate less vulnerability towards mitochondrial toxins than will

neurons (Almeida *et al.*, 2001; Pellerin and Magistretti, 2003).

Triorganotins, including TBT-Cl, have been observed to disturb mitochondrial activity, binding to a component of the ATP synthase complex and inhibiting mitochondrial ATP synthesis (Corsini *et al.*, 1998; von Ballmoos *et al.*, 2004). Stridh *et al.*, (1999a) found that TBT-Cl induced ATP depletion in Jurkat T-lymohocytes but that glycolytic ATP production could be maintained by the addition of glucose to the medium. The group also postulated that TBT-Cl would be an efficient ATP-depleting agent in cells of low glycolytic capacity, such as neurons. A possible explanation of the order of the sensitivity of the cell systems regarding ATP depletion therefore, is that the NT2.N/A co-culture was able to invoke glycolysis as a way of maintaining superior ATP levels, in comparison with the NT2.N mono-culture.

Exposure of the cell systems to non-cytotoxic concentrations of TBT-Cl for 4-hours caused an initial progressive increase in caspase-3 activity, which peaked and then declined to control levels, in all four cell cultures. The order of decreasing sensitivity of the cell cultures regarding the maximum significant increase above the untreated control was CCF-STTG1 > NT2.N/A > NT2.N > NT2.D1.

TBT-Cl at concentrations around 1 μM has previously been shown to acutely increase the activity of caspase-3 in a variety of cultures, with numerous cell types also showing characteristic signs of an apoptotic mode of cell death following 2-36 hours exposure. These include primary rat thymocytes (Gennari *et al.*, 2000; Okada *et al.*, 2000) and hepatocytes (Jurkiewicz *et al.*, 2004), human peripheral blood lymphocytes (Stridh *et al.*, 2001), the human Hut-78 and Jurkat T-lymohocyte cell lines (Stridh *et al.*, 1999b; Stridh *et al.*, 1999c) and in hippocampal neurons of organotypic slice cultures from immature rats (Mizuhashi *et al.*, 2000a). The TBT-Cl concentration required to induce apoptosis in these cells is in good agreement with the concentrations of TBT-Cl required to activate caspase-3 in the cell systems in the present study (0.3 – 2 μM). For example, upon exposure of rat hepatocytes to 2.5 μM TBT-Cl, release of the pro-apoptotic factor cytochrome c (cyt-c) from mitochondria into the cytosol was apparent after 15 minutes of exposure. The activity of initiator caspase-9 was observed to increase after 30 minutes, followed by caspase-3 activation and initiation of

dismantlement of the cell (Jurkiewicz *et al.*, 2004). Exposure of rat thymocytes to TBT-Cl (3 μM) also led to the release of cyt-c from the mitochondrial membrane into the cytosol, followed by caspase-3 activation (Gennari *et al.*, 2000). Taken together these data suggest that a range of cell-types are susceptible to acute TBT-Cl induced caspase-3 activation and may explain why all the cell systems in the current study demonstrated increased caspase-3 activation to various extents following 4-hours exposure to the tin compound.

When the Hut-78 cell line was exposed to increasing concentrations of TBT-Cl for 3-hours, the number of apoptotic cells peaked at 2 μM, with necrosis being the primary mode of cell death at higher concentrations (Stridh *et al.*, 1999c). Necrosis was also found to be the mode of cell death at lower concentrations of TBT-Cl (0.5 μM) in primary rat cortical neurons (Nakatsu *et al.*, 2006b). These data correlate with the present observations in that in all cell systems, the level of TBT-Cl induced capase-3 activation reached a maximum and the then declined with increasing toxin concentration.

Gennari *et al.*, (2000) found that TBT-Cl induced ROS production and the release of cyt-c were reduced by BAPTA, an intracellular Ca^{2+} chelator, indicating the important role of Ca^{2+} during these early intracellular events. Furthermore, they demonstrated that Z-DEVD FMK (a mainly caspase-3 inhibitor) decreased apoptotic cell death, confirming the role of capase-3 in activation of TBT-Cl induced apoptosis. Therefore, the increase in capase-3 activity observed in all the cell systems following exposure to non-cytotoxic levels of TBT-Cl for 4-hours, suggests that a decrease in cell viability due to apoptosis will result at a later time point. Another consideration is that whilst TBT-Cl has been shown to induce caspase-3 activation and apoptosis in numerous cell-types, the consequences may be greater in the nervous system owing to the irreplaceable nature of neurons.

It is considered that prevention of a default apoptotic programme by oxidative stress, or metabolic situations precluding caspase activation, may result in necrosis (Stridh *et al.*, 1999a). As mentioned, one metabolic parameter that has been shown to determine the mode of death is the intracellular ATP concentration and is considered that a severe

depletion would be sufficient to block apoptosis and switch the mode of cell death to necrosis (Leist *et al.*, 1997). Stridh *et al.*, (1999a) found that 10 μM TBT-Cl caused disturbance of mitochondrial energy metabolism and inhibition of mitochondrial glycolytic ATP synthesis, leading to a necrotic mode of cell death in the Jurkat T-lymohocyte cell line. However, when glycolytic ATP production was maintained by addition of glucose to the medium, TBT-Cl caused cyt-c release into the cytoplasm and caspase-3 activation, followed by a decrease in cell viability owing to apoptosis. Indeed, regarding the NT2.N/A, NT2.N and NT2.D1 cultures, a higher maximum level of caspase-3 activation was mirrored by maintenance of higher ATP levels upon TBT-Cl exposure. Conversely, the high level of caspase-3 activation in the CCF-STTG1 cell line was not reflected by the decline in ATP levels to ~ 37 % observed. The CCF-STGG1 cell line also demonstrated the highest increase in hydrogen peroxide (discussed below). It has been reported that H_2O_2 can induce the release of cyt-c into the cytosol, followed by caspase-9 and -3 activation leading to apoptosis (Saito *et al.*, 2006).

Glutathione has an important role in protecting cells against oxidative stress. TBT-Cl at 0.3 μM was found to lead to almost total depletion of GSH in rat thymocytes (Okada *et al.*, 2000). It may be suggested that if a similar depletion occurs in neuronal cells, that this would greatly increase the vulnerability of the nervous system to subsequent oxidative insult.

Cultured neurons have been reported to be more vulnerable than cultured astrocytes to apoptotic cell death or necrosis caused by oxidative stress. This may be due to the lower concentrations of GSH found in neurons, compared with astrocytic cells (Wullner *et al.*, 1999). Indeed in co-culture, astrocytes have been demonstrated to protect neuronal cells against ROS induced toxicity by maintaining neuronal GSH levels (Iwata-Ichikawa *et al.*, 1999). This is in agreement with the observation that the NT2.N/A co-culture was able to maintain its GSH levels at control values, whereas the NT2.N mono-culture experienced a ~ 40 % depletion. TBT-C1 completely depleted GSH levels in the NT2.D1 and CCF-STTG1 cells with increasing concentration.

Antioxidants such as GSH are consumed against increased oxidants and their

concentration decreases, with subsequent oxidative stress. This is in agreement with the observations of the present study. H_2O_2 levels in the CCF-STTG1 initially remained low but at concentrations above 0.5 μM, levels climbed sharply. This observation correlated well with the GSH data, in that GSH levels were not observed to fall in the CCF-STTG1 until concentrations above 0.5 μM TBT-Cl were employed and then declined sharply. This may suggest that GSH was consumed as a result of increasing hydrogen peroxide formation due to TBT-Cl exposure.

The extent of GSH depletion and increase in H_2O_2 in the remaining cultures correlated less well. For example, the NT2.N/A culture maintained GSH levels at control values, yet an increase in H_2O_2 levels comparable with the GSH depleted NT2.D1 cell line, was also observed. Some groups consider the ability of astroglial cells to protect neurons against H_2O_2 to be related predominantly to the capacity of these cells to remove the peroxide using GSH as a substrate of glutathione peroxidase (Drukarch *et al.*, 1997; Dringen *et al.*, 1999a). It has also been postulated that catalase plays a predominant protecting role within astrocytes, via H_2O_2 decomposition (Desagher *et al.*, 1996). It is possible therefore that the increase in H_2O_2 observed in the NT2.N/A culture was as a result of catalase depletion rather than reduction of GSH. Mizuhashi *et al.*, (2000a) found that addition of catalase virtually abolished the cytotoxicity caused by exposure of cultures of rat hippocampal neurons to 5 μM TBT-Cl. Superoxide dismutase had little effect, suggesting the ROS generated following exposure to TBT-Cl, may be composed more of H_2O_2, than superoxide ($O_2^{-\bullet}$) .

Many chemical and physical treatments capable of inducing apoptosis are also associated with oxidative stress and it is considered that TBT-Cl induced toxicity may be mediated in part by ROS generation (Gennari *et al.*, 2000). Indeed, hydrogen peroxide levels generated as a result of TBT-Cl exposure correlated more closely with caspase-3 activation than with GSH depletion.

In summary, the biochemical endpoints were intended to establish the ability of the cell systems to predict the intrinsic neurotoxic potential of TBT-Cl. However, the compound is able to cross the BBB and has the potential to accumulate in lipid rich organs such as the brain as a result of its bioavailability from consumption of

contaminated fish in some areas. It may therefore be considered that the low micromolar concentrations of TBT-Cl that were capable of inducing metabolic perturbations in this study are physiologically relevant. As such, TBT-Cl was generally capable of inducing effects on ATP, GSH, capase-3 and H_2O_2 in all of the cell systems at low micromolar, non-cytotoxic concentrations.

The NT2.N/A co-culture maintained overall superior ATP and GSH levels in comparison with the NT2.N mono-culture, in response to TBT-Cl, which may be indicative of astrocytic protective capabilities. However, levels of caspase-3 activation and H_2O_2 generation were similar in the mono and co-cultures, which may indicate that the number of cells with the potential to undergo cell-death by apoptosis at a later time-point as a result of metabolic perturbations may be similar.

With the exception of hydrogen peroxide levels, the metabolic endpoints examined were generally able to differentiate between the cell system responses but not in a manner consistent with specific neurotoxicity. However, whilst TBT-Cl has been shown to cause apoptosis and a decrease in cell viability in numerous cell-types, as previously discussed, due to their irreplaceable nature neurons may prevail as the most vulnerable cell-type. Also, additional factors regarding the uniqueness of neuronal cells may render them more susceptible to toxicity induced by TBT-Cl and other compounds. For example, whilst ATP is present in all metabolically active cells, the CNS has particularly high metabolic demands for numerous processes, including excitatory signalling, axonal transport, maintenance of the cytoskeleton and driving essential ion transporters such as the Na^+,K^+-ATPase and Ca^{2+}-ATPase (Gregus and Klaassen, 2001). Alterations in mitochondrial integrity and ATP depletion in neuronal cultures following exposure to neurotoxic compounds, frequently occur earlier than effects on membrane permeability (Massicotte *et al.*, 2005). It is considered that generally astrocytes will demonstrate less vulnerability to mitochondrial toxins than will neurons (Almeida *et al.*, 2001; Pellerin and Magistretti, 2003) and that if energy levels of astrocytes can be preserved, for example through glycolysis, then cellular defence mechanisms may reverse or impede injury to brain cells caused by ROS release from ATP depleted cells (Sharma *et al.*, 2003).

Alterations in Ca^{2+} homeostasis resulting from exposure of the cell systems to TBT-Cl were not examined. However, high intracellular Ca^{2+} levels may lead to cell death via over-activation of destructive Ca^{2+}-dependent enzymes (Sun *et al.*, 2005) and it has been suggested that the earliest event triggered by TBT-Cl treatment is an increase in Ca^{2+} (Corsini *et al.*, 1998). TBT-Cl at concentrations comparable with those used in this study induced Ca^{2+} overload in various cell types, including cortical neurons, hippocampal slices and PC12 cells (Mizuhashi *et al.*, 2000a; Nakatsu *et al.*, 2006b). Additionally, exposure of the rodent keratinocyte cell line HEL30 to 5 μM TBT-Cl, caused a ten-fold increase in intracellular Ca^{2+} after 4 min, with ROS generation after 15 min. Prevention of Ca^{2+} increase using calcium channel blockers prevented ROS production and cell death, suggesting that alterations in Ca^{2+} homeostasis may initiate TBT-Cl induced oxidative stress (Corsini *et al.*, 1998). Similarly, TBT-Cl (2 μM) was found to cause a rapid Ca^{2+} increase in PC12 neuronal cells, followed by death of 90 % of cells after 6 hours. The use of a Ca^{2+} chelator decreased the level of cell death, suggesting Ca^{2+} may contribute to TBT-Cl induced cytotoxicity (Nakatsu *et al.*, 2006b). Therefore, in order to further compare the response of the cell systems towards TBT-Cl, a measure of Ca^{2+} perturbation could be considered a relevant addition to the endpoint battery.

Similar concentrations of TBT-Cl to those used in the present study have also been implicated in excitotoxicity. In addition to its necessary transmission functions, glutamate acts as a potent neurotoxin when present at high concentrations at glutamatergic synapses (Ye and Sontheimer, 1999; Sandhu *et al.*, 2003), with over stimulation of glutamate receptors inducing excitotoxic neuronal death (Had-Aissouni *et al.*, 2002). Nakatsu *et al.*, (2006a) studied the involvement of glutamate in TBT-Cl induced neurotoxicity in rat cortical neuronal cultures. Exposure of the cells to the IC_{50} concentration of TBT-Cl (0.5 μM) for 30 min resulted in an increased concentration of extracellular glutamate and prior incubation of cells with a glutamate receptor antagonist (MK801) alleviated cell death at 24-hours to only 13%. Astrocytic processes closely encapsulate synapses and normally efficiently maintain extracellular glutamate concentrations at low micromolar levels (Ye *et al.*, 1999; Daniels and Brown, 2001). As mentioned the cell viability IC_{50} values demonstrated that TBT-Cl decreased cell viability more in the NT2.N than the NT2.N/A cultures after 4- and 24-hours exposure.

It may be hypothesised that glutamate clearance by NT2 astrocytic cells may have contributed to the improvement in cell survival observed in comparison with the neuronal mono-culture. Further investigation would be required to establish this.

5.4.5 Summary

To summarise overall, a greater variation in cell system responses was more apparent when cell viability was not compromised. For example, the IC_{50} values obtained for the reportedly non-toxic 2,3- and 3,4-HD, were generally identical for the different cell systems. However, both the α-hexanediones were capable of inducing effects on ATP, GSH and capase-3 which differentiated between the cell system responses but not in a manner consistent with neurotoxicity. The known chronic neurotoxicant 2,5-HD was also capable of inducing acute effects on the biochemical endpoints. It was not consistently more toxic to the differentiated neuronal cell systems in comparison with the continuous cell lines but did induce caspase-3 activation specifically in the NT2.N/A co-culture.

Following exposure to micromolar concentrations of the known acute neurotoxicant TMT-Cl, the NT2.N mono-culture was consistently one of the most vulnerable cell systems. The NT2.N/A co-culture was the least sensitive cell system and it appeared that the presence of NT2 astrocytes was important in modulating the response of the NT2 neurons to TMT-Cl. The known acute neurotoxicant and immunosuppressant TBT-Cl was also generally capable of inducing biochemical effects in all of the cell systems at very low micromolar, non-cytotoxic concentrations. However, in both cases, it was not clear whether the cell system responses were consistent with specific acute neurotoxicity.

Chapter 6 – Conclusions and future experimental approaches

Many thousands of new chemicals enter commerce each year, which require hazard assessment and may prove highly toxic to the nervous system (Atterwill *et al.*, 1994; Coecke *et al.*, 2006). Additionally, the recent update of the EC chemical testing policy will necessitate the evaluation of the neurotoxic potential of over 30,000 'existing' substances via establishment of the REACH (Registration, Evaluation and Authorisation of Chemicals) system. The use of *in vitro* cell culture data may greatly accelerate the neurotoxic hazard identification process in an ethical and economic manner to meet the increasing demands of the pharmaceutical industry and the REACH strategy. However, up to now, no *in vitro* methods for evaluating the human neurotoxic potential of a chemical have been validated and those proposed are mainly animal derived systems (Coecke *et al.*, 2006).

No single *in vitro* system is able to model complexity of the *in vivo* nervous system and as such a tiered *in vitro* neurotoxicity test strategy has been proposed (Atterwill *et al.*, 1994; Coecke *et al.*, 2006). Such a stepwise approach progresses from a first-tier preliminary screening battery aimed at the rapid differentiation of neurotoxicants from cytotoxicants and rank chemicals for cytotoxic potency, to more defined neurospecific mechanistic questions relating to the *in vivo* situation (Veronesi, 1992). At the current stage, this approach is not intended to replace existing *in vivo* testing, rather to provide a quick and relatively inexpensive system for assessing the basic neurotoxic potential of many chemicals (Coecke *et al.*, 2006).

A first-tier screening battery for differentiating cytotoxicants from neurotoxicants should consist of an appropriate collection of cell systems and general biochemical and specific endpoints, with appraisal using a variety of test chemicals. Regarding the identification of potential human neurotoxins, the most relevant cell system for inclusion in a screening battery would be human-derived to facilitate extrapolation from *in vitro* to *in vivo* and ideally reflect both the important *in vivo* neuronal-astrocytic relationship and the terminally differentiated neuronal state.

Hence, the aim of the research presented here was the preliminary development of such

a human cell line based, post-mitotic, neuronal-astrocytic cell system (NT2.N/A), suitable for inclusion in a test battery for the first-tier, rapid preliminary screening of new and existing compounds for acute neurotoxic potential. The suitability of the NT2.N/A co-culture cell system to predict correctly acute neurotoxicity was appraised in comparison with a number of other human cell lines (NT2.N mono-, CCF-STTG1 astrocytoma and NT2.D1 neuronal precursor cultures), using a measure of basal cytotoxicity and a number of biochemical rather than neurospecific endpoints.

An initial objective of the study was to produce cultures of terminally differentiated NT2.N and NT2.N/A cells in a timely and convenient format for the high throughput screening of potential neurotoxins. In this respect, the novel use of CellBIND 6-well plates in place of the traditional pdl/lam coated plastic, allowed the production of sufficient numbers of cells for toxicity studies and conferred numerous advantages regarding cost, throughput, ease of use and preservation of cellular interactions.

NT2.N mono-cultures were successfully produced that demonstrated the morphological characteristics and marker expression expected of post-mitotic CNS neurons. *In vivo*, astrocytes outnumber neurons by at least 10:1 but have been shown to provide a protective function over neurons at a ratio of 1:4, *in vitro* (Gegg et al., 2003). In the present study, NT2.N/A cultures were produced with a characteristic pattern of neuronal and astrocytic marker expression and a ratio of 2:1 astrocytes:neurons. This ratio demonstrated evidence of an astrocytic protective effect when examining cell system responses using both cytotoxic and non-cytotoxic endpoints. Both the mono- and co-culture neuronal-based systems appeared to be terminally differentiated. It was thus considered that the novel use of NT2.N and NT2.A cells in a system for the identification of potential neurotoxins would be particularly relevant to the human situation as *in vivo* most neurons are post-mitotic and usually cannot be replaced by the proliferation of surviving cells if lost to toxic damage.

It was important to incorporate a measure of basal cytotoxicity into the stepwise assessment of the test chemicals for neurotoxic potential. As such, it was found using the MTT assay to determine acute basal cytotoxic potential (IC_{50} concentration at 4- and 24-hours), that the different cell systems could rank the chemicals according to

potency. Much lower micromolar concentrations of the acute neurotoxins TMT-Cl and TBT-Cl were required to induce cell-death in comparison with the millimolar concentrations of the chronic neurotoxin 2,5- and the low-level toxins 2,3- and 3,4-HD. Significant differences between cell system responses could not consistently be attributed to the presence or absence of neuronal features. However, the basal cytotoxicity data did provide some preliminary evidence of the value of astrocytes in cytotoxicity assays, with the NT2.N/A co-culture frequently demonstrating reduced vulnerability in comparison with the NT2.N mono-culture. It was considered that a greater variation in cell system responses, for example, due to inclusion of more than one cellular-target, may be more apparent at non-cytotoxic levels rather than overt toxicity measured for IC_{50} values.

The mechanisms underlying the neurotoxic effect of a compound are often a result of a subtle disruption to basic biochemical processes. In order to meet the high throughput needs of the REACH strategy, an objective of the study was to develop sensitive protocols for the rapid and accurate collection of several biochemical endpoints, including the measurement of ATP, hydrogen peroxide, glutathione and additionally caspase-3 levels. With the exception of the interference experienced regarding the α-hexanediones and the Amplex red assay, this objective was achieved.

The biochemical endpoints selected have limited ability to detect neural-specific effects. However, the nervous system is particularly susceptible to toxicants that disrupt energy metabolism and redox status. Thus, it was hypothesised that a clear and greater sensitivity to non-cytotoxic concentrations of known acute neurotoxins in the neuronal-like cell systems, would indicate the presence of a potentially neurospecific toxic mechanism. Additionally, it was considered that diminished vulnerability of the NT2.N/A co-culture compared with the NT2.N mono-culture may be evidence of an astrocytic protective effect relevant to the *in vivo* situation and demonstrate the suitability of inclusion of both neuronal and astrocytic cell-types in a cell system for differentiating cytotoxicity from neurotoxicity.

A greater variation in cell system responses was indeed more apparent at lower levels of toxicity. For example, the IC_{50} values obtained for the non-toxic 2,3- and 3,4-HD,

demonstrated the chemicals to be only weakly cytotoxic and the cell systems demonstrated identical responses. However, both the α-hexanediones were capable of inducing effects on ATP, GSH and caspase-3, which discriminated between the cell systems, though not in a manner consistent with neurotoxicity. The remaining chemicals were also capable of inducing effects on the biochemical endpoints at non-cytotoxic concentrations and discriminated between the cell system responses to varying degrees. When the different cultures were exposed acutely to 2,5-HD, the known chronic neurotoxicant was capable of inducing acute effects on biochemical endpoints but was no more toxic to the differentiated neuronal cell systems than the continuous CCF-STTG1 and NT2.D1 cell lines. Thus, it may be concluded that using this test strategy, 2,5-HD - whilst cytotoxic at high concentrations - did not demonstrate specific acute neurotoxic potential.

The NT2.N mono-culture was consistently one of the most vulnerable cell systems following exposure to non-cytotoxic micromolar concentrations of the known acute neurotoxicant TMT-Cl. The NT2.N/A co-culture was the least sensitive and it appeared that the presence of NT2 astrocytes was important in modulating the response of the NT2 neurons to TMT-Cl. However, it was not clear whether the cell-system responses specifically indicated neurotoxicity. The known acute neurotoxicant and immunosuppressant TBT-Cl was generally capable of inducing effects on ATP, GSH, capase-3 and H_2O_2 in all of the cultures at very low micromolar, non-cytotoxic concentrations. However, the order of sensitivity of the cell systems was not consistent with specific neurotoxicity.

It is well established that the metabolic and protective support offered by astrocytes to neurons may provide increased tolerance of neurons to some toxic insults. Indeed, the NT2 astrocytes appeared to contribute to NT2 neuronal well being following exposure to all the test chemicals. For example, the differentiated NT2.N/A co-culture model was capable of maintaining superior ATP and GSH levels and reduced H_2O_2 levels in comparison with the NT2.N mono-culture. This could be indicative of augmented astrocytic defence mechanisms that may aid neuronal recovery and survival. However, generally, the extent of caspase-3 activation was actually greater in the NT2.N/A co-culture. *In vivo* this may be an advantageous response, as an apoptotic mode of cell-

death would prevent an inflammatory necrotic outcome which is damaging to neighbouring cells and suggests astrocytes may be necessary for the expression of certain toxic effects.

Conversely, in response to the test chemicals, the CCF-STTG1 cell line did not consistently demonstrate the vulnerability expected of astrocytes as judged from the 2,5-HD, TMT-Cl and TBT-Cl compound literature. It is possible that this non-differentiated astrocytic model may not phenotypically reflect *in vivo* astrocytic behaviour closely enough to be a suitable cell system for the screening of chemicals for neurotoxic potential.

Astrocytes are less susceptible to damage than neurons but may become activated in response to toxic insult *in vivo*, a reaction (astrogliosis) that may be associated with enhanced metabolic status (Pekny and Nilsson, 2005). Accordingly, the NT2.N/A co-culture demonstrated an increase in GSH and ATP above control levels upon exposure to TMT-Cl, a known inducer of astrogliosis. This suggests the NT2 astrocytes became activated in response to TMT-Cl, which is relevant to the *in vivo* situation and supports their inclusion in the test system. However, that the NT2 astrocytes demonstrated an astrogliotic response to TMT-Cl was not confirmed by increased positive staining for GFAP, a specific marker of astrocytic reactive response to nervous system injury or toxic insult (Tilson, 2000). Thus, chemical-induced increases in GFAP as a biomarker of neurotoxic effect may be a desirable addition to the endpoint battery.

Drugs and neurotoxins may act directly on neural tissues. However, often they require some form of bioactivation, which is usually hepatic but may occur within the neuron itself and thus modulate some CNS drug responses (Ravindranath *et al.*, 1995; Ravindranath, 1998). Additionally, due to the low rate of metabolism and elimination found in the nervous system, many lipid soluble toxins that cross the BBB have the potential to accumulate due to the high lipid content of the brain (Anthony *et al.*, 2001). In the present study, due to the low metabolic capability of cell cultures, where possible the ultimate toxic metabolites of the test chemicals were employed, such as 2,5-hexanedione in the case of n-hexane. Relating the effects detected at the compound concentration applied to the cell systems, to the effects that would be caused by the

compound concentration that actually reaches the target cells *in vivo*, was beyond the scope of this study.

It is widely considered that when initially screening a compound, it is actually advantageous to examine the intrinsic toxicity of the chemical in a controlled defined system, without the associated *in vivo* complicating factors. Although the *in vivo* blood levels and kinetics of the test chemicals would eventually require consideration, intrinsic neurotoxic hazard identification may be addressed using a first-tier preliminary screening battery, with incorporation of compound kinetic data being more critical when results from neurospecific endpoints are evaluated at a later testing stage. However, human and animal neural tissues may differ greatly in their susceptibility to neurotoxins and in the present study, it was necessary to consider species differences when examining the response of the cell-systems to TMT-Cl. As discussed, sensitivity to TMT-Cl has been seen to vary in between species and cell type, with rodent derived neurons demonstrating up to a 1000-fold greater vulnerability than do human based systems, including human foetal cerebral neurons and the neuronal based cell systems employed in the current study. One of the factors postulated is the higher capability of human foetal and NT2 neurons to buffer calcium (Almaas *et al.*, 2002). In the present study, toxin effects on cellular Ca^{2+} levels were not determined but overall the TMT-Cl data obtained supports the view that the use of human cells would reduce the need for such species extrapolation when assessing human neurotoxic hazard.

To summarise, although simple non-specific biochemical assays are required to distinguish basal cytotoxicity from specific neurotoxicity, neurotoxicants were not generally distinguishable from cytotoxicants in the current study; casting some doubt on the expectation that neurotoxicants would be more toxic to cell systems with the greatest number of neuronal properties. However, the cell systems and endpoints used here did distinguish known acute neurotoxicants from cytotoxicants, regarding the toxin concentrations required to elicit a response at sub-lethal concentrations.

The results do sustain the view that the NT2.N and NT2.N/A cultures may prove to be a useful *in vitro* alternative to human primary neural tissues for neurotoxicological testing. Additionally, the preliminary data suggests that whilst the support offered by

astrocytes to neurons may provide increased tolerance of neurons to some toxins, astrocytes may also be necessary for the expression of certain neuronal responses, for example apoptosis. Thus, this study demonstrates that neuronal-astrocytic interactions have important implications in neurotoxicity and provides evidence of the greater degree of relevance to the *in vivo* heterogeneous nervous system offered by an *in vitro* integrated population of human neurons and astrocytes.

In conclusion, in order to better reflect the *in vivo* situation, the findings presented here support the inclusion of both, neuronal and astrocytic, post-mitotic, human cell lines in a cell system intended for incorporation in a test battery for the first-tier rapid pre-screening of new and existing compounds for acute neurotoxic potential.

6.1 Future experimental approaches

The results presented here highlight the limitations encountered when using a relatively small number of *in vitro* endpoints, to identify the potential of chemicals to induce a variety of types of neurotoxicity and cytotoxicity. However, the impetus for the development of human based *in vitro* testing strategies capable of identifying neurotoxicants remains. The ideal preliminary screening system would identify those neurotoxic chemicals with low associated cytotoxicity, as in terms of hazard to human health this renders neurotoxicity the most significant property of a compound. Once validated, the incorporation of such a neurotoxicity screening battery into the REACH strategy would aid the ethical, economical, rapid and relevant testing of existing and new chemicals.

Regarding the continued development of a first-tier preliminary screening battery to differentiate neurotoxicants from cytotoxicants, further work could continue to investigate the test battery described by the current study, with the supplementation of further appropriate non-specific and specific endpoints and test chemicals, to state definitively if cell system responses were consistent with specific neurotoxicity.

The European Centre for Validation of Alternative Methods (ECVAM) has recently highlighted a batch of test chemicals for evaluating the suitability of *in vitro* cell-

systems for detecting neurotoxicity. These include the known neurotoxins 5- and 6-hydroxydopamine, aluminium chloride, cadmium chloride, chloroquine diphosphate, L-glutamate, propane-1,2-diol and the non-neurotoxic camptothecin and sodium chloride (Gartlon *et al.*, 2006). Such chemicals are commercially available and could thus be easily incorporated into the further development of a preliminary neurotoxicity screening battery.

It has been hypothesised that three key mitochondrial related disorders are involved in apoptotic or necrotic neuronal cell death inflicted by toxins; an increase in intracellular reactive oxygen species (ROS) commensurate with impaired antioxidant function, depletion in cellular energy and an increase in intracellular calcium (Ca^{2+}) levels (Gartlon *et al.*, 2006). Toxicants may induce elevation of Ca^{2+} levels by inducing leakage from storage organelles, damage to the plasma membrane promoting its extracellular influx, or inhibition of efflux through inhibition of Ca^{2+} transporters or depletion of the ATP driving force (Gregus and Klaassen, 2001).

Raised intracellular Ca^{2+} can lead to the disassociation of microfilaments, resulting in plasma membrane blebbing that predisposes the membrane to rupture and activation of Ca^{2+} dependent hydrolytic enzymes that degrade proteins, phospholipids and nucleic acids, leading to necrosis or activation of apoptotic cell death (McCarthy *et al.*, 2004). Additionally, excess Ca^{2+} causes increased production of ROS leading to oxidative stress, oxidative inactivation of thiol dependent Ca^{2+} pumps and ATP depletion (Gregus and Klaassen, 2001; Brookes *et al.*, 2004). Oxidative damage, aberrant calcium homeostasis and metabolic compromise interact with each other intimately, forming a deleterious network which is important regarding cell viability in both neural and non-neural tissues (Ying, 1996). Thus, the addition of cellular calcium concentration imaging and examination of the protective effects of Ca^{2+} chelators, to this test strategy could also be considered as an appropriate general non-cytotoxic endpoint to predict toxic effects which may ultimately compromise cell viability.

Cell damage can cause the mitochondrial matrix to expand and the inner-membrane to lose its electro-gradient. Such mitochondrial membrane potential (MMP) depolarisation can cause increased ROS production and inhibition of ATP synthesis (Polster and

Fiskum, 2004). Thus measurement of the ability of a toxin to depolarise the MMP may be considered a desirable addition to the endpoint battery and this may be achieved using the straight-forward JC-1 assay. The JC-1 dye enters cells, forms aggregates and exhibits a spectral shift from green to red only in healthy mitochondria with polarised membranes. Therefore, a population of cells undergoing toxicant-induced MMP depolarisation would be expected to display a greater proportion of green fluorescence in comparison with a control culture (Gartlon *et al.*, 2006).

As the Amplex red assay was found to be unsuitable for use with two of the test chemicals, in future it may be desirable to employ a different measure of ROS. One such widely used assay uses the fluorescent probe 2',7'-dichlorofluorescein (DCFH). Diacetylated forms of DCFH (DCFH-DA) are non-fluorescent until the acetate groups are removed by intracellular esterases and oxidation occurs within the cell. The resulting increase in fluorescence may then be detected with a fluorescent microplate reader, flow cytometer, etc. Therefore, following its loading into cells, DCFH-DA has been utilised to quantify cellular ROS production following exposure to toxins (Amoroso *et al.*, 1999; Mahrouf *et al.*, 2006). This technique was briefly examined during the current study. However, it was found that in the absence of cells (and therefore esterases), DCFH-DA still produced a fluorescent signal of increasing magnitude upon exposure to increasing concentrations of H_2O_2, suggesting auto-oxidation of the probe (data not included). Indeed, some other groups consider the commonly used DCFH-DA fluorometric assay to be unreliable and subject to artefacts of autooxidation (Ingram *et al.*, 2003). However, this method could be examined further to determine its suitability for inclusion in the biochemical endpoint battery.

Alternatively, various chemilumigenic substrates have been employed to monitor the extracellular release of ROS by cells, including luminol, lucigenin and pholasin. The intensity of the chemiluminescence is proportional to the amount of ROS in a sample (Hasegawa *et al.*, 2000; Kopprasch *et al.*, 2003). The substrates differ with respect to their sensitivity as a result of different, as yet largely unknown, molecular mechanisms leading to light emission following oxidation. It is possible one of these substrates may prove a useful addition to the test strategy.

A further endpoint appropriate for incorporation into the screening battery is the measurement of test chemical effect on glutamate levels. In the CNS, glutamate is the most abundant excitatory neurotransmitter. It is widely distributed and plays an important role in many biochemical pathways and physiological functions, including the maintenance of calcium homeostasis (Sandhu *et al.*, 2003). Its physiological and pathological effects in the CNS are mediated mainly via two types of ionotropic glutamate receptors, the NMDA receptor and the non-NMDA receptor. Activation of NMDA receptors allows influx of extracellular Ca^{2+} but excessive release of glutamate causes prolonged stimulation of NMDA receptors, inducing Ca^{2+} overload with activation of Ca^{2+} dependent enzymes, the production of ROS and neuronal death (excitotoxicity) (Garcia and Massieu, 2003). Excitotoxicity has been reported to play an important role in the neurotoxicity of numerous compounds, for example, tributyltin chloride (Nakatsu *et al.*, 2006a).

Astrocytic processes closely encapsulate synapses and normally efficiently maintain extracellular glutamate concentrations at low micromolar levels to prevent against excitotoxicity (Ye *et al.*, 1999; Daniels and Brown, 2001). An increase in extracellular glutamate may occur owing to induced efflux from neurons or astrocytes or due to impaired astrocytic uptake as a result of a toxic insult. Such glutamate released into the culture medium may be easily measured with an Amplex red Glutamic Acid/Glutamate Oxidase fluorescence assay kit. However, possible interference of test chemicals with the kit components must be examined. Additionally, alleviation of cell death due to prior incubation of cells with the glutamate receptor antagonist MK-801 or CNQX, may confirm that glutamate and glutamate receptors are involved in test chemical toxicity (Sandhu *et al.*, 2003).

As previously introduced, the vulnerability of foetal human neurons to excitatory amino acids develops over a prolonged period compared with cortical rat neurons, as foetal human neurons constitutively express less than 10 % of the functional NMDA receptors of primary rat cultures (Almaas *et al.*, 2002). NT2 neurons have been shown to exhibit both N-methyl-D-aspartate (NMDA) and non-NMDA glutamate receptor channels at similar levels as human foetal neurons (Hartley *et al.*, 1999; Almaas *et al.*, 2002). Additionally, NT2 astrocytes have been previously demonstrated to possess high

affinity, functional, glutamate transporting proteins and to contain glutamine synthase, for the breakdown of glutamate to non-toxic glutamine (Sandhu *et al.*, 2003). Therefore, it may be hypothesised that NT2 based neuronal and astrocytic cultures would be ideal for the relevant screening of human neurotoxins for excitotoxic potential.

Several cellular perturbations may be observed soon after toxin exposure, such as caspase-3 activation, ATP depletion and changes in intracellular and extracellular Ca^{2+} levels. Thus a 4-hour exposure of the cell systems is a useful initial time point for the examination of toxicity on the biochemical endpoints. However in future, depending on the choice of endpoint, the addition of further acute time points such as 24-hours may prove helpful. For example, a 24-hour exposure period may allow for TMT-Cl induced, astrocytic, TNF-α release, to result in measurable effects at the level of protein expression. Additionally, as a 24-hour time point has been used previously in the examination of the neurotoxic potential of chemicals at non-cytotoxic concentrations, it may facilitate comparison of data obtained with the literature. Furthermore, previous studies have shown that following 72-hours exposure, *in vitro* basal cytotoxicity assay IC_{50} values give a 70 % predictivity of acute oral rodent LD_{50} values (Gartlon *et al.*, 2006). Despite the extrapolation problems presented by species differences, such an *in vivo* comparison point is important in the validation process.

As discussed, the NT2 astrocytes appeared to contribute to NT2 neuronal well being following exposure to all the test chemicals, with the NT2.N/A co-culture maintaining superior ATP and GSH levels and reduced H_2O_2 levels in comparison with the NT2.N mono-culture. However, neurospecific endpoints would be required to offer more distinct evidence that NT2 neuronal function and survival is improved following toxic insult in the presence of NT2 astrocytes. Among the specific neurochemical measurements that have been previously proposed are assays for neural enzymes such as glutamic acid decarboxylase, dopamine hydroxylase, tyrosine hydroxylase and glutamine synthetase and also acetylcholinesterase and neuron-specific enolase activity (Veronesi, 1992; Costa, 1998b; Coecke *et al.*, 2006).

Additionally, in future, it may be desirable to characterise further the NT2.N and

NT2.N/A cell systems. Western blotting could be used to verify whether the NT2.N cells express neuronal markers characteristic of CNS neurons, for example NeuN, a protein specifically localised in the nucleus of terminally differentiated CNS neurons (Pleasure *et al.*, 1992; Younkin *et al.*, 1993; Megiorni *et al.*, 2005). Neurons typically have a single axon and multiple dendrites that could be distinguished in the NT2.N and NT2.N/A cultures by several differentially distributed molecular markers, using specific staining and fluorescent microscopy. For example, the axon is rich in highly phosphorylated NF proteins and tau, whilst dendrites have primarily hypophosphorylated variants and MAP2 (Pleasure *et al.*, 1992).

Due to their cytoarchitecture, neuronal phenotypes are known to be particularly prone to cell death through cytoskeleton modifications to the axons, dendrites and/or cell body and toxicants can induce such damage at non-cytotoxic concentrations. Also, changes to the astrocytic cytoskeleton may lead to a reactive hypertrophic response or loss of processes, cell swelling and perturbation of homeostatic control (Cookson and Pentreath, 1994; Gartlon *et al.*, 2006). Therefore, cytoskeletal related endpoints may be useful for differentiating neurotoxic from cytotoxic chemicals. For example, it may be desirable to perform enzyme linked, immunoabsorbent assays (ELISAs) in order to quantify cell-type specific, toxicant induced cytoskeleton changes to MAPs, neurofilaments (NFs) and glial fibrillary acidic protein (GFAP). This technique uses antibodies against specific intracellular markers and a secondary antibody coupled to an enzyme that converts an applied substrate to elicit a chromogenic or fluorescent signal. Levels of cytokines such as TNF-α can also be determined by ELISA techniques, which may be useful when examining chemicals such as TMT-Cl, which are reported to cause astrogliosis. However, all such ELISA procedures are most straightforward and economical when carried out on cells grown and exposed to toxin in a 96-well plate. Thus, an initial obstacle would be adaptation of existing protocols to growth of NT2.N and NT2.N/A cells in CellBIND 6-well plates.

Whilst the usefulness of the NT2.N and NT2.N/A cell systems have been demonstrated by the current study, the addition of a number of other human cell cultures to the screening battery may offer further useful information. A few groups have attempted to produce pure cultures of NT2 astrocytes (NT2.A) from a mixed culture of NT2.N/A cells, via exploitation of differential adhesion properties (Sandhu *et al.*, 2002; Stewart

et al., 2003). It appears that in co-culture, the NT2.N cells are effectively loosely held on a layer of NT2.A cells and that following shaking for a length of time, the NT2.N cells may be washed off into a separate vessel, leaving a purified NT2.A mono-culture. It would be advantageous to develop such a purification protocol within the laboratory in order to better examine the response of astrocytes to neurotoxic insult, without the presence of neurons. In studies presented in this thesis, the CCF-STTG1 cell line was employed for this purpose. However, it did not demonstrate the vulnerability expected in response to the test chemicals, which may have been due to its mitotic status or lack of closeness to the astrocytic phenotype. Comparison with the vulnerability of an NT2.A mono-culture towards the test-chemicals may offer further insights into this problem as well as enabling a more complete determination of the suitability of the NT2.N/A cell system for the screening of potential neurotoxins. Also, the employment of a completely non-neuronal cell line in addition to the NT2.D1 neuronal precursor cell line, (e.g. the HepG2 hepatocellular carcinoma cell line), could potentially distinguish neuronal and non neuronal responses more clearly.

In order to be designated truly neuronal, neurons in culture must possess an action potential (Younkin *et al.*, 1993). It has been previously demonstrated by Hartley *et al.*, (1999) that NT2.N cells in the absence of astrocytes have weak and uncommon action potentials. However, co-culture with primary embryonic rat astrocytes enhanced the electrophysiological characteristics of NT2.N neurons, which expressed high-amplitude action potentials of short duration, characteristic of those of primary neurons in the CNS. During the current research, preliminary whole-cell electrical recordings were carried out by Dr Ian Stanford (Aston University, UK) to investigate the presence of an action potential of an NT2 neuron in co-culture with NT2 astrocytes plated on a pdl/lam coverslip. Whilst a pseudo-action potential was obtained (data not shown), the results were inconclusive and there was insufficient time for repetition. Thus, in future it would be useful to repeat this procedure, both for an NT2 neuron in mono-culture and in co-culture with NT2 astrocytes, in order to investigate any difference in amplitude and duration of the action potential observed.

Retinoic acid (RA) treatment of NT2.D1 cells induces growth arrest and terminal differentiation along the neuronal pathway, with accumulation of cells in the G1/G0

phase (Baldassarre *et al.*, 2000). In order to confirm the post-mitotic status of cultures of NT2.N and NT2.N/A cells, cell density was regularly estimated for eight weeks using the MTT assay. In future, it may be desirable to undertake a more accurate DNA cell cycle analysis using the nucleoid stain propidium iodide (PI) in combination with flow cytometry. Information that may be derived from this method includes the percentage of nucleoids in the G0/G1 (senescent) and G2/M (dividing) phases and the abundance of apoptotic nucleoids (Nicoletti *et al.*, 1991). This technique has been previously developed within the group (Zilz *et al.*, 2007).

The proportion of immunostained GFAP positive astrocytes to β-tubulin III positive neurons in batches of NT2.N/A was estimated to be 2:1 by manual counting using a fluorescent microscope, which was in good agreement with the literature. However, re-examination of the same slides using a confocal microscope demonstrated that the aggregations of neuronal bodies had a 3D nature and thus it may be desirable to estimate the ratio of cell types to a higher degree of accuracy. In future, fluorescence-activated cell sorting (FACS) may prove a more reliable and rapid method for the counting of densely packed heterogeneous populations. Sergent-Tanguy *et al.*, (2003) have developed such a FACS method to determine the proportion of neurons and astrocytes in mixed primary cultures from postnatal rat cerebellum. Following dissociation of the cell population by trypsin, the group employed antibodies against the same intracellular, neuronal (β-tubulin III) and astrocytic (GFAP) markers as the present study. Following conjugation of the primary antibodies to fluorescent conjugated secondary antibodies, fluorescence signals were discriminated and different cell types quantified using a FACS flow cytometer. Regarding the NT2.N/A co-culture, this may also prove a useful tool for specifically quantifying the decrease in neuronal compared with astrocytic cell-viability, following exposure to a range of cytotoxic concentrations of test chemicals.

List of References

Almaas, R., Saugstad, O. D., Pleasure, D., Rootwelt, T. 2002. Neuronal formation of free radicals plays a minor role in hypoxic cell death in human NT2-N neurons. Pediatric Research 51, 136-143.

Almeida, A., Almeida, J., Bolanos, J. P., Moncada, S. 2001. Different responses of astrocytes and neurons to nitric oxide: The role of glycolytically generated ATP in astrocyte protection. Proceedings of the National Academy of Sciences of the United States of America 98, 15294-15299.

Amoroso, S., Gioielli, A., Cataldi, M., Di Renzo, G., Annunziato, L. 1999. In the neuronal cell line SH-SY5Y, oxidative stress-induced free radical overproduction causes cell death without any participation of intracellular Ca(2+) increase. Biochimica Et Biophysica Acta 1452, 151-160.

Andersson, M., Sjostrand, J., Petersen, A., Honarvar, A. K. S., Karlsson, J. O. 2000. Caspase and proteasesome activity during staurosporin-induced apoptosis in lens epithelial cells. Investigative Ophthalmology & Visual Science 41, 2623-2632.

Andrews, P. W. 1984. Retinoic acid induces neuronal differentiation of a cloned human embryonal carcinoma cell line in vitro. Developmental Biology 103, 285-293.

Andrews, P. W. 1988. Human Teratocarcinomas. Biochimica Et Biophysica Acta 948, 17-36.

Andrews, P. W., Damjanov, I., Simon, D., Banting, G. S., Carlin, C., Dracopoli, N. C., Fogh, J. 1984. Pluripotent embryonal carcinoma clones derived from the human teratocarcinoma cell line Tera-2 - Differentiation in vivo and in vitro. Laboratory Investigation 50, 147-162.

Ankarcrona, M., Dypbukt, J. M., Bonfoco, E., Zhivotovsky, B., Orrenius, S., Lipton, S. A., Nicotera, P. 1995. Glutamate-induced neuronal death - a succession of necrosis or apoptosis depending on mitochondrial-function. Neuron 15, 961-973.

Anthony, D. C., Montine, T. J., Valentine, W. M., Graham, D. G. (2001). Chapter 16: Toxic Responses of the Nervous System. In *Casarett and Doull's Toxicology: The Basic Science of Poisons* (C. D. Klassen, Ed.), pp. 535-564. McGraw-Hill, London.

Appel, K. E. 2004. Organotin compounds: Toxicokinetic aspects. Drug Metabolism Reviews 36, 763-786.

Aschner, M., Aschner, J. L. 1992. Cellular and molecular effects of trimethyltin and triethyltin: Relevance to organotin neurotoxicity. Neuroscience and Biobehavioral Reviews 16, 427-435.

Atterwill, C. K., Bruinink, A., Drejer, J., Duarte, E., Abdulla, E. M., Meredith, C., Nicotera, P., Regan, C., Rodriguezfarre, E., Simpson, M. G., Smith, R.,

Veronesi, B., Vijverberg, H., Walum, E., Williams, D. C. 1994. In-vitro neurotoxicity testing - the report and recommendations of ECVAM workshop-3. ATLA-Alternatives to Laboratory Animals 22, 350-362.

Atterwill, C. K., Davenportjones, J., Goonetilleke, S., Johnston, H., Purcell, W., Thomas, S. M., West, M., Williams, S. 1993. New models for the in-vitro assessment of neurotoxicity in the nervous-system and the preliminary validation stages of a tiered-test model. Toxicology in Vitro 7, 569-580.

Ba, F., Pang, P. K. T., Benishin, C. G. 2003. The establishment of a reliable cytotoxic system with SK-N-SH neuroblastoma cell culture. Journal of Neuroscience Methods 123, 11-22.

Baldassarre, G., Boccia, A., Bruni, P., Sandomenico, C., Barone, M. V., Pepe, S., Angrisano, T., Belletti, B., Motti, M. L., Fusco, A., Viglietto, G. 2000. Retinoic acid induces neuronal differentiation of embryonal carcinoma cells by reducing proteasome-dependent proteolysis of the cyclin-dependent inhibitor p27. Cell Growth & Differentiation 11, 517-526.

Bani-Yaghoub, M., Bechberger, J. F., Naus, C. C. 1997. Reduction of connexin43 expression and dye-coupling during neuronal differentiation of human NTera2/clone D1 cells. Journal of Neuroscience Research 49, 19-31.

Bani-Yaghoub, M., Felker, J. M., Naus, C. C. G. 1999. Human NT2/D1 cells differentiate into functional astrocytes. Neuroreport 10, 3843-3846.

Barna, B. P., Chou, S. M., Jacobs, B., Ransohoff, R. M., Hahn, J. F., Bay, J. W. 1985. Enhanced DNA-synthesis of human glial-cells exposed to human-leukocyte products. Journal of Neuroimmunology 10, 151-158.

Belizario, J. E., Lorite, M. J., Tisdale, M. J. 2001. Cleavage of caspases-1, -3, -6, -8 and -9 substrates by proteases in skeletal muscles from mice undergoing cancer cachexia. British Journal of Cancer, 1135-1140.

Betz, N., Farfan, A., O'Brian, M. 2003. Detecting caspase activity in staurosporine-treated human neuroblastoma cells using fluorescent and luminescent methods. Cell Notes, 9-10

Boegner, F., Gruning, W., Stoltenburgdidinger, G., Marx, P., Altenkirch, H. 1992. 2,5-Hexanedione is a potent gliatoxin in in vitro-cell cultures of the nervous-system. Neurotoxicology 13, 151-154.

Brecht, S., Gelderblom, M., Srinivasan, A., Mielke, K., Dityateva, G., Herdegen, T. 2001. Caspase-3 activation and DNA fragmentation in primary hippocampal neurons following glutamate excitotoxicity. Molecular Brain Research 94, 25-34.

Broadhead, C. L., Bottrill, K. 1997. Strategies for replacing animals in biomedical research. Molecular Medicine Today 3, 483-487.

Bronstein, D. M., PerezOtano, I., Sun, V., Sawin, S. B. M., Chan, J., Wu, G. C., Hudson, P. M., Kong, L. Y., Hong, J. S., McMillian, M. K. 1995. Glia-

dependent neurotoxicity and neuroprotection in mesencephalic cultures. Brain Research 704, 112-116.

Brookes, P. S., Yoon, Y. S., Robotham, J. L., Anders, M. W., Sheu, S. S. 2004. Calcium, ATP, and ROS: a mitochondrial love-hate triangle. American Journal of Physiology-Cell Physiology 287, C817-C833.

Brown, D. R. 1999. Dependence of neurones on astrocytes in a coculture system renders neurones sensitive to transforming growth factor beta 1-induced glutamate toxicity. Journal of Neurochemistry 72, 943-953.

Buckley, P. (1997). Chapter 9: The Nervous System. In *Target Organ Pathology: A Basic Text* (J. Turton,J. Hoosen, Eds.), pp. 273-310. Taylor and Francis, London.

Cardoso, S. M., Rego, A. C., Penacho, N., Oliveira, C. R. 2004. Apoptotic cell death induced by hydrogen peroxide in NT2 parental and mitochondrial DNA depleted cells. Neurochemistry International 45, 693-698.

Cardoso, S. M., Swerdlow, R. H., Oliveira, C. R. 2002. Induction of cytochrome c-mediated apoptosis by amyloid beta 25-35 requires functional mitochondria. Brain Research 931, 117-125.

Carmignoto, G. 2000. Reciprocal communication systems between astrocytes and neurones. Progress in Neurobiology 62, 561-581.

Chen, H. F., Hee, S. S. Q. 1995. Ketone Ec(50) Values in the Microtox Test. Ecotoxicology and Environmental Safety 30, 120-123.

Clarke, J. B., Fortes, M. A., Giovanni, A., Brewster, D. W. 1996. Modification of an enzymatic glutathione assay for the microtiter plate and the determination of glutathione in rat primary cortical cells. Toxicology Methods 6, 223-230.

Coecke, S., Eskes, C., Gartlon, J., Kinsner, A., Price, A., van Vliet, E., Prieto, P., Boveri, M., Bremer, S., Adler, S., Pellizzer, C., Wendel, A., Hartung, T. 2006. The value of alternative testing for neurotoxicity in the context of regulatory needs. Environmental Toxicology and Pharmacology 21, 153-167.

Combes, R. D. 2005. Assessing risk to humans from chemical exposure by using non-animal test data. Toxicology in Vitro 19, 921-924.

Cookson, M. R., McClean, R., Williams, S. P., Davenportjones, J., Egan, C., Ohare, S., Atterwill, C. K., Pentreath, V. W. 1994. Use of astrocytes for in-vitro neurotoxicity testing. Toxicology in Vitro 8, 817-819.

Cookson, M. R., Mead, C., Austwick, S. M., Pentreath, V. W. 1995. Use of the MTT assay for estimating toxicity in primary astrocyte and C6 glioma cell-cultures. Toxicology in Vitro 9, 39-42.

Cookson, M. R., Pentreath, V. W. 1994. Alterations in the glial fibrillary acidic protein-content of primary astrocyte cultures for evaluation of glial-cell toxicity.

Toxicology in Vitro 8, 351-356.

Corsini, E., Viviani, B., Marinovich, M., Galli, C. L. 1997. Role of mitochondria and calcium ions in tributyltin-induced gene regulatory pathways. Toxicology and Applied Pharmacology 145, 74-81.

Corsini, E., Viviani, B., Marinovich, M., Galli, C. L. 1998. Primary role of mitochondria and calcium ions in the induction of reactive oxygen species by external stimuli such as triorganotins. Toxicology in Vitro 12, 551-556.

Costa, L. G. 1998a. Biochemical and molecular neurotoxicology: relevance to biomarker development, neurotoxicity testing and risk assessment. Toxicology Letters 103, 417-421.

Costa, L. G. 1998b. Neurotoxicity testing: A discussion of in vitro alternatives. Environmental Health Perspectives 106, 505-510.

Couri, D., Milks, M. 1982. Toxicity and metabolism of the neurotoxic hexacarbons normal-hexane, 2-hexanone, and 2,5-hexanedione. Annual Review of Pharmacology and Toxicology 22, 145-166.

Cree, I. A., Andreotti, P. E. 1997. Measurement of cytotoxicity by ATP-based luminescence assay in primary cell cultures and cell lines. Toxicology in Vitro 11, 553-556.

Cristofol, R. M., Gasso, S., Vilchez, D., Pertusa, M., Rodriguez-Farre, E., Sanfeliu, C. 2004. Neurotoxic effects of trimethyltin and triethyltin on human fetal neuron and astrocyte cultures: A comparative study with rat neuronal cultures and human cell lines. Toxicology Letters 152, 35-46.

Daniels, M., Brown, D. R. 2001. Astrocytes regulate N-methyl-D-aspartate receptor subunit composition increasing neuronal sensitivity to excitotoxicity. Journal of Biological Chemistry 276, 22446-22452.

Decaprio, A. P. 1987. n-Hexane neurotoxicity - a mechanism involving pyrrole adduct formation in axonal cytoskeletal protein. Neurotoxicology 8, 199-210.

Decaprio, A. P., Jackowski, S. J., Regan, K. A. 1987. Mechanism offormation and quantitation of imines, pyrroles, and stable nonpyrrole adducts in 2,5-hexanedione-treated protein. Molecular Pharmacology 32, 542-548.

Del Rio, M. J., Velez-Pardo, C. 2002. Monoamine neurotoxins-induced apoptosis in lymphocytes by a common oxidative stress mechanism: involvement of hydrogen peroxide (H2O2), caspase-3, and nuclear factor kappa-B (NF-kappa B), p53, c-Jun transcription factors. Biochemical Pharmacology 63, 677-688.

Denizot, F., Lang, R. 1986. Rapid colorimetric assay for cell-growth and survival - modifications to the tetrazolium dye procedure giving improved sensitivity and reliability. Journal of Immunological Methods, 271-277.

Desagher, S., Glowinski, J., Premont, J. 1996. Astrocytes protect neurons from

hydrogen peroxide toxicity. Journal of Neuroscience 16, 2553-2562.

Desagher, S., Glowinski, J., Premont, J. 1997. Pyruvate protects neurons against hydrogen peroxide-induced toxicity. Journal of Neuroscience 17, 9060-9067.

Doctor, S. V., Sultatos, L. G., Murphy, S. D. 1983. Distribution of trimethyltin in various tissues of the male-mouse. Toxicology Letters 17, 43-48.

dos Santos, C. R., Passarelli, M. M., Nascimento, E. D. 2002. Evaluation of 2,5-hexanedione in urine of workers exposed to n-hexane in Brazilian shoe factories. Journal of Chromatography B-Analytical Technologies in the Biomedical and Life Sciences 778, 237-244.

Dringen, R. 2000. Metabolism and functions of glutathione in brain. Progress in Neurobiology, 649-671.

Dringen, R., Gutterer, J. M., Hirrlinger, J. 2000. Glutathione metabolism in brain - Metabolic interaction between astrocytes and neurons in the defense against reactive oxygen species. European Journal of Biochemistry 267, 4912-4916.

Dringen, R., Kussmaul, L., Gutterer, J. M., Hirrlinger, J., Hamprecht, B. 1999a. The glutathione system of peroxide detoxification is less efficient in neurons than in astroglial cells. Journal of Neurochemistry 72, 2523-2530.

Dringen, R., Pfeiffer, B., Hamprecht, B. 1999b. Synthesis of the antioxidant glutathione in neurons: supply by astrocytes of CysGly as precursor for neuronal glutathione. Journal of Neuroscience 19, 562-569.

Drukarch, B., Schepens, E., Jongenelen, C. A. M., Stoof, J. C., Langeveld, C. H. 1997. Astrocyte-mediated enhancement of neuronal survival is abolished by glutathione deficiency. Brain Research 770, 123-130.

Durham, H. D. 1988. Aggregation of intermediate filaments by 2,5-hexanedione - comparison of effects on neurofilaments, gfap-filaments and vimentin-filaments in dissociated cultures of mouse spinal-cord dorsal-root ganglia. Journal of Neuropathology and Experimental Neurology 47, 432-442.

EC (2001). European Commission White Paper on a Strategy for a Future Chemicals Policy (COM Brussels 88 final).

Edelstein, C. L., Shi, Y. X., Schrier, R. W. 1999. Role of caspases in hypoxia-induced necrosis of rat renal proximal tubules. Journal of the American Society of Nephrology 10, 1940-1949.

Eisenbrand, G., Pool-Zobel, B., Baker, V., Balls, M., Blaaubocr, B. J., Boobis, A., Carere, A., Kevekordes, S., Lhuguenot, J. C., Pieters, R., Kleiner, J. 2002. Methods of in vitro toxicology. Food and Chemical Toxicology 40, 193-236.

Elsabbagh, H. S., Moussa, S. Z., El-Tawil, O. S. 2002. Neurotoxicologic sequelae of tributyltin intoxication in rats. Pharmacological Research 45, 201-206.

Erel, O. 2005. A new automated colorimetric method for measuring total oxidant

status. Clinical Biochemistry 38, 1103-1111.

Eskes, C., Juillerat-Jeanneret, L., Leuba, G., Honegger, P., Monnet-Tschudi, F. 2003. Involvement of microglia-neuron interactions in the tumor necrosis factor-alpha release, microglial activation, and neurodegeneration induced by trimethyltin. Journal of Neuroscience Research 71, 583-590.

Eyer, C. L., Rio, C., Smith, J. R. 2000. Trimethyltin reduces ATP levels and MTT reduction in the LRM55 rat astrocytoma cell line. In Vitro and Molecular Toxicology 13, 263-268.

FAO/WHO (1999). International Programme on Chemical Safety, WHO Food Additives Series: 42. Joint FAO/WHO Expert Commitee on Food Additives (JECFA).

Ferraris, M., Radice, S., Catalani, P., Francolini, M., Marabini, L., Chiesara, E. 2002. Early oxidative damage in primary cultured trout hepatocytes: a time course study. Aquatic Toxicology 59, 283-296.

Fiedorowicz, A., Figiel, L., Kaminska, B., Zaremba, M., Wilk, S., Oderfeld-Nowak, B. 2001. Dentate granule neuron apoptosis and glia activation in murine hippocampus induced by trimethyltin exposure. Brain Research 912, 116-127.

Fields, R. D., Stevens-Graham, B. 2002. Neuroscience - New insights into neuron-glia communication. Science 298, 556-562.

Figiel, I., Fiedorowicz, A. 2002. Trimethyltin-evoked neuronal apoptosis and glia response in mixed cultures of rat hippocampal dentate gyrus: A new model for the study of the cell type-specific influence of neurotoxins. Neurotoxicology 23, 77-86.

Florea, A. M., Splettstoesser, F., Dopp, E., Rettenmeier, A. W., Busselberg, D. 2005. Modulation of intracellular calcium homeostasis by trimethyltin chloride in human tumour cells: Neuroblastoma SY5Y and cervix adenocarcinoma HeLaS3. Toxicology 216, 1-8.

Fonck, C., Baudry, M. 2003. Rapid reduction of ATP synthesis and lack of free radical formation by MPP+ in rat brain synaptosomes and mitochondria. Brain Research 975, 214-221.

Fujii, J., Iuchi, Y., Matsuki, S., Ishii, T. 2003. Cooperative function of antioxidant and redox systems against oxidative stress in male reproductive tissues. Asian Journal of Andrology 5, 231-242.

Gabryel, B., Adamek, M., Pudelko, A., Malecki, A., Trzeciak, H. I. 2002. Piracetam and vinpocetine exert cytoprotective activity and prevent apoptosis of astrocytes in vitro in hypoxia and reoxygenation. Neurotoxicology 23, 19-31.

Garcia, O., Massieu, L. 2003. Glutamate uptake inhibitor L-Trans-pyrrolidine 2,4-dicarboxylate becomes neurotoxic in the presence of subthreshold concentrations of mitochondrial toxin 3-nitropropionate: Involvement of mitochondrial reducing activity and ATP production. Journal of Neuroscience

Research 74, 956-966.

Gartlon, J., Kinsner, A., Bal-Price, A., Coecke, S., Clothier, R. H. 2006. Evaluation of a proposed in vitro test strategy using neuronal and non-neuronal cell systems for detecting neurotoxicity. Toxicology in Vitro 20, 1569-1581.

Gegg, M. E., Beltran, B., Salas-Pino, S., Bolanos, J. P., Clark, J. B., Moncada, S., Heales, S. J. 2003. Differential effect of nitric oxide on glutathione metabolism and mitochondrial function in astrocytes and neurones: implications for neuroprotection/neurodegeneration? Journal of Neurochemistry 86, 228-237.

Geller, H. M., Cheng, K. Y., Goldsmith, N. K., Romero, A. A., Zhang, A. L., Morris, E. J., Grandison, L. 2001. Oxidative stress mediates neuronal DNA damage and apoptosis in response to cytosine arabinoside. Journal of Neurochemistry 78, 265-275.

Geloso, M. C., Vercelli, A., Corvino, V., Repici, M., Boca, M., Haglid, K., Zelano, G., Michetti, F. 2002. Cyclooxygenase-2 and caspase 3 expression in trimethyltin-induced apoptosis in the mouse hippocampus. Experimental Neurology 175, 152-160.

Gennari, A., Viviani, B., Galli, C. L., Marinovich, M., Pieters, R., Corsini, E. 2000. Organotins induce apoptosis by disturbance of [Ca2+](i) and mitochondrial activity, causing oxidative stress and activation of caspases in rat thymocytes. Toxicology and Applied Pharmacology 169, 185-190.

Gregus, Z., Klaassen, C. (2001). Chapter 3: Mechanisms of Toxicity In *Casarett and Doull's Toxicology: The Basic Science of Poisons* (C. D. Klaassen, Ed.), pp. 38-73. McGraw-Hill, London.

Griffin, J. L., O'Donnell, J. M., White, L. T., Hajjar, R. J., Lewandowski, E. D. 2000. Postnatal expression and activity of the mitochondrial 2-oxoglutarate-malate carrier in intact hearts. American Journal of Physiology - Cell Physiology 279, 1704-1709.

Griffioen, K. J. S., Ghribi, O., Fox, N., Savory, J., DeWitt, D. A. 2004. Aluminum maltolate-induced toxicity in NT2 cells occurs through apoptosis and includes cytochrome c release. Neurotoxicology 25, 859-867.

Guillemain, I., Alonso, G., Patey, G., Privat, A., Chaudieu, I. 2000. Human NT2 neurons express a large variety of neurotransmission phenotypes in vitro. Journal of Comparative Neurology 422, 380-395.

Gunasekar, P., Li, L., Prabhakaran, K., Eybl, V., Borowitz, J. L., Isom, G. E. 2001a. Mechanisms of the apoptotic and necrotic actions of trimethyltin in cerebellar granule cells. Toxicological Sciences 64, 83-89.

Gunasekar, P. G., Mickova, V., Kotyzova, D., Li, L., Borowitz, J. L., Eybl, V., Isom, G. E. 2001b. Role of astrocytes in trimethyltin neurotoxicity. Journal of Biochemical and Molecular Toxicology 15, 256-262.

Had-Aissouni, L., Re, D. B., Nieoullon, A., Goff, L. K. L. 2002. Importance of

astrocytic inactivation of synaptically released glutamate for cell survival in the central nervous system-are astrocytes vulnerable to low intracellular glutamate concentrations? Journal of Physiology-Paris 96, 317-322.

Hanks, J. H. 1975. Hanks' balanced salt solution and pH control. Methods in Cell Science V1, 3-4.

Harlow, E., Lane, D. (1998). *Antibodies: A laboratory manual.* Cold Spring Harbor Laboratory Press, New York.

Harris, J. B., Blain, P. G. 2004. Neurotoxicology: What the neurologist needs to know. Journal of Neurology Neurosurgery and Psychiatry 75, 29-34.

Harry, G. J., Billingsley, M., Bruinink, A., Campbell, I. L., Classen, W., Dorman, D. C., Galli, C., Ray, D., Smith, R. A., Tilson, H. A. 1998. In vitro techniques for the assessment of neurotoxicity. Environmental Health Perspectives 106, 131-158.

Hartley, C. L., Anderson, V. E. R., Anderson, B. H., Robertson, J. 1997. Acrylamide and 2,5-hexanedione induce collapse of neurofilaments in SH-SY5Y human neuroblastoma cells to form perikaryal inclusion bodies. Neuropathology and Applied Neurobiology 23, 364-372.

Hartley, R. S., Margulis, M., Fishman, P. S., Lee, V. M. Y., Tang, C. M. 1999. Functional synapses are formed between human NTera2 (NT2N, hNT) neurons grown on astrocytes. Journal of Comparative Neurology 407, 1-10.

Hasegawa, H., Suzuki, K., Suzuki, K., Nakaji, S., Sugawara, K. 2000. Effects of zinc on the reactive oxygen species generating capacity of human neutrophils and on the serum opsonic activity in vitro. Luminescence 15, 321-327.

Heijink, E., Scholten, S. W., Bolhuis, P. A., de Wolff, F. A. 2000. Effects of 2,5-hexanedione on calpain-mediated degradation of human neurofilaments in vitro. Chemico-Biological Interactions 129, 231-247.

Hernandez-Viadel, M., Montoliu, C., Monfort, P., Canales, J. J., Erceg, S., Rowan, M., Ceccatelli, S., Felipo, V. 2003. Chronic exposure to 2,5-hexanedione impairs the glutamate-nitric oxide-cyclic GMP pathway in cerebellar neurons in culture and in rat brain in vivo. Neurochemistry International 42, 525-533.

Horrocks, G. A., Lauder, L., Stewart, R., Przyborski, S. 2003. Formation of neurospheres from human embryonal carcinoma stem cells. Biochemical and Biophysical Research Communications 304, 411-416.

Hu, X. T. 2003. Proteolytic signaling by TNF alpha: caspase activation and I kappa B degradation. Cytokine 21, 286-294.

Ingram, J. L., Rice, A. B., Santos, J., Van Houten, B., Bonner, J. C. 2003. Vanadium-induced HB-EGF expression in human lung fibroblasts is oxidant dependent and requires MAP kinases. American Journal of Physiology - Lung Cellular and Molecular Physiology 284, L774-782.

Inna Kruman, Q. G. M. P. M. 1998. Calcium and reactive oxygen species mediate staurosporine-induced mitochondrial dysfunction and apoptosis in PC12 cells. Journal of Neuroscience Research 51, 293-308.

IPCS (1990). International programme on chemical safety, Environmental health criteria: Series 116 Tributyltin compounds. World Health Organisation (WHO).

IPCS (1991). International programme on chemical safety, n-Hexane. ICSC: 0279. CEC.

Iwasaki, K., Tsuruta, H. 1984. Molecular mechanism of hexane neuropathy: Significant differences in pharmacokinetics between 2.3-, 2.4-, and 2.5-hexanedione. Industrial Health 22, 177-187.

Iwata-Ichikawa, E., Kondo, Y., Miyazaki, I., Asanuma, M., Ogawa, N. 1999. Glial cells protect neurons against oxidative stress via transcriptional up-regulation of the glutathione synthesis. Journal of Neurochemistry 72, 2334-2344.

Jenkins, S. M., Barone, S. 2004. The neurotoxicant trimethyltin induces apoptosis via caspase activation, p38 protein kinase, and oxidative stress in PC12 cells. Toxicology Letters 147, 63-72.

Jenkins, S. M., Ehman, K., Barone, S., Jr. 2004. Structure-activity comparison of organotin species: dibutyltin is a developmental neurotoxicant in vitro and in vivo. Developmental Brain Research 151, 1-12.

Ji, L. L. 1999. Antioxidants and oxidative stress in exercise. Proceedings of the Society for Experimental Biology and Medicine 222, 283-292.

Jimenez, A., Jorda, E. G., Verdaguer, E., Pubill, D., Sureda, F. X., Canudas, A. M., Escubedo, E., Camarasa, J., Camins, A., Pallas, M. 2004. Neurotoxicity of amphetamine derivatives is mediated by caspase pathway activation in rat cerebellar granule cells. Toxicology and Applied Pharmacology 196, 223-234.

Jones-Villeneuve, E. M. V., McBurney, M. W., Rogers, K. A., Kalnins, V. I. 1982. Retinoic Acid Induces Embryonal Carcinoma-Cells to Differentiate into Neurons and Glial-Cells. Journal of Cell Biology 94, 253-262.

Jurkiewicz, M., Averill-Bates, D. A., Marion, M. 2004. Involvement of mitochondrial and death receptor pathways in tributyltin-induced apoptosis in rat hepatocytes. Biochimica Et Biophysica Acta-Molecular Cell Research 1693, 15-27.

Kandel, E. R., Schwartz, J. H., Jessell, T. M. (2000). Part VIII: The Development of the Nervous System. In *Principles of Neural Science* (E.R. Kandel, J. H. Schwartz,T. M. Jessell, Eds.), pp. 1019-1168. McGraw-Hill, Maidenhead.

Karpiak, V. C., Eyer, C. L. 1999. Differential gliotoxicity of organotins. Cell Biology and Toxicology 15, 261-268.

Kerr, J. F., Wyllie, A. H., Currie, A. R. 1972. Apoptosis: a basic biological phenomenon with wide-ranging implications in tissue kinetics. British Journal

of Cancer 26, 239-257.

Kerr, J. F. R. 2002. History of the events leading to the formulation of the apoptosis concept. Toxicology 181-182, 471-474.

Kimmel, E. C., Fish, R. H., Casida, J. E. 1977. Bio-Organotin Chemistry - Metabolism of Organotin Compounds in Microsomal Monooxygenase Systems and in Mammals. Journal of Agricultural and Food Chemistry 25, 1-9.

Kirkpatrick, L., Brady, S. (1998). Chapter 11: The Cytoskeleton of Neurons and Glia In *Basic Neurochemistry: Molecular, Cellular and Medical Aspects* (G. J. Siegel, B. W. Agranoff, R. W. Albers, S. K. Fisher,M. D. Uhler, Eds.), pp. 135-174. Lippincott, Williams and Wilkins, London.

Kleinsmith, L. J., Kish, V. M. (1995). Chapter 17: Neurons and Synaptic Signalling In *Principles of Cell and Molecular Biology* (L. J. Kleinsmith,V. M. Kish, Eds.), pp. 747-776. HaperCollins, Glasgow.

Kondziolka, D., Wechsler, L., Goldstein, S., Meltzer, C., Thulborn, K. R., Gebel, J., Jannetta, P., DeCesare, S., Elder, E. M., McGrogan, M., Reitman, M. A., Bynum, L. 2000. Transplantation of cultured human neuronal cells for patients with stroke. Neurology 55, 565-569.

Koo, H. N., Hong, S. H., Kim, C. Y., Ahn, J. W., Lee, Y. G., Kim, J. J., Lyu, Y. S., Kim, H. M. 2002. Inhibitory effect of apoptosis in human astrocytes CCF-STTG1 cells by lemon oil. Pharmacological Research 45, 469-473.

Kopin, I. J. 1987. MPTP - an industrial-chemical and contaminant of illicit narcotics stimulates a new era in research on Parkinsons-disease. Environmental Health Perspectives 75, 45-51.

Kopprasch, S., Pietzsch, J., Graessler, J. 2003. Validation of different chemilumigenic substrates for detecting extracellular generation of reactive oxygen species by phagocytes and endothelial cells. Luminescence 18, 268-273.

Lamarche, F., Gonthier, B., Signorini, N., Eysseric, H., Barret, L. 2003. Acute exposure of cultured neurones to ethanol results in reversible DNA single-strand breaks; Whereas chronic exposure causes loss of cell viability. Alcohol and Alcoholism, 550-558.

Langlois, A., Duval, D. 1997. Differentiation of human NT2 cells into neurons and glia. Methods in Cell Science 19, 213-219.

Lavastre, V., Girard, D. 2002. Tributyltin induces human neutrophil apoptosis and selective degradation of cytoskeletal proteins by caspases. Journal of Toxicology and Environmental Health-Part A 65, 1013-1024.

Lee, V. M. Y., Andrews, P. W. 1986. Differentiation of Ntera-2 clonal human embryonal carcinoma-cells into neurons involves the induction of all 3 neurofilament proteins. Journal of Neuroscience 6, 514-521.

Lee, W. T., Itoh, T., Pleasure, D. 2002. Acute and chronic alterations in calcium

homeostasis in 3-nitropropionic acid-treated human NT2-N neurons. Neuroscience 113, 699-708.

Lehning, E. J., Dyer, K. S., Jortner, B. S., Lopachin, R. M. 1995. Axonal atrophy is a specific component of 2,5-hexanedione peripheral neuropathy. Toxicology and Applied Pharmacology 135, 58-66.

Leist, M., Single, B., Castoldi, A. F., Kuhnle, S., Nicotera, P. 1997. Intracellular adenosine triphosphate (ATP) concentration: A switch in the decision between apoptosis and necrosis. Journal of Experimental Medicine 185, 1481-1486.

Lemasters, J. J., Hackenbrock, C. E. 1973. Adenosine triphosphate: continuous measurement in mitochondrial suspension by firefly luciferase luminescence. Biochemical and Biophysical Research Communications 55, 1262-1270.

Leypoldt, F., Lewerenz, J., Methner, A. 2001. Identification of genes up-regulated by retinoic-acid-induced differentiation of the human neuronal precursor cell line NTERA-2 cl.D1. Journal of Neurochemistry 76, 806-814.

Lily, O., Palace, J., Vincent, A. 2004. Serum autoantibodies to cell surface determinants in multiple sclerosis: a flow cytometric study. Brain 127, 269-279.

LoPachin, R. M. 2000. Redefining toxic distal axonopathies. Toxicology Letters 112, 23-33.

Lopachin, R. M., Aschner, M. 1993. Glial neuronal interactions - relevance to neurotoxic mechanisms. Toxicology and Applied Pharmacology 118, 141-158.

LoPachin, R. M., DeCaprio, A. P. 2004. gamma-Diketone neuropathy: axon atrophy and the role of cytoskeletal protein adduction. Toxicology and Applied Pharmacology 199, 20-34.

LoPachin, R. M., DeCaprio, A. P. 2005. Protein adduct formation as a molecular mechanism in neurotoxicity. Toxicological Sciences 86, 214-225.

LoPachin, R. M., Lehning, E. J., Opanashuk, L. A., Jortner, B. S. 2000. Rate of neurotoxicant exposure determines morphologic manifestations of distal axonopathy. Toxicology and Applied Pharmacology 167, 75-86.

Lu, W., Maheshwari, A., Misiuta, I., Fox, S. E., Chen, N., Tanja, Z. B., Zigova, T., Christensen, R. D., Calhoun, D. A. 2005. Neutrophil-specific chemokines are produced by astrocytic cells but not by neuronal cells. Developmental Brain Research 155, 127-134.

Lundin, A., Hasenson, M., Persson, J., Pousette, A. 1986. Estimation of Biomass in Growing Cell lines by Adenosine-Triphosphate Assay. Methods in Enzymology 133, 27-42.

Mahrouf, M., Ouslimani, N., Peynet, J., Djelidi, R., Couturier, M., Therond, P., Legrand, A., Beaudeux, J. L. 2006. Metformin reduces angiotensin-mediated intracellular production of reactive oxygen species in endothelial cells through

the inhibition of protein kinase C. Biochemical Pharmacology 72, 176-183.

Maier, W. E., Brown, H. W., Tilson, H. A., Luster, M. I., Harry, G. J. 1995. Trimethyltin increases interleukin(Il)1-alpha, Il-6 and tumor-necrosis-factor-alpha messenger-RNA levels in rat hippocampus. Journal of Neuroimmunology 59, 65-75.

Makar, T. K., Nedergaard, M., Preuss, A., Gelbard, A. S., Perumal, A. S., Cooper, A. J. 1994. Vitamin E, ascorbate, glutathione, glutathione disulfide, and enzymes of glutathione metabolism in cultures of chick astrocytes and neurons: evidence that astrocytes play an important role in antioxidative processes in the brain. Journal of Neurochemistry 62, 45-53.

Mandavilli, B. S., Boldogh, I., Van Houten, B. 2005. 3-Nitropropionic acid-induced hydrogen peroxide, mitochondrial DNA damage, and cell death are attenuated by Bcl-2 overexpression in PC12 cells. Molecular Brain Research 133, 215-223.

Manthorpe, M., Engvall, E., Ruoslahti, E., Longo, F. M., Davis, G. E., Varon, S. 1983. Laminin promotes neuritic regeneration from cultured peripheral and central neurons. Journal of Cell Biology 97, 1882-1890.

Marcaida, G., Minana, M. D., Grisolia, S., Felipo, V. 1997. Determination of intracellular ATP in primary cultures of neurons. Brain Research Protocols 1, 75-78.

Marchal-Victorion, S., Deleyrolle, L., De Weille, J., Saunier, A., Dromard, C., Sandillon, F., Privat, A., Hugnot, J. P. 2003. The human NTERA2 neural cell line generates neurons on growth under neural stem cell conditions and exhibits characteristics of radial glial cells. Molecular and Cellular Neuroscience 24, 198-213.

Marini, A. M., Nowak, T. S. 2000. Metabolic effects of 1-methyl-4-phenylpyridinium (MPP+) in primary neuron cultures. Journal of Neuroscience Research 62, 814-820.

Martin, L. J., Al-Abdulla, N. A., Brambrink, A. M., Kirsch, J. R., Sieber, F. E., Portera-Cailliau, C. 1998. Neurodegeneration in excitotoxicity, global cerebral ischemia, and target deprivation: A perspective on the contributions of apoptosis and necrosis. Brain Research Bulletin 46, 281-309.

Massicotte, C., Knight, K., Van Der Schyf, C. J., Jortner, B. S., Ehrich, M. 2005. Effects of organophosphorus compounds on ATP production and mitochondrial integrity in cultured cells. Neurotoxicity Research 7, 203-217.

Mayan, O., Teixiera, J. P., Alves, S., Azevedo, C. 2002. Urinary 2,5 hexanedione as a biomarker of n-hexane exposure. Biomarkers 7, 299-305.

McCaffery, P., Drager, U. C. 2000. Regulation of retinoic acid signaling in the embryonic nervous system: a master differentiation factor. Cytokine & Growth Factor Reviews 11, 233-249.

McCarthy, S., Somayajulu, M., Sikorska, M., Borowy-Borowski, H., Pandey, S. 2004. Paraquat induces oxidative stress and neuronal cell death; neuroprotection by water-soluble Coenzyme Q10. Toxicology and Applied Pharmacology 201, 21-31.

McConkey, D. J. 1998. Biochemical determinants of apoptosis and necrosis. Toxicology Letters 99, 157-168.

McLaughlin, B. A., Nelson, D., Silver, I. A., Erecinska, M., Chesselet, M. F. 1998. Methylmalonate toxicity in primary neuronal cultures. Neuroscience 86, 279-290.

Medrano, C. J., LoPachin, R. M. 1989. Effects of acrylamide and 2,5-hexanedione on brain mitochondrial respiration. Neurotoxicology 10, 249-255.

Megiorni, F., Mora, B., Indovina, P., Mazzilli, M. C. 2005. Expression of neuronal markers during NTera2/cloneD1 differentiation cell aggregation method. Neuroscience Letters 373, 105-109.

Mentz, S., de Lacalle, S., Baerga-Ortiz, A., Knauer, M. F., Knauer, D. J., Komives, E. A. 1999. Mechanism of thrombin clearance by human astrocytoma cells. Journal of Neurochemistry 72, 980-987.

Merrick, S. E., Trojanowski, J. Q., Lee, V. M. Y. 1997. Selective destruction of stable microtubules and axons by inhibitors of protein serine/threonine phosphatases in cultured human neurons (NT2N cells). Journal of Neuroscience 17, 5726-5737.

Misiuta, I. E., Anderson, L., McGrogan, M. P., Sanberg, P. R., Willing, A. E., Zigova, T. 2003. The transcription factor Nurr1 in human NT2 cells and hNT neurons. Developmental Brain Research 145, 107-115.

Misiuta, I. E., Saporta, S., Sanberg, P. R., Zigova, T., Willing, A. E. 2006. Influence of retinoic acid and lithium on proliferation and dopaminergic potential of human NT2 cells. Journal of Neuroscience Research 83, 668-679.

Mizuhashi, S., Ikegaya, Y., Matsuki, N. 2000a. Cytotoxicity of tributyltin in rat hippocampal slice cultures. Neuroscience Research 38, 35-42.

Mizuhashi, S., Ikegaya, Y., Nishiyama, N., Matsuki, N. 2000b. Cortical astrocytes exposed to tributyltin undergo morphological changes in vitro. Japanese Journal of Pharmacology 84, 339-346.

Mohanty, J. G., Jaffe, J. S., Schulman, E. S., Raible, D. G. 1997. A highly sensitive fluorescent micro-assay of H2O2 release from activated human leukocytes using a dihydroxyphenoxazine derivative. Journal of Immunological Methods 202, 133-141.

Mosmann, T. 1983. Rapid colorimetric assay for cellular growth and survival - application to proliferation and cyto-toxicity assays. Journal of Immunological Methods, 55-63.

Na, H. J., Koo, H. N., Lee, G. G., Yoo, S. J., Park, J. H., Lyu, Y. S., Kim, H. M. 2001. Juniper oil inhibits the heat shock-induced apoptosis via preventing the caspase-3 activation in human astrocytes CCF-STTG1 cells. Clinica Chimica Acta 314, 215-220.

Nakatsu, Y., Kotake, Y., Komasaka, K., Hakozaki, H., Taguchi, R., Kume, T., Akaike, A., Ohta, S. 2006a. Glutamate excitotoxicity is involved in cell death caused by tributyltin in cultured rat cortical neurons. Toxicological Sciences 89, 235-242.

Nakatsu, Y., Kotake, Y., Ohta, S. 2006b. Tributyltin-induced cell death is mediated by calpain in PC12 cells. Neurotoxicology 27, 587-593.

Naus, C. C., Bani-Yaghoub, M. 1998. Gap junctional communication in the developing central nervous system. Cell Biology International 22, 751-763.

Nelson, P. T., Kondziolka, D., Wechsler, L., Goldstein, S., Gebel, J., DeCesare, S., Elder, E. M., Zhang, P. J., Jacobs, A., McGrogan, M., Lee, V. M. Y., Trojanowski, J. Q. 2002. Clonal human (hNT) neuron grafts for stroke therapy - Neuropathology in a patient 27 months after implantation. American Journal of Pathology 160, 1201-1206.

Nicoletti, I., Migliorati, G., Pagliacci, M. C., Grignani, F., Riccardi, C. 1991. A rapid and simple method for measuring thymocyte apoptosis by propidium iodide staining and flow cytometry. Journal of Immunological Methods 139, 271-279.

Nicotera, P., Orrenius, S. 1998. The role of calcium in apoptosis. Cell Calcium 23, 173-180.

Nobel, C. S. I., Kimland, M., Nicholson, D. W., Orrenius, S., Slater, A. F. G. 1997. Disulfiram is a potent inhibitor of proteases of the caspase family. Chemical Research in Toxicology 10, 1319-1324.

Nohl, H., Kozlov, A. V., Gille, L., Staniek, K. 2003. Cell respiration and formation of reactive oxygen species: facts and artefacts. Biochemical Society Transactions 31, 1308-1311.

North, R. A., Verkhratsky, A. 2006. Purinergic transmission in the central nervous system. Pflugers Archiv-European Journal of Physiology 452, 479-485.

O'Callaghan, J. P. 1991. Assessment of neurotoxicity: Use of glial fibrillary acidic protein as a biomarker. Biomedical and Environmental Sciences 4, 197-206.

O'Callaghan, J. P., Jensen, K. F., Miller, D. B. 1995. Quantitative aspects of drug and toxicant-induced astrogliosis. Neurochemistry International 26, 115-124.

O'Donnell, T. J., Nathan, C. F., Lanks, K., Deboer, C. J., Delaharpe, J. 1987. Secretion of pyruvate - an antioxidant defense of mammalian-cells. Journal of Experimental Medicine 165, 500-514.

Ochu, E. E., Rothwell, N. J., Waters, C. M. 1998. Caspases mediate 6-hydroxydopamine-induced apoptosis but not necrosis in PC12 cells. Journal of

Neurochemistry 70, 2637-2640.

OECD (2004). OECD series on testing and assessment. Number 20: guidance document for neurotoxicity testing.

Ogawa, Y., Shimizu, H., Kim, S. U. 1996. 2,5-Hexanedione induced apoptosis in cultured mouse DRG neurons. International Archives of Occupational and Environmental Health 68, 495-497.

Okada, Y., Oyama, Y., Chikahisa, L., Satoh, M., Kanemaru, K., Sakai, H., Noda, K. 2000. Tri-n-butyltin-induced change in cellular level of glutathione in rat thymocytes: a flow cytometric study. Toxicology Letters 117, 123-128.

Opdyke, D. L. J. 1979. Monographs on fragrance raw materials. Food and Cosmetics Toxicology 17, 357-371.

Owens, C. W., Belcher, R. V. 1965. A colorimetric micro-method for the determination of glutathione. The Biochemical Journal 94, 705-711.

Paquet-Durand, F., Gierse, A., Bicker, G. 2006. Diltiazem protects human NT-2 neurons against excitotoxic damage in a model of simulated ischemia. Brain Research 1124, 45-54.

Paquet-Durand, F., Tan, S. M., Bicker, G. 2003. Turning teratocarcinoma cells into neurons: rapid differentiation of NT-2 cells in floating spheres. Developmental Brain Research 142, 161-167.

Parkinson, F. E., Friesen, J., Krizanac-Bengez, L., Janigro, D. 2003. Use of a three-dimensional in vitro model of the rat blood-brain barrier to assay nucleoside efflux from brain. Brain Research, 233-241.

Pei, W., Misumi, J., Kubota, N., Morikawa, M., Kimura, N. 2007. Two new reactive targets of 2,5-hexanedione in vitro - beta-alanine and glycine. Amino Acids 32, 261-264.

Pekny, M., Nilsson, M. 2005. Astrocyte activation and reactive gliosis. Glia 50, 427-434.

Pellerin, L., Magistretti, P. J. 2003. How to balance the brain energy budget while spending glucose differently. Journal of Physiology-London 546, 325-325.

Perea, G., Araque, A. 2002. Communication between astrocytes and neurons: a complex language. Journal of Physiology-Paris 96, 199-207.

Petty, R. D., Sutherland, L. A., Hunter, E. M., Cree, I. A. 1995. Comparison of MTT and ATP-based assays for the measurement of viable cell number. Journal of Bioluminescence and Chemiluminescence 10, 29-34.

Piwocka, K., Jaruga, E., Skierski, J., Gradzka, I., Sikora, E. 2001. Effect of glutathione depletion on caspase-3 independent apoptosis pathway induced by curcumin in Jurkat cells. Free Radical Biology and Medicine 31, 670-678.

Pleasure, S. J., Page, C., Lee, V. M. Y. 1992. Pure, postmitotic, polarized human neurons derived from Ntera-2 cells provide a system for expressing exogenous proteins in terminally differentiated neurons. Journal of Neuroscience 2, 1802-1815.

Polster, B. M., Fiskum, G. 2004. Mitochondrial mechanisms of neural cell apoptosis. Journal of Neurochemistry 90, 1281-1289.

Pong, K., Doctrow, S. R., Huffman, K., Adinolfi, C. A., Baudry, M. 2001. Attenuation of staurosporine-induced apoptosis, oxidative stress, and mitochondrial dysfunction by synthetic superoxide dismutase and catalase mimetics, in cultured cortical neurons. Experimental Neurology 171, 84-97.

Prieto, M. J., Marhuenda, D., Roel, J., Cardona, A. 2003. Free and total 2,5-hexanedione in biological monitoring of workers exposed to n-hexane in the shoe industry. Toxicology Letters 145, 249-260.

Przyborski, S. A., Morton, I. E., Wood, A., Andrews, P. W. 2000. Developmental regulation of neurogenesis in the pluripotent human embryonal carcinoma cell line NTERA-2. European Journal of Neuroscience 12, 3521-3528.

Purchase, I. F. H., Botham, P. A., Bruner, L. H., Flint, O. P., Frazier, J. M., Stokes, W. S. 1998. Workshop overview: Scientific and regulatory challenges for the reduction, refinement, and replacement of animals in toxicity testing. Toxicological Sciences 43, 86-101.

Putnam, K. P., Bombick, D. W., Doolittle, D. J. 2002. Evaluation of eight in vitro assays for assessing the cytotoxicity of cigarette smoke condensate. Toxicology in Vitro 16, 599-607.

Ramirez, G., Alvarez, A., Garcia-Abreu, J., Gomes, F. C. A., Moura-Neto, V., Maccioni, R. B. 1999. Regulatory roles of microtubule-associated proteins in neuronal morphogenesis. Involvement of the extracellular matrix. Brazilian Journal of Medical and Biological Research 32, 611-618.

Ravindranath, V. 1998. Metabolism of xenobiotics in the central nervous system - Implications and challenges. Biochemical Pharmacology 56, 547-551.

Ravindranath, V., Bhamre, S., Bhagwat, S. V., Anandatheerthavarada, H. K., Shankar, S. K., Tirumalai, P. S. 1995. Xenobiotic metabolism in brain. Toxicology Letters 82-83, 633-638.

Reine, C. S. (1998). Chapter 1: Neurocellular Anatomy. In *Basic Neurochemistry: Molecular, Cellular and Medical Aspects* (G. J. Siegel, B. W. Agranoff, R. W. Albers, S. K. Fisher,M. D. Uhler, Eds.), pp. 3-30. Lippincott, Williams and Wilkins, London.

Richter-Landsberg, C., Besser, A. 1994. Effects of organotins on rat brain astrocytes in culture. Journal of Neurochemistry 63, 2202-2209.

Rogers, S. L., Letourneau, P. C., Palm, S. L., McCarthy, J., Furcht, L. T. 1983. Neurite extension by peripheral and central nervous-system neurons in response to

substratum-bound fibronectin and laminin. Developmental Biology 98, 212-220.

Rohl, C., Gulden, M., Seibert, H. 2001. Toxicity of organotin compounds in primary cultures of rat cortical astrocytes. Cell Biology and Toxicology 17, 23-32.

Rootwelt, T., Dunn, M., Yudkoff, M., Itoh, T., Almaas, R., Pleasure, D. 1998. Hypoxic cell death in human NT2-N neurons: Involvement of NMDA and non-NMDA glutamate receptors. Journal of Neurochemistry 71, 1544-1553.

Ross, S. A., McCaffery, P. J., Drager, U. C., De Luca, L. M. 2000. Retinoids in embryonal development. Physiological Reviews 80, 1021-1054.

Russell, W. M. S., Burch, R. L. (1959). *The Principles of Humane Experimental Technique*. Methuen, London.

Sagara, J. I., Makino, N., Bannai, S. 1996. Glutathione efflux from cultured astrocytes. Journal of Neurochemistry 66, 1876-1881.

Saito, Y., Nishio, K., Ogawa, Y., Kimata, J., Kinumi, T., Yoshida, Y., Noguchi, N., Niki, E. 2006. Turning point in apoptosis/necrosis induced by hydrogen peroxide. Free Radical Research 40, 619-630.

Sandhu, J. K., Pandey, S., Ribecco-Lutkiewicz, M., Monette, R., Borowy-Borowski, H., Walker, P. R., Sikorska, M. 2003. Molecular mechanisms of glutamate neurotoxicity in mixed cultures of NT2-derived neurons and astrocytes: Protective effects of coenzyme Q(10). Journal of Neuroscience Research 72, 691-703.

Sandhu, J. K., Sikorska, M., Walker, P. R. 2002. Characterization of astrocytes derived from human NTera-2/D1 embryonal carcinoma cells. Journal of Neuroscience Research 68, 604-614.

Sanfeliu, C., Cristofol, R., Toran, N., Rodriguez-Farre, E., Kim, S. U. 1999. Use of human central nervous system cell cultures in neurotoxicity testing. Toxicology in Vitro 13, 753-759.

Sass, J. B., Ang, L. C., Juurlink, B. H. J. 1993. A simple, yet versatile, coculture method for examining neuron-glia interactions. Journal of Neuroscience Methods 47, 115-121.

Schmuck, G., Ahr, H. J., Schluter, G. 2000. Rat cortical neuron cultures: An in vitro model for differentiating mechanisms of chemically induced neurotoxicity. In Vitro & Molecular Toxicology-a Journal of Basic and Applied Research 13, 37-49.

Schuliga, M., Chouchane, S., Snow, E. T. 2002. Upregulation of glutathione-related genes and enzyme activities in cultured human cells by sublethal concentrations of inorganic arsenic. Toxicological Sciences 70, 183-192.

Seeley, R. R., Stephens, T. D., Tate, P. (1998a). Chapter 3: Structure and Function of the Cell. In *Anatomy and Physiology* (R. R. Seeley, T. D. Stephens,P. Tate,

Eds.), pp. 57-99. McGraw-Hill, Maidenhead.

Seeley, R. R., Stephens, T. D., Tate, P. (1998b). Chapter 12: Functional Organisation of Nervous Tissue. In *Anatomy and Physiology* (R. R. Seeley, T. D. Stephens, P. Tate, Eds.), pp. 354-376. McGraw-Hill, Maidenhead.

Selkoe, D. J., Luckenbilledds, L., Shelanski, M. L. 1978. Effects of neurotoxic industrial solvents on cultured neuroblastoma-cells - Methyl normal-butyl ketone, normal-hexane and derivatives. Journal of Neuropathology and Experimental Neurology 37, 768-789.

Sergent-Tanguy, S., Chagneau, C., Neveu, I., Naveilhan, P. 2003. Fluorescent activated cell sorting (FACS): a rapid and reliable method to estimate the number of neurons in a mixed population. Journal of Neuroscience Methods 129, 73-79.

Seyfried, T. N., Mukherjee, P. 2005. Targeting energy metabolism in brain cancer: review and hypothesis. Nutrition and Metabolism 2, 30-39.

Sharma, P., Karian, J., Sharma, S., Liu, S. Z., Mongan, P. D. 2003. Pyruvate ameliorates post ischemic injury of rat astrocytes and protects them against PARP mediated cell death. Brain Research 992, 104-113.

Shimizu, T., Uehara, T., Nomura, Y. 2004. Possible involvement of pyruvate kinase in acquisition of tolerance to hypoxic stress in glial cells. Journal of Neurochemistry 91, 167-175.

Sickles, D. W., Fowler, S. R., Testino, A. R. 1990. Effects of neurofilamentous axonopathy-producing neurotoxicants on in vitro production of ATP by brain mitochondria. Brain Research 528, 25-31.

Sies, H. 1999. Glutathione and its role in cellular functions. Free Radical Biology and Medicine 27, 916-921.

Silverthorn, D. (1998a). Chapter 8: The Nervous System. In *Human Physiology: An Integrated Approach* (D. K. Brake, Ed.), pp. 201-234. Prentice-Hall, London.

Silverthorn, D. (1998b). Chapter 9: The Central Nervous System. In *Human Physiology: An Integrated Approach* (D. K. Brake, Ed.), pp. 235-262. Prentice-Hall, London.

Sladowski, D., Combes, R., van der Valk, J., Nawrot, I., Gut, G. 2005. ESTIV questionnaire on the acquisition and use of primary human cells and tissue in toxicology. Toxicology in Vitro 19, 1009-1013.

Snoeij, N. J., Penninks, A. H., Seinen, W. 1987. Biological-activity of organotin compounds - an overview. Environmental Research 44, 335-353.

Spencer, P. S., Couri, D., Schaumburg, H. H. (1980). Chapter 32: n-Hexane and methyl n-butyl ketone. In *Experimental and Clinical Neurotoxicology* (P. S. Spencer,H. H. Schaumburg, Eds.), pp. 456-475. Oxford University Press, Oxford.

Stewart, R., Christie, V. B., Przyborski, S. A. 2003. Manipulation of human pluripotent

embryonal carcinoma stem cells and the development of neural subtypes. Stem Cells 21, 248-256.

Stipani, I., Mangiullo, G., Stipani, V., Daddabbo, L., Natuzzi, D., Palmieri, F. 1996. Inhibition of the reconstituted mitochondrial oxoglutarate carrier by arginine-specific reagents. Archives of Biochemistry and Biophysics 331, 48-54.

Stridh, H., Cotgreave, I., Muller, M., Orrenius, S., Gigliotti, D. 2001. Organotin-induced caspase activation and apoptosis in human peripheral blood lymphocytes. Chemical Research in Toxicology 14, 791-798.

Stridh, H., Fava, E., Single, B., Nicotera, P., Orrenius, S., Leist, M. 1999a. Tributyltin-induced apoptosis requires glycolytic adenosine trisphosphate production. Chemical Research in Toxicology 12, 874-882.

Stridh, H., Gigliotti, D., Orrenius, S., Cotgreave, I. 1999b. The role of calcium in pre- and postmitochondrial events in tributyltin-induced T-cell apoptosis. Biochemical and Biophysical Research Communications 266, 460-465.

Stridh, H., Orrenius, S., Hampton, M. B. 1999c. Caspase involvement in the induction of apoptosis by the environmental toxicants tributyltin and triphenyltin. Toxicology and Applied Pharmacology 156, 141-146.

Stryer, L. (1995). *Biochemistry.* W. H. Freeman and Company, New York.

Sun, G. Y., Xu, J. F., Jensen, M. D., Yu, S., Wood, W. G., Gonzalez, F. A., Simonyi, A., Sun, A. Y., Weisman, G. A. 2005. Phospholipase A(2) in astrocytes - Responses to oxidative stress, inflammation, and G protein-coupled receptor agonists. Molecular Neurobiology 31, 27-41.

Sureda, F. X., Gabriel, C., Comas, J., Pallas, M., Escubedo, E., Camarasa, J., Camins, A. 1999. Evaluation of free radical production, mitochondrial membrane potential and cytoplasmic calcium in mammalian neurons by flow cytometry. Brain Research - Brain Research Protocols 4, 280-287.

Tada, H., Shiho, O., Kuroshima, K., Koyama, M., Tsukamoto, K. 1986. An Improved Colorimetric Assay for Interleukin-2. Journal of Immunological Methods 93, 157-165.

Tahti, H., Nevala, H., Toimela, T. 2003. Refining in vitro neurotoxicity testing - The development of blood-brain barrier models. ATLA-Alternatives to Laboratory Animals 31, 273-276.

Takuma, K., Baba, A., Matsuda, T. 2004. Astrocyte apoptosis: implications for neuroprotection. Progress in Neurobiology 72, 111-127.

Talanian, R. V., Quinlan, C., Trautz, S., Hackett, M. C., Mankovich, J. A., Banach, D., Ghayur, T., Brady, K. D., Wong, W. W. 1997. Substrate specificities of caspase family proteases. Journal of Biological Chemistry 272, 9677-9682.

Tamagno, E., Aragno, M., Parola, M., Parola, S., Brignardello, E., Boccuzzi, G., Danni, O. 2000. NT2 neurons, a classical model for Alzheimer's disease, are highly

susceptible to oxidative stress. Neuroreport 11, 1865-1869.

Tietze, F. 1969. Enzymic method for quantitative determination of nanogram amounts of total and oxidized glutathione: applications to mammalian blood and other tissues. Analytical Biochemistry 27, 502-522.

Tieu, K., Ashe, P. C., Zuo, D. M., Yu, P. H. 2001. Inhibition of 6-hydroxydopamine-induced p53 expression and survival of neuroblastoma cells following interaction with astrocytes. Neuroscience 103, 125-132.

Tilson, H. A. 2000. New horizons: Future directions in neurotoxicology. Environmental Health Perspectives 108, 439-441.

Van-Heijst, A. (1999). Group Poisons Information Monograph G019: Trimethyltin compounds. International Programme on Chemical Safety.

Van den Pol, A. N., Spencer, D. D. 2000. Differential neurite growth on astrocyte substrates: Interspecies facilitation in green fluorescent protein-transfected rat and human neurons. Neuroscience 95, 603-616.

Van Houten, B., Woshner, V., Santos, J. H. 2006. Role of mitochondrial DNA in toxic responses to oxidative stress. DNA Repair (Amst) 5, 145-152.

Verdaguer, E., Garcia-Jorda, E., Jimenez, A., Stranges, A., Sureda, F. X., Canudas, A. M., Escubedo, E., Camarasa, J., Pallas, M., Camins, A. 2002. Kainic acid-induced neuronal cell death in cerebellar granule cells is not prevented by caspase inhibitors. British Journal of Pharmacology 135, 1297-1307.

Verderio, C., Matteoli, M. 2001. ATP mediates calcium signaling between astrocytes and microglial cells: modulation by IFN-gamma. Journal of Immunology 166, 6383-6391.

Veronesi, B. 1992. Invitro Screening Batteries for Neurotoxicants. Neurotoxicology 13, 185-195.

Viviani, B., Corsini, E., Galli, C. L., Marinovich, M. 1998a. Glia increase degeneration of hippocampal neurons through release of tumor necrosis factor-alpha. Toxicology and Applied Pharmacology 150, 271-276.

Viviani, B., Corsini, E., Galli, C. L., Padovani, A., Ciusani, E., Marinovich, M. 2000. Dying neural cells activate glia through the release of a protease product. Glia 32, 84-90.

Viviani, B., Corsini, E., Pesenti, M., Galli, C. L., Marinovich, M. 2001. Trimethyltin-activated cyclooxygenase stimulates tumor necrosis factor-alpha release from glial cells through reactive oxygen species. Toxicology and Applied Pharmacology 172, 93-97.

Viviani, B., Galli, C. L., Marinovich, M. 1998b. Trimethyltin but not triethyltin induces specific neural cell death through the protein stannin. Neuroscience Research Communications 23, 139-149.

von Ballmoos, C., Brunner, J., Dimroth, P. 2004. The ion channel of F-ATP synthase is the target of toxic organotin compounds. Proceedings of the National Academy of Sciences U S A 101, 11239-11244.

Votyakova, T. V., Reynolds, I. J. 2004. Detection of hydrogen peroxide with Amplex Red: interference by NADH and reduced glutathione auto-oxidation. Archives of Biochemistry and Biophysics 431, 138-144.

Wang, F. X., Cynader, M. S. 2001. Pyruvate released by astrocytes protects neurons from copper-catalyzed cysteine neurotoxicity. The Journal of Neuroscience 21, 3322-3331.

Wang, S., Rosengren, L. E., Hamberger, A., Haglid, K. G. 1998. An acquired sensitivity to H2O2-induced apoptosis during neuronal differentiation of NT2/D1 cells. Neuroreport 9, 3207-3211.

Wang, W., Ballatori, N. 1998. Endogenous Glutathione Conjugates: Occurrence and Biological Functions. Pharmacological Reviews 50, 335-356.

Watts, L. T., Rathinam, M. L., Schenker, S., Henderson, G. I. 2005. Astrocytes protect neurons from ethanol-induced oxidative stress and apoptotic death. Journal of Neuroscience Research 80, 655-666.

Woehrling, E. K., Zilz, T. R., Coleman, M. D. 2006. The toxicity of hexanedione isomers in neural and astrocytic cell lines. Environmental Toxicology and Pharmacology 22, 249-254.

Wondrak, G. T., Cervantes-Laurean, D., Roberts, M. J., Qasem, J. G., Kim, M., Jacobson, E. L., Jacobson, M. K. 2002. Identification of alpha-dicarbonyl scavengers for cellular protection against carbonyl stress. Biochemical Pharmacology 63, 361-373.

Wu, V. W., Schwartz, J. P. 1998. Cell culture models for reactive gliosis: New perspectives. Journal of Neuroscience Research 51, 675-681.

Wullner, U., Seyfried, J., Groscurth, P., Beinroth, S., Winter, S., Gleichmann, M., Hencka, M., Loschmann, P. A., Schulz, J. B., Weller, M., Klockgether, T. 1999. Glutathione depletion and neuronal cell death: the role of reactive oxygen intermediates and mitochondrial function. Brain Research 826, 53-62.

Xu, L. J., Lee, J. E., Giffard, R. G. 1999. Overexpression of bcl-2, bcl-x(L) or hsp70 in murine cortical astrocytes reduces injury of co-cultured neurons. Neuroscience Letters, 193-197.

Ye, Z. C., Rothstein, J. D., Sontheimer, H. 1999. Compromised glutamate transport in human glioma cells: Reduction-mislocalization of sodium-dependent glutamate transporters and enhanced activity of cystine-glutamate exchange. Journal of Neuroscience 19, 10767-10777.

Ye, Z. C., Sontheimer, H. 1999. Glioma cells release excitotoxic concentrations of glutamate. Cancer Research 59, 4383-4391.

Ying, W. 1996. A new hypothesis of neurodegenerative diseases: The deleterious network hypothesis. Medical Hypotheses 47, 307-313.

Younkin, D. P., Tang, C. M., Hardy, M., Reddy, U. R., Shi, Q. Y., Pleasure, S. J., Lee, V. M. Y., Pleasure, D. 1993. Inducible expression of neuronal glutamate receptor channels in the NT2 human cell line. Proceedings of the National Academy of Sciences of the United States of America 90, 2174-2178.

Yu, K., Kennedy, C. A., O'Neill, M. M., Barton, R. W., Tatake, R. J. 2001. Disparate cleavage of poly-(ADP-ribose)-polymerase (PARP) and a synthetic tetrapeptide, DEVD, by apoptotic cells. Apoptosis 6, 151-160.

Yu, P. H., Zuo, D. M. 1997. Enhanced tolerance of neuroblastoma cells towards the neurotoxin 6-hydroxydopamine following specific cell-cell interaction with primary astrocytes. Neuroscience 78, 903-912.

Zhang, Y. S., Liu, Q., Liu, Q. J., Duan, H. W., He, F. S., Zheng, Y. S. 2006. Effect of 2,5-hexanedione on calcium homeostasis of motor neuron. Chinese Journal of Industrial Hygiene and Occupational Diseases 24, 270-272.

Zhou, J. L., Liang, J. H., Zheng, J. W., Li, C. L. 2004. Nerve growth factor protects R2 cells against neurotoxicity induced by methamphetamine. Toxicology Letters 150, 221-227.

Zhou, M. J., Diwu, Z. J., Panchuk-Voloshina, N., Haugland, R. P. 1997. A stable nonfluorescent derivative of resorufin for the fluorometric determination of trace hydrogen peroxide: Applications in detecting the activity of phagocyte NADPH oxidase and other oxidases. Analytical Biochemistry 253, 162-168.

Zhu, M. S., Spink, D. C., Yan, B., Bank, S., Decaprio, A. P. 1995. Inhibition of 2,5-hexanedione-induced protein cross-linking by biological thiols - chemical mechanisms and toxicological implications. Chemical Research in Toxicology 8, 764-771.

Zilz, T. R., Griffiths, H. R., Coleman, M. D. 2007. Apoptotic and necrotic effects of hexanedione derivatives on the human neuroblastoma line SK-N-SH. Toxicology 231, 210-214.